Weak Localisation Corrections to Electrical and Thermal Conductivity in Superconducting Metals

by

Jacob Spink

A thesis submitted to the
University of Birmingham
for the degree of
DOCTOR OF PHILOSOPHY

School of Physics and Astronomy
College of Engineering and Physical Sciences
University of Birmingham
July 20, 2023

ABSTRACT

This thesis examines the weak localisation correction to electrical and thermal conductivity in superconductors. We propose that the thermal conductivity may be the better candidate to detect weak localisation effects in superconductors, due to the absence of the supercurrent. We provide an analytic calculation of the weak localisation correction to thermal conductivity in a superconductor with the phase coherence lifetime, τ_ϕ, included as a phenomenological parameter. We then examine the case where magnetic impurities are the source of the phase breaking. We provide a thorough derivation of the analytic behaviour in the calculation of the electrical and thermal conductivity with magnetic impurities. We evaluate the full frequency dependent form of the cooperon including magnetic impurities and find the leading order form in the limit of weak doping with magnetic impurities. We provide a partial calculation of the weak localisation correction to thermal conductivity in superconductors weakly-doped with magnetic impurities.

ACKNOWLEDGEMENTS

Cheers Rob.

CONTENTS

LIST OF FIGURES

CHAPTER 1

INTRODUCTION

1.1 Introduction to the Introduction

We will begin this thesis with a discussion of the history of transport phenomena, beginning from the turn of the 20th century with Drude's model for conductivity, all the way through to the development of quantum field theory techniques. Of course this discussion cannot hope to include everything, nor dive too deep into the mathematical details of the various models we will mention. The objective is simply to give a qualitative overview, highlighting the key points that are of relevance to the contents of this thesis.

We will use this background to build up a picture of why we are interested in the theory of weak localisation effects in the thermal conductivity of superconductors, concluding the chapter with an outline of the contents of the rest of the thesis.

1.2 A Brief History of Transport Phenomena

1.2.1 From Classical to Quantum

In 1900 Drude proposed a simple model for conductivity in a metal, motivated by the discovery of the electron only three years prior by J. J. Thomson. In this model the mobile electrons in the metal are treated in the same way as a dilute neutral ideal gas, so their

dynamics are described by the kinetic theory of gases. Understanding that the metal was net-neutral, there was assumed to be some static background of heavy, positively charged particles, i.e. the ion-cores, a new notion at the time [1]. When an electric field is applied, the electrons move on average through the metal, scattering elastically with the ions with a characteristic scattering rate, τ_0^{-1}. Using this relatively simple model, Drude was able to derive an equation for the electrical conductivity, σ in terms of quantities that were all measurable, except for the scattering rate,

$$\sigma = \frac{ne^2\tau_0}{m}\,, \tag{1.1}$$

where n is the number density of electrons, m the mass of the electron and e the charge.

Drude also used this model to predict the contribution to thermal conductivity from the mobile electrons, finding

$$\kappa = \frac{3n\tau_0 k_B^2 T}{2m}\,. \tag{1.2}$$

It had been known for some time that the ratio of thermal and electrical conductivity of metals appeared to be a universal constant, this fact known as the Wiedemann-Franz law, and the constant known as the Lorenz number, L. The Drude results predict this ratio to be

$$\frac{\kappa T}{\sigma} = \frac{3}{2}\left(\frac{k_B T}{e}\right)^2 = L\,, \tag{1.3}$$

which is remarkably close to the measured values; only approximately a factor of 2 out. However, this close agreement was in fact a coincidence, due to two incorrect values obtained from the kinetic theory of gases fortuitously cancelling in the derivation of the thermal conductivity. The specific heat per electron was assumed to be $c_v = \frac{3}{2}k_B$ (as it would be in a conventional monotomic gas [2]) which turns out to be approximately a factor of 100 too large at room temperature, whereas, the average of the square of the ve-

locity used in the derivation was a factor of 100 too small. Although the predicted Lorenz number was close to correct, many other thermal properties were far off the observed results as result of using a Maxwell-Boltzmann distribution for the electrons.

With the advent of quantum mechanics around this time, improvements to the understanding of specific heat were also under way. Boltzmann's classical model treated each atom as trapped in a harmonic well formed by the interactions with its neighbours. The model predicted a constant specific heat of $3k_B$ per atom, obeying the so called law of Dulong-Petit that had been known since the early 1800s. This 'law' was reasonably accurate for a number for materials at room temperature, but it was clear from experiment that the specific heat was not a constant at low temperatures. In 1907, Einstein proposed a model where the atoms were instead treated as quantum harmonic oscillators, with a oscillation frequency know as the Einstein frequency, ω. In the limit $k_BT \gg \hbar\omega$ it recovered the Dulong-Petit law and at low temperatures predicted the specific heat decreased with temperature as an exponential. Experimental findings showed that the dependence of the specific heat at low temperatures went as T^3, plus a small part linear in T that becomes significant at very low temperatures. In 1912 Debye was able to explain the T^3 dependence by realising that the oscillations of the atoms could be treated as sound waves, and quantised in the same way as Planck's quantisation of light. Using a linear dispersion for the sound waves, $\omega(\mathbf{k}) = v|\mathbf{k}|$, where v is the speed of sound, the Debye model yields for the specific heat in the low temperature limit,

$$C = \frac{12\pi^2 N k_B}{5}\left(\frac{k_B T}{\hbar\omega_D}\right)^3 = \frac{12\pi^2 N k_B}{5}\left(\frac{T}{T_D}\right)^3, \tag{1.4}$$

where ω_D is the Debye frequency and T_D is the Debye temperature [2]. This expression is only valid for low temperature, more precisely $T \ll T_D$, because it includes sounds wave modes up to infinite momentum. In the low temperature regime the large momentum modes are not occupied, thus do not contribute to the value of the specific heat, but at higher temperatures, there needs to be a cut-off so that the number of modes included

does not exceed the actual available degrees of freedom of the system. In this model the number of degrees of freedom is $3N$, where N is the number of atoms and the factor of three arising from the three Cartesian directions in which the atoms can oscillate. The derivation has been cleverly constructed so that the cut-off frequency is in fact the Debye frequency. In the limit $T \gg T_D$, the Debye model also recovers the Dulong-Petit result, so is overall very successful. The one remaining question is the source of the term in the specific heat that is linear is T, that seemed to become significant at very low temperatures.

After the discovery of the Pauli-exclusion principle in 1925 and subsequent development of Fermi-Dirac statistics in 1926, Sommerfeld realised the Drude model could be generalised to incorporate the Fermi distribution [2]. The usage of the Fermi-Dirac distribution, as opposed the Maxwell-Boltzmann distribution, resolved issues of the Drude model pertaining to quantities that depended on the form of the distribution. Because the electrical conductivity in the Drude model is not one such quantity, the Sommerfeld model reproduces this result. However, the specific heat is altered by the new distribution. One finds the specific heat is a function of temperature that is linear in T, demonstrating that the contribution to the specific heat at lower temperatures in metals is in fact coming from the specific heat of the electrons. This specific heat is in the order of $k_B T/E_F$ smaller than predicted by the Drude model (where E_F is the Fermi energy) and the averaged velocity term the same order larger. These factors then cancel, explaining why the Drude model's prediction of the Lorenz number is so close. In the Sommerfeld model the Lorenz number is found to be

$$\frac{\kappa T}{\sigma} = \frac{\pi^2}{3}\left(\frac{k_B T}{e}\right)^2, \tag{1.5}$$

which is in good agreement with measured values, and also in good agreement with predictions from microscopic theory, but more on that later.

The Sommerfeld model was not without its problems however. Although the form of

the electrical conductivity is identical to the Drude model, and hence the values of the scattering rates deduced from it, when calculating the mean-free path, $l_0 = v\tau_0$, the larger value for the velocity was now predicting values of l_0 up to hundreds of atomic-spacings at room temperature, whereas the Drude model would yield mean-free-paths in the order of one atomic-spacing. Surprisingly, considering the scattering mechanism was assumed to be due the collisions with the ions, the Drude model actually seemed to predict mean-free-paths more in line with this assumption (albeit somewhat coincidentally once again). This begs the question is the Sommerfeld model's prediction of such long mean-free paths correct? It turns out that it *is* correct, but the Sommerfeld model could not offer any insight as to how the electrons were able to travel so far through the metal without colliding with the ions.

The resolution to this issue came in 1928 with Bloch's theorem, discovered not long after the Schrödinger equation. The major difference of Bloch's theorem compared to the Drude and Sommerfeld models, is that it addresses the periodic potential acting on the electrons due to the lattice of positive ions; whereas the previous model are completely free-electron models. Bloch's theorem also departs with the naïve picture of electrons scattering off of ions as the source of resistance and instead employs a plane wave solution to the Schrödinger equation, which, because the ion potential is included intrinsically as part of the solution, cannot be the source of the scattering. In fact, in a perfectly periodic lattice the model would predict that the electrons are able to travel through the lattice uninhibited and hence lead to an infinite conductivity. The reality is that imperfections in the lattice, due to vacancies, impurities and thermal excitations are abundant, and will all prevent the lattice from being exactly periodic, and hence the conductivity will be finite in practice. Hence, this model was more successful in providing an explanation for why the mean-free paths are so much longer than typical atomic spacing.

The fuller treatment of the lattice also improved understanding of the role of phonons. By examining a one-dimensional, monoatomic toy model of a lattice, one can find a dispersion relation of the phonons where $\omega \propto |\sin(ka/2)|$, where a is the atomic spacing.

So Debye's assumption of a linear dispersion was a good approximation for small momenta, but breaks down at the Brillouin zone boundaries. By counting normal modes of the system we can also provide a more fundamental footing for the cut-off predicted in Debye's model. Of course real materials have a much more complex dispersion relations and normal modes, but we are interested solely in the thermal conductivity, and the phonon picture is helpful in demonstrating how the lattice contributes to the thermal conductivity. We can construct a simple picture where the thermal transport due to the lattice is treated as the transport of a phonon gas, and hence will be described by the kinetic theory of gases, similar to the Drude conductivity. This yields

$$\kappa = \frac{1}{3} n c_v v^2 \tau_{ph} \,, \tag{1.6}$$

where n is the number density of phonons, c_v the heat capacity per phonon, v is the speed of sound and τ_{ph} some characteristic scattering rate of the phonons. In pure metals this contribution is very small in comparison to contributions from the electrons at all temperatures, but in dirty samples where the mean free path of the electrons is reduced the contributions can become comparable at higher temperatures [3].

1.2.2 Superconductivity

During this time where theories of conductivity for metals were moving from a classical to a quantum picture, superconductivity was discovered. First in 1911 with Kamerlingh-Onnes' measurement of the resistivity of mercury [4], where he observed the resistivity dropped sharply to zero at 4K [5]. So a superconductor is a 'perfect' conductor but this is not the entire story. If a superconductor was only a perfect conductor it would exhibit a phenomena known as 'field-locking'. In a perfect conductor the magnetic field inside the bulk is not able to change, this means that if a superconductor was cooled to below the transition temperature without a field applied, any subsequent applied field would be expelled. But if it were cooled with the field already applied, the field would be locked

in. In 1933, Meissner and Oschenfeld found that the magnetic field is always expelled regardless of when it is applied [6], dubbed the Meissner effect. So superconductors are also perfect diamagnets. This effect also implied that superconductivity will be destroyed by the application of a critical magnetic field.

These two key electrodynamic properties of superconductors were explained phenomenologically by Fritz and Heinz London in 1935 using classical electromagnetism [7], named London theory. This predicted that the magnetic field would die-off exponentially inside the superconductor, with a characteristic length scale called the penetration depth, λ. This was superseded by Ginzburg-Landau theory in 1950 [8]: a quantum phenomenological theory in which a complex order parameter, Ψ, was used to describe the superconducting electrons, with the density of superconducting electrons given by $n_s = |\Psi|^2$. One of the major successes of Ginzburg-Landau theory was in handling the intermediate state of superconductors, that occurs at magnetic fields close to the critical value, in which superconducting and normal domains coexist in the material. The theory includes a length scale called the coherence length, ξ, that characterises the range of order in the superconducting electrons [9]. For typical pure metal superconductors that were investigated at the time, $\lambda \ll \xi$, and GL-theory predicts this ratio leads to a positive energy cost for the boundary. In 1957, Abrikosov showed that when $\xi < \sqrt{2}\lambda$, there would be a negative cost for domain walls [10]. This predicted a regime, called the mixed state, where when a magnetic field would be able to penetrate the superconductor in an array of flux vortices, each carrying a quantum of flux. This regime would occur with magnetic fields applied with strength over the lower critical field, H_{c1}, as as the magnetic field was increase from here, the vortex density would increase up until a upper critical field, H_{c2} where the superconductivity is fully destroyed [11]. Superconductors of this nature were called type-II superconductors, and typically occurred in alloys, and the type of superconductivity found in pure metals was called type-I.

The breakthrough for the microscopic theory of superconductivity came in 1956, when Cooper showed that if there were a weak attractive potential between a pair electrons it

would be energetically favourable for them form a bound pair with opposite spin and momenta to each other [12]. One year later Bardeen, Cooper and Schrieffer would extend this model, demonstrating that entire Fermi-sea of electrons would be unstable to the formation of these Cooper pairs and so would, at absolute zero at least, all pair-up and form a superconducting condensate [13]. This microscopic description, on top of being consistent with the electrodynamics we discussed above, successfully explained why there was an energy-gap, Δ, in the excitation spectrum of most superconductors. This is because there is a minimum energy of 2Δ required in order to excite the electrons out of the cooper pair condensate before they can be excited. At finite temperature, electrons are able to be thermally excited out of the condensate leading to a 'two-fluid' picture, where the electrons can be thought of as co-existing superconducting condensate and thermally excited quasi-particles that conduct normally.

It is important to mention at this point, that it is possible for a superconducting state to exist without a gap in the energy spectrum, for example in superconductors containing magnetic impurities, and that superconductivity is characterised fundamentally by the existence of the pair correlations and not the presence of a gap [14]. In 1958, Matthias et. al. observed that doping lanthanum with small concentrations of paramagnetic rare earth elements lead to a reduction in the transition temperature. This was then examined theoretically by Abrikosov and Gor'kov explaining the decrease in transition temperature, but also predicted that the gap would be suppressed. At a critical concentration of impurities the superconductor would become 'gapless' (about 91% of the concentration required to completely destroy the superconductivity at 0K) [15]. This prediction was confirmed experimentally in 1962 by Reif and Woolf in thin films of indium doped with iron [16].

We have discussed that the superconducting state requires an attractive potential between electrons to form, so where does this potential arise from, especially considering that we know that the Coulomb interaction between electrons will actually repel them? In 1950 Frölich was the first to suggest the interaction of the electrons with the lattice

could lead to an effective attractive potential between electrons [17] and this was supported experimentally by the discovery of the isotope effect [18, 19]. This effect is that if measurements are made on samples made from from different isotopes of the same element, one would find the transition temperatures are dependent on the isotopic mass. A physical picture of this effective attraction is as an electron passes through the lattice its negative charge will attract the positively charged lattice ions, causing them to move toward it. Because the lattice ions are much heavier than the electron, the lattice takes a longer time to relax back to its initial position than it take for the electron to move on. Thus, the electron will leave behind a area of positive charge density, which in turn will attract another electron toward where the first electron just was. Hence, there is an effective attraction between the two electrons. So long as this potential exceeds the Coulomb repulsion, Cooper's condition for pairing would be satisfied. This picture can also be formulated in terms of the exchange of virtual phonons between the pairing electrons. The BCS theory approximates this interaction as a featureless interaction of constant strength between electrons within ω_D of the Fermi surface.

1.2.3 Microscopic theories of conductivity

Development of a microscopic theory of quantum transport would take off in 1955 with Matsubara introducing a methodology for quantum field theory at finite temperatures, encapsulating statistical physics into the theory [20]. By making use of this formalism, along with Kubo's linear response theory [21, 22] and Edwards' method for averaging over impurity distributions [23], Langer published a trio of papers in 1960, 1961 and 1962 that successfully reproduced the Drude conductivity at finite temperature using a fully microscopic method [24, 25, 26]. Around the same time as these developments the BCS theory of superconductivity [13] was cast into quantum field theoretic language separately by Gor'kov [27] and Nambu [28].

Shortly after, Langer [29] applied the methodology used for the Drude conductivity to thermal conductivity in the normal state and Ambegaokar and Tewordt [30] extended the

microscopic theory for thermal conductivity into the superconducting regime. However, we must note that there are number of theoretical hurdles to overcome when considering the microscopic theory of thermal currents. First and foremost is that, because temperature is a statistical property of the system, there is no Hamiltonian that describes the application of a temperature gradient; so there is immediately a difficulty in applying Kubo's formula in this context. Furthermore, thermal averaging that takes place in the Kubo formula assumes a constant temperature, which is incompatible with the thermal gradient that is the cause of the current [31]. Luttinger was able to shed some light on this issue, demonstrating that one can construct energy flows in the system by using a fictitious potential, analogous to a gravitational field, and from this extract thermal coefficients both in the normal and superconducting states [32, 33]. However one has to be careful about the exact definition of what constitutes a thermal current, there are several constructions one may take, that if treated self-consistently will all lead to correct evaluation of thermal coefficients. An excellent discussion of this is provided in Mahan [31], but a key take-away for our purposes is that the rate of change of entropy, rather than energy, is really the important quantity for thermal transport.

The advent of field-theoretic methods, whilst successfully explaining basic transport phenomena, like the Drude conductivity, opened the door to exploring from a theoretical perspective more interesting quantum effects in electron transport. Honorable mentions go to electron-electron interactions via the Coulomb force [34] and fluctuation conductivity close to the transition temperature in superconductors, due to finite-lifetime virtual Cooper pairs [35, 36, 37]. The focus of this thesis is on weak-localisation effects due to quantum interference of the electrons with disorder, which we will now discuss in more detail.

1.3 Weak Localisation

In as early as 1966 Langer and Neal [38], in an attempt to go beyond lowest order perturbation theory in the impurity scattering in conductivity calculations, noted that a certain class of diagram (known as the maximally-crossed diagrams) in the perturbation expansion each contributed a small logarithmic term to the conductivity, and that this occurred at all orders of the perturbation expansion. They highlighted this would cause potential divergence issues, but was simply presented as a mathematical difficulty that may need to be overcome and was not given any physical interpretation. It was not until the late 1970s with the development of the scaling theory of localisation [39] that this class of diagram was identified with the quantum interference effect corresponding to coherent back-scattering of the electrons due to impurities. This effect leads to a decreased probability of electron transport and hence a reduction in conductivity, and so was called weak-localisation. The term 'weak' here is an important distinction here with regards the scaling theory of localisation. The weak localisation effect occurs well in the metallic regime, when the disorder is not too strong, and hence can be considered as a perturbative correction to the metallic behaviour described by Bloch's theorem. In terms of wave functions, we can say that at long enough time scales the wave functions of the electrons will be extensive over the system size. For stronger disorder the spatial extent of the wave function can become exponentially suppressed and we will be in the realm of stronger localisation effects, i.e. Anderson localisation [40]. In this thesis we will only be concerned with weak localisation.

Gorkov et. al. calculated the weak localisation correction to conductivity using field-theory by considering the full infinite sum of maximally-crossed diagrams in 1979 [41]. The weak localisation correction exists in one, two and three dimensions, but the two-dimensional case is of particular interest because provides the largest correction. In experiments in thin metallic films the correction to the resistance is in the order of $10^{-3} - 10^{-2}$ and can be measured with an accuracy of $\sim 1\%$ [42]. The form of the correction predicted

by theory, and confirmed experimentally, is logarithmic,

$$\delta\sigma \propto \ln\left(\frac{\tau_\phi}{\tau_0}\right), \tag{1.7}$$

where τ_0 is the elastic scattering lifetime (the same as found in the Drude formula) and τ_ϕ is the phase coherence lifetime. Because weak localisation is a quantum coherence effect between electrons, τ_ϕ measures the characteristic time the over which electron wave-function maintains its phase. If the phase of the wave functions are sufficiently 'scrambled' between scattering events the coherence between the electrons, and hence the weak localisation, will be destroyed. As a general rule, the phase coherence lifetime increases as temperature decreases, so the effect will be most prominent at low temperatures. The exact form of this temperature dependence will depend on the particular mechanisms contributing toward it, so theoretical determination of the temperature dependence of different mechanisms is an important tool for understanding which effects are present in experiment. An example of a direct measurement of a logarithmic dependence in the resistance of a thin film of AuPd obtained by Dolan and Osheroof is shown in figure 1.1 [43]. Unfortunately, to complicate matters Altshuler et. al. demonstrated that the electron-electron interaction correction to conductivity we mentioned briefly in the previous section would also yield a logarithmic correction at low temperatures. So experiment would have to develop a means to distinguish between the two effects. To understand this let us discuss some of the sources of phase breaking.

The types of effects that can cause 'scrambling' of the phase can be broken up broadly into two categories. Firstly, there are inelastic scattering processes, the most prevalent of which is electron-electron interactions. The phase coherence lifetime due to electron-electron interactions was first calculated by Fukuyama and Abrahams [44] and a fairly comprehensive discussion of this can be found in Altshuler and Aronov [45]. This is not a particularly controllable effect though and we essentially at at the mercy of the particular system for how significant this will be. Secondly, there are time-reversal symmetry

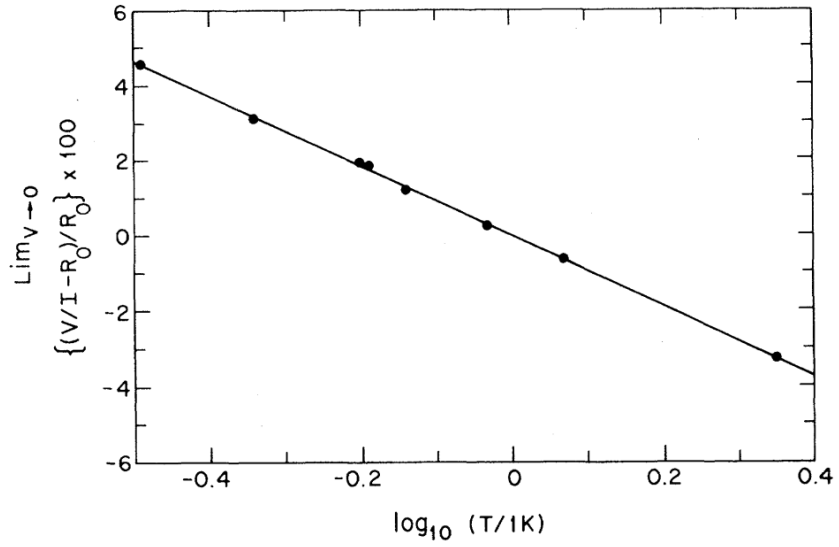

Figure 1.1: Figure taken from Dolan and Osheroff [43]. An example of the correction to resistance increasing logarithmically with decreasing temperature in a thin film of AuPd.

breaking processes. The examples we will be interested in are magnetic impurities and the application of a magnetic field. For experiment the magnetic field is a powerful tool, especially in two dimensions, where the field can be applied perpendicular to the films. This is because by increasing the magnetic field, the phase coherence lifetime, and hence the weak localisation correction, is decreased. Because the application of a magnetic field is so controllable it can be used to switch-off the correction, and so measurements of the magneto-resistance of thin films has become the favoured method for detecting weak-localisation effects [42].

An example of a magneto resistance curve for a thin film of Mg is shown in figure 1.2. We can see in the upper set of curves, at zero applied field, the resistance increases with decreasing temperature. As the field is applied the effect is killed off and this leaves a peak in the centre of the figure. In the lower figure the Mg has been doped with 1% of Au, this introduces spin-orbit scattering. This is a time-reversal breaking process similar to the spin-flip scattering of magnetic impurities, however it actually has the effect to decrease the resistance, hence this effect is called weak anti-localisation. This effect can be seen in the figure as the peak in the centre being inverted for the MgAu film.

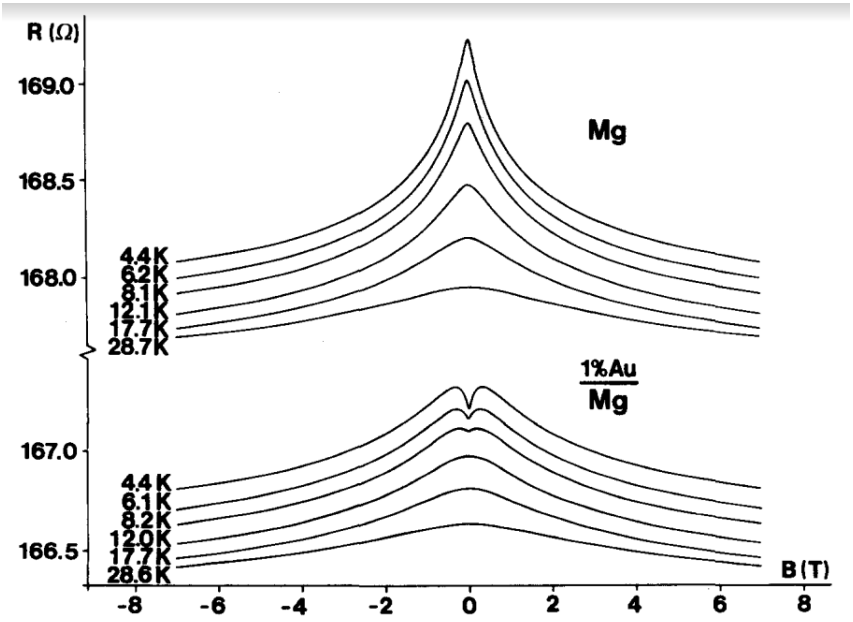

Figure 1.2: Figure taken from Bergmann [42]. The figure displays the magneto-resistance curves for a thin film of Mg. The upper image displays the increasing resistance with decreasing temperature when no field is applied corresponding to weak localisation effect. As the magnetic field is increased (going outward in each curve) this effect is killed off. The lower figure shows the film after it has been doped with a small amount of Au, this introduces spin orbit scattering that inverts the effect, called weak anti-localisation.

1.4 Motivation of the Thesis

The objective of this thesis is to extend the theoretical framework of weak localisation correction calculation to the thermal conductivity of s-wave superconductors and to, in particular, examine the case where the phase-breaking mechanism is provided by magnetic impurities. In this section we will build up a picture of why this is of interest.

The understanding of weak localisation effects in normal metals has been so well studied that it has moved from being a theoretical point of interest to a tool for material science. That is to say, by fitting experimental results to the theory, weak localisation experiments have become a method to probe the particular scattering rates in materials. Typically, experiments of this type are conducted by looking at the electrical conductivity rather than the thermal. This is because weak-localisation effects are caused only by the interaction of the electrons with impurities and do not include any two-body interaction effects. Hence the effect will be identical for the electrical conductivity and electronic

thermal conductivity (i.e. the contribution to thermal conductivity from the electrons specifically) and so the Wiedemann-Franz law persists for this correction, and there is perhaps not much one can learn from thermal measurements that one cannot find by electrical measurements, that are relatively easier to perform. As far as the author is aware the only experimental measurement of the weak localisation correction to thermal conductivity in the normal state is by Bayot et. al. [46].

There has been recent experimental interest in weak localisation effects in materials with superconducting properties. One study on a $LaAlO_3/SrTiO_3$ interface system [47], and another on topologically-insulating Sb_2Te_3 nanoplates [48], both observed weak localisation and superconducting transitions in their samples. However, they were primarily focused on the interplay between weak localisation and weak anti-localisation corrections to electrical conductivity above the transition. Some studies have examined more generally the transition from the normal state to the superconducting state, taking into account all quantum contributions to conductivity,including the weak localisation correction, electron-electron interactions and superconducting fluctuations. Such as in ultra thin TiN films [49] and in strained $Sn_{1-x}In_xTe$ thin films [50]. But once again, as these studies used electrical conductivity, there was no probe of weak localisation firmly in the superconducting state.

There still remains a significant gap in experimental study of weak localisation inside the superconducting state itself. To understand why, we consider the two-fluid picture of superconductivity. In the superconducting state at finite temperatures, some of the electrons form the condensate that carries the supercurrent and some are thermally excited out of the condensate (referred to as the quasiparticles) that can still carry a normal current. The quasi-particles still have, in principle, a weak localisation correction to their contribution to the conductivity. However, the quasiparticle current is shorted-out by the supercurrent, so this small correction is essentially impossible to resolve in measurements of the electrical conductivity. Considering that historically most weak localisation experiments have been conducted with electrical conductivity, we can see why there would be

little interest in the superconducting state. This is where thermal conductivity becomes an interesting prospect. Because the condensate does not carry entropy, it does not carry a thermal current and hence only the quasi-particles will contribute the the electronic thermal conductivity. Without the issue of the supercurrent eclipsing the conductivity measurement, it should in principle be possible to resolve the weak localisation correction to thermal conductivity in a superconductor, as experiments are able to accurately measure thermal conductivities well down into the millikelivin range [51, 52, 53]. Thus, by having a working theory of weak localisation in the superconducting state, we can match the theory to experiment in order to probe how the phase coherence lifetime is affected by the superconducting state.

Although we have argued that thermal conductivity is a good candidate for measuring weak localisation in superconductors, there are some additional considerations with regards to experimental measurements that we must address. We have discussed that the most reliable method for measurements of the weak localisation in the normal state relies on the application of a magnetic field. This presents an immediate problem in the superconducting state, as the magnetic field will suppress the superconductivity. So rather than only destroy the weak localisation correction, the magnetic field will introduce a number of competing effects that will be difficult to distinguish. In the case of thermal conductivity, the break-down of the condensate should lead to an increase in conductivity, due to the increase in number of available quasi-particles for thermal transport. This effect may mask the increase in conductivity that we would expect from the destruction of the weak-localisation contribution. Therefore, we expect that a more direct measurement of the temperature dependence of the conductivity would be a more viable option than examination of magneto-resistance curves. However, a measurement of this type comes with its own complications.

Firstly, the weak localisation effect affects the contribution to the thermal conductivity from the electron transport. However there is also a contribution from the transport of phonons, such that the thermal conductivity can be written as the sum of the two

parts, $\kappa = \kappa_e + \kappa_{ph}$. Each of these terms can then be split into two contributions. The electron term has a contribution from scattering with impurities and from scattering with the phonons. The phonon term also has a contribution from scattering with impurities and a contribution from scattering off the electrons [54]. The best candidate materials for experiment would be those in which there is a temperature region where the effects involving the phonons are minimised and the primary term contributing to the thermal conductivity comes from the electronic component whose mean-free path is limited by scattering with the impurities, as well as having a significant weak localisation effect in that region. Of course it may not be possible to find a case where the phononic effects are entirely negligible, but because the weak localisation correction is expected to be $1 - 10\%$ of the electronic contribution, maximising the electronic part compared to the phononic will lead to the best chance of resolving the correction. In this case one would have to have an understanding of the temperature dependencies of the phononic effects so that one could distinguish them from the weak localisation correction by fitting the shapes of the temperature-conductivity curves. As the focus of this thesis is entirely on the electronic thermal conductivity, we will direct the reader to Gladstone et. al. [55] and Ginsberg and Hebel [54] in Parks' treatise and Rickayzen [9] for reviews on the phononic thermal conductivity.

The second effect we will consider is once again best framed within the two fluid picture of superconductivity, as this will inform where measurements should be focused in the temperature range (it is useful to express this on a scale on 0 to 1 in the reduced temperature T/T_c). As the temperature is decreased below T_c the number of quasiparticles available to participate in thermal conductivity will decrease as they will become part of the condensate. This will cause a suppression of the electronic thermal conductivity as temperature is decreased, an example of which for aluminium can be seen in figure 1.3, where the ratio of superconducting to normal thermal conductivity is shown as a function of T/T_c. Therefore, we should direct attention to the higher-temperature region, just below T_c, as the phononic contribution may become comparable to that of the electronic

contribution lower in the temperature range [56].

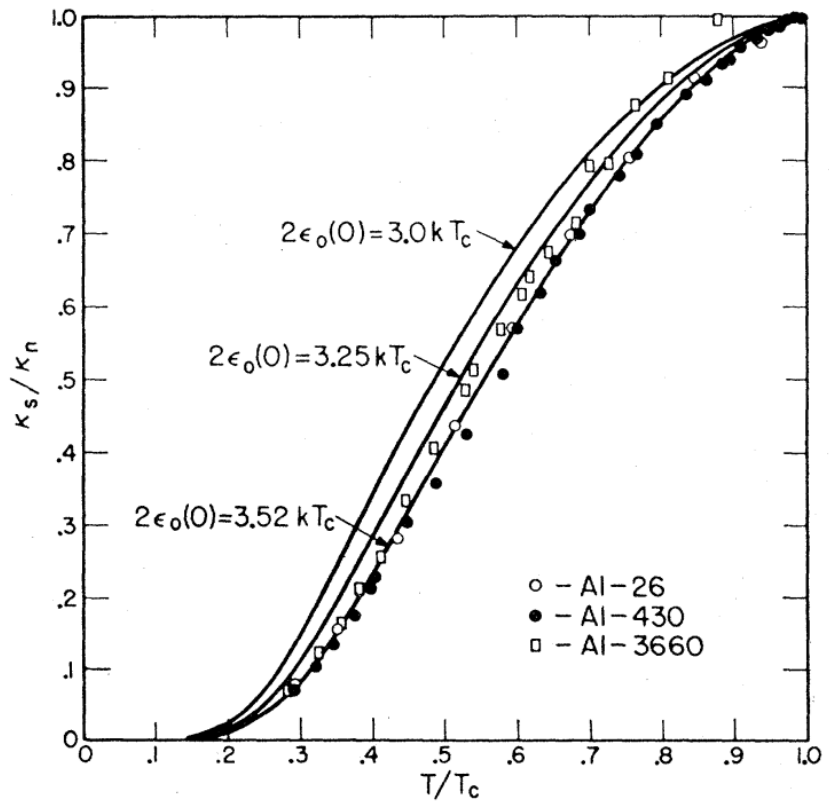

Figure 1.3: Figure taken from Satterthwaite [57]. The ratio of superconducting to normal thermal conductivity of Aluminium as a function of temperature normalised to the critical temperature. The dots are the experimental data for three different specimens and the solid lines are theoretical curves based on the calculation of Bardeen et. al. [58] with three different fitting parameters for the gap.

Now that we have discussed the experimental background, we will discuss the theoretical work that has examined weak localisation in superconductors. Smith and Ambegaokar found the correction to the number density of superconducting electrons from the weak localisation effect in dirty s-wave superconductors [59], Yang et. al. calculated this correction in d-wave superconductors [60] and Jujo has calculated the effect of weak localisation on the linear absorption in s-wave superconductors [61]. All of these studies have been concerned with the effects of weak localisation on properties of superconductors other than the conductivity itself. Only two studies have examined the correction to thermal conductivity, one of which is in a superconductor-normal-superconductor junction system [62], which is not of as much interest to us, and the other is the recent work of González

Rosado et. al. [63]. In the latter paper the weak localisation correction to thermal conductivity in s-wave superconductors is calculated, with the phase breaking rate included as a phenomenological parameter. The clean and dirty limits are examined and particular attention is drawn to the temperature region $T \approx 0.9T_c$ as the optimum region for observing the correction, which is in agreement with the arguments we have outlined above. Thus, in this thesis, we aim to develop a methodology for the calculation of weak localisation corrections in the superconducting state and verify the results of this paper for dirty superconductors in this high temperature region.

The next step to take from a theoretical standpoint is to be able to include mechanisms for phase breaking directly into the calculation. González Rosado et. al. included a brief look at the inclusion of spin-orbit scattering, but found that the correction in this case is functionally the same as their results with the phenomenological parameter, only with an additional factor of $-1/2$, meaning the result is weak anti-localisation instead as expected. Reizer has developed much of the theory of phase coherence lifetime due to electron-electron interactions in the superconducting state [64], however this work is rather complex from a theoretical standpoint. As well as this, when electron-electron interactions are an appreciable source of phase breaking for the weak localisation effect, they typically will cause their own correction to conductivity that can difficult to resolve from the weak localisation correction.

The primary original work in this thesis will be the development of the theory of weak localisation in superconductors where magnetic impurities provide the limiting source of the phase coherence lifetime. We are motivated to choose magnetic impurities because these are a relatively simple dephasing mechanism that one can include directly into the formalism. Their effect on most common physical properties, such as the order parameter and the conductivity, have been established for some time (see Maki's chapter in Parks' treatise for a good summary [14]). The only work the author is aware of to date that covers the theory of weak localisation with magnetic impurities is in the work of Smith [65]. However, this work does not examine the correction to conductivity, but the correction

the superconducting density of states.

Like magnetic fields, magnetic impurities will act to suppress the superconductivity and because they are a strong source of phase breaking there should be a doping concentration that is high enough for them to be the dominant source of phase breaking, but low enough such that the superconductivity is not strongly suppressed. In the case of thin films, in which the weak localisation is most prominent, the doping concentration should be a controllable parameter, as the magnetic impurities can be purposefully dispersed into the sample during or after the growth of the film.

1.5 Summary of the Contents of this Thesis

The remainder of this thesis will be mathematical in nature and consist primarily of the derivation of results, gradually increasing in complexity with each chapter. To that end, we begin in Chapter 2 by establishing the mathematical techniques related to Green's functions and diagrammatic quantum field theory that we will make heavy use of in the rest of the thesis. Then in Chapter 3, we make use of these techniques to derive a number of important results relating to transport phenomena in the normal state, starting with Drude's results for electrical conductivity and the electronic component of the thermal conductivity. We then introduce the weak localisation effect and calculate the correction for both electrical and thermal conductivity. We conclude the chapter by examining the superconducting transition through the lens of quantum fluctuations in the normal state just above the transition temperature.

In Chapter 4 we introduce the Nambu-Gorkov formalism for performing calculations of transport properties in BCS-type superconductors, then go on to use these to derive some rudimentary results such as the gap parameter, the transition temperature and the superconducting carrier density. We also provide an analytic expression for the frequency-dependent linear response to an electromagnetic field in a superconductor, which describes the infrared absorption and transmission of the superconductor. We then derive the

electronic component of thermal conductivity in the superconducting state.

In Chapter 5 we move on to weak localisation effects in the superconducting state, which is the beginning of the original work of this thesis. First we demonstrate how to construct a cooperon in the Nambu-Gorkov formalism in isolation, utilising the outer-product of Pauli matrices to encode the information of both vertices of the cooperon in one function. We then use this to calculate the weak localisation correction to electrical and thermal conductivity. Here we focus on the thermal conductivity, because the supercurrent will short-out the electrical conductivity, meaning the weak localisation correction to the quasi-particles will be negligible in comparison to the supercurrent. We introduce the phase-breaking rate as a phenomenological parameter in the thermal weak localisation to provide a cut-off for the correction. We find that our results are in agreement with those of González Rosado et. al. for the case of the dirty superconductor in the upper temperature range of the superconducting state [63].

Chapter 6 introduces magnetic impurities into the Nambu-Gorkov formalism. We once again treat the linear response of the superconductor, now doped with magnetic impurities, to both an electromagnetic field and a temperature gradient to obtain analytic expressions for the electrical and thermal conductivity. We in particular hope to shed some light on the process of analytic continuation of the linear response functions in this regime, as this is particularly poorly demonstrated in the literature. In the second half of the chapter we provide a full derivation of the form of the cooperon in a superconductor containing paramagnetic impurities, similarly to that which can be found in the work of Smith [65]. Here we depart from Smith's previous work as we take the leading order approximation for weak doping with magnetic impurities whilst retaining the full frequency dependence of the cooperon, such that analytic continuation is still possible. The previous work was only concerned with the correction to number density of superconducting electrons, thus the frequency could be taken to zero at this stage. We then go on to progress with the weak localisation calculation as far as analytic methods can take us. We are able to complete this calculation up to the point where we could perform analytic

continuation in the same way as outlined in the first half of the chapter. It is possible to perform this analytic continuation stage exactly, however there is no neat simplification, leading to an explosion in the number of terms. Therefore we end this chapter with a discussion of behaviour we might expect from the analytic continuation and potential avenues for future work.

CHAPTER 2

THE METHODOLOGY OF GREEN'S FUNCTIONS FOR TRANSPORT

In this chapter we will lay the groundwork for the diagrammatic quantum field theory, which will be the method that all calculation in the thesis will utilise. Firstly, we will discuss Green's functions and their function in the context of diagrammatics. In the next, section we will establish the main types of Green's functions that are of interest to us and establish their analytic properties. With the mathematical formalities out of the way, we then move on to deriving the single particle Green's function, which is perhaps the most fundamental object in the diagrammatic theory. We will then use it in the perturbation expansion for a one-body and two-body potential. The chapter culminates with the derivation of the impurity Green's function, which will be used in the remainder of the thesis, as it describes the propagation of electrons in disordered systems. This section importantly discusses the process of ensemble averaging, which bridges the gap between particular distributions of impurities on the microscopic level and macroscopic observables, such as conductivity, where the impurity distributions appear homogeneous.

2.1 Motivating Green's Functions

When considering the microscopic theory of electrical and thermal transport, one is dealing with a system of many electrons which may be interacting with one another and their environment, hence many body quantum field theory is the natural language with which to approach this problem. Broadly speaking quantum field theory is approached in one of two equivalent ways: path integral formulation or diagrammatics. For certain applications the path integral approach proves a more powerful tool, however we will be making heavy use of perturbative expansions and diagrammatics offers a much more simple and direct route to this objective. This methodology is well established and can be found in a number of standard texts. The structure presented here follows most closely that found in refs [56, 66], but the reader may also find useful ref [67].

The diagrammatic approach uses Green's functions as the primary objects that power the theory, but what is a Green's function in this context? In mathematics, they are encountered as a means to solve linear differential equations; where loosely they can be thought of as the inverse of the differential operator, such that applying the differential operator to the Green's function yields a delta function source, or an impulse. In a classical physical context, this method is employed in electrostatics to find the electrical potential ϕ generated by a fixed charge distribution [66],

$$\nabla^2\phi(\mathbf{r}) = -\frac{\rho_e(\mathbf{r})}{\varepsilon_0}\,, \tag{2.1}$$

$$\text{define} \quad \nabla^2 G(\mathbf{r}) = \delta(\mathbf{r})\,,$$

$$\Rightarrow \phi(\mathbf{r}) = -\frac{1}{\varepsilon_0}\int \mathrm{d}^3 r\, G(\mathbf{r}-\mathbf{r}')\rho_e(\mathbf{r}')\,. \tag{2.2}$$

So we have reduced the problem down to solving the much differential equation for $G(\mathbf{r})$,

which can be solved immediately with a Fourier transformation yielding

$$\begin{aligned} G(\mathbf{k}) &= -\frac{1}{k^2}\,, \\ \Rightarrow G(\mathbf{r}) &= -\int \frac{\mathrm{d}\mathbf{k}}{(2\pi)^3}\frac{e^{i\mathbf{k}\cdot\mathbf{r}}}{k^2} = -\frac{1}{4\pi|\mathbf{r}|}\,. \end{aligned} \tag{2.3}$$

Now this can simply be substituted back into equation 2.2 to obtain the well known equation for the potential

$$\phi(\mathbf{r}) = \frac{1}{4\pi\epsilon_0}\int \mathrm{d}\mathbf{r}'\,\frac{\rho_e(\mathbf{r})}{|\mathbf{r}-\mathbf{r}'|} \tag{2.4}$$

We can also apply this same concept to quantum mechanical problems. Consider the time-dependent Schrödinger equations (with $\hbar = 1$) for a free particle and a particle in a potential, $V(\mathbf{r})$,

$$[i\partial_t - H_0(\mathbf{r})]\psi_0(\mathbf{r},t) = 0\,, \tag{2.5a}$$

$$\text{and} \quad [i\partial_t - H_0(\mathbf{r}) - V(\mathbf{r})]\psi(\mathbf{r},t) = 0\,, \tag{2.5b}$$

where we know the eigenstates of H_0 and want to find out about the full Hamiltonian by treating the potential as a perturbation. The Green's functions for these equations can then be defined as

$$[i\partial_t - H_0(\mathbf{r})]G_0(\mathbf{r},t,\mathbf{r}',t') = \delta(\mathbf{r}-\mathbf{r}')\delta(t-t') \tag{2.6a}$$

$$\text{and} \quad [i\partial_t - H_0(\mathbf{r}) - V(\mathbf{r})]G(\mathbf{r},t,\mathbf{r}',t') = \delta(\mathbf{r}-\mathbf{r}')\delta(t-t')\,, \tag{2.6b}$$

then because

$$G^{-1}(\mathbf{r},t)G(\mathbf{r},t,\mathbf{r}',t') = \delta(\mathbf{r}-\mathbf{r}')\delta(t-t')\,, \tag{2.7}$$

the inverse of the Green's functions are given by

$$G_0^{-1}(\mathbf{r},t) = i\partial_t - H_0(\mathbf{r}) \tag{2.8a}$$

$$\text{and} \quad G^{-1}(\mathbf{r},t) = i\partial_t - H_0(\mathbf{r}) - V(\mathbf{r})\,. \tag{2.8b}$$

Now by inspection we can see that the solution to equation 2.5 is

$$\begin{aligned} \psi(\mathbf{r},t) &= \psi_0(\mathbf{r},t) + \int \mathrm{d}\mathbf{r}'\,\mathrm{d}t\, G_0(\mathbf{r},t,\mathbf{r}',t')V(\mathbf{r}')\psi(\mathbf{r}',t')\,, \\ \text{or equally} \quad \psi(\mathbf{r},t) &= \psi_0(\mathbf{r},t) + \int \mathrm{d}\mathbf{r}'\,\mathrm{d}t\, G(\mathbf{r},t,\mathbf{r}',t')V(\mathbf{r}')\psi_0(\mathbf{r}',t')\,, \end{aligned} \tag{2.9}$$

which can be verified by substituting the form of $\psi(\mathbf{r},t)$ back into the Schrödinger equation along with using the definitions of the inverse Green's functions. These integral equation can be solved iteratively to yield

$$\begin{aligned} & G = G_0 + G_0VG_0 + G_0VG_0VG_0 + \ldots\,, \\ \Rightarrow \quad & G = G_0 + G_0VG \\ & \quad = (G_0^{-1} - V)^{-1}\,; \end{aligned} \tag{2.10}$$

where equations of this type are known as Dyson equations. This approach of using a perturbation to a known Hamiltonian to obtain a Dyson equation will be reflected as we extend this formalism up into the realms of quantum field theory, as it allows us to obtain a Green's function for the Hamiltonian we are interested in, given we know the Green's function for the simpler unperturbed Hamiltonian and the form of the interaction. This leads us a building block approach where we can repeat this process up from a very simple single particle Green's function to obtain Green's functions that include information about more and more interactions, as long as we can add these interactions to the Hamiltonian in a perturbative way.

However there is some subtlety when comparing single particle quantum mechanics

to the full many body problem. In the Shrödinger equation example above the Green's function relates the wavefunction at times t' and t,

$$\psi(\mathbf{r}, t) = \int \mathrm{d}\mathbf{r}' \, G(\mathbf{r}, t; \mathbf{r}', t)\psi(\mathbf{r}', t') \, . \tag{2.11}$$

For this reason these Green's functions are also referred to as propagators, as they propagate the wavefunction through time and space. But when we construct Green's functions in diagrammatic quantum field theory they turn out to be the solutions to equations of motion, as opposed to the differential operator acting on the full wavefunction as in the Schrödinger equation example. As such they do not contain all the information in the many body wavefunction, but instead the information relevant for the equation of motion we have constructed [66].

2.2 General Properties of Green's Function

Before examining in detail the single particle Green's function, we will summarise some of the important properties of the types of Green's functions of which we will make use. At this stage, the general form of the Green's functions will be introduced without much motivation, however it will become more clear when we look at the single particle case. As well, the retarded Green's function we will discuss next naturally arises in the Kubo formula for the linear response of a system to a small perturbation (see appendix A for a full derivation), which is the context in which we wish to use the Green's functions.

The retarded Green's function relating two time dependent operators $A(t)$ and $B(t')$ is given by

$$G^R(t, t') = -i \left\langle [A(t), B(t')]_\eta \right\rangle \Theta(t - t') \, ; \tag{2.12}$$

$$\text{where} \quad [A(t), B(t')]_\eta = A(t)B(t') + \eta B(t')A(t) \, ,$$

where $\eta = +1$ for fermionic operators and -1 for bosonic operators. This Green's function

is the one that arises naturally in linear response theory and is known as retarded because the Heaviside function, $\Theta(t-t')$, enforces the correct causality: in this case that the response of $A(t)$ comes after the perturbation caused by $B(t')$. Similarly, there is an advanced Green's function given by

$$G^A(t,t') = i\,\langle [A(t), B(t')]_\eta \rangle\, \Theta(t'-t)\,, \tag{2.13}$$

which relates $A(t)$ to $B(t')$ at a later time t'. The advanced Green's function will not be nearly as important to us- being interested in response to perturbations. The angled brackets denote thermal averaging with respect to the density matrix, $\rho = e^{-\beta H}$, of a Hamiltonian, H,

$$\langle A(t)B(t')\rangle = \frac{1}{Z}\,\mathrm{Tr}\big\{e^{-\beta H}A(t)B(t')\big\} \quad , \quad Z = \mathrm{Tr}\big\{e^{-\beta H}\big\}\,, \tag{2.14}$$

where Z is the partition function [56].

The next type of Green's function we will examine is the temperature Green's function, named as such because it is constructed to allow us to perform calculations at finite temperatures [56]. This is achieved by making use of the formal similarity between the statistical density matrix, $e^{-\beta H}$, and the quantum mechanical time-evolution operator, e^{-iHt} [68]. This similarity is exploited by performing the Wick rotation from real time, t, into imaginary time, $-i\tau$, causing the time-evolution and density matrix to have the same functional form. Furthermore, the time domain is transformed from $t \in [-\infty, \infty]$ to $\tau \in [0, \beta]$ (where $\beta = 1/T$ and $k_B = 1$), meaning that integrals over real time are cast into integrals up to the reciprocal temperature, thereby encoding the information about the system temperature into calculations. The Green's function has the form

$$\begin{aligned} G(\tau,\tau') &= -\,\langle \mathcal{T}_\tau A(-i\tau)B(-i\tau')\rangle \\ &= -\,\langle A(-i\tau)B(-i\tau')\rangle\,\Theta(\tau-\tau') + \eta\,\langle B(-i\tau')A(-i\tau)\rangle\,\Theta(\tau'-\tau)\,; \end{aligned} \tag{2.15}$$

where $\mathcal{T}_\tau$ is the imaginary time ordering operator, whose definition is as equation 2.15. Note that all of the following still holds when we extend this formalism to a grand canonical ensemble, where our density matrix and time evolution operators will be given instead by

$$\rho = e^{-\beta(H-\mu N)} \quad \text{and} \quad U(t) = e^{-i(H-\mu N))t}\,. \tag{2.16}$$

When we have Green's functions that are functions of only two times, by using the cyclic property of the trace, the time dependence of one operator may be shifted onto the other, making the Green's functions only functions of time differences:

$$G^R(t,t') = -i\,\langle[A(t-t'),B(0)]_\eta\rangle\,\Theta(t-t') = G^R(t-t')\,, \tag{2.17a}$$

$$G^A(t,t') = -i\,\langle[A(t-t'),B(0)]_\eta\rangle\,\Theta(t'-t) = G^A(t-t')\,, \tag{2.17b}$$

$$G(\tau,\tau') = -\,\langle\mathcal{T}_\tau A(-i\tau+i\tau')B(0)\rangle = G(\tau-\tau')\,. \tag{2.17c}$$

This means that we can Fourier transform with respect to their time differences, but we must treat the real time and imaginary time differently due to their different domains.

Beginning with the real time Green's functions, the Fourier transform for the retarded Green's function is given by

$$G^\wedge(\Omega) = \int_{-\infty}^{\infty} \mathrm{d}t\, G^R(t-t')e^{i\Omega(t-t')}\,, \tag{2.18}$$

where Ω is in general a complex number and so we must be careful about where the function is analytic. If we write Ω as its real and imaginary parts, $\Omega = \omega + i\delta$ (ω, $\delta \in \mathbb{R}$), it is clear that the integral converges for $\delta > 0$ i.e. in the upper half plane (hence why we have suggestively labelled it with an upwards arrow), provided the correlation does not grow faster than an exponential; a reasonable assumption for most real systems. If we take the limit that the imaginary part goes to zero, we obtain the retarded Green's

function in frequency space,

$$G^R(\omega) = \lim_{\delta \to 0} G^\wedge(\omega + i\delta)\,, \tag{2.19}$$

this gives the response of the system to a perturbation of frequency ω. Similarly for the advanced Green's function, we find it is analytic in the lower half plane and we have

$$G^\vee(\Omega) = \int_{-\infty}^{\infty} \mathrm{d}t\, G^A(t-t') e^{i\Omega(t-t')}\,, \tag{2.20a}$$

$$G^A(\omega) = \lim_{\delta \to 0} G^\vee(\omega - i\delta)\,; \tag{2.20b}$$

where we have assumed for now that the Fourier transform of the retarded and advanced Green's functions do not necessarily yield the same function, so we have defined another Green's function, $G^\vee(\Omega)$, to denote it is analytic in the lower half plane. The Green's functions $G^\wedge(\Omega)$ and $G^\vee(\Omega)$ can be written in terms of a spectral function

$$G^\wedge(\Omega) = G^\vee(\Omega) = \int_{-\infty}^{\infty} \frac{\mathcal{A}(x)}{\Omega - x}\,; \tag{2.21}$$

where it so happens that the spectral function has the same form for both, only distinguished by their regions of analyticity [56]. Hence, there is a single function, $G(\Omega)$, that is analytic in both the upper and lower half plane that equals G^R as the real axis is approached from above and G^A when approached from below. One must be careful on the real axis due to this break in analyticity, as there is a branch cut given by

$$\begin{aligned} G^R(\omega) - G^A(\omega) &= \lim_{\delta \to 0}[G(\omega + i\delta) - G(\omega - i\delta)] \\ &= \lim_{\delta \to 0} \int_{-\infty}^{\infty} \mathrm{d}x\, \mathcal{A}(x) \left[\frac{1}{\omega + i\delta - x} - \frac{1}{\omega - i\delta - x} \right] \\ &= -2\pi i \mathcal{A}(\omega)\,. \end{aligned} \tag{2.22}$$

Where we have made use of the Plemelj formula

$$\int_{-\infty}^{\infty} \mathrm{d}x \, \frac{\mathcal{A}(x)}{\omega \pm i\delta - x} = \mp \pi i \mathcal{A}(x) + \mathcal{P} \int_{-\infty}^{\infty} \frac{\mathcal{A}(x)}{\omega - x} \,, \tag{2.23}$$

with $\mathcal{P}$ being the principle part. So the spectral function is related to the difference between the retarded and advanced Green's functions [56].

The temperature Green's function requires different treatment because it has a finite time domain, so the solutions must be periodic and hence there will be discrete frequency modes. Start by choosing $\tau' = \beta$ and $0 < \tau < \beta$, therefore due to the time ordering operator we will only be left with the term corresponding to $\tau < \tau'$, then we use the cyclic property of the trace to show that the temperature Green's functions are periodic,

$$\begin{aligned} G(\tau - \beta) &= \eta \left\langle B(0) A(-i\tau + i\beta) \right\rangle \\ &= \frac{\eta}{Z} \operatorname{Tr}\left\{ e^{-\beta H} B(0) e^{(\tau-\beta)H} A(0) e^{-(\tau-\beta)H} \right\} \\ &= \eta \left\langle A(0) B(i\tau) \right\rangle \\ &= -\eta G(\tau) \,. \end{aligned} \tag{2.24}$$

Note that bosonic and fermionic operators will have different Fourier transforms, due to the sign of η. For bosonic operators, the temperature Green's functions are periodic over the interval $0 < \tau \leq \beta$ and hence can be expanded in terms of exponentials $e^{-i\omega_l \tau}$, where $\omega_l = \frac{2\pi l}{\beta}$:

$$\begin{aligned} G(i\omega_l) &= \int_0^\beta \mathrm{d}\tau \, e^{i\omega_l \tau} G(\tau) \\ \text{and} \quad G(\tau) &= \frac{1}{\beta} \sum_{\omega_l} G(i\omega_l) e^{-i\omega_l \tau} \,. \end{aligned} \tag{2.25}$$

Whereas for fermonic operators the Green's functions are anti-periodic over $0 < \tau \leq \beta$ and hence the Fourier series can be constructed in the same way only with frequency modes of $\varepsilon_l = \frac{2\pi}{\beta}\left(l + \frac{1}{2}\right)$ [56].

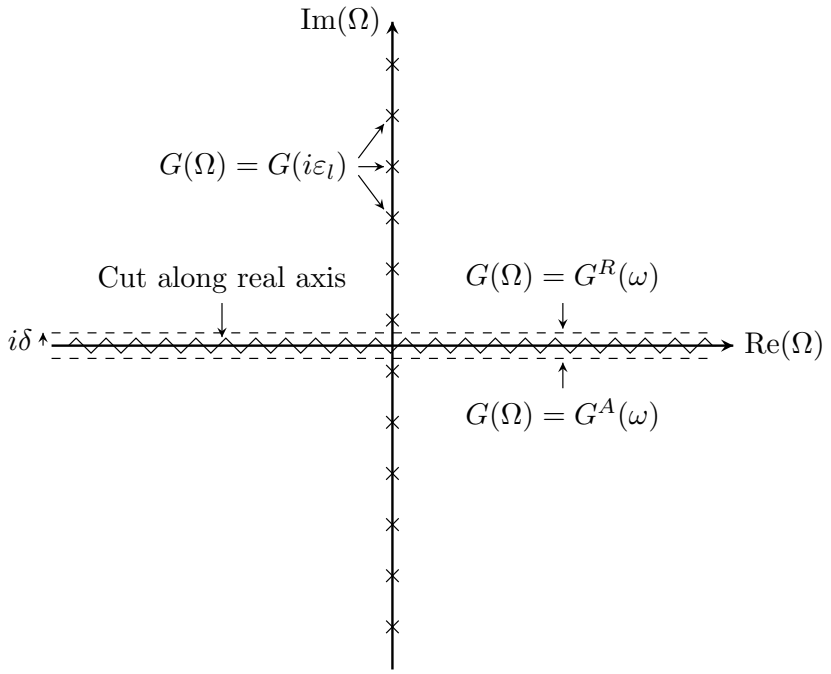

Figure 2.1: This schematic shows the important features of Green's functions on the complex frequency plane. $G(\Omega)$ is analytic in the upper and lower half planes and equals the retarded Green's function, $G^R(\omega)$, just above the real axis and the advanced Green's function, $G^A(\omega)$, just below; with a break in analyticity when crossing the real axis. Up the imaginary axis the Green's function is equal to the temperature Green's function at the Matsubara frequencies depicted by the crosses.

These discrete frequencies in the imaginary time regime are known as Matsubara frequencies and lie up the imaginary axis in the complex Ω plane, as shown in figure 2.1. The spectral function related to these Matsubara Green's functions is exactly the same as for the real time case, but now

$$G(i\omega_l) = \int_{-\infty}^{\infty} \mathrm{d}x \, \frac{\mathcal{A}(x)}{i\omega_l - x} \quad \text{or} \quad G(i\varepsilon_l) = \int_{-\infty}^{\infty} \mathrm{d}x \, \frac{\mathcal{A}(x)}{i\varepsilon_l - x} \tag{2.26}$$

As the retarded, advanced and Matsubara Green's functions can all be defined by a single spectral function, for a given problem there should be a single Green's function, $G(\Omega)$, that is analytic in the upper and lower half planes and yields all the aforementioned Green's functions at the appropriate points on the complex plane. However, to uniquely define $G(\Omega)$ we must also use the condition that $G(\Omega)$ must fall off to zero at least as fast as Ω^{-1} as $|\Omega| \to \infty$ [56].

2.3 The Single Particle Green's Function

Now we will turn our attention to the single particle Green's function, that will constitute the fundamental building blocks of the many body framework. Consider the time-ordered correlation function between two particle field operators

$$\left\langle \psi(\mathbf{r},t)\psi^{\dagger}(\mathbf{r}',t')\right\rangle \Theta(t-t')\,. \tag{2.27}$$

This object describes the expectation of a particle to be created at $(\mathbf{r}',t')$ and later annihilated at $(\mathbf{r},t)$, or in other words the propagation of the particle. From this we can construct a retarded Green's function as per equation 2.12,

$$G_0^R(\mathbf{r},t;\mathbf{r}',t') = -i\left\langle \left[\psi(\mathbf{r},t),\,\psi^{\dagger}(\mathbf{r}',t')\right]_{\eta}\right\rangle \Theta(t-t')\,. \tag{2.28}$$

So there is a term as in equation 2.27 describing a particle propagator, but also a second term of the form $\left\langle \psi^{\dagger}(\mathbf{r}',t')\psi(\mathbf{r},t)\right\rangle$ that corresponds to a hole propagator. So the inclusion of the commutator encapsulates the fact that the propagation of a particle forward in time is equivalent to the propagator of a hole backward in time.

Although the retarded Green's functions are those that arise naturally in linear response theory, we will find that is is most practical to operate using temperature Green's functions during calculations and then use analytic continuation to recover the retarded Green's function from the temperature Green's function. The single particle temperature Green's function is defined by

$$\begin{aligned} G_0(\mathbf{r}_1,\tau_1;\mathbf{r}_2,\tau_2) &= -\left\langle \mathcal{T}_{\tau}\psi(\mathbf{r}_1,-i\tau_1)\psi^{\dagger}(\mathbf{r}_2,-i\tau_2)\right\rangle\,, \\ \text{where}\quad \psi(\mathbf{r},-i\tau) &= e^{H\tau}\psi(\mathbf{r})e^{-H\tau} \\ \text{and}\quad \psi^{\dagger}(\mathbf{r},-i\tau) &= e^{H\tau}\psi^{\dagger}(\mathbf{r})e^{-H\tau}\,. \end{aligned} \tag{2.29}$$

One must be careful about the Hermitian conjugation as

$$[\psi(\mathbf{r}, -i\tau)]^\dagger = \psi^\dagger(\mathbf{r}, i\tau) \neq \psi^\dagger(\mathbf{r}, -i\tau)\,, \tag{2.30}$$

thus to avoid confusion we employ the notation

$$\psi(\mathbf{r}, \tau) = \psi(\mathbf{r}, -i\tau)\,, \quad \psi^\dagger(\mathbf{r}, \tau) = \psi^\dagger(\mathbf{r}, -i\tau)\,. \tag{2.31}$$

Now to evaluate this propagator in the simplest case, we take a translationally invariant system of non-interacting particles. The translational invariance means our Green's function only depends on spatial differences $\mathbf{r} = \mathbf{r}_1 - \mathbf{r}_2$ and we already established that the Green's functions are only dependent on time differences, $\tau = \tau_1 - \tau_2$, therefore we can write our propagator in terms of single arguments,

$$G_0(\mathbf{r}_1, \tau_1; \mathbf{r}_2, \tau_2) \to G_0(\mathbf{r}, \tau)\,. \tag{2.32}$$

Now we can expand the field operators in terms of single particle creation and annihilation operators:

$$\psi(\mathbf{r}_1, \tau_1) = \frac{1}{\sqrt{\mathcal{V}}} \sum_{\mathbf{k}} e^{i\mathbf{k}\cdot\mathbf{r}_1} c_{\mathbf{k}}(\tau_1)\,, \quad \psi^\dagger(\mathbf{r}_2, \tau_2) = \frac{1}{\sqrt{\mathcal{V}}} \sum_{\mathbf{k}'} e^{-i\mathbf{k}'\cdot\mathbf{r}_2} c^\dagger_{\mathbf{k}'}(\tau_2)\,, \tag{2.33}$$

where the operators obey the usual commutation relations $\left[c_{\mathbf{k}},\, c^\dagger_{\mathbf{k}'}\right]_\eta = \delta_{\mathbf{k}\mathbf{k}'}$ and $\mathcal{V}$ is the system volume. Substituting the equations in 2.33 into equation 2.29 yields

$$\begin{aligned} G_0(\mathbf{r}, \tau) &= -\frac{1}{\mathcal{V}} \sum_{\mathbf{k}} e^{i\mathbf{k}\cdot\mathbf{r}} \left\langle \mathcal{T}_\tau c_{\mathbf{k}}(\tau) c^\dagger_{\mathbf{k}}(0) \right\rangle = \frac{1}{\mathcal{V}} \sum_{\mathbf{k}} e^{i\mathbf{k}\cdot\mathbf{r}} G(\mathbf{k}, \tau) \\ \Rightarrow G_0(\mathbf{k}, \tau) &= -\left\langle \mathcal{T}_\tau c_{\mathbf{k}}(\tau) c^\dagger_{\mathbf{k}}(0) \right\rangle\,. \end{aligned} \tag{2.34}$$

The system of non-interacting particles can be described by the Hamiltonian

$$H_0 = \sum_{\mathbf{k}} \xi_{\mathbf{k}} c^\dagger_{\mathbf{k}} c_{\mathbf{k}} \,, \tag{2.35}$$

where ξ_k is the energy of a particle of momentum, $\mathbf{k}$. By making use of the commutation relations it can be shown for this Hamiltonian that

$$\begin{aligned} c_{\mathbf{k}}(\tau) &= e^{H_0\tau} c_{\mathbf{k}} e^{-H_0\tau} = c_{\mathbf{k}} e^{-\xi_{\mathbf{k}}\tau} \,, \\ \Rightarrow G_0(\mathbf{k},\tau) &= -\left\langle \mathcal{T}_\tau c_{\mathbf{k}} e^{-\xi_{\mathbf{k}}\tau} c^\dagger_{\mathbf{k}} \right\rangle \\ &= \left[-\left\langle c_{\mathbf{k}} c^\dagger_{\mathbf{k}} \right\rangle \Theta(\tau) + \eta \left\langle c^\dagger_{\mathbf{k}} c_{\mathbf{k}} \right\rangle \Theta(-\tau) \right] e^{-\xi_{\mathbf{k}}\tau} \,. \end{aligned} \tag{2.36}$$

Now we wish to Fourier transform this to Matsubara frequencies, but this must be performed separately for the bosonic and fermionic cases because of both the η factor, as well as because of the differing occupation factors given by $\left\langle c^\dagger_{\mathbf{k}} c_{\mathbf{k}} \right\rangle = b(\xi_{\mathbf{k}})$, $f(\xi_{\mathbf{k}})$ for the bosonic and fermionic cases respectively. Thus, for the fermionic case we have that

$$\begin{aligned} G_0(\mathbf{k},\tau) &= [-(1-f(\xi_{\mathbf{k}}))\Theta(\tau) + f(\xi_{\mathbf{k}})\Theta(-\tau)] e^{-\xi_{\mathbf{k}}\tau} \\ \therefore G_0^F(\mathbf{k}, i\varepsilon_l) &= -(1-f(\xi_{\mathbf{k}})) \int_0^\beta \mathrm{d}\tau \, e^{(i\varepsilon_l - \xi_{\mathbf{k}})\tau} \\ &= -(1-f(\xi_{\mathbf{k}})) \frac{e^{(i\varepsilon_l - \xi_{\mathbf{k}})\beta} - 1}{i\varepsilon_l - \xi_{\mathbf{k}}} = \frac{1}{i\varepsilon_l - \xi_{\mathbf{k}}} \end{aligned} \tag{2.37}$$

One can follow a similar process for the bosonic case [66] and it so happens that the functional form is identical, save for the bosonic Matsubara frequencies , thus in total we have

$$G_0^B(\mathbf{k}, i\omega_l) = \frac{1}{i\omega_l - \xi_{\mathbf{k}}} \quad \text{and} \quad G_0^F(\mathbf{k}, i\varepsilon_l) = \frac{1}{i\varepsilon_l - \xi_{\mathbf{k}}} \,. \tag{2.38}$$

By comparing this back to our definition for the spectral function, given by equation 2.26, we can immediately deduce that the spectral function must be given by a simple delta

function,

$$\mathcal{A}(x) = \delta(x - \xi_{\mathbf{k}})\,. \tag{2.39}$$

which makes the analytic continuation from the imaginary time Green's functions to the retarded and advanced Green's functions trivial, by simply replacing $i\omega_l, i\varepsilon_l \mapsto \omega + i\delta$ and $i\omega_l, i\varepsilon_l \mapsto \omega - i\delta$ respectively,

$$G_0^{R,A} = \frac{1}{\omega - \xi_{\mathbf{k}} \pm i\delta}\,. \tag{2.40}$$

Now that we have obtained the form of the most basic objects that will make up our framework we can use them as the zeroth order term in a perturbation expansion to construct Green's functions that describe more complex Hamiltonians. The first case we will examine the addition of a one-body interaction to the non-interacting Hamiltonian.

2.4 Perturbation Theory for a One-body Potential

Now we will consider the addition of a single particle potential, $U(\mathbf{r}, \tau)$, to the free particle Hamiltonian, H_0, given in equation 2.35. If this interaction is sufficiently weak we can treat this interaction as a perturbation on H_0. We define temperature Green's functions for this similarly to the Schrödinger equation, as in equation 2.6:

$$\left[\frac{\partial}{\partial\tau_1} + h_0(\mathbf{r}_1) + U(\mathbf{r}_1, \tau_1)\right] G(\mathbf{r}_1, \tau_1; \mathbf{r}_2, \tau_2) = -\delta(\mathbf{r}_1 - \mathbf{r}_2)\delta(\tau_1 - \tau_2) \tag{2.41a}$$

$$\text{and} \quad \left[\frac{\partial}{\partial\tau_1} + h_0(\mathbf{r}_1)\right] G_0(\mathbf{r}_1, \tau_1; \mathbf{r}_2, \tau_2) = -\delta(\mathbf{r}_1 - \mathbf{r}_2)\delta(\tau_1 - \tau_2)\,, \tag{2.41b}$$

$$\text{where} \quad h_0(\mathbf{r}) = -\frac{1}{2m}\boldsymbol{\nabla}_{\mathbf{r}}^2 - \mu\,.$$

Subject to the usual periodicity condition

$$G(\mathbf{r}_1, \tau_1 + \beta; \mathbf{r}_2, \tau_2) = -\eta G(\mathbf{r}_1, \tau_1; \mathbf{r}_2, \tau_2). \tag{2.42}$$

From now we will compactify our notation to 4-positions, $(1) = (\mathbf{r}_1, \tau_1)$, such that

$$\begin{aligned} &G(1,2) = G(\mathbf{r}_1, \tau_1; \mathbf{r}_2, \tau_2) \quad \text{and} \quad \delta(1,2) = \delta(\mathbf{r}_1 - \mathbf{r}_2)\delta(\tau_1 - \tau_2)\,, \\ &\Rightarrow \left[\frac{\partial}{\partial \tau_1} + h_0(1) + U(1)\right] G(1,2) = -\delta(1,2) \qquad (2.43a) \\ &\quad \text{and} \quad \left[\frac{\partial}{\partial \tau_1} + h_0(1)\right] G_0(1,2) = -\delta(1,2)\,. \qquad (2.43b) \end{aligned}$$

From the equations in 2.43 we can find an integral equation

$$\begin{aligned} G(1,2) &= G_0(1,2) + \int \mathrm{d}1'\, G_0(1,1')U(1')G(1',2)\,, \qquad (2.44) \\ \text{where} \quad \int \mathrm{d}1' &= \int_0^\beta \mathrm{d}\tau_1' \int_{\mathcal{V}} \mathrm{d}\mathbf{r}_1'\,. \end{aligned}$$

By equating powers of U a recursion formula can be found,

$$\begin{aligned} G(1,2) &= \sum_{n=0}^{\infty} G_n(1,2)\,, \qquad (2.45) \\ \text{with} \quad G_{n+1} &= \int \mathrm{d}n'\, G_0(1,n')U(n')G_n(n',2)\,. \end{aligned}$$

This can be expressed as an infinite series expansion of G_0 in powers of U,

$$\begin{aligned} G(1,2) = G_0(1,2) &+ \int \mathrm{d}1'\, G_0(1,1')U(1')G_0(1',2) \\ &+ \int \mathrm{d}1'\,\mathrm{d}2'\, G_0(1,1')U(1')G_0(1',2')U(2')G_0(2',2) \qquad (2.46) \\ &+ \int \mathrm{d}1'\,\mathrm{d}2'\,\mathrm{d}3'\, G_0(1,1')U(1')G_0(1',2')U(2')G_0(2',3')U(3')G_0(3',2) + ... \end{aligned}$$

We can represent this expansion diagrammatically (figure 2.2), remembering that G_0 represents the propagation of a particle from (2) to (1), thus we represent this as a line directed from (2) to (1). The full perturbed GF, G, is represented as a thick line. The 4-positions that appear in the G are called the external vertices. Interactions with the one body potential occur at internal vertices (dashed 4-positions in the above equations) and

these are integrated over to take into account all possible positions and times at which this interaction can occur. We represent these interactions as crosses in the diagrams.

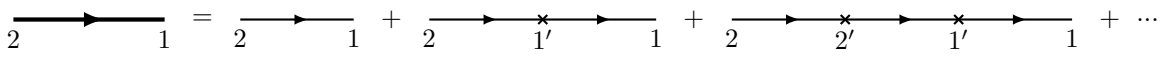

Figure 2.2: The diagrammatic representation of the perturbation expansion for the Green's function of a particle in a one-body external potential. The thick line is the full GF, the thins lines are the single particle GFs in the absence of the potential and the crosses are interactions with the one-body potential.

2.5 Perturbation Theory for a Two-body Potential

Now we will extend our treatment in the previous section further to consider the addition of a two body interaction potential term to the Hamiltonian:

$$\begin{aligned} H(\tau) &= H_0(\tau) + H_{\text{int}}\,, \\ \text{where} \quad H_0(\tau) &= \int \mathrm{d}\mathbf{r}\, \psi^\dagger(\mathbf{r}) h(\mathbf{r},\tau)\psi(\mathbf{r})\,, \\ \text{with} \quad h(\mathbf{r},\tau) &= -\frac{1}{2m}\boldsymbol{\nabla}^2_{\mathbf{r}} - \mu + U(\mathbf{r},\tau) \\ \text{and} \quad H_{\text{int}}(\tau) &= \frac{1}{2}\int \mathrm{d}\mathbf{r}\,\mathrm{d}\mathbf{r}'\,\mathrm{d}\tau'\, \psi^\dagger(\mathbf{r})\psi^\dagger(\mathbf{r}')V(\mathbf{r}-\mathbf{r}')\delta(\tau-\tau')\psi(\mathbf{r}')\psi(\mathbf{r})\,. \end{aligned} \tag{2.47}$$

So now our new 'unperturbed' Hamiltonian contains the one-body interaction and so the corresponding zeroth order Green's function we will do the two-body perturbation with carries the information about the one-body potential already. This a prime example of the 'building blocks' approach we can take using diagrammatic QTF, where if a Green's function is known we can use it as the effective G_0 in a further perturbation regime. Note that the delta function in the interaction term means we are considering an instantaneous interaction. Diagrammatically we represent the two body interaction as a dashed line connecting the 4-positions $(1')$ and $(2')$, that we know must be at the same τ due to the delta function.

Now that we have two body interactions, the particle whose propagation we are consid-

ering can now be affected by the other particles in our many body problem and *visa versa*. But formally the Green's functions are constructed to describe the propagation of the particle with the rest of the many body state restored to its initial state. Diagrammatically this means that we may have interaction lines connecting the main 'backbone' particle propagation to other particle propagators, but these extra sections of propagators cannot have any external vertices (they must be closed loops). Furthermore internal vertices forming sections of the diagram that are completely disconnected from the 'backbone' that connects the eternal vertices (that is that there are no interaction lines connecting the two or more distinct parts) are found to formally cancel in the perturbation expansion. This follows logically realising that disconnected sections of the diagram correspond to background processes that do not interact with the particle propagator we are interested in, so should have no affect on its dynamics.

The full derivation of the diagrammatic expansion of the two body expansion can be summarised in essentially two steps: firstly, the full Green's function is expanded in of the two body interaction, each term including a many-particle Green's function of the unperturbed system; secondly, Wick's theorem is used to express the many-particle Green's function in terms of single particle Green's functions that we know. Then each of the terms of the expansion can be expressed in terms of Feynman diagrams by establishing a set of conventions, or Feynman rules, for what each element of the diagram corresponds to in terms of the integral equations. Here we will omit the details of the proof as these are quite tedious and can be found in a number of standard texts (see [67, 66, 68, 56]); instead, we will simply summarise the Feynman rules as per Rickayzen's convention [56].

If we remove the time dependence from the one-body potential, $U(\mathbf{r}, \tau) \to U(\mathbf{r})$ then our Hamiltonian has spatial and temporal invariance and we can easily Fourier transform from $G(1, 2)$ to $G(\mathbf{k}, \varepsilon)$, so that we can construct our Feynman rules in terms of momenta and energies (or equivalently frequencies as $\hbar = 1$). For the n^{th} order contribution to $G(\mathbf{k}, \varepsilon)$ one must draw all topologically distinct connected diagrams that:

(i) Each contain two external vertices 1 and 2.

(ii) Each contain $2n$ internal vertices.

(iii) All internal vertices are connected in pairs by dashed interaction lines.

(iv) Solid electron lines are drawn with exactly one entering and exiting each internal vertex, one exiting external vertex 2 and one entering external vertex 1.

Then the Feynman rules are:

(i) Assign a momentum $\mathbf{k}$ and energy ε to the particle lines entering and exiting the diagram.

(ii) Assign a momentum $\mathbf{k}_i$ and energy ε_i to each internal particle line such that energy and momentum are conserved at each vertex.

(iii) Introduce a factor $G_0(\mathbf{k}_i, \varepsilon_i)$ for each line carrying the respective energy and momentum labels.

(iv) Introduce a factor $-V(\mathbf{k}_i)$ for each dashed interaction line.

(v) Sum over all n arbitrary internal energies ε_i and sum or integrate over all internal momenta $\mathbf{k}_i$.

(vi) Introduce a factor T for each internal energy and a factor $\mathcal{V}^{-n}$ for each discrete internal momentum or $(2\pi)^{-3n}$ if the momenta are continuous.

(vii) Introduce a factor $(-\eta)$ for each closed particle loop for spinless particles or (-2η) for spin-1/2 Fermions.

2.6 Single Particle Green's Function with Disorder

For real systems we will want to include the effect of disorder/impurities on our electron propagators. Take a model where all the impurities are alike, such that we can construct

a one-body potential

$$U(\mathbf{r}) = \sum_{i=1}^{N_\alpha} u(\mathbf{r} - \mathbf{R}_i)\,, \tag{2.48}$$

where $u(\mathbf{r} - \mathbf{R}_i)$ is the potential due to an impurity located at $\mathbf{R}_i$ and the number of impurities is N_α. Thus we can employ the same iterative solution to the integral equations as in section 2.4 (equation 2.46). But at the level of measurements made on a macroscopic scale, such as the conductivity, the impurity distribution appears homogeneous. Therefore, we need not be concerned with a particular distribution of impurities, but rather a average over possible distributions. This corresponds to considering the ensemble average of the Green's function,

$$\langle G(1,2)\rangle_{\text{ens}}\ , \tag{2.49}$$

and because G_0 is independent of the impurities, this amounts to calculating the ensemble averages of the impurities distributions at each order in U,

$$\langle U(1')\rangle_{\text{ens}}\ , \quad \langle U(1')U(2')\rangle_{\text{ens}}\ , \quad \langle U(1')U(2')U(3')\rangle_{\text{ens}}\ , \quad \text{etc.}\,. \tag{2.50}$$

If one can assume that the distribution of impurities is independent and random, which tends to be a reasonable assumption for a low concentration of impurities, then one finds that $\langle G(1,2)\rangle_{\text{ens}}$ can be represented by a diagrammatic expansion as in figure 2.3. Where the thick line is $\langle G(1,2)\rangle_{\text{ens}}$, the thin lines are the bare electron propagators G_0, the crosses represent an impurity at position $\mathbf{R}_i$ and the dotted lines are the interaction between the electron and the impurity. The contributions from averages to only first order in U, i.e. $\langle U\rangle_{\text{ens}}$, only amount to a constant shift in energy level and no dynamical effects, so these have been absorbed into the chemical potential without loss of generality.

A Dyson equation can be formed from this infinite set of diagrams by identifying a 'self-energy' part, Σ, that contains the complete set of interactions with impurities that

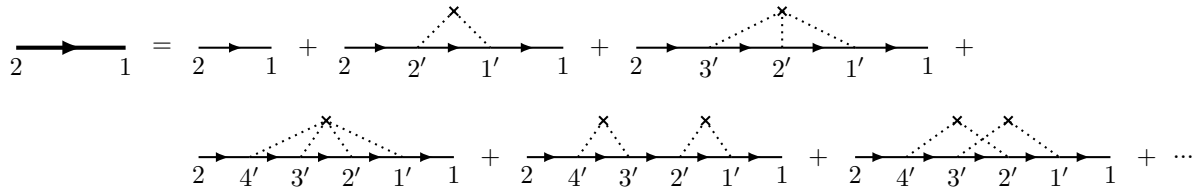

Figure 2.3: The beginning of the full diagrammatic series for the impurity averaged Green's function. The bold arrow is the full Green's function including all terms in the perturbation expansion, the thin arrows are the unpurturbed clean Green's function and the dotted lines are the interaction with the impurity, represented by the cross.

cannot be separated by breaking a single electron line to form two simpler diagrams. Because the ensemble averaging automatically ensures translational invariance we can Fourier transform to momentum and energy so we have

$$\langle G(\mathbf{k}, i\varepsilon)\rangle_{\text{ens}} = \left[G_0^{-1}(\mathbf{k}, i\varepsilon) - \Sigma^{-1}(\mathbf{k}, i\varepsilon)\right]^{-1}; \tag{2.51}$$

note that from here we will drop the integer subscript from the Matsubara frequencies and the inclusion of the i in the argument will imply we are working with Matsubara frequencies. The simplest approximation that can be taken is to take the self energy part to be as shown in figure 2.4; known as the first Born approximation. This is useful in the case where the scattering by the impurities in very weak, because we have chosen to neglect terms including three or more scatterings with the same impurity, which intuitively will be suppressed when scattering is highly improbable. Less intuitively though it also discards all contributions that include any crossing or nesting of impurity scatterings. This can be justified because it can be shown that contributions of these types carry a

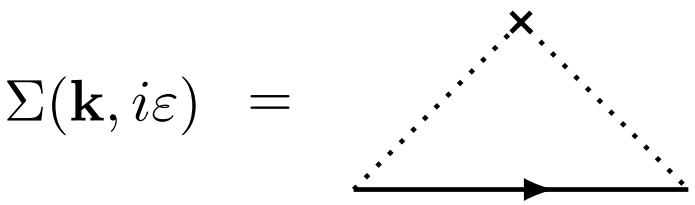

Figure 2.4: The self energy part in the First born approximation, found when considering only the leading contribution at each order in U. The Green's function is the unperturbed G_0.

factor of $(k_F l_0)^{-1}$ compared to the other diagrams at the same order. Then because the impurity scattering is weak the mean free path, l_0, is very large and this factor suppresses the diagrams containing these types of impurity interactions.

The mean free path can be related to the characteristic scattering lifetime, τ_0, by $l_0 = v_F \tau_0$. The scattering lifetime is defined as

$$\frac{1}{\tau_0} = 2\pi N(0) n_{\text{imp}} |U|^2 \,; \tag{2.52}$$

where $N(0)$ is the density of states (DoS) at the Fermi surface per spin, n_{imp} is the number density of impurities and $|U|$ is the strength of the potential. Given this definition of the scattering lifetime it is also the case that the self-energy part as in figure 2.4 is given by

$$\Sigma(\mathbf{k}, i\varepsilon) = \sum_{\mathbf{k}'} G_0(\mathbf{k}', i\varepsilon) \frac{1}{2\pi N(0)\tau_0} = \sum_{\mathbf{k}'} \frac{1}{i\varepsilon - \xi_{\mathbf{k}'}} \frac{1}{2\pi N(0)\tau_0} \,. \tag{2.53}$$

In these two equations we have made the assumption that, because we are considering transport, the only electrons that are relevant are those that are close to the Fermi surface. As a result of this the scattering off the impurity only contributes $(2\pi N(0)\tau_0)^{-1}$ to the self energy part: a factor that is independent of both momentum and energy. Because of this assumption we can change our sum to an integral and extend the limits to infinity, as the integrand will decay sufficiently rapidly away from zero:

$$\Sigma(\mathbf{k}, i\varepsilon) = -\frac{1}{2\pi\tau_0} \int_{-\infty}^{\infty} \mathrm{d}\xi \, \frac{i\varepsilon + \xi}{\varepsilon^2 + \xi^2} \,. \tag{2.54}$$

The second term is odd and so will evaluate to zero and the first term is the standard integral for $\arctan(\varepsilon)$ and therefore when the limits are taken

$$\begin{aligned} \Sigma(\mathbf{k}, i\varepsilon) &= -\frac{i}{2\tau_0} \operatorname{sgn}(\varepsilon) \,, \\ \Rightarrow \langle G(\mathbf{k}, i\varepsilon) \rangle_{\text{ens}} &= \frac{1}{i\varepsilon - \xi_k + \frac{i}{2\tau_0} \operatorname{sgn}(\varepsilon)} \,. \end{aligned} \tag{2.55}$$

As we will be considering the transport properties of disordered systems, this impurity Green's function will be the primarily building block of diagrammatic calculations.

CHAPTER 3

CONDUCTIVITY IN THE NORMAL STATE

In the previous chapter we established the diagrammatic methodology we require to perform calculations within the thesis. Now in this chapter we will put it use for the electronic transport in metals in the normal state. We will use diagrammatic quantum field theory to calculate the classical result of Drude conductivity for electrical conductivity and then the electronic thermal conductivity; in doing so we will have verified the Wiedemann-Franz relation.

In section 3.3, we introduce the primary quantum interference effect of interest: the weak localisation effect. We discuss the physical picture of the effect and how this relates to the maximally-crossed diagrams that are used to calculate the weak localisation correction to conductivity. In section 3.4, we derive the form of the cooperon, which is a diagrammatic object that allows us to encapsulate the behaviour of the infinite set of maximally-crossed diagrams into one term. We then use this in the following section to calculate the weak localisation correction to both electrical and electronic thermal conductivity, and show that the Wiedemann-Franz relation still holds for the corrections. We then end the chapter by examining another diagrammatic object known as the pair propagator, which is related to the superconducting transition and use it to calculate the

transition temperature.

3.1 Drude Conductivity

We wish to show that in the simplest approximation our quantum field theory methods can reproduce the classical result of the Drude conductivity,

$$\sigma = \frac{ne^2\tau_0}{m}\,. \tag{3.1}$$

This will serve as an important proof of concept. Of course, this is using a very powerful and complex method to obtain a relatively simple result, however this result is the baseline against which all the more interesting quantum effects will be compared, so we must be sure that we can successfully reproduce Drude to have any faith in the quantum corrections we will go on to calculate. The structure of this calculation will follow that shown in ref [56].

To do this we consider a disordered metal in the presence of a weak electric field, $\mathbf{E}$, with corresponding vector potential, $\mathbf{A}$, related by

$$\mathbf{E}(\mathbf{r},t) = -\frac{\partial \mathbf{A}(\mathbf{r},t)}{\partial t}\,. \tag{3.2}$$

The Hamiltonian describing this can written as

$$H = \sum_\sigma \int \mathrm{d}^3 r\, \psi^\dagger_\sigma(\mathbf{r}) \left[\frac{(-i\boldsymbol{\nabla} - e\mathbf{A})^2}{2m} + U(\mathbf{r})\right] \psi_\sigma(\mathbf{r})\,, \tag{3.3}$$

to which a current density per spin can be associated (see appendix B):

$$\begin{aligned}
\mathbf{j}_\sigma(\mathbf{r}) &= \mathbf{j}^{\boldsymbol{\nabla}}_\sigma(\mathbf{r}) + \mathbf{j}^{\mathbf{A}}_\sigma(\mathbf{r})\,,\\
\mathbf{j}^{\boldsymbol{\nabla}}_\sigma(\mathbf{r}) &= \frac{ie}{2m}\Big(\psi^\dagger_\sigma(\mathbf{r})\boldsymbol{\nabla}\psi_\sigma(\mathbf{r}) - \boldsymbol{\nabla}\psi^\dagger_\sigma(\mathbf{r})\psi_\sigma(\mathbf{r})\Big)\,,\\
\mathbf{j}^{\mathbf{A}}_\sigma(\mathbf{r}) &= -\frac{e^2}{m}\mathbf{A}(\mathbf{r})\psi^\dagger_\sigma(\mathbf{r})\psi_\sigma(\mathbf{r})\,;
\end{aligned} \tag{3.4}$$

where we have suggestively split the current density operator into two parts: the paramagnetic part, $\mathbf{j}^{\boldsymbol{\nabla}}$, and the diamagnetic part, $\mathbf{j}^{\mathbf{A}}$.

To extract a macroscopic observable such as the conductivity, we must find the macroscopic current density, $\mathbf{J}$, from the current density operator. The macroscopic current does not depend on microscopic details of the system, or in other words it is an averaged quantity, and so can be related to the microscopic operator by

$$\mathbf{J}(\mathbf{r},t) = \sum_{\sigma} \langle \mathbf{j}_{\sigma}(\mathbf{r},t) \rangle_{0,\text{ens}} \,. \tag{3.5}$$

The average here denotes first taking a thermal expectation value with respect to the unperturbed Hamiltonian, H_0, and then taking an ensemble average over all possible impurity distributions. To obtain the leading-order approximation of the conductivity, we will appeal to the linear response of the system to the $\mathbf{A}$-field. The diamagnetic term is already linear in $\mathbf{A}$ so we can immediately average this term, but for the paramagnetic term we must apply Kubo's formula to obtain for the α^{th} component of $\mathbf{J}$ (see appendix A for a derivation of Kubo's formula),

$$\begin{aligned} \mathbf{J}_{\sigma\alpha}(\mathbf{r},t) = \langle \mathbf{j}_{\sigma\alpha}(\mathbf{r},t) \rangle_{0,\text{ens}} = &- \frac{e^2}{m} \mathbf{A}(\mathbf{r},t) \left\langle \psi^{\dagger}_{\sigma}(\mathbf{r}) \psi_{\sigma}(\mathbf{r}) \right\rangle_{0,\text{ens}} \\ &- \int_0^{\infty} \mathrm{d}t' \int_{\mathcal{V}} \mathrm{d}^3 r' \, \mathbf{A}_{\beta}(\mathbf{r}',t') \left\langle G^{R,E}_{\alpha\beta\sigma}(\mathbf{r},t,\mathbf{r}',t') \right\rangle_{\text{ens}} , \end{aligned} \tag{3.6}$$

$$\text{where} \quad G^{R,E}_{\alpha\beta\sigma}(\mathbf{r},t,\mathbf{r}',t') = \left\langle \left[\mathbf{j}^{\boldsymbol{\nabla}}_{\sigma\alpha}(\mathbf{r},t),\, \mathbf{j}^{\boldsymbol{\nabla}}_{\sigma\beta}(\mathbf{r}',t') \right] \right\rangle_0 . \tag{3.7}$$

Note that we are using the summation convention where repeated index, β, is being summed over. The first term can be evaluated immediately because the expectation value, $\left\langle \psi^{\dagger}_{\sigma} \psi_{\sigma} \right\rangle$ simply gives the number density per spin, so

$$\left\langle \mathbf{j}^{\mathbf{A}}_{\sigma\alpha}(\mathbf{r},t) \right\rangle = -\frac{n_{\sigma} e^2}{m} \mathbf{A}_{\beta}(\mathbf{r},t) \delta_{\alpha\beta} \,. \tag{3.8}$$

The second term we have written in terms of the current-current Green's function

$$\left\langle G^{R,E}_{\alpha\beta\sigma}(1,1')\right\rangle_{\text{ens}} = -i\left\langle\left[\mathbf{j}^{\boldsymbol{\nabla}}_{\sigma\alpha}(1),\mathbf{j}^{\boldsymbol{\nabla}}_{\sigma\beta}(1')\right]\right\rangle_{0,\text{ens}}, \tag{3.9}$$

where we have switched to the 4-position notation. Because we are ensemble averaging, translational invariance is ensured, so we can write

$$\left\langle G^{R,E}_{\alpha\beta\sigma}(1,1')\right\rangle_{\text{ens}} = G^{R,E}_{\alpha\beta\sigma}(1-1'), \tag{3.10}$$

where for now we will use the convention that the Green's functions written in terms of differences have had the ensemble average completed. This gives the integral in equation 3.6 the form of a convolution, and hence we can immediately Fourier transform to obtain

$$\left\langle\mathbf{j}^{\boldsymbol{\nabla}}_{\sigma\alpha}(\mathbf{q},\omega)\right\rangle = -\mathbf{A}_{\beta}(\mathbf{q},\omega)G^{R,E}_{\alpha\beta\sigma}(\mathbf{q},\omega). \tag{3.11}$$

Now switch to working with the temperature Green's functions,

$$G^{E}_{\alpha\beta\sigma}(1,1') = -\left\langle\mathcal{T}_{\tau}\,\mathbf{j}^{\boldsymbol{\nabla}}_{\sigma\alpha}(1)\mathbf{j}^{\boldsymbol{\nabla}}_{\sigma\beta}(1')\right\rangle_{0}, \tag{3.12}$$

from which we can extract the retarded Green's function by appropriate analytic continuation. The 4-position labels now contain the imaginary time, so $(1) = (\mathbf{r},\tau)$ and the average, $\langle ...\rangle_0$, denotes a thermal average for a particular impurity distribution. We substitute in for the current operators, but we do so introducing two extra degrees of freedom, 2 and $2'$, such that we can subscript the $\boldsymbol{\nabla}$ operators to indicate which operator they should act on. Then we can later take the limit that $2 \to 1_{-}$ and $2' \to 1'_{-}$ to eliminate the fictitious degrees of freedom whilst preserving correct time ordering. Doing this

we obtain

$$G^E_{\alpha\beta\sigma}(1,1') = \frac{e^2}{4m^2}(\boldsymbol{\nabla}_{2\alpha} - \boldsymbol{\nabla}_{1\alpha})(\boldsymbol{\nabla}_{2'\beta} - \boldsymbol{\nabla}_{1'\beta}) \left\langle \mathcal{T}_\tau \psi^\dagger_\sigma(1)\psi_\sigma(2)\psi^\dagger_\sigma(1')\psi_\sigma(2') \right\rangle_0$$
$$= \frac{e^2}{4m^2}(\boldsymbol{\nabla}_2 - \boldsymbol{\nabla}_1)_\alpha(\boldsymbol{\nabla}_{2'} - \boldsymbol{\nabla}_{1'})_\beta \, G_\sigma(2,2';1,1') \,. \tag{3.13}$$

The Green's function in equation 3.13 is a two-particle Green's function that can be written in terms of the single-particle electron Green's functions in the presence of disorder by making use of Wick's theorem,

$$G_{2,\sigma}(2,2';1,1') = G_\sigma(2,1)G_\sigma(2',1') - G_\sigma(2,1')G_\sigma(2',1) \,. \tag{3.14}$$

Diagrammatically these two terms can be represented as in figure 3.1. The first term turns out to be zero as each single-particle Green's function corresponds to the expectation value of the current density at a point in the absence of an applied field, which is of course zero. We take the ensemble average of the remaining second term, where we will assume that

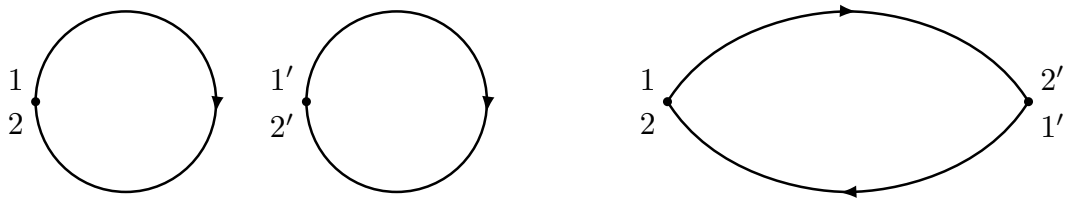

Figure 3.1: The diagrammatic representation of the two terms obtained from the Wick expansion of the two particle Green's function in terms of single particle Green's functions.

the disorder is sufficiently weak such that there will be no interference terms between the two propagators. This means that the average of the product can be treated as the

product of the averages (which is not true in general) i.e.

$$\begin{aligned}\langle G_\sigma(2,2';1,1')\rangle_{\text{ens}} &= -\langle G_\sigma(2,1')G_\sigma(2',1)\rangle_{\text{ens}} \\ &= -\langle G_\sigma(2,1')\rangle_{\text{ens}}\langle G_\sigma(2',1)\rangle_{\text{ens}} \\ &= -G_\sigma(2-1')G_\sigma(2'-1)\,. \end{aligned} \tag{3.15}$$

Now that the Green's functions are the translationally invariant impurity Green's functions that we calculated in section 2, they can be Fourier transformed easily and the limits $2 \to 1$ and $2' \to 1'$ taken to obtain

$$G^E_{\alpha\beta\sigma}(\mathbf{q}, i\omega) = \frac{e^2}{4m^2\mathcal{V}} T\sum_{\mathbf{k},\varepsilon}(2\mathbf{k}+\mathbf{q})_\alpha(2\mathbf{k}+\mathbf{q})_\beta G_\sigma(\mathbf{k}+\mathbf{q}, i\varepsilon+i\omega)G_\sigma(\mathbf{k}, i\varepsilon)\,. \tag{3.16}$$

Thus, by also performing the trivial Fourier transform on the diamagnetic term, we can write the problem in terms of the linear response function, K^E. Note that the problem is also completely spin-independent so we can simply drop the spin factor and introduce a factor of two, this yields:

$$\mathbf{J}_\alpha(\mathbf{q},\omega) = -K^E_{\alpha\beta}(\mathbf{q},\omega)\mathbf{A}_\beta(\mathbf{q},\omega) = \frac{K^E_{\alpha\beta}(\mathbf{q},\omega)\mathbf{E}_\beta(\mathbf{q},\omega)}{-i\omega} = \sigma_{\alpha\beta}(\mathbf{q},\omega)\mathbf{E}_\beta(\mathbf{q},\omega)\,, \tag{3.17}$$

$$\text{with} \quad K^E_{\alpha\beta}(\mathbf{q},\omega) = G^{R,E}_{\alpha\beta}(\mathbf{q},\omega) + \frac{ne^2}{m}\delta_{\alpha\beta}\,. \tag{3.18}$$

From this set of equations we see that if we evaluate the temperature Green's function in equation 3.16, and analytically continue it to real frequencies, then we can read off the conductivity tensor, $\sigma_{\alpha\beta}(\mathbf{q},\omega)$.

Substituting in the the impurity averaged Green's functions given in equation 2.55 leads to

$$\begin{aligned}G^E_{\alpha\beta}(\mathbf{q}, i\omega) = \frac{2e^2T}{4m^2\mathcal{V}}\sum_{\mathbf{k}\varepsilon}&(2\mathbf{k}+\mathbf{q})_\alpha(2\mathbf{k}+\mathbf{q})_\beta \\ &\times \frac{1}{i\varepsilon + i\omega - \xi_{k+q} + \frac{i}{2\tau_0}\operatorname{sgn}(\varepsilon+\omega)}\frac{1}{i\varepsilon - \xi_k + \frac{i}{2\tau_0}\operatorname{sgn}(\varepsilon)}\,. \end{aligned} \tag{3.19}$$

For most cases of interest the wavelength of the applied field will be much longer than the Fermi-wavelength, or in terms of momenta $|\mathbf{q}| \ll |\mathbf{k}|$. In particular for a uniform applied field, $\mathbf{q} = 0$. In this regime only electrons close to the Fermi surface will be involved in the transport, so we can approximate $|\mathbf{k}| \approx k_F$. This can also be interpreted the Green's functions being peaked around the Fermi-surface with a width proportional to $\mathbf{q}$. This allows the Green's function to be simplified to

$$\begin{aligned} G^E_{\alpha\beta}(\mathbf{q}, i\omega) =& \frac{2e^2 N(0) T}{m^2} \int \frac{d\Omega}{4\pi} \mathbf{k}_{\mathrm{F}\alpha} \mathbf{k}_{\mathrm{F}\beta} \int_{-\infty}^{\infty} d\xi_k \\ & \times \sum_{\varepsilon} \frac{1}{i\varepsilon - \xi_k + \frac{i}{2\tau_0}\mathrm{sgn}(\varepsilon)} \frac{1}{i\varepsilon + i\omega - \xi_k - \mu_\theta + \frac{i}{2\tau_0}\mathrm{sgn}(\varepsilon + \omega)} \,. \end{aligned} \tag{3.20}$$

We have converted the sum over momentum to an integral over the kinetic energy, ξ_k, and surface integral over $\mathrm{d}\Omega = \mathrm{d}\theta \mathrm{d}\phi \sin\theta$; this introduces a factor of the density of states at the Fermi surface, $N(0)$. The factor $\mu_\theta = \mathbf{v}_F \cdot \mathbf{q} = v_F q \cos\theta$ is the first-order term in $\mathbf{q}$ from ξ_{k+q}. Note that the summation over frequency and integration over energy are purposefully ordered, and one must in general be careful for divergence issues when exchanging the order. This calculation is an instance where the logarithmic divergence of the integral does not allow for a trivial interchanging of the order. However, we show in appendix C that careful treatment of this simply leads to a term that exactly cancels the contribution from the diamagnetic part. So here we will make the ansatz that we can simply exchange the order without issue and this will cancel the diamagnetic part, and so we obtain

$$\begin{aligned} K^E_{\alpha\beta}(\mathbf{q}, i\omega) =& \frac{2e^2 N(0) T}{m^2} \int \frac{d\Omega}{4\pi} \mathbf{k}_{\mathrm{F}\alpha} \mathbf{k}_{\mathrm{F}\beta} \\ & \times \sum_{\varepsilon} \int_{-\infty}^{\infty} d\xi \, \frac{1}{\xi - i\varepsilon - \frac{i}{2\tau_0}\mathrm{sgn}(\varepsilon)} \frac{1}{\xi + \mu_\theta - i\varepsilon - i\omega - \frac{i}{2\tau_0}\mathrm{sgn}(\varepsilon + \omega)} \,. \end{aligned} \tag{3.21}$$

We compute the integral over $d\xi$ using a contour integral, but it will only be non-zero if the two poles are in opposite half planes. We can without loss of generality choose $\varepsilon < 0$ and $\varepsilon + \omega > 0$ (we will obtain exactly the same result choosing the other way around), to

give

$$\begin{aligned} K^E_{\alpha\beta}(\mathbf{q}, i\omega) =& \frac{2e^2N(0)T}{m^2}\int\frac{d\Omega}{4\pi}\mathbf{k}_{\mathrm{F}\alpha}\mathbf{k}_{\mathrm{F}\beta} \\ & \times\sum_\varepsilon\int_{-\infty}^{\infty}d\xi\,\frac{1}{\xi - i\varepsilon + \frac{i}{2\tau_0}}\frac{1}{\xi + \mu_\theta - i\varepsilon - i\omega - \frac{i}{2\tau_0}}\,\Theta(-\varepsilon)\Theta(\varepsilon+\omega) \\ =& \frac{2e^2N(0)T}{m^2}\int\frac{d\Omega}{4\pi}\mathbf{k}_{\mathrm{F}\alpha}\mathbf{k}_{\mathrm{F}\beta} \\ & \times\sum_\varepsilon\oint_\Gamma dz\,\frac{1}{z - i\varepsilon + \frac{i}{2\tau_0}}\frac{1}{z + \mu_\theta - i\varepsilon - i\omega - \frac{i}{2\tau_0}}\,\Theta(-\varepsilon)\Theta(\varepsilon+\omega)\,. \end{aligned} \tag{3.22}$$

The contour Γ closes in the upper half plane, and hence we pick up the residue at $z = i\varepsilon + i\omega - \mu_\theta + \frac{i}{2\tau_0}$ yielding

$$K^E_{\alpha\beta}(\mathbf{q}, i\omega) = \frac{2e^2N(0)T}{m^2}\int\frac{d\Omega}{4\pi}\mathbf{k}_{\mathrm{F}\alpha}\mathbf{k}_{\mathrm{F}\beta}\sum_\varepsilon\frac{2\pi i}{i\omega - \mu_\theta + \frac{i}{\tau_0}}\,\Theta(-\varepsilon)\Theta(\varepsilon+\omega)\,. \tag{3.23}$$

Now the term inside the sum over ε has no ε-dependence, so only the Θ-functions determine the value of the sum, therefore we can use the result

$$T\sum_\varepsilon\Theta(-\varepsilon)\Theta(\varepsilon+\omega) = \frac{\omega}{2\pi}\,, \tag{3.24}$$

to find

$$K^E_{\alpha\beta}(\mathbf{q}, i\omega) = \frac{2e^2N(0)}{m^2}\int\frac{d\Omega}{4\pi}\mathbf{k}_{\mathrm{F}\alpha}\mathbf{k}_{\mathrm{F}\beta}\frac{\omega\tau_0}{1 + \omega\tau_0 + i\mu_\theta\tau_0}\,. \tag{3.25}$$

The Drude conductivity is obtained when the electric field is static and uniform, there we only require the Fourier components with $\mathbf{q} = 0$ and $\omega = 0$. So set $\mathbf{q} = 0$ now to yield

$$K^E_{\alpha\beta}(0, i\omega) = \frac{2e^2N(0)}{m^2}\frac{k_F^2}{3}\delta_{\alpha\beta}\frac{\omega\tau_0}{1+\omega\tau_0} = \frac{ne^2\tau_0}{m}\frac{\omega}{1+\omega\tau_0}\delta_{\alpha\beta}\,. \tag{3.26}$$

Now we can analytically continue from Matsubara frequencies to real frequencies by taking

$i\omega \to \omega$ and then set $\omega = 0$ and $\alpha = \beta$ to obtain the d.c. conductivity:

$$K^E_{\alpha\beta}(0,\omega) = \frac{ne^2\tau_0}{m}\frac{-i\omega}{1-i\omega\tau_0}\delta_{\alpha\beta}\,, \tag{3.27a}$$

$$\therefore \sigma_{\alpha\beta}(\omega) = \frac{ne^2\tau_0}{m}\frac{1}{1-i\omega\tau_0}\delta_{\alpha\beta}\,, \tag{3.27b}$$

$$\sigma_{\text{Drude}} = \sigma_{\alpha\alpha}(0) = \frac{ne^2\tau_0}{m}\,. \tag{3.27c}$$

We have therefore successfully reproduced the classical Drude conductivity result using diagrammatic field theory techniques.

3.2 Thermal Conductivity of Electron Transport

For the calculation of the thermal conductivity the process is similar to that of the electrical conductivity, except that the Green's function that the Kubo formula yields is now the heat current-heat current Green's function,

$$G^T_{\alpha\beta\sigma}(1,1') = -\left\langle \mathcal{T}_\tau\, \mathbf{j}^T_{\sigma\alpha}(1)\mathbf{j}^T_{\sigma\beta}(1')\right\rangle_0\,. \tag{3.28}$$

The derivation of this is not as simple as that of the electrical conductivity, where it is possible to write a Hamiltonian describing the applied electrical field. Whereas, we cannot write a Hamiltonian for the application of a thermal gradient, as it is a statistical property of the system. However, Luttinger [32] demonstrated that one could circumvent this issue by instead studying a Hamiltonian with a field, analogous to a gravitational field, along with Einstein relations to find the thermal transport coefficients. The appropriate form for the heat-current operator to use in the Green's function is

$$\mathbf{j}^T_\sigma(1) = -\frac{i}{2m}\Big(\partial_\tau\psi^\dagger_\sigma(1)\boldsymbol{\nabla}\psi_\sigma(1) + \boldsymbol{\nabla}\psi^\dagger_\sigma(1)\partial_\tau\psi_\sigma(1)\Big)\,, \tag{3.29}$$

where ∂_τ is the partial derivative with respect to imaginary time, which is the form found in ref [30]. In general, one must be careful to ensure that the heat-current operator is

appropriate choice for the system in question, however, we can simply use the Wiedemann-Franz relation to confirm that our heat-current operator is the correct choice (further discussion of the construction of the heat-current operator can be found in refs [31, 69]).

We can extract the differential operators in the heat current - heat current Green's function in the same way as in equation 3.13, leading to

$$G^T_{\alpha\beta\sigma}(1,1') = \frac{1}{4m^2}(\partial_{\tau 1}\boldsymbol{\nabla}_2 + \partial_{\tau 2}\boldsymbol{\nabla}_1)_\alpha(\partial_{\tau 1'}\boldsymbol{\nabla}_{2'} + \partial_{\tau 2'}\boldsymbol{\nabla}_{1'})_\beta G_\sigma(2,2';1,1')\,. \tag{3.30}$$

The principal difference in this case is that when the temporal Fourier transform takes place, the time derivatives will bring down factors of the Matsubara frequencies, yielding

$$\begin{aligned} G^T_{\alpha\beta\sigma}(\mathbf{q},i\omega) = -\frac{2T}{4m^2\mathcal{V}}\sum_{\mathbf{k}\varepsilon}\big(\varepsilon(\mathbf{k}+\mathbf{q}) + (\varepsilon+\omega)\mathbf{k}\big)_\alpha\big(\varepsilon(\mathbf{k}+\mathbf{q}) + (\varepsilon+\omega)\mathbf{k}\big)_\beta \\ \times G_\sigma(\mathbf{k}+\mathbf{q}, i\varepsilon + i\omega)G_\sigma(\mathbf{k}, i\varepsilon)\,. \end{aligned} \tag{3.31}$$

Once again the linear response function is obtained by simply inverting the order of the momentum and frequency sums and is related to the thermal conductivity, κ, by the relation

$$T\kappa_{\alpha\beta}(\mathbf{q},\omega) = \frac{K^T_{\alpha\beta}(\mathbf{q},\omega)}{-i\omega} \tag{3.32}$$

Making use of the assumption $|\mathbf{q}| \ll |\mathbf{k}|$, and gaining a factor of 2 for each spin, we can therefore write

$$\begin{aligned} K^T_{\alpha\beta}(\mathbf{q},i\omega) = &-\frac{2N(0)T}{m^2}\int\frac{\mathrm{d}\Omega}{4\pi}\mathbf{k}_{\mathrm{F}\alpha}\mathbf{k}_{\mathrm{F}\beta}\sum_\varepsilon\left(\varepsilon+\frac{\omega}{2}\right)^2 \\ &\times\int_{-\infty}^{\infty}d\xi\,\frac{1}{\xi - i\varepsilon - \frac{i}{2\tau_0}\mathrm{sgn}(\varepsilon)}\frac{1}{\xi+\mu_\theta - i\varepsilon - i\omega - \frac{i}{2\tau_0}\mathrm{sgn}(\varepsilon+\omega)}\,. \end{aligned} \tag{3.33}$$

This calculation is then identical to that of the electrical conductivity until the sum over

Matsubara frequencies, where instead we have

$$K^T_{\alpha\beta}(\mathbf{q}, i\omega) = -\frac{2N(0)}{m^2}\int \frac{d\Omega}{4\pi}\mathbf{k}_{\mathrm{F}\alpha}\mathbf{k}_{\mathrm{F}\beta}\frac{2\pi\tau_0}{1+\omega\tau_0+i\mu_\theta\tau_0} \times T\sum_{\varepsilon}\left(\varepsilon+\frac{\omega}{2}\right)^2\Theta(-\varepsilon)\Theta(\varepsilon+\omega)\,. \tag{3.34}$$

The Matsubara sum can be reformulated using $\varepsilon = 2\pi T\big(l-\frac{1}{2}\big)$ and $\omega = 2\pi T m$, and because the Θ-functions limit the sum to $-\omega < \varepsilon < 0$ we also transform $\varepsilon \to -\varepsilon$, which leads to

$$\begin{aligned} S(i\omega) &= T\sum_{\varepsilon}\left(\varepsilon+\frac{\omega}{2}\right)^2\Theta(-\varepsilon(\varepsilon+\omega)) \\ &= T(2\pi T)^2\sum_{l=1}^{m}\left(l^2-(m+1)l+\frac{1}{4}(m+1)^2\right). \end{aligned} \tag{3.35}$$

To solve the sum use the following standard results

$$\sum_{l=1}^{m} l^2 = \frac{m(m+1)(2m+1)}{6} \tag{3.36a}$$

$$\sum_{l=1}^{m} l = \frac{m(m+1)}{2} \tag{3.36b}$$

$$\sum_{l=1}^{m} 1 = m\,. \tag{3.36c}$$

After simplifying and substituting back for the Matsubara frequency we get

$$\begin{aligned} S(i\omega) &= T(2\pi T)^2\frac{m(m^2-1)}{12} \\ &= \frac{(2\pi T)^2}{12}\frac{\omega}{2\pi}\left(\frac{\omega^2}{(2\pi T)^2}-1\right). \end{aligned} \tag{3.37}$$

Now substituting this back into the linear response function and setting $\mathbf{q} = 0$ we obtain

$$\begin{aligned} K^T_{\alpha\beta}(0, i\omega) &= -\frac{2N(0)k_F^2}{3m^2}\delta_{\alpha\beta}\frac{\pi^2T^2}{3}\frac{\omega\tau_0}{1+\omega\tau_0}\left(\frac{\omega^2}{(2\pi T)^2} - 1\right) \\ &= \frac{n\tau_0}{m}\frac{\pi^2T^2}{3}\frac{\omega}{1+\omega\tau_0}\left(1 - \frac{\omega^2}{(2\pi T)^2}\right)\delta_{\alpha\beta}\,. \end{aligned} \tag{3.38}$$

For thermal conductivity we will only be concerned with the 'd.c.' result corresponding to $\omega = 0$. Hence, we can discard the term cubic in ω as we will be taking the limit $\omega \to 0$ anyway. At this stage we can also analytically continue $i\omega \to \omega + i\delta$ to obtain the retarded linear response function,

$$\therefore K^T_{\alpha\beta}(0, \omega) = \frac{n\tau_0}{m}\frac{\pi^2T^2}{3}\frac{-i\omega}{1-i\omega\tau_0}\delta_{\alpha\beta}\,. \tag{3.39}$$

Finally, from this we can obtain the thermal conductivity using equation 3.32,

$$T\kappa = \frac{\pi^2T^2}{3}\frac{n\tau_0}{m}\,. \tag{3.40}$$

To be reassured that this method for finding the thermal conductivity is valid we can confirm our result is consistent with the Wiedemann-Franz law [3] which states that for electron gases at sufficiently high temperatures (such that other quantum effects do not interfere) the ratio of the thermal and electrical conductivity is given by

$$\frac{T\kappa}{\sigma} = \frac{\pi^2T^2}{3e^2}\,. \tag{3.41}$$

Or if we restore the Boltzmann factor it can also be written as

$$\frac{\kappa}{T\sigma} = \frac{\pi^2k_{\mathrm{B}}^2}{3e^2} = L\,, \tag{3.42}$$

where L is the Lorenz factor. Clearly our calculation satisfies this relation so we can be satisfied that our choice of heat-current operator is appropriate. The inclusion of

time derivatives in the operator will mean that we will always get an additional factor proportional to a Matsubara frequency on the vertex in thermal calculations compared to electrical.

3.3 Quantum Interference Effects and Weak localisation

The major advantage of calculating the conductivity using diagrammatic field theory techniques is the ease at which interference effects can be included. In this section we will expand upon the Drude calculation by including the weak localisation correction to the conductivity.

In the Drude calculation the only impurity scattering terms included are those that scatter off the same impurity and interference between scattering off different impurities are not included. This is a good approximation at higher temperatures because the phase coherence lifetime, τ_ϕ, is small in comparison the the impurity scattering lifetime, τ_0. This means that as the electron propagates its quantum mechanical phase is scrambled, or 'dephased', on average in between each impurity scattering event. So any coherent scattering is averaged out and hence interference effects can be neglected. However as the temperature is lowered the phase coherence lifetime, or equivalently the phase coherence length l_ϕ, will increase and when $\tau_\phi > \tau_0$ scattering on different impurities can interfere [66]. When the coherence length is such that it is comparable to the system size, L, we enter the so called mesoscopic regime where all manner of quantum effects become important.

We will be interested in the case where the sample is sufficiently large so that $l_0 \ll l_\phi \ll L$, this is because we can still ensemble average in this regime which eliminates most of the interference effects. The important class of diagrams that survive the ensemble averaging are the maximally-crossed diagrams that correspond to weak localisation [38, 41].

We can see why this is the case by examining the problem from the more physical

perspective of the paths the electrons take through the metal as they conduct. We will follow the interpretation of Altshuler and Aronov [45] and consider the probability of a particle travelling from point A to point B,

$$P(A \to B) = \left| \sum_i A_i \right|^2 = \sum_i |A_i|^2 + \sum_{i \neq j} A_i A_j^* \,, \tag{3.43}$$

where A_i is the probability amplitude for the particle travelling along the i^{th} path. The first term is simply the sum of all the probabilities of travelling down each path and the second term comes from the interference between the different paths. The averaging over impurity positions will mean that most pairs of paths will have negligible interference, because the averaging usually destroys any coherence between the paths. The class of paths where the interference survives the averaging are depicted in the lowest path in figure 3.2: the so-called self-intersecting paths.

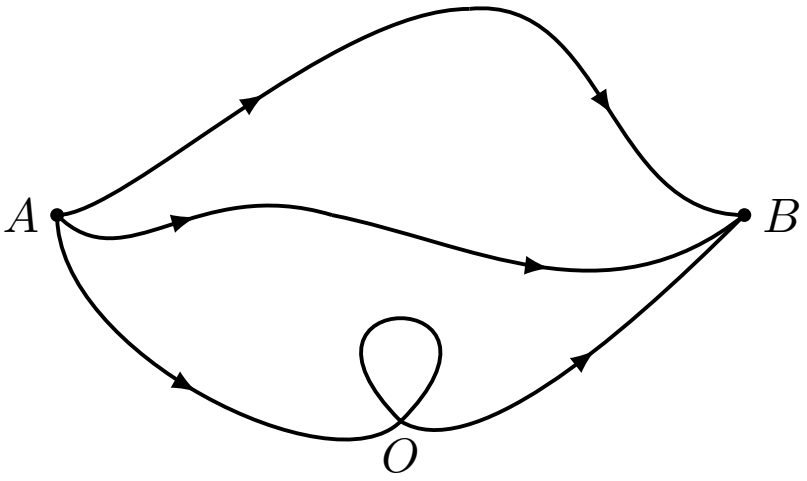

Figure 3.2: A visual representation of a few possible paths through a space an particle could take when propagating from point A to point B. The bottom path shows a self-intersecting path, where the particle passes through the point O twice. Paths of this type lead to a increased probability of remaining at point O, hence leading to a decrease in conductivity.

The path in the figure actually depicts two possible paths: the particle first travels from A to O; then it can travel around the loop in either the clockwise or anticlockwise direction (which we will label as A_1 and A_2 respectively); then it continues on from O to

B. For the particle to have travelled around the same loop but in the opposite direction, it must have scattered off the same impurities but in the opposite order [66]. Therefore, the two paths will have picked up the same phase as they travelled around the loop, meaning their relative phase is always zero and hence they will constructively interfere. Then the probability of finding the particle at O is given by

$$|A_1|^2 + |A_2|^2 + 2\,\mathrm{Re}[A_1 A_2^*] = 4|A_1|^2\,, \tag{3.44}$$

which is a factor 2 larger than if there was no coherence and we could ignore the interference term. This means that for self-interesting paths there is a higher probability of remaining at the point O and thereby a lower probability of reaching point B, thus leading to a reduction in the conductivity. This is the origin of the name 'weak localisation'.

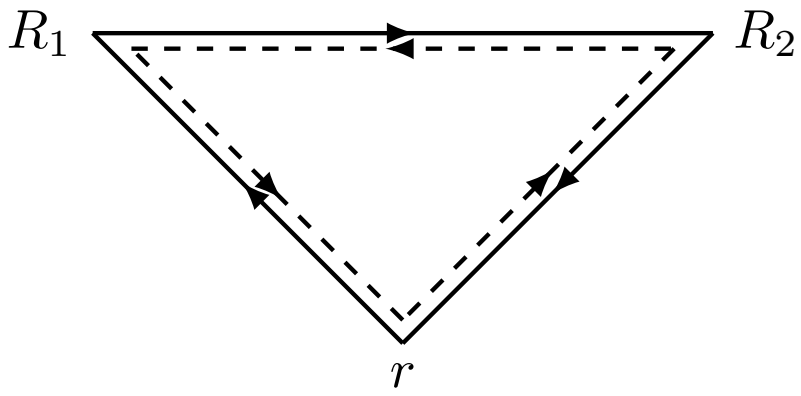

Figure 3.3: A representation of two time-reversed paths that an electron could take when travelling from point r and scattering off two impurities, before returning to r. One path propagates to R_1 first, the R_2, and visa versa. If the propagators in between each impurity are identical, up to their direction, the two paths will constructively interfere.

To demonstrate why the maximally-crossed diagrams correspond to these self intersecting paths, we will examine the simplest case where two such time reversed paths can be constructed, following the discussion in Bruus and Flensburg [66]. Suppose we have two impurities, as shown in figure 3.3. One path scatters off the impurity at position R_1 first, then off the impurity at R_2 then returns to the starting point r and the other path scatters first off R_2 and then off R_1. The probability amplitudes of these two paths can

be related to Green's functions by

$$A_1 \propto \lim_{r' \to r} \left[G_0^R(r, R_1, \varepsilon) U G_0^R(R_1, R_2, \varepsilon) U G_0^R(R_2, r', \varepsilon) \right]$$
$$A_2 \propto \lim_{r' \to r} \left[G_0^R(r, R_2, \varepsilon) U G_0^R(R_2, R_1, \varepsilon) U G_0^R(R_1, r', \varepsilon) \right], \tag{3.45}$$

where we assume that the impurity interaction is short-ranged, so the one-body potential is given by

$$U(r) = \sum_i U \delta(r - R_i)\,. \tag{3.46}$$

Since the Green's function is time-translationally invariant, we have taken the temporal Fourier transformation. Now the quantum correction due to this interference is given by

$$\mathrm{Re}[A_1 A_2^*] \propto \lim_{r' \to r} \mathrm{Re} \Big[G_0^R(r, R_1, \varepsilon) U G_0^R(R_1, R_2, \varepsilon) U G_0^R(R_2, r', \varepsilon) \times \left(G^R(r, R_2, \varepsilon) U G^R(R_2, R_1, \varepsilon) U G^R(R_1, r', \varepsilon) \right)^* \Big] \tag{3.47}$$

and after ensemble averaging over the impurity positions we can take the spatial Fourier transform to obtain

$$\langle \delta P(O) \rangle_{\mathrm{ens}} \propto \mathrm{Re} \frac{1}{\mathcal{V}^4} \sum_{k_1 k_2 k_3 q} G_0^R(q - k_1, \varepsilon) U G_0^R(q - k_2, \varepsilon) U G_0^R(q - k_3, \varepsilon) \times G_0^A(k_1, \varepsilon) U G_0^A(k_2, \varepsilon) U G_0^A(k_3, \varepsilon)\,. \tag{3.48}$$

This is can be represented diagrammatically as the first diagram in figure 3.4. It is straightforward to see how this process can be repeated for increasing numbers of impurities leading to diagrams such as the second and third in the figure. Therefore, to calculate the weak localisation correction to the conductivity, we must sum up the infinite class of such diagrams, restoring the appropriate factors and sums in analogy with the Drude calculation that would arise from Kubo formula.

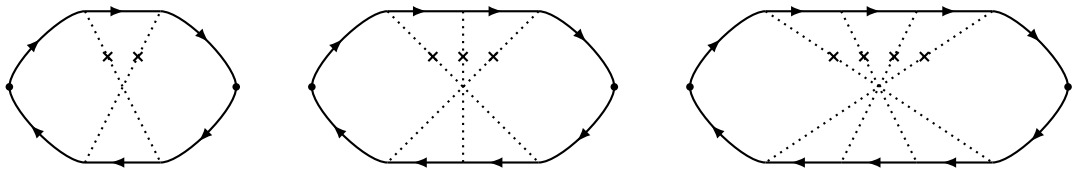

Figure 3.4: The first three diagrams in the series of maximally crossed diagrams that arise when considering the self intersecting paths that give rise to the weak localisation correction to conductivity. The upper Green's functions are retarded, the lower are advanced and the the upper and lower Green's functions scatter off the same local impurities, represented by the crosses, in a time reversed order.

3.4 Calculation of the Cooperon

Since we need to sum an infinite series of diagrams, it is appropriate to construct a Dyson equation. The way to approach this for the maximally crossed diagrams is to realise that we can construct a ladder of impurities by twisting the diagram around as in figure 3.5. We can then take the ladder sum and compute it in isolation. This infinite impurity ladder is shown in figure 3.6 and is known as the cooperon. It can be represented in terms the Dyson equation form in the lower line of the figure to give

$$\begin{aligned} \Gamma_{\mathrm{C}}(\mathbf{q}, i\varepsilon, i\varepsilon + i\omega) &= \Gamma_0 + \Gamma_0 \Sigma_{\mathrm{C}}(\mathbf{q}, i\varepsilon, i\varepsilon + i\omega)\Gamma_{\mathrm{C}}(\mathbf{q}, i\varepsilon, i\varepsilon + i\omega) \qquad (3.49) \\ \text{with} \quad \Gamma_0 &= \frac{1}{2\pi N(0)\tau_0} \\ \text{and} \quad \Sigma_{\mathrm{C}}(\mathbf{q}, i\varepsilon, i\varepsilon + i\omega) &= \sum_{\mathbf{k}} G(\mathbf{q}-\mathbf{k}, i\varepsilon + i\omega) G(\mathbf{k}, i\varepsilon)\,. \end{aligned}$$

Calculating the cooperon is therefore reduced to calculating the self-energy part, Σ_{C}, and then simply substituting it and the impurity line contribution, Γ_0 back into the Dyson equation. Using the impurity Green's function given in equation 2.55, we have

$$\begin{aligned} \Sigma_{\mathrm{C}}(\mathbf{q}, i\varepsilon, i\varepsilon + i\omega) =& \sum_{\mathbf{k}} \frac{1}{i\varepsilon + i\omega - \xi_{q-k} + \frac{i}{2\tau_0}\mathrm{sgn}(\varepsilon+\omega)} \frac{1}{i\varepsilon - \xi_k + \frac{i}{2\tau_0}\mathrm{sgn}(\varepsilon)} \qquad (3.50) \\ =& N(0) \int \frac{d\Omega}{4\pi} \int_{-\infty}^{\infty} d\xi \, \frac{1}{\xi - \mu_\theta - i\varepsilon - i\omega - \frac{i}{2\tau_0}\mathrm{sgn}(\varepsilon+\omega)} \frac{1}{\xi - i\varepsilon - \frac{i}{2\tau_0}\mathrm{sgn}(\varepsilon)}\,, \end{aligned}$$

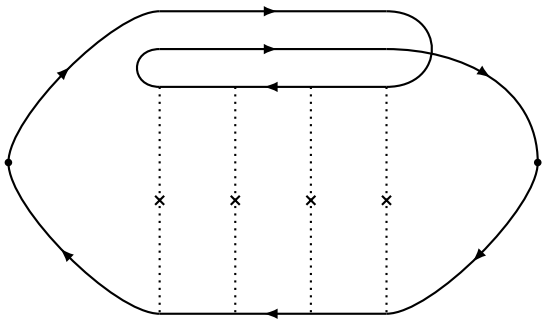

Figure 3.5: An example of a maximally crossed diagram where the propagator lines have been twisted, so the impurity lines are displayed a a 'ladder' of impurity interaction lines in a particle-particle or hole-hole channel.

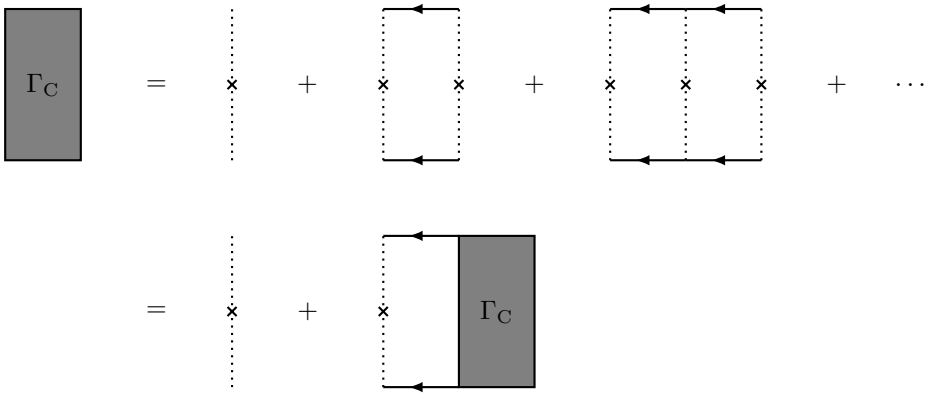

Figure 3.6: The upper line in the figure displays the first first terms in infinite series of the cooperon. The lower line displays the infinite sum as a Dyson equation.

where we are in the diffusive limit, $|\mathbf{q}| \ll l_0^{-1}$, along with once again being primarily interested in long wavelength applied fields and so $|q| \ll |k| \sim k_F$. The integral over dξ can be completed using a contour integral, choosing $\omega > 0$, which yields

$$\Sigma_{\mathrm{C}}(\mathbf{q}, i\varepsilon, i\varepsilon + i\omega) = 2\pi N(0)\tau_0 \int \frac{d\Omega}{4\pi} \frac{1}{1 + \omega\tau_0 - i\mu_\theta \tau_0} \, \Theta(-\varepsilon(\varepsilon + \omega)) \,. \tag{3.51}$$

Using the fact that we are in the diffusive limit, which implies the limits $\omega\tau_0 \ll 1$ and $ql_0 \ll 1$, we can expand out the denominator to leading order

$$\Sigma_{\mathrm{C}}(\mathbf{q}, i\varepsilon, i\varepsilon + i\omega) \approx 2\pi N(0)\tau_0 \int \frac{d\Omega}{4\pi} \Big(1 - \omega\tau_0 + i\mathbf{v}_F \cdot \mathbf{q}\tau_0 - (\mathbf{v}_F \cdot \mathbf{q}\tau_0)^2\Big) \,. \tag{3.52}$$

When the angular integration is completed, the first order term $\mathbf{v}_F \cdot \mathbf{q}$ will average to zero, hence why the leading order term in ql is quadratic. This leads to

$$\Sigma_{\mathrm{C}}(\mathbf{q}, i\varepsilon, i\varepsilon + i\omega) = 2\pi N(0)\tau_0\big(1 - (Dq^2 + \omega)\tau_0\big)\,, \tag{3.53}$$

where $D = \frac{v_F^2 \tau_0}{d}$ is the diffusion constant. Substituting equation 3.53 back into the Dyson equation, we obtain

$$\Gamma_{\mathrm{C}}(\mathbf{q}, i\varepsilon, i\varepsilon + i\omega) = \frac{\Gamma_0}{1 - \Gamma_0\Sigma_{\mathrm{D}}} = \frac{1}{2\pi N(0)\tau_0^2}\frac{1}{Dq^2 + \omega} \quad \text{for} \quad \omega > 0\,. \tag{3.54}$$

If we were to take the poles to have opposite signs, i.e. $\varepsilon > 0$ and $\varepsilon + \omega < 0$ and hence $\omega < 0$, we get the same result apart from the sign of ω:

$$\Gamma_{\mathrm{C}}(\mathbf{q}, i\varepsilon, i\varepsilon + i\omega) = \frac{1}{2\pi N(0)\tau_0^2}\frac{1}{Dq^2 - \omega} \quad \text{for} \quad \omega < 0\,. \tag{3.55}$$

Hence we can combine the two regimes like so

$$\Gamma_{\mathrm{C}}(\mathbf{q}, i\varepsilon, i\varepsilon + i\omega) = \frac{1}{2\pi N(0)\tau_0^2}\frac{1}{Dq^2 + |\omega|}\,\Theta(-\varepsilon(\varepsilon + \omega))\,. \tag{3.56}$$

One can see that that the cooperon has a pole at $q \to 0$, $\omega \to 0$ and though this does not pose a problem for the form of the cooperon in isolation, when we use it to calculate weak localisation effects we will be integrating over $\mathrm{d}\mathbf{q}$ and so this causes divergence issues unless the pole is cut off. The cooperon describes phase coherence between paths, so fortunately it is naturally cutoff by the phase coherence length l_ϕ, Remembering that at length scales above this the phase is scrambled and there is no reduction in conductivity. We could introduce this cutoff by changing the lower limit of the $\mathrm{d}q$ integral to $q = l_\phi^{-1}$, but more conveniently it is equivalent to leave the lower limit and introduce into the

denominator the phase breaking rate, τ_ϕ^{-1},

$$\Gamma_{\rm C}(\mathbf{q},,i\varepsilon,i\varepsilon+i\omega)=\frac{1}{2\pi N(0)\tau_0^2}\frac{1}{Dq^2+|\omega|+\tau_\phi^{-1}}\Theta(-\varepsilon(\varepsilon+\omega))\,. \tag{3.57}$$

3.5 Weak Localisation Correction to Electrical and Thermal Conductivity

3.5.1 Correction to Electrical Conductivity

To calculate the weak localisation correction to conductivity we can set up a bubble diagram including the cooperon, which includes all the maximally crossed diagrams up to infinite order; this diagram is shown in figure 3.7. We will start by calculating the correction to electrical conductivity, where, by following the same diagrammatic construction we used for the Drude calculation, we can write the linear response function as

$$K_{\alpha\beta}^{\rm WL,E}(0,i\omega)=\frac{2T}{\mathcal{V}^2}\sum_{\varepsilon}\sum_{\mathbf{kq}}\Big(\frac{e\mathbf{k}}{m}\Big)_\alpha\Big(\frac{e(\mathbf{q}-\mathbf{k})}{m}\Big)_\beta G(\mathbf{k},i\varepsilon+i\omega)G(\mathbf{q}-\mathbf{k},i\varepsilon+i\omega)$$
$$\times G(\mathbf{q}-\mathbf{k},i\epsilon)G(\mathbf{k},i\varepsilon)\frac{\Theta(-\varepsilon(\varepsilon+\omega))}{2\pi N(0)\tau_0^2(Dq^2+|\omega|+\tau_\phi^{-1})}\,. \tag{3.58}$$

We have the external momentum set to zero here, so this corresponds to the application of a uniform field. The inclusion of the cooperon in the weak localisation bubble implies that this calculation must also be in the diffusive limit and hence we can take $|\mathbf{q}|\ll|\mathbf{k}|\sim k_F$. Thus, we can replace the Green's functions with argument $(\mathbf{q}-\mathbf{k})$ with $G(\mathbf{k})$, also using the fact that the Green's function is even in $\mathbf{k}$. This simplifies the linear repose function to

$$K_{\alpha\beta}^{\rm WL,E}(0,i\omega)=-\frac{2e^2T}{m^2\mathcal{V}^2}\sum_{\varepsilon}\sum_{\mathbf{kq}}\mathbf{k}_{F\alpha}\mathbf{k}_{F\alpha}G(\mathbf{k},i\varepsilon+i\omega)^2G(\mathbf{k},i\epsilon)^2$$
$$\times\frac{\Theta(-\varepsilon(\varepsilon+\omega))}{2\pi N(0)\tau_0^2(Dq^2+|\omega|+\tau_\phi^{-1})}\,. \tag{3.59}$$

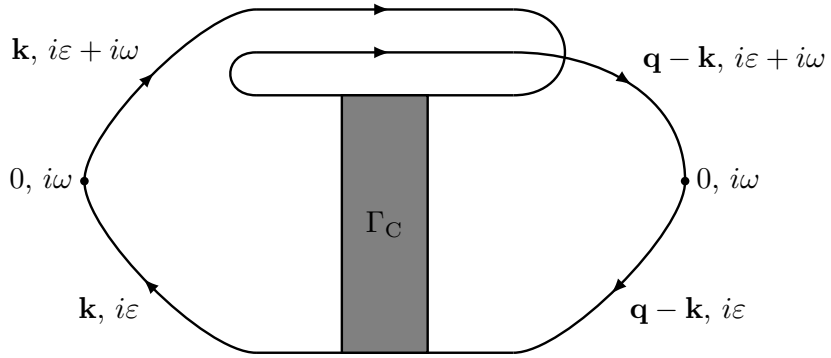

Figure 3.7: A diagrammatic representation of the weak localisation correction to the Drude conductivity.

Unlike the Drude calculation, there are no divergence issues to be concerned with, because we have three sums but four Green's functions, and so we can interchange the order of integrations/sums freely. So starting with the integral over $\mathbf{k}$, assuming isotropy so the angular dependence of the vertex parts can be approximated to simply $\frac{k_F}{d}$, where d is the dimensionality of the system. The cooperon part is only dependent on q and ε so the integral over $\mathbf{k}$ only contains the Green's functions and can be computed from the standard formula in the diffusive limit,

$$\sum_{\mathbf{k}} G^+(\mathbf{k}, i\omega_1)^n G^-(\mathbf{k}, i\omega_2)^m = 2\pi N(0)\tau_0 \frac{(m+n-2)!}{(m-1)!(n-1)!}(-i\tau_0)^{n-1}(i\tau_0)^{m-1}\,, \tag{3.60}$$

where $\omega_1 > 0$ and $\omega_2 < 0$ (see appendix D for a full derivation of this result). So in this case with $n, m = 2$ we are left with

$$K^{\mathrm{WL},E}_{\alpha\beta}(0, i\omega) = -\frac{2e^2 k_F^2 \delta_{\alpha\beta}}{m^2 d}\frac{T}{\mathcal{V}}\sum_{\varepsilon}\Theta(-\varepsilon(\varepsilon+\omega))\sum_{\mathbf{q}}\frac{4\pi N(0)\tau_0^3}{2\pi N(0)\tau_0^2(Dq^2 + |\omega| + \tau_\phi^{-1})}\,. \tag{3.61}$$

Next we can complete the sum over ε trivially and simplify the pre-factor to get

$$K^{\mathrm{WL},E}_{\alpha\beta}(0, i\omega) = -4e^2 D\delta_{\alpha\beta}\frac{\omega}{2\pi}\frac{1}{\mathcal{V}}\sum_{\mathbf{q}}\frac{1}{Dq^2 + |\omega| + \tau_\phi^{-1}}\,. \tag{3.62}$$

We then follow the same steps as in the Drude calculation to obtain the d.c. conductivity

from the linear response function: analytically continue $i\omega \to \omega + i\delta$; divide by $-i\omega$; set $\omega \to 0$; take the diagonal component. After doing all of this we are left with

$$\sigma^{\mathrm{WL}} = -\frac{2e^2 D}{\pi} \frac{1}{\mathcal{V}} \sum_{\mathbf{q}} \frac{1}{Dq^2 + \tau_\phi^{-1}} \,. \tag{3.63}$$

We can write this sum as an integral in d-dimensions, like so,

$$\sigma^{\mathrm{WL}} = -\frac{2e^2 D}{\pi} \int \frac{\mathrm{d}^d q}{(2\pi)^d} \frac{1}{Dq^2 + \tau_\phi^{-1}} \,. \tag{3.64}$$

Remembering that for the cooperon calculation to be valid we made the assumption that $ql_0 \ll 1$, meaning we must cutoff the upper limit of the q integral at l_0^{-1}. Hence, we have

$$\sigma^{\mathrm{WL}} = -\frac{e^2}{\pi}\sqrt{D\tau_\phi} \qquad \text{when} \quad d = 1 \,, \tag{3.65a}$$

$$\sigma^{\mathrm{WL}} = -\frac{e^2}{2\pi^2} \ln\left(\frac{\tau_\phi}{\tau_0}\right) \qquad \text{when} \quad d = 2 \,, \tag{3.65b}$$

$$\text{and} \quad \sigma^{\mathrm{WL}} = -\frac{e^2}{\pi^3\sqrt{D\tau_0}} + \frac{e^2}{2\pi^2\sqrt{D\tau_\phi}} \qquad \text{when} \quad d = 3 \,, \tag{3.65c}$$

where we have used $\tau_\phi \gg \tau_0$, recalling that we need phase coherence to persist over many collisions with the static impurities to have this effect. We can also write the correction in terms of scattering lengths,

$$\sigma^{\mathrm{WL}} = -\frac{e^2}{\pi} l_\phi \qquad \text{when} \quad d = 1 \,, \tag{3.66a}$$

$$\sigma^{\mathrm{WL}} = -\frac{e^2}{\pi^2} \ln\left(\frac{l_\phi}{l_0}\right) \qquad \text{when} \quad d = 2 \,, \tag{3.66b}$$

$$\text{and} \quad \sigma^{\mathrm{WL}} = -\frac{e^2}{\pi^3 l_0} + \frac{e^2}{2\pi^2 l_\phi} \qquad \text{when} \quad d = 3 \,. \tag{3.66c}$$

3.5.2 The Phase Coherence Lifetime

Typically the phase coherence lifetime is dependent on temperature as an inverse power law, $\tau_\phi \propto T^{-p}$ [66]. Therefore, it is a increasing function with decreasing temperature. In the two-dimensional case this means we have a logarithmic correction to the conductivity

(both electrical and thermal) that decreases the conductivity as temperature is decreased, regardless of the exact value of p. We are most interested in the two-dimensional case because it typically has a much larger correction than in three-dimensions. The logarithmic dependence is also helpful for detecting the effect in experiments, because it is distinct from the power law behaviour from the leading order parts of the conductivity.

To understand why the weak localisation effect in three dimensions is much smaller than in two dimensions, we recall the picture of self-intersecting paths. The paths the electron takes as it propagates, colliding with impurities, can be interpreted as a random walk [45]. In a random walk, the ratio of paths that self intersect to the set of all possible paths in decreases with increasing dimensions dimensions. This not difficulty to reason intuitively, because the higher the dimension, at any given point in the path there are more possible directions the particle could travel, and hence a lower probability of travelling back to a point it has already been.

This argument is most easily interpreted in one-dimensional systems. In this case any back-scattering at all will immediately lead to a self intersection, as the electron can only travel back exactly the way it came. So in one dimension, weak localisation effects can become very large even with weak disorder. In fact, it can be shown that a particle in a one-dimensional random potential is always localised [66]. Conversely, in three dimensions we may have to introduce a lot of disorder to be able to generate appreciable weak localisation effects.

Recall that in all of this discussion, we have included τ_ϕ as a phenomenological parameter, understanding that we need a cut-off for the $1/Dq^2$ in the cooperon. We discussed some of the sources of phase breaking in section 1.3 but we will reiterate them here. Mechanisms that cause phase breaking can either be inelastic processes or time-reversal symmetry breaking processes. The primary inelastic process at low temperatures is electron-electron interactions. Fukuyama and Abrahams calculated the electron-electron phase

breaking rate [44] to have a temperature dependence of

$$\tau_\phi^{-1} \propto T \ln(T)\,. \tag{3.67}$$

It is important to mention that the application of magnetic field is a time-reversal symmetry breaking mechanism, because of its importance in identifying weak localisation effects in experiments. However, in this context it not so much a used as a cut-off to the correction, instead magnetic fields strong enough to completely destroy the effect are applied in order to generate magneto-resistance curves. The other phase breaking mechanism of this type we will be interested in is magnetic impurities. In this case the phase coherence between paths is destroyed when the electron interacts with the magnetic impurity because it scrambles its spin state. When magnetic impurities are the dominant phase breaking mechanism, i.e. $\tau_\phi \sim \tau_s$. where τ_s is the characteristic scattering time with magnetic impurities, we must therefore have $\tau_s >> \tau_0$. This means the concentration of magnetic impurities must be much less than the concentration of non-magnetic impurities to be in the correct regime for weak localisation. If $\tau_s \sim \tau_0$ we weak localisation effect will be destroyed as the spin will be scrambled on average in between scattering events with the non-magnetic impurities. Magnetic impurities, like non-magnetic, are a static effect and we would not expect them to have any temperature dependence.

3.5.3 Correction to Thermal Conductivity

When comparing the Drude electrical and thermal conductivity we confirmed the Wiedemann Franz relationship using microscopic theory, so it is a natural continuation to ask where this 'law' breaks down. It was shown by Chester and Thellung [70] in a very general sense, using the method of exact-eigenstates, that for a system of non interacting electrons involving only elastic scattering that the Wiedemann-Franz law should always hold. The weak localisation effect satisfies this criterion, discussed explicitly by Kearney and Butcher [71], so we expect the relation to hold. To calculate the weak localisation

correction to thermal conductivity via a microscopic means we need only change the contribution from the vertex in the same way as we did for the Drude conductivity. This means that the linear response function we have to compute will instead be

$$K_{\alpha\beta}^{\mathrm{WL},T}(0,i\omega) = -\frac{2T}{m^2\mathcal{V}^2}\sum_{\varepsilon}\sum_{\mathbf{kq}}\mathbf{k}_{F\alpha}\mathbf{k}_{F\beta}\Big(i\varepsilon+\frac{i\omega}{2}\Big)^2 G(\mathbf{k},i\varepsilon+i\omega)^2 G(\mathbf{k},i\epsilon)^2 \times \frac{\Theta(-\varepsilon(\varepsilon+\omega))}{2\pi N(0)\tau_0^2(Dq^2+|\omega|+\tau_\phi^{-1})}\,. \tag{3.68}$$

Simplifying this down we are left with

$$K_{\alpha\beta}^{\mathrm{WL},T}(0,i\omega) = 4D\delta_{\alpha\beta}\frac{T}{\mathcal{V}}\sum_{\varepsilon}\Big(\varepsilon+\frac{\omega}{2}\Big)^2\Theta(-\varepsilon(\varepsilon+\omega))\sum_{\mathbf{q}}\frac{1}{Dq^2+|\omega|+\tau_\phi^{-1}}\,. \tag{3.69}$$

So note the only difference between this and the electrical case is the form of the sum and a factor of e^2. The sum we have already completed in equation 3.37 and so one easily verifies that the Wiedemann-Franz law holds for the weak localisation corrections to electrical conductivity and thermal conductivity, and so they will simply be related by the Lorenz factor,

$$T\kappa^{\mathrm{WL}} = \frac{\pi^2T^2}{3e^2}\sigma^{\mathrm{WL}}\,. \tag{3.70}$$

In a way that is more useful for our methodology, we can say generally that if the thermal conductivity and electrical conductivity calculations differ only by a factor of $(\varepsilon+\omega/2)^2$ in the sum over Matsubara frequencies, then the Wiedemann-Franz law should hold. However, as we will be moving on to superconducting systems shortly, this will be the last time that this condition will be satisfied moving forward.

3.6 The Transition to the Superconducting State

The next quantum effect we consider is related to the transition from the normal state to the superconducting state. We consider the BCS theory of superconductivity that states that below the critical temperature, T_c, due to an effective phonon-mediated attractive potential, it is energetically favourable for electrons of opposite spin and momenta to pair up into bosonic quasi-particles called cooper pairs. These cooper pairs then form a condensate that is able to carry and electrical current without dissipation, a super-current, leading to a massive increase in the conductivity, or equivalently a nearly zero resistance. The form of the phonon potential is assumed to be featureless and constant, V, and only active within a shell of width $\pm\omega_{\mathrm{D}}$ around the Fermi surface, where ω_{D} is the Debye frequency: a typical phonon energy.

In the next chapter we will address how to deal with the superconducting state with diagrammatic field theory. Here we will examine the instability in the normal state as the superconducting state is approached from above the transition temperature. A transition to the superconducting state that involved the condensate instantaneously forming at T_c with zero Cooper-pairs present above T_c, would lead to the resistance dropping to zero as a step function at the transition; this is know as a a first-order transition. However, the decrease in resistance is observed to be a smooth curve with a finite width: a second-order transition. This is due to superconducting fluctuations above T_c, where finite-lifetime cooper pairs are formed, temporarily creating a superconducting channel. Intuitively one would expect this to increase conductivity and as T_c is approached the lifetime of these fluctuations will increase, leading to the smooth second-order transition one expects.

We will not be going into the detail of calculating the contribution of superconducting fluctuations to conductivity above T_c, that were calculated in a trio of papers by Aslamazov and Larkin, Maki and Thompson [35, 36, 37]. We can however, relatively easily reproduce some important results about the superconducting state, such as the critical temperature, by calculating the pair propagator that appears in the diagrams for superconducting fluctuations.

The pair propagator is an infinite ladder sum, similar to the cooperon, that physically corresponds to the finite-lifetime virtual cooper pair channel. In the case of a 'clean' superconductor with no impurities, the ladder consists of the BCS interaction between particle-particle or hole-hole pairs, shown in figure 3.8, as opposed to the impurity lines in the case of the cooperon. We will begin with calculating the clean pair propagator, $L_0(\mathbf{q}, i\omega)$, before moving to the full pair propagator including impurities, $L(\mathbf{q}, i\omega)$.

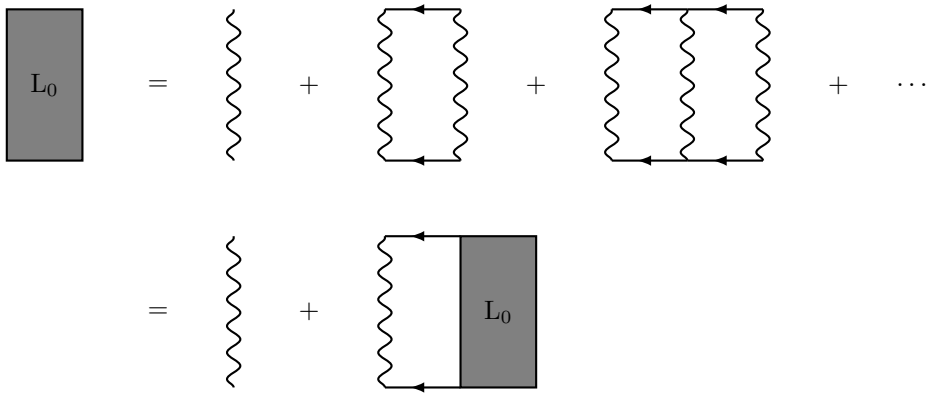

Figure 3.8: Diagrammatic representation of the infinite summation series for the pair propagator in a clean superconductor and in the lower line the corresponding Dyson equation.

As usual we can construct the Dyson equation for the infinite sum like so

$$L_0^{-1}(\mathbf{q}, i\omega) = V^{-1} - \Sigma_{L_0}(\mathbf{q}, i\omega)\,, \tag{3.71}$$

where the wavy line corresponds to the featureless BCS interaction, given by the constant V. As we are considering a clean superconductor the self-energy part will consist of clean Green's functions with opposite sign of momenta, remembering that cooper pairs are formed of electrons with opposite momenta and spin:

$$\begin{aligned}\Sigma_{L_0}(\mathbf{q}, i\omega) &= \frac{T}{\mathcal{V}} \sum_{\varepsilon} \sum_{\mathbf{k}} G_0(\mathbf{k}+\mathbf{q}, i\varepsilon + i\omega) G_0(-\mathbf{k}, -i\varepsilon) \\ &= T \sum_{\varepsilon} N(0) \int \frac{d\Omega}{4\pi} \int_{-\infty}^{\infty} d\xi_k \, \frac{1}{\xi_{k+q} - i\varepsilon - i\omega} \, \frac{1}{\xi_k + i\varepsilon}\,. \end{aligned} \tag{3.72}$$

First, we will restrict ourselves to the case where $\omega > 0$. We can solve the integral using

a contour, which will only be non-zero if the poles are in opposite half planes, leading to contributions from $\varepsilon > 0$ and $\varepsilon < -\omega$:

$$\Sigma_{L_0}(\mathbf{q}, i\omega) = N(0)T\left(\sum_{\varepsilon>0} + \sum_{\varepsilon<\omega}\right)\int \frac{d\Omega}{4\pi}\oint \mathrm{d}z\, \frac{1}{z+\mu_\theta - i\varepsilon - i\omega}\,\frac{1}{z+i\varepsilon} \tag{3.73}$$

By making the substitution $\varepsilon \mapsto -\varepsilon - \omega$ in the latter contribution and taking the residues, we have

$$\Sigma_{L_0}(\mathbf{q}, i\omega) = 2\pi N(0)T\sum_{\varepsilon>0}\int \frac{d\Omega}{4\pi}\left(\frac{1}{2\varepsilon+\omega-\mu_\theta} + \frac{1}{2\varepsilon+\omega+\mu_\theta}\right) \tag{3.74}$$

The denominator can then be expanded in the same way as equation 3.52 and the angular integral average away the linear term in μ_θ, leaving only the quadratic term. Hence, the two contributions are in fact equal, just leading to a factor of two, yielding

$$\Sigma_{L_0}(\mathbf{q}, i\omega) = 4\pi N(0)T\sum_{\varepsilon>0}\left(\frac{1}{2\varepsilon+\omega} - \frac{v_F^2 q^2}{3(2\varepsilon+\omega)^3}\right) \quad \text{for} \quad \omega > 0\,. \tag{3.75}$$

If one was to repeat for $\omega < 0$, we simply find the sign of ω is switched and hence we can combine the two regimes, like so

$$\Sigma_{L_0}(\mathbf{q}, i\omega) = 4\pi N(0)T\sum_{\varepsilon>0}\left(\frac{1}{2\varepsilon+|\omega|} - \frac{v_F^2 q^2}{3(2\varepsilon+|\omega|)^3}\right) \quad \text{for} \quad \omega > 0\,. \tag{3.76}$$

To evaluate the first term an upper cutoff must be introduced to avoid the logarithmic divergence that corresponds to the region of validity of the BCS interaction, $\varepsilon \sim \omega_D$:

$$4\pi N(0)T\sum_{\varepsilon>0}\frac{1}{2\varepsilon+|\omega|} = N(0)\sum_{l=0}^{\frac{\omega_D}{2\pi T}}\frac{1}{l+\frac{1}{2}+\frac{|\omega|}{4\pi T}}\,. \tag{3.77}$$

Sums of this form may be calculated using the difference equation of the digamma function,

$$\sum_{k=0}^{N} \frac{1}{k+a} = \psi(N+a+1) - \psi(a) \tag{3.78}$$

$$\Rightarrow N(0) \sum_{l=0}^{\frac{\omega_D}{2\pi T}} \frac{1}{l + \frac{1}{2} + \frac{|\omega|}{4\pi T}} = N(0)\left(\psi\Big(\frac{\omega_D}{2\pi T} + \frac{|\omega|}{4\pi T} + \frac{3}{2}\Big) - \psi\Big(\frac{|\omega|}{4\pi T} + \frac{1}{2}\Big)\right) \tag{3.79}$$

For a superconductor, typically $\frac{\omega_D}{2\pi T} \gg 1$ and for very large arguments $\psi(x) \sim \ln(x)$, hence we can say

$$N(0) \sum_{l=0}^{\frac{\omega_D}{2\pi T}} \frac{1}{l + \frac{1}{2} + \frac{|\omega|}{4\pi T}} \simeq N(0)\left(\ln\Big(\frac{\omega_D}{2\pi T}\Big) - \psi\Big(\frac{|\omega|}{4\pi T} + \frac{1}{2}\Big)\right). \tag{3.80}$$

Now consider the second term

$$4\pi N(0) T \sum_{\epsilon>0} \frac{1}{(2\epsilon + |\omega|)^3} = \frac{N(0)}{(4\pi T)^2} \sum_{l=0}^{\infty} \frac{1}{(l + \frac{1}{2} + \frac{|\omega|}{4\pi T})^3}\,. \tag{3.81}$$

As this term will contribute higher order terms we will only take the leading order contribution that comes from when $\omega = 0$. This puts the sum in the form of a Hurwitz-zeta function,

$$\zeta(s, q) = \sum_{l=0}^{\infty} \frac{1}{(l+q)^s}, \tag{3.82}$$

with $s = 3$ and $q = \frac{1}{2}$. In the $q = \frac{1}{2}$ case there is a simple relation to the Riemann zeta function that we can use, given by

$$\zeta\Big(s, \frac{1}{2}\Big) = (2^s - 1)\zeta(s)\,, \tag{3.83a}$$

$$\therefore \zeta\Big(3, \frac{1}{2}\Big) = 7\zeta(3)\,. \tag{3.83b}$$

Putting this all together gives

$$\Sigma_{L_0}(\mathbf{q}, i\omega) = N(0)\bigg(\ln\Big(\frac{\omega_D}{2\pi T}\Big) - \psi\Big(\frac{|\omega|}{4\pi T} + \frac{1}{2}\Big) - \frac{v_F^2 q^2}{3}\frac{7\zeta(3)}{16\pi^2 T^2}\bigg), \tag{3.84a}$$

$$\Rightarrow L_0^{-1}(\mathbf{q}, i\omega) = V^{-1} - N(0)\bigg(\ln\Big(\frac{\omega_D}{2\pi T}\Big) - \psi\Big(\frac{|\omega|}{4\pi T} + \frac{1}{2}\Big) - \frac{7v_F^2 q^2 \zeta(3)}{48\pi^2 T^2}\bigg). \tag{3.84b}$$

We can find the critical temperature for a clean superconductor, which we will label as $T_{c,0}$, by finding the value of T for which $L_0^{-1}(0,0) = 0$. This is because a divergence in the pair propagator will cause a divergence in the fluctuation conductivity diagrams and hence signals the onset of the Cooper instability and therefore the superconducting regime. So we have

$$0 = V^{-1} - N(0)\bigg(\ln\bigg(\frac{\omega_D}{2\pi T_{c,0}}\bigg) - \psi\Big(\frac{1}{2}\Big)\bigg). \tag{3.85}$$

After using the standard result $\psi(\frac{1}{2}) = -2\ln 2 - \gamma$ (where γ is the Euler-Mascheroni constant) and a simple rearrangement, we can obtain the well-known BCS result for the critical temperature,

$$T_{c,0} = \frac{2e^{\gamma}}{\pi}\omega_D \exp\bigg(-\frac{1}{N(0)V}\bigg) \simeq 1.13\omega_D \exp\bigg(-\frac{1}{N(0)V}\bigg). \tag{3.86}$$

As equation 3.85 is identically zero we can subtract it from 3.84b to write the pair propagator in terms of the transition temperature,

$$L_0^{-1}(\mathbf{q}, i\omega) = N(0)\bigg(\ln\bigg(\frac{T}{T_{c,0}}\bigg) + \psi\Big(\frac{|\omega|}{4\pi T} + \frac{1}{2}\Big) - \psi\Big(\frac{1}{2}\Big) + \frac{7v_F^2 q^2 \zeta(3)}{48\pi^2 T^2}\bigg). \tag{3.87}$$

To consider the pair propagator in the presence of disorder, the Dyson equation is altered to be as in figure 3.9, where now the electron propagators are the impurity Green's functions and cooperon interference terms are inserted in between each BCS interaction line. This of course also means we will be again working in the diffusive limit. So the

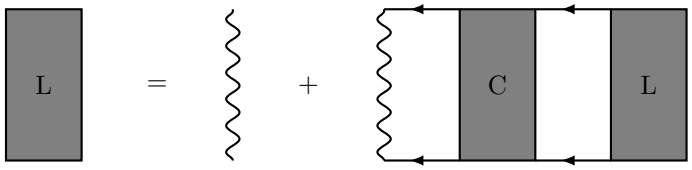

Figure 3.9: The Dyson equation for the pair propagator in a dirty superconductor. The self-energy part now contains a cooperon.

Dyson equation and self-energy part can be written as,

$$L^{-1}(\mathbf{q}, i\omega) = V^{-1} - \Sigma_L^{-1}(\mathbf{q}, i\omega) \tag{3.88}$$

$$\begin{aligned}\Sigma_L(\mathbf{q}, i\omega) =& \frac{2T}{\mathcal{V}^2} \sum_{\mathbf{k}\mathbf{k}'} \sum_{\varepsilon} G(\mathbf{k}+\mathbf{q}, i\varepsilon + i\omega) G(\mathbf{k}'+\mathbf{q}, i\varepsilon + i\omega) \\ & \times G(-\mathbf{k}, -i\varepsilon) G(-\mathbf{k}', -i\varepsilon) \frac{\Theta(\varepsilon(\varepsilon+\omega))}{2\pi N(0)\tau^2 (Dq^2 + 2\varepsilon + \omega + \tau_\phi^{-1})}\end{aligned} \tag{3.89}$$

We can switch the order of summations as there are no divergence issues. Using the standard diffusive integral result from appendix D we can easily complete the integrals over $\mathbf{k}$ and $\mathbf{k}'$ to obtain

$$\Sigma_L(\mathbf{q}, i\omega) = 4\pi N(0) T \sum_{\varepsilon > 0} \frac{1}{Dq^2 + 2\varepsilon + |\omega| + \tau_\phi^{-1}} \,. \tag{3.90}$$

Again, this is logarithmically divergent, so we introduce the cutoff $\varepsilon \sim \omega_D$.

$$\Sigma_L(\mathbf{q}, i\omega) = N(0) \sum_{l=0}^{\frac{\omega_D}{2\pi T}} \frac{1}{l + \frac{1}{2} + \frac{Dq^2 + |\omega| + \tau_\phi^{-1}}{4\pi T}} \,. \tag{3.91}$$

Using the same result as in equation 3.80, we have

$$\Sigma_L(\mathbf{q}, i\omega) = N(0) \bigg(\ln\Big(\frac{\omega_D}{2\pi T}\Big) - \psi\Big(\frac{1}{2} + \frac{Dq^2 + |\omega| + \tau_\phi^{-1}}{4\pi T}\Big) \bigg) \tag{3.92}$$

$$\therefore L^{-1}(\mathbf{q}, i\omega) = V^{-1} - N(0) \bigg(\ln\Big(\frac{\omega_D}{2\pi T}\Big) - \psi\Big(\frac{1}{2} + \frac{Dq^2 + |\omega| + \tau_\phi^{-1}}{4\pi T}\Big) \bigg) \,. \tag{3.93}$$

Again L will diverge as $\mathbf{q} \to 0$ and $\omega \to 0$ giving us the value of T_c

$$V^{-1} = N(0)\left(\ln\left(\frac{\omega_D}{2\pi T_c}\right) - \psi\left(\frac{1}{2} + \frac{1}{4\pi T_c \tau_{\phi,c}}\right)\right), \tag{3.94}$$

noting that if τ_ϕ is temperature dependent it will be the value at T_c, $\tau_{\phi,c}$. If $\tau_\phi^{-1} = 0$ we will simply recover the result as for $T_{c,0}$, agreeing with the result that the critical temperature for BCS superconductors is robust to doping with non-magnetic impurities. Now we can use the expression for T_c to simplify yielding:

$$L^{-1}(\mathbf{q}, i\omega) = N(0)\left(\ln\left(\frac{T}{T_c}\right) + \psi\left(\frac{1}{2} + \frac{Dq^2 + |\omega| + \tau_\phi^{-1}}{4\pi T}\right) - \psi\left(\frac{1}{2} + \frac{1}{4\pi T_c \tau_{\phi,c}}\right)\right). \tag{3.95}$$

These will be important results to keep in mind in the following chapter where we will move on to using the Green's function formalism in the superconducting regime, because we should be able to recover these result when calculating T_c from below the superconducting transition as well.

CHAPTER 4

CONDUCTIVITY IN THE SUPERCONDUCTING STATE

To be able to perform calculations for systems in the superconducting state we must have Green's functions that explicitly contain information about the formation of Cooper pairs. In the following section we will show the construction of the Nambu-Gorkov description of superconducting Green's functions which contains this information for a clean superconductor. In section 4.2, we will extend the formalism to dirty superconductors by adding an impurity scattering term. In section 4.3 we use the dirty Nambu-Green's functions to construct the linear response fuction of the superconductor to an applied electromagnetic field. Firstly, we use it to calculate the number density of superconducting electrons by taking the $\omega \to 0$ limit. Everything mentioned so far is fairly standard practice and can be found in a number of texts (see [56, 66, 68] for example).

In the second part of this section, we calculate the frequency-dependent response, which requires proper treatment of the analytic continuation to real frequencies. This was first calculated by Abrikosov and Gor'kov [72] and can also be found in ref [67]. In section 4.4 we turn our attention to calculating the electronic thermal conductivity of the superconductor, reproducing the result found in Ambegaokar and Griffin [30], which reveals the exponential suppression of the thermal conductivity at low temperatures.

4.1 Nambu-Gorkov Formalism for Diagrammatics in the Superconducting State

We begin with the simple BCS model for a clean superconductor described by the following interacting Hamiltonian which contains a constant potential within the shell of size ω_D about the Fermi surface,

$$H(\tau) = H_0 + H_{int} = \sum_{\mathbf{k}\sigma} \xi_k c^\dagger_{\mathbf{k}\sigma}(\tau) c_{\mathbf{k}\sigma}(\tau) - \frac{V}{2} \sum_{\mathbf{k}\mathbf{k}'\mathbf{q}\sigma} c^\dagger_{\mathbf{k}\sigma}(\tau) c^\dagger_{\mathbf{q}-\mathbf{k}\bar{\sigma}}(\tau) c_{\mathbf{q}-\mathbf{k}'\bar{\sigma}}(\tau) c_{\mathbf{k}'\sigma}(\tau)\,. \quad (4.1)$$

where we take the convention that $\bar{\sigma}$ is the opposite spin to σ and, thus, repeated σ's are the same spin-species. For now we will drop the τ's out of the notation for convenience and we will return them when necessary. To include the Cooper instability into the theory, when considering relevant correlations there will be new non-zero terms corresponding to electron-electron and hole-hole pairing. For s-wave pairing we have

$$\begin{aligned} \langle c_{\mathbf{q}-\mathbf{k}\downarrow}(\tau) c_{\mathbf{k}\uparrow}(0)\rangle &= b_{\mathbf{k}}\, \delta(\mathbf{q})\, \delta(\tau)\,, \\ \left\langle c^\dagger_{\mathbf{k}\uparrow}(\tau) c^\dagger_{\mathbf{q}-\mathbf{k}\downarrow}(0)\right\rangle &= b^*_{\mathbf{k}}\, \delta(\mathbf{q})\, \delta(\tau)\,, \\ \langle c_{\mathbf{q}-\mathbf{k}\sigma} c_{\mathbf{k}\sigma}\rangle &= 0 \\ \text{and} \quad \left\langle c^\dagger_{\mathbf{k}\sigma} c^\dagger_{\mathbf{q}-\mathbf{k}\sigma}\right\rangle &= 0\,, \end{aligned} \quad (4.2)$$

where $b^*_{\mathbf{k}}$ and $b_{\mathbf{k}}$ are the expectation values for the creation of a cooper pair made up of electrons or holes (respectively) with momenta $\pm\mathbf{k}$. We assume that the Cooper pair quasiparticle operator $c^\dagger_{\mathbf{k}\sigma} c^\dagger_{\mathbf{q}-\mathbf{k}\bar{\sigma}}$ is close to its expectation value, so that we can represent it as its expectation value plus small fluctuations about the expectation value,

$$\begin{aligned} c^\dagger_{\mathbf{k}\sigma} c^\dagger_{\mathbf{q}-\mathbf{k}\bar{\sigma}} &= \left\langle c^\dagger_{\mathbf{k}\sigma} c^\dagger_{\mathbf{q}-\mathbf{k}\bar{\sigma}}\right\rangle + \delta(c^\dagger_{\mathbf{k}\sigma} c^\dagger_{\mathbf{q}-\mathbf{k}\bar{\sigma}}) \\ &= \left\langle c^\dagger_{\mathbf{k}\sigma} c^\dagger_{\mathbf{q}-\mathbf{k}\bar{\sigma}}\right\rangle + \left(c^\dagger_{\mathbf{k}\sigma} c^\dagger_{\mathbf{q}-\mathbf{k}\bar{\sigma}} - \left\langle c^\dagger_{\mathbf{k}\sigma} c^\dagger_{\mathbf{q}-\mathbf{k}\bar{\sigma}}\right\rangle\right). \end{aligned} \quad (4.3)$$

Now we can use this approximation to perform a 'mean-field' approximation on the interaction term, where we can ignore terms quadratic in the fluctuations,

$$H_{\text{int}} = -\frac{V}{2}\sum_{\mathbf{k}\mathbf{k}'\mathbf{q}\sigma} c^{\dagger}_{\mathbf{k}\sigma}c^{\dagger}_{\mathbf{q}-\mathbf{k}\bar{\sigma}}c_{\mathbf{q}-\mathbf{k}'\bar{\sigma}}c_{\mathbf{k}'\sigma} \simeq -\sum_{\mathbf{k}}\left[\Delta c^{\dagger}_{\mathbf{k}\uparrow}c^{\dagger}_{-\mathbf{k}\downarrow} + \Delta^{*}c_{-\mathbf{k}\downarrow}c_{\mathbf{k}\uparrow} - \Delta b^{*}_{\mathbf{k}}\right]. \tag{4.4}$$

where we have defined the internal pairing field

$$\Delta = V\sum_{\mathbf{k}} b_{\mathbf{k}}\,, \tag{4.5}$$

that's value is to be obtained self consistently. Hence, after absorbing any non-dynamical terms into the chemical potential, the mean field Hamiltonian we are left with is

$$H = H_0 + H_{BCS} = \sum_{\mathbf{k}\sigma}\xi_k c^{\dagger}_{\mathbf{k}\sigma}c_{\mathbf{k}\sigma} - \sum_{\mathbf{k}}\left[\Delta c^{\dagger}_{\mathbf{k}\uparrow}c^{\dagger}_{-\mathbf{k}\downarrow} + \Delta^{*}c_{-\mathbf{k}\downarrow}c_{\mathbf{k}\uparrow}\right]. \tag{4.6}$$

We now obtain the equations of motion for the electron creation and annihilation operators using Heisenberg's equation of motion:

$$\frac{\mathrm{d}A(\tau)}{\mathrm{d}\tau} = \big[H(\tau), A(\tau)\big]\,. \tag{4.7}$$

As we are working with Fermionic operators and in the Hamiltonian all the terms appears as pairs of operators, we will make use of the following relation in order to switch the commutator in Heisenberg's equation of motion to appropriate anticommutators:

$$\big[AB, C\big] = A\big\{B, C\big\} - \big\{C, A\big\}B\,. \tag{4.8}$$

Using this along with standard anticommutation relations we find the set of equations of motion:

$$\frac{\mathrm{d}c^{\dagger}_{\mathbf{k}\uparrow}(\tau)}{\mathrm{d}\tau} = \xi_k c^{\dagger}_{\mathbf{k}\uparrow}(\tau) - \Delta^* c_{-\mathbf{k}\downarrow}(\tau)\,, \tag{4.9a}$$

$$\frac{\mathrm{d}c_{\mathbf{k}\uparrow}(\tau)}{\mathrm{d}\tau} = -\xi_k c_{\mathbf{k}\uparrow}(\tau) + \Delta c^{\dagger}_{-\mathbf{k}\downarrow}(\tau)\,, \tag{4.9b}$$

$$\frac{\mathrm{d}c^{\dagger}_{-\mathbf{k}\downarrow}(\tau)}{\mathrm{d}\tau} = \xi_k c^{\dagger}_{-\mathbf{k}\downarrow}(\tau) + \Delta^* c_{\mathbf{k}\uparrow}(\tau)\,, \tag{4.9c}$$

$$\frac{\mathrm{d}c_{-\mathbf{k}\downarrow}(\tau)}{\mathrm{d}\tau} = -\xi_k c_{-\mathbf{k}\downarrow}(\tau) - \Delta c^{\dagger}_{\mathbf{k}\uparrow}(\tau)\,. \tag{4.9d}$$

Each of the above equations of motion can be related to an equation of motion for a particular Green's function. Two of the Green's functions are normal electron propagators that we have encountered before in the normal state, but the other two are new Green's functions called the anomalous, or off-diagonal, Green's functions. These Green's functions correspond to the creation or annihilation of Cooper pair quasiparticles in the Cooper pair condensate, and will be denoted by F. The set of four Green's functions we will be concerned with is shown below, where we have temporal invariance such that the imaginary time can be defined by a single difference variable, $\tau = \tau_1 - \tau_2$,

$$G_{\uparrow}(\mathbf{k},\tau) = -\left\langle \mathcal{T}_{\tau} c_{\mathbf{k}\uparrow}(\tau) c^{\dagger}_{\mathbf{k}\uparrow}(0) \right\rangle\,, \tag{4.10a}$$

$$-G_{\downarrow}(-\mathbf{k},-\tau) = -\left\langle \mathcal{T}_{\tau} c^{\dagger}_{\mathbf{k}\downarrow}(\tau) c_{-\mathbf{k}\downarrow}(0) \right\rangle\,, \tag{4.10b}$$

$$F^{\dagger}(\mathbf{k},\tau) = -\left\langle \mathcal{T}_{\tau} c^{\dagger}_{-\mathbf{k}\downarrow}(\tau) c^{\dagger}_{\mathbf{k}\uparrow}(0) \right\rangle\,, \tag{4.10c}$$

$$F(\mathbf{k},-\tau) = -\left\langle \mathcal{T}_{\tau} c_{\mathbf{k}\uparrow}(\tau) c_{-\mathbf{k}\downarrow}(0) \right\rangle\,. \tag{4.10d}$$

Now we can use the equations of motion for the electron operators to find a set of equations for our Green's functions that relate them to one another:

$$\frac{\mathrm{d}}{\mathrm{d}\tau}G_\uparrow(\mathbf{k},\tau) = -\xi_k G_\uparrow(\mathbf{k},\tau) + \Delta F^\dagger(\mathbf{k},\tau) - \delta(\tau)\,, \tag{4.11a}$$

$$\frac{\mathrm{d}}{\mathrm{d}\tau}\big(-G_\downarrow(-\mathbf{k},-\tau)\big) = \xi_k\big(-G_\downarrow(-\mathbf{k},-\tau)\big) + \Delta^* F(\mathbf{k},-\tau) - \delta(\tau)\,, \tag{4.11b}$$

$$\frac{\mathrm{d}}{\mathrm{d}\tau}F^\dagger(\mathbf{k},\tau) = \xi_k F^\dagger(\mathbf{k},\tau) + \Delta^* G_\uparrow(\mathbf{k},\tau)\,, \tag{4.11c}$$

$$\frac{\mathrm{d}}{\mathrm{d}\tau}F(\mathbf{k},-\tau) = -\xi_k F(\mathbf{k},-\tau) + \Delta\big(-G_\downarrow(-\mathbf{k},-\tau)\big)\,. \tag{4.11d}$$

We can represent this system of four equations as 2×2 matrix equation by defining spinors,

$$\alpha_{\mathbf{k}}(\tau) = \begin{pmatrix} c_{\mathbf{k}\uparrow}(\tau) \\ c^\dagger_{-\mathbf{k}\downarrow}(\tau) \end{pmatrix} \quad \text{and} \quad \alpha^\dagger_{\mathbf{k}}(\tau) = \begin{pmatrix} c^\dagger_{\mathbf{k}\uparrow}(\tau) & c_{-\mathbf{k}\downarrow}(\tau) \end{pmatrix}, \tag{4.12}$$

and a corresponding matrix Green's function

$$\begin{aligned} \mathcal{G}(\mathbf{k},\tau) &= -\left\langle \mathcal{T}_\tau \alpha_{\mathbf{k}}(\tau)\alpha^\dagger_{\mathbf{k}}(0)\right\rangle \\ &= \begin{pmatrix} -\left\langle \mathcal{T}_\tau c_{\mathbf{k}\uparrow}(\tau)c^\dagger_{\mathbf{k}\uparrow}(0)\right\rangle & -\langle \mathcal{T}_\tau c_{\mathbf{k}\uparrow}(\tau)c_{-\mathbf{k}\downarrow}(0)\rangle \\ -\left\langle \mathcal{T}_\tau c^\dagger_{-\mathbf{k}\downarrow}(\tau)c^\dagger_{\mathbf{k}\uparrow}(0)\right\rangle & -\left\langle \mathcal{T}_\tau c^\dagger_{-\mathbf{k}\downarrow}(\tau)c_{-\mathbf{k}\downarrow}(0)\right\rangle \end{pmatrix} \\ &= \begin{pmatrix} G_\uparrow(\mathbf{k},\tau) & F(\mathbf{k},-\tau) \\ F^\dagger(\mathbf{k},\tau) & -G_\downarrow(-\mathbf{k},-\tau) \end{pmatrix} \end{aligned} \tag{4.13}$$

The set of equations of motion can then be represented in this matrix form,

$$\begin{aligned}\frac{\mathrm{d}}{\mathrm{d}\tau}\mathcal{G}(\mathbf{k},\tau) =& \begin{pmatrix} -\delta(\tau) - \xi_k G_\uparrow + \Delta F^\dagger & -\xi_k F + \Delta(-G_\downarrow) \\ \xi_k F^\dagger + \Delta^\dagger G_\uparrow & -\delta(\tau) + \xi_k(-G_\downarrow) + \Delta^* F \end{pmatrix} \\ =& -\delta(\tau)\begin{pmatrix} 1 & 0 \\ 0 & 1 \end{pmatrix} - \xi_k \begin{pmatrix} G_\uparrow & F \\ -F^\dagger & -(-G_\downarrow) \end{pmatrix} \\ &+ \Delta \begin{pmatrix} F^\dagger & (-G_\downarrow) \\ 0 & 0 \end{pmatrix} + \Delta^* \begin{pmatrix} 0 & 0 \\ G_\uparrow & F \end{pmatrix} \\ =& -\delta(\tau)\sigma_0 - \xi_k \sigma_z \mathcal{G} + (\Delta\sigma_+ + \Delta^*\sigma_-)\mathcal{G}\,, \end{aligned} \tag{4.14}$$

where σ_x, σ_y, etc. are the usual Pauli matrices. In general, Δ is complex, but unless one is looking at calculations relating more than one distinct superconducting region, such as in Josephson junctions, the complex phase will never manifest in the calculation. So for now we will set Δ to be real and we will see this will not affect the result of these calculations to follow. Therefore, after applying this simplification and rearranging we have

$$\Big(\frac{\mathrm{d}}{\mathrm{d}\tau}\sigma_0 + \xi_k\sigma_z - \Delta\sigma_x\Big)\mathcal{G}(\mathbf{k},\tau) = -\delta(\tau)\sigma_0\,. \tag{4.15}$$

From here we drop the identity matrices, σ_0, for convenience and the absence of a Pauli matrix will imply there is an identity. We next Fourier transform this equation in imaginary time,

$$\begin{aligned}\Big(\frac{\mathrm{d}}{\mathrm{d}\tau} + \xi_k\sigma_z - \Delta\sigma_x\Big)T\sum_\varepsilon \mathcal{G}(\mathbf{k},i\varepsilon)e^{-i\varepsilon\tau} &= -\delta(\tau)\,, \\ \Rightarrow \mathcal{G}(\mathbf{k},i\varepsilon) &= \frac{1}{i\varepsilon - \xi_k\sigma_z + \Delta\sigma_x}\,. \end{aligned} \tag{4.16}$$

We wish to remove the Pauli matrices from the denominator as these will be difficult to deal with. To do this we note that,

$$\begin{aligned}
&\big(i\varepsilon - \xi_k\sigma_z + \Delta\sigma_x\big)\big(i\varepsilon + \xi_k\sigma_z - \Delta\sigma_x\big) \\
&= -\varepsilon^2 - \xi_k^2\sigma_z^2 - \Delta^2\sigma_x^2 - \xi_k\Delta(\sigma_x\sigma_z + \sigma_z\sigma_x) + i\varepsilon(\xi_k\sigma_z - \Delta\sigma_x) - i\varepsilon(\xi_k\sigma_z - \Delta\sigma_x) \\
&= -\varepsilon^2 - \xi_k^2 - \Delta^2\,, \qquad (4.17)
\end{aligned}$$

since $\sigma_x^2 = \sigma_z^2 = \sigma_0$ and $(\sigma_x\sigma_z + \sigma_z\sigma_x) = 0$. Multiplying the denominator of equation 4.16 by $i\varepsilon + \xi_k\sigma_z - \Delta\sigma_x$ then gives

$$\mathcal{G}(\mathbf{k}, i\varepsilon) = \frac{i\varepsilon + \xi_k\sigma_z - \Delta\sigma_x}{-\varepsilon^2 - \xi_k^2 - \Delta^2} \qquad (4.18)$$

Sometimes, we will find it useful to write this Green's function in terms of the quantity $E_k^2 = \xi_k^2 + \Delta^2$ instead.

This matrix Green's function is the primary object with which we will build the diagrammatic description of the superconducting state, analogous to the free single-electron Green's function that was derived in section 2.3. By analogy to the normal state formalism, we can construct a set of Feynman rules for the perturbation expansion of these matrix Green's functions. These turn out to be the same as described as in section 2.5 except:

(i) The solid electron lines now represent the matrix Green's function, $\mathcal{G}$.

(ii) Electron-Coulomb and electron-phonon vertices now carry a factor of σ_z.

(iii) The order of matrices follows the order they appear along the diagram.

(iv) For any closed loop, the trace is taken over matrices that appear in the loop.

we now wish to find the form of Δ self consistently between the original definition in equation 4.5 and the matrix Green's function in equation 4.18 that we have just defined

using it. We can relate $b_{\mathbf{k}}$ to the anomalous Green's function by noting,

$$\begin{aligned} b_{\mathbf{k}} &= F(\mathbf{k}, -\tau)\Big|_{\tau=0_-} = \mathrm{Tr}\left\{\sigma_- \mathcal{G}(\mathbf{k}, \tau = 0_-)\right\} \\ &= \mathrm{Tr}\left\{\sigma_- T \sum_{\varepsilon} e^{-i\varepsilon 0_-} \frac{i\varepsilon + \xi_k \sigma_z - \Delta\sigma_x}{-\varepsilon^2 - \xi_k^2 - \Delta^2}\right\} \quad ; \quad e^{-i\varepsilon 0_-} = 1 \\ &= T \sum_{\varepsilon} \mathrm{Tr}\left\{\frac{i\varepsilon\sigma_- + \xi_k \sigma_- \sigma_z - \Delta\sigma_- \sigma_x}{-\varepsilon^2 - \xi_k^2 - \Delta^2}\right\}. \end{aligned} \tag{4.19}$$

Using $\mathrm{Tr}\{\sigma_-\} = 0$, $\mathrm{Tr}\{\sigma_-\sigma_z\} = 0$ and $\mathrm{Tr}\{\sigma_-\sigma_x\} = 1$, we are only left with one term in the numerator after taking the trace, leaving

$$\begin{aligned} b_{\mathbf{k}} &= -T \sum_{\varepsilon} \frac{\Delta}{-\varepsilon^2 - \xi_k^2 - \Delta^2}, \\ \Rightarrow 1 &= V \sum_{\mathbf{k}} T \sum_{\varepsilon} \frac{1}{\varepsilon^2 + \xi_k^2 + \Delta^2}. \end{aligned} \tag{4.20}$$

We can now compute the sum over Matsubara frequencies to simplify this equation using the usual residue method,

$$\begin{aligned} T \sum_{\varepsilon} \frac{1}{\varepsilon^2 + E_k^2} &= \frac{1}{2\pi i} \oint dz \, \frac{f(z)}{z^2 - E_k^2} = -\sum \mathrm{Res}\left(\frac{f(z)}{z^2 - E_k^2}\right) \\ &= \frac{1}{2E_k} \tanh\left(\frac{E_k}{2T}\right) = \frac{1}{2E_k}\big(1 - 2f(E_k)\big) \end{aligned} \tag{4.21}$$

Substituting this back into the self consistency equation we have

$$\begin{aligned} 1 &= V \sum_{\mathbf{k}} \frac{\tanh\left(\frac{E_k}{2T}\right)}{2E_k}, \\ \Rightarrow 1 &= N(0)V \int_0^{\omega_D} d\xi \, \frac{\tanh\left(\frac{\sqrt{\xi^2+\Delta^2}}{2T}\right)}{\sqrt{\xi^2 + \Delta^2}}. \end{aligned} \tag{4.22}$$

This is the simplest general closed form of the self consistency equation for Δ, although in general this integral is not analytically tractable and must be tackled numerically. Note that the upper limit of the momentum sum has been cut-off by the Debye frequency, due

to the nature of the BCS interaction. It is solvable in two important case, as we will show shortly. We first calculate an alternative form of the self consistency equation switching the order of sums and computing the sum over momenta,

$$\begin{aligned} 1 &= VT\sum_{\varepsilon}\sum_{\mathbf{k}}\frac{1}{\varepsilon^2+\xi_k^2+\Delta^2} \\ &= N(0)VT\sum_{\varepsilon}\int_{-\infty}^{\infty}d\xi_k\,\frac{1}{\xi_k^2+\varepsilon^2+\Delta^2}\,, \\ \therefore 1 &= \pi N(0)VT\sum_{\varepsilon}\frac{1}{\sqrt{\varepsilon^2+\Delta^2}} = 2\pi N(0)VT\sum_{\varepsilon>0}\frac{1}{\sqrt{\varepsilon^2+\Delta^2}}\,. \end{aligned} \tag{4.23}$$

This form can formally be proven to be equivalent to the other by performing the contour integral around the Matsubara frequencies in the complex ε plane whilst properly addressing the branch cut caused by the square root. This second form is again not in general analytically tractable, but leaves us with a sum over Matsubara frequencies instead of an integral over energy. So we are free to choose the form that is most convenient for us in a given situation.

We now examine the behaviour of the self-consistency equation at important points. We will perform these calculations with the form involving the sum over Matsubara frequencies, because we wish to show that we can produce the same results as the first form with which one usually derives these BCS results. Firstly, we should be able to find the critical temperature by setting $\Delta = 0$, as this corresponds to the situation where cooper pair formation is no longer energetically favourable to form Cooper pairs. This leads to

$$1 = 2\pi N(0)VT_{c,0}\sum_{\varepsilon>0}\frac{1}{\varepsilon} = N(0)V\sum_{l=0}^{\frac{\omega_D}{2\pi T_{c,0}}}\frac{1}{l+\frac{1}{2}}\,. \tag{4.24}$$

We then can proceed as in the calculation of the pair propagator by using the diagamma function identity to obtain

$$1 = N(0)V\left(\psi\Big(\frac{\omega_D}{2\pi T_{c,0}}+\frac{3}{2}\Big)-\psi\Big(\frac{1}{2}\Big)\right). \tag{4.25}$$

Noting that $\psi(x) \sim \ln(x)$ for $x \gg 1$, as in equation 3.86, this can then be rearranged to give the expected result for the critical temperature,

$$T_{c,0} = \frac{2e^{\gamma}}{\pi}\omega_D \exp\left(-\frac{1}{N(0)V}\right) \approx 1.13\omega_D \exp\left(-\frac{1}{N(0)V}\right). \tag{4.26}$$

Now consider the limit $T \to 0$, which should correspond to the largest value of Δ, as physically we expect the condensate to contain more Cooper pairs the lower the temperature. Our sum over Matsubara frequencies goes in steps of $2\pi T$, so in this limit we can write the sum as an integral, where we must impose an upper cut off of ω_D to avoid the integral diverging,

$$\begin{aligned} 1 &= N(0)V \int_0^{\omega_D} d\epsilon \, \frac{1}{\sqrt{\epsilon^2 + \Delta^2(T=0)}} \\ &= N(0)V \text{arcsinh}\left(\frac{\omega_D}{\Delta(0)}\right) = N(0)V \ln\left(\frac{\omega_D}{\Delta(0)} + \sqrt{\frac{\omega_D^2}{\Delta^2(0)} + 1}\right) \end{aligned} \tag{4.27}$$

Using $\omega_D \gg \Delta(0)$, as the Debye energy is a much higher energy scale than any superconducting energy scale, this equation becomes

$$\begin{aligned} 1 &= N(0)V \ln\left(\frac{2\omega_D}{\Delta(0)}\right), \\ \Rightarrow \Delta(0) &= 2\omega_D \exp\left(-\frac{1}{N(0)V}\right), \end{aligned} \tag{4.28}$$

which agrees with the standard result from BCS theory.

4.2 Nambu-Gorkov Diagrammatic Formalism for a Dirty Superconductor

The next step is to add impurities to the Nambu-Gorkov formalism to be able to deal with dirty superconductors. We therefore add an impurity term to the Hamiltonian. However now because of the impurity distribution there will be no translational invariance

until we ensemble average over impurity distributions, so instead we will write the BCS Hamiltonian in real space,

$$H = H_0 + H_{int} + H_{imp} \tag{4.29a}$$

$$H_0 = \sum_\sigma \int \mathrm{d}\mathbf{r}\, \psi_\sigma^\dagger(\mathbf{r}) \left(\frac{\boldsymbol{\nabla}^2}{2m} - \mu \right) \psi_\sigma(\mathbf{r}) \tag{4.29b}$$

$$H_{int} = -\frac{V}{2} \sum_\sigma \int \mathrm{d}\mathbf{r}\, \mathrm{d}\mathbf{r}'\, \psi_\sigma^\dagger(\mathbf{r}) \psi_{\bar{\sigma}}^\dagger(\mathbf{r}') \psi_{\bar{\sigma}}(r') \psi_\sigma(\mathbf{r}) \tag{4.29c}$$

$$H_{imp} = \sum_\sigma \int \mathrm{d}\mathbf{r} \sum_i u(\mathbf{r} - \mathbf{R}_i) \psi_\sigma^\dagger(\mathbf{r}) \psi_\sigma(\mathbf{r}) \tag{4.29d}$$

We can rewrite these in terms of real space Nambu-Gorkov operators,

$$\Psi(\mathbf{r}) = \begin{pmatrix} \psi_\uparrow(\mathbf{r}) \\ \psi_\downarrow^\dagger(\mathbf{r}) \end{pmatrix} \quad ; \quad \Psi^\dagger(\mathbf{r}) = \begin{pmatrix} \psi_\uparrow^\dagger(\mathbf{r}) & \psi_\downarrow(\mathbf{r}) \end{pmatrix} \tag{4.30a}$$

$$\Rightarrow H_0 = \int \mathrm{d}\mathbf{r}\, \Psi^\dagger(\mathbf{r}) \left(\frac{\boldsymbol{\nabla}^2}{2m} - \mu \right) \sigma_z \Psi(\mathbf{r}) \tag{4.30b}$$

$$H_{int} = -\frac{V}{2} \int \mathrm{d}\mathbf{r}\, \mathrm{d}\mathbf{r}'\, \Psi^\dagger(\mathbf{r}) \sigma_z \Psi(\mathbf{r}) \Psi^\dagger(\mathbf{r}') \sigma_z \Psi(\mathbf{r}') \tag{4.30c}$$

$$H_{imp} = \int \mathrm{d}\mathbf{r} \sum_i u(\mathbf{r} - \mathbf{R}_i) \Psi^\dagger(\mathbf{r}) \sigma_z \Psi(\mathbf{r}) \tag{4.30d}$$

Using the mean field approximation on the interaction term we can obtain the BCS term and then write it in terms of the Nambu-spinors like so

$$\begin{aligned} H_{BCS} &= -\Delta \int \mathrm{d}\mathbf{r} \left(\psi_\uparrow^\dagger(\mathbf{r}) \psi_\downarrow^\dagger(\mathbf{r}) + \psi_\downarrow(\mathbf{r}) \psi_\uparrow(\mathbf{r}) \right) \\ &= -\Delta \int \mathrm{d}\mathbf{r}\, \Psi^\dagger(\mathbf{r}) \sigma_x \Psi(\mathbf{r})\,. \end{aligned} \tag{4.31}$$

We can then construct equations of motion in the same way as the clean case. It is clear that the impurity has functionally the same matrix behaviour as the unperturbed term, H_0, so will also carry a σ_z after following through this process. Since we have a particular impurity configuration that has not yet been ensemble averaged here, we do not have

translational invariance, so we will work in terms of real space operators,

$$\left[\frac{\mathrm{d}}{\mathrm{d}\tau}+\left(\frac{\boldsymbol{\nabla}}{2m}-\mu\right)\sigma_z+\sum_i u(\mathbf{r}-\mathbf{R}_i)\sigma_z-\Delta\sigma_x\right]\mathcal{G}(\mathbf{r},\mathbf{r}';\tau)=-\delta(\mathbf{r}-\mathbf{r}')\delta(\tau)\,. \tag{4.32}$$

To proceed, we ensemble average over impurity positions which works essentially identically to the impurity Green's function in section 2.6, only now following the additional diagrammatic rules for the Nambu-Gorkov Green's functions outlined above. By treating the impurity term as a perturbative correction to the clean BCS Green's function, we can construct a Dyson equation,

$$\mathcal{G}^{-1}=\mathcal{G}_0^{-1}-\Sigma_{imp}\,. \tag{4.33}$$

Assuming a sufficiently low impurity concentrations, we can take the first Born approximation. In this regime the self-energy contribution, shown diagrammatically in figure 4.1, is given by

$$\Sigma_{imp}(i\varepsilon)=n_{imp}|U|^2\sum_k \sigma_z\mathcal{G}_0(\mathbf{k},i\varepsilon)\sigma_z\,, \tag{4.34}$$

where we have taken the impurity interaction to be instantaneous and point-like with strength U so

$$u(\mathbf{r}-\mathbf{R}_i)=U\delta(\mathbf{r}-\mathbf{R}_i)\,. \tag{4.35}$$

Noting that commuting the σ_z through the Green's function will simply switch the sign of the σ_x term, we can solve the expression for Σ_{imp},

$$\begin{aligned}\Sigma_{imp}&=-n_{imp}N(0)|U|^2\int_{-\infty}^{\infty}\mathrm{d}\xi_k\,\frac{i\varepsilon+\xi_k\sigma_z+\Delta\sigma_x}{\varepsilon^2+\xi_k^2+\Delta^2}\\&=-n_{imp}N(0)|U|^2\pi\frac{i\varepsilon+\Delta\sigma_x}{\sqrt{\varepsilon^2+\Delta^2}}\,.\end{aligned} \tag{4.36}$$

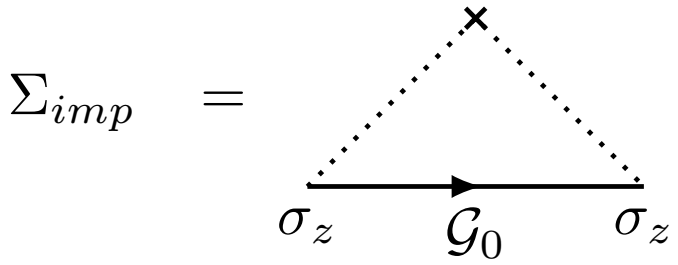

Figure 4.1: Self-energy part for the scattering with impurities in the superconducting state, where the first born approximation has been taken.

Substituting this expression back into equation 4.33 and using the definition for the scattering rate, given in equation 2.52, we find

$$\mathcal{G}^{-1} = i\varepsilon\left(1 + \frac{1}{2\tau_0}\frac{1}{\sqrt{\varepsilon^2+\Delta^2}}\right) - \xi_k\sigma_z + \Delta\left(1 + \frac{1}{2\tau_0}\frac{1}{\sqrt{\varepsilon^2+\Delta^2}}\right)\sigma_x\,. \tag{4.37}$$

From this we define new variables for the dirty Nambu Green's function,

$$\bar{\varepsilon} = \varepsilon\left(1 + \frac{1}{2\tau_0\sqrt{\varepsilon^2+\Delta^2}}\right) \quad \text{and} \quad \bar{\Delta} = \Delta\left(1 + \frac{1}{2\tau_0\sqrt{\varepsilon^2+\Delta^2}}\right), \tag{4.38}$$

$$\Rightarrow \mathcal{G}^{-1} = i\bar{\varepsilon} - \xi_k\sigma_z + \bar{\Delta}\sigma_x\,. \tag{4.39}$$

If we opt to slightly extend our treatment we can use the full Green's function in the self-energy diagram, which diagrammatically amounts to including the nested diagrams in our Dyson equation. So we have

$$\Sigma_{imp}(i\varepsilon) = n_{imp}|U|^2\sum_k \sigma_z\mathcal{G}(\mathbf{k}, i\varepsilon)\sigma_z\,. \tag{4.40}$$

Now we must make an ansatz for the form of the self-energy part and solve self-consistently, as now the form of $\mathcal{G}$depends on itself. We make the ansatz that the Full Green's function has the same form as equation 4.39. So from the form of the Dyson equation we can deduce that this requires

$$\Sigma_{imp} = i(\varepsilon - \bar{\varepsilon}) + (\Delta - \bar{\Delta})\sigma_x\,, \tag{4.41}$$

and we must solve this self-consistently with

$$\Sigma_{imp} = -\, n_{imp} N(0) |U|^2 \int_{-\infty}^{\infty} \mathrm{d}\xi_k \, \frac{i\bar{\varepsilon} + \xi_k \sigma_z + \bar{\Delta}\sigma_x}{\bar{\varepsilon}^2 + \xi_k^2 + \bar{\Delta}^2} \,. \tag{4.42}$$

This integral is solved identically to equation 4.36 and by equating the coefficients of the Pauli matrices with equation 4.41 we find

$$\varepsilon = \bar{\varepsilon}\left(1 - \frac{1}{2\tau_0\sqrt{\bar{\varepsilon}^2 + \bar{\Delta}^2}}\right) \quad \text{and} \quad \Delta = \bar{\Delta}\left(1 - \frac{1}{2\tau_0\sqrt{\bar{\varepsilon}^2 + \bar{\Delta}^2}}\right). \tag{4.43}$$

It is important to note the relation between the ratios of the clean and dirty variables,

$$\frac{\bar{\varepsilon}}{\bar{\Delta}} = \frac{\varepsilon}{\Delta} \,. \tag{4.44}$$

This is the case both when the nested diagrams are included and when they are not, and by using this relation one can go between equations 4.38 and 4.44. So including the full Green's function in the self-energy contribution has not changed the form of the Green's function and hence we have for the dirty Nambu-Green's function,

$$\mathcal{G} = \frac{i\bar{\varepsilon} + \xi_k \sigma_z - \bar{\Delta}\sigma_x}{-\bar{\varepsilon}^2 - \xi_k^2 - \bar{\Delta}^2} \,. \tag{4.45}$$

If one returns to equation 4.20 to self consistently determine the gap but now using the impurity superconducting Green's functions, one can see that the extra factors from $\bar{\varepsilon}$ and $\bar{\Delta}$ will cancel out and the gap equation will be the same as in the clean case. In other words the gap is independent of impurities so long as the above ratio holds. Similarly the transition temperature is also unaffected by these impurities.

4.3 Linear Response of a Superconductor to an Electromagnetic Field

Calculating the linear response function of the superconductor in an applied electromagnetic field encapsulates a number of interesting effects, depending on which limiting cases are taken. We will find the carrier density of superconducting carriers by finding $\mathbf{K}(0,0)$. Furthermore, as discussed in Rickayzen [9], the condition for infinite conductivity is

$$\lim_{\omega\to 0}\lim_{\mathbf{q}\to 0} K^E(\mathbf{q},\omega) = \text{non-zero constant}\,, \tag{4.46}$$

and for the Meissner effect is

$$\lim_{\mathbf{q}\to 0}\lim_{\omega\to 0} K^E(\mathbf{q},\omega) = \text{non-zero constant}\,. \tag{4.47}$$

We will also calculate the long wavelength response to an alternating field given by $K^E(0,\omega)$, which describes infrared absorption and transmission [67].

4.3.1 Construction of the Linear Response Function and the Superconducting Carrier Density

The construction of the linear response function is exactly analogous to the normal state Drude calculation (section 3.1), the only difference is that we will be constructing the 'bubble' Drude diagram using Nambu Green's functions. To demonstrate this analogy we need only show that we can replace the electron operators, $c^{(\dagger)}_{\mathbf{k},\sigma}$, with the Nambu spinors,

$\alpha_{\mathbf{k}}^{(\dagger)}$, so we examine the current operator in momentum space,

$$\begin{aligned}\mathbf{j}^{\boldsymbol{\nabla}}(\mathbf{q}) =& \frac{e}{2m}\sum_{\mathbf{k},\sigma}(2\mathbf{k}+\mathbf{q})c^{\dagger}_{\mathbf{k}\sigma}c_{\mathbf{k}+\mathbf{q}\sigma} \\ =& \frac{e}{2m}\sum_{\mathbf{k}}(2\mathbf{k}+\mathbf{q})\Big(c^{\dagger}_{\mathbf{k}\uparrow}c_{\mathbf{k}+\mathbf{q}\uparrow}+c_{-\mathbf{k}\downarrow}c^{\dagger}_{-\mathbf{k}-\mathbf{q}\downarrow}-\delta_{\mathbf{q},0}\Big) \\ =& \frac{e}{2m}\sum_{\mathbf{k}}(2\mathbf{k}+\mathbf{q})\alpha^{\dagger}_{\mathbf{k}}\alpha_{\mathbf{k}+\mathbf{q}}\,. \end{aligned} \tag{4.48}$$

In the second line we have expanded out the sum over spin and substituted $\mathbf{k}\mapsto-\mathbf{k}-\mathbf{q}$ in the second term, then commuted the operators yielding a delta function, however the delta function will evaluate to zero under the sum over $\mathbf{k}$, because when $\mathbf{q}=0$ it is odd in $\mathbf{k}$. Thus, the current operator can be written in terms of the Nambu-spinors and the rest of the derivation using Kubo's formula follows straightforwardly. The linear response function is given by the diagram in figure 4.2. Using the appropriate diagrammatic rules for the Nambu Green's functions this diagram can be written as,

$$\mathcal{G}^{E}_{\alpha\beta}(\mathbf{q},i\omega)=\frac{e^2T}{4m^2\mathcal{V}}\sum_{\mathbf{k},\varepsilon}(2\mathbf{k}+\mathbf{q})_{\alpha}(2\mathbf{k}+\mathbf{q})_{\beta}\,\mathrm{Tr}[\mathcal{G}(\mathbf{k},i\varepsilon)\mathcal{G}(k+q,i\varepsilon+i\omega)]\,, \tag{4.49}$$

where the Green's functions are those for the dirty superconductor, as this will yield both the clean and dirty results upon taking the appropriate limits. As in normal state result,

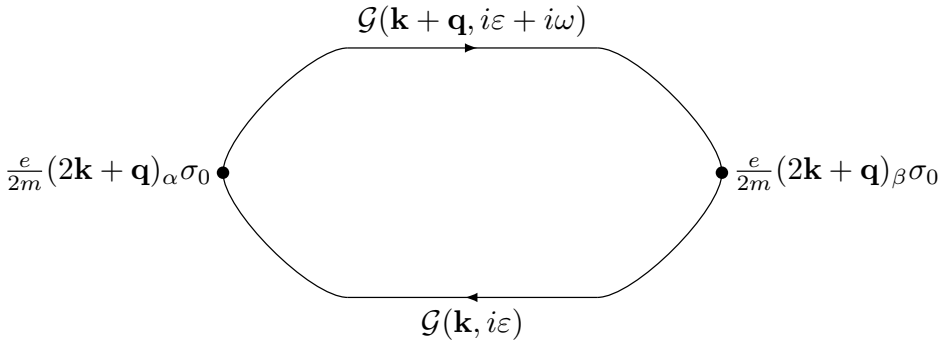

Figure 4.2: Diagrammatic representation of the linear response of a superconductor to an electromagnetic field

we will take the small momentum limit, $|\mathbf{q}| \to 0$ and $|\mathbf{k}| \sim k_F$, leading to

$$\mathcal{G}^E_{\alpha\beta}(0, i\omega) = \frac{e^2 k_F^2 N(0)}{3m^2}\delta_{\alpha\beta}\int_{-\infty}^{\infty} \mathrm{d}\xi_k\, T\sum_{\varepsilon} \mathrm{Tr}\left[\frac{i\bar{\varepsilon} + \xi_k\sigma_z - \bar{\Delta}\sigma_x}{\bar{\varepsilon}^2 + \xi_k^2 + \bar{\Delta}^2}\frac{i\bar{\varepsilon}' + \xi_k\sigma_z - \bar{\Delta}'\sigma_x}{\bar{\varepsilon}'^2 + \xi_k^2 + \bar{\Delta}'^2}\right], \tag{4.50}$$

where $\bar{\varepsilon}' = \bar{\varepsilon} + \omega$, $\bar{\Delta} = \bar{\Delta}(\varepsilon)$ and $\bar{\Delta}' = \bar{\Delta}(\varepsilon + \omega)$. We can invert the order of the sum and integral to obtain the linear response function, as we will have an exact cancellation with the diamagnetic term. This must be the case because at any stage we could take the limit $\Delta \to 0$ and the calculation should collapse to the normal state calculation. Thus we have

$$\mathcal{K}^E_{\alpha\beta}(0, i\omega) = \frac{ne^2}{2m}\delta_{\alpha\beta}T\sum_{\varepsilon}\int_{-\infty}^{\infty} \mathrm{d}\xi_k\, \mathrm{Tr}\left[\frac{i\bar{\varepsilon} + \xi_k\sigma_z - \bar{\Delta}\sigma_x}{\bar{\varepsilon}^2 + \xi_k^2 + \bar{\Delta}^2}\frac{i\bar{\varepsilon}' + \xi_k\sigma_z - \bar{\Delta}'\sigma_x}{\bar{\varepsilon}'^2 + \xi_k^2 + \bar{\Delta}'^2}\right]. \tag{4.51}$$

The only terms in the trace that will give a non-zero contribution are the terms that carry a identity matrix, which will give $\mathrm{Tr}\{\sigma_0\} = 2$. This leads to

$$\mathcal{K}^E_{\alpha\beta}(0, i\omega) = \frac{ne^2}{m}\delta_{\alpha\beta}T\sum_{\varepsilon}\int_{-\infty}^{\infty} \mathrm{d}\xi_k\, \frac{\xi_k^2 - \bar{\varepsilon}\bar{\varepsilon}' + \bar{\Delta}\bar{\Delta}'}{(\xi_k^2 + \bar{E}^2)(\xi_k^2 + \bar{E}'^2)}, \tag{4.52}$$

where $\bar{E}^2 = \bar{\varepsilon}^2 + \bar{\Delta}^2$ and $\bar{E}'^2 = \bar{\varepsilon}'^2 + \bar{\Delta}'^2$. These integrals can be performed using the standard results

$$\int_{-\infty}^{\infty} \mathrm{d}\xi\, \frac{\xi^2}{(\xi^2 + a^2)(\xi^2 + b^2)} = \frac{\pi}{a + b} \tag{4.53a}$$

$$\text{and} \quad \int_{-\infty}^{\infty} \mathrm{d}\xi\, \frac{1}{(\xi^2 + a^2)(\xi^2 + b^2)} = \frac{\pi}{ab(a + b)}, \tag{4.53b}$$

subject to the condition $\mathrm{Re}\{a\}, \mathrm{Re}\{b\} > 0$ (this will be of importance later when it comes to analytic continuation). Using the above results yields

$$\mathcal{K}^E_{\alpha\beta}(0, i\omega) = \frac{\pi ne^2}{m}\delta_{\alpha\beta}T\sum_{\varepsilon}\frac{\bar{E}\bar{E}' + \bar{\Delta}\bar{\Delta}' - \bar{\varepsilon}\bar{\varepsilon}'}{\bar{E}\bar{E}'(\bar{E} + \bar{E}')}. \tag{4.54}$$

Using the relations in equation 4.38 and cancelling the factors in the denominator and numerator, along with the additional relation,

$$\bar{E} = \frac{1}{2\tau_0}(1 + 2\tau_0 E)\,, \tag{4.55}$$

we can obtain an expression for the linear response entirely in terms of the unperturbed frequency and gap parameters,

$$\mathcal{K}^E_{\alpha\beta}(0, i\omega) = \frac{\pi n e^2 \tau_0}{m}\delta_{\alpha\beta} T \sum_{\varepsilon} \frac{EE' + \Delta^2 - \varepsilon\varepsilon'}{EE'(1 + \tau_0 E + \tau_0 E')}\,. \tag{4.56}$$

To calculate the number density of superconducting electrons, n_s, we take the limit $\omega \to 0$ and use the relation

$$\mathcal{K}^E_{\alpha\beta}(0, 0) = \frac{n_s e^2}{m}\delta_{\alpha\beta}\,. \tag{4.57}$$

This relationship can be understood because the condensate's response to the applied field will be purely diamagnetic. The only contributions to the paramagnetic part will be from quasiparticle excitations out of the condensate, leading to a result of order ω. So when we take the limit $\omega \to 0$ the paramagnetic part will vanish leaving only the diamagnetic part, with only the superconducting electrons contributing to it, hence why it has the factor of n_s. When we take $\omega \to 0$ the linear response function becomes

$$\begin{aligned}\mathcal{K}^E_{\alpha\beta}(0, 0) =& \frac{\pi n e^2 \tau_0}{m}\delta_{\alpha\beta} T \sum_{\varepsilon} \frac{E^2 + \Delta^2 - \varepsilon^2}{E^2(1 + 2\tau_0 E)} \\ =& \frac{2\pi n e^2 \tau_0}{m}\delta_{\alpha\beta} T \sum_{\varepsilon} \frac{\Delta^2}{(\varepsilon^2 + \Delta^2)(1 + 2\tau_0\sqrt{\varepsilon^2 + \Delta^2})}\,.\end{aligned} \tag{4.58}$$

Using equation 4.57 we obtain for the superconducting carrier density,

$$n_s = 2\pi n \tau_0 T \sum_{\varepsilon} \frac{\Delta^2}{(\varepsilon^2 + \Delta^2)(1 + 2\tau_0\sqrt{\varepsilon^2 + \Delta^2})}\,. \tag{4.59}$$

In this model the gap does not depend on the frequency of the applied field, ω, so we have taken $\Delta = \Delta'$.

Using this expression we can examine the two extreme limits: the dirty case ($1 \gg \Delta\tau_0$) and the clean case ($1 \ll \Delta\tau_0$). Because the $2\tau_0\sqrt{\varepsilon^2 + \Delta^2}$ term is of order $\Delta\tau_0$, in the clean case we have

$$n_{s,0} = \pi n T \sum_{\varepsilon} \frac{\Delta^2}{(\varepsilon^2 + \Delta^2)^{\frac{3}{2}}}\,, \tag{4.60}$$

but we are going to be primarily interested in superconductors with impurities so we will not invest any more time into the clean limit. In the dirty limit the superconducting carrier density is given by

$$n_s = 2\pi n \tau_0 T \sum_{\varepsilon} \frac{\Delta^2}{\varepsilon^2 + \Delta^2}. \tag{4.61}$$

Using the standard method to convert a Matsubara sum into a contour integral, shown in appendix E, we obtain

$$\begin{aligned} n_s =& -2\pi n \Delta^2 \tau_0 \frac{i}{2\pi} \oint_\Gamma \mathrm{d}z\, \frac{f(z)}{(z-\Delta)(z+\Delta)} \\ =& -\pi n \Delta \tau_0 [f(\Delta) - f(-\Delta)] \\ =& \pi n \Delta \tau_0 \tanh \frac{\Delta}{2T}\,. \end{aligned} \tag{4.62}$$

4.3.2 Long-wavelength Response to an Alternating Electromagnetic Field

Continuing in the dirty limit, we can calculate the full ω dependence of the linear response function, with $\mathbf{q} \to 0$; meaning a long-wavelength response. As we mentioned earlier, this corresponds to infrared absorption and transmission in the superconductor.

Equation 4.56 in the dirty limit reduces to

$$\begin{aligned}\mathcal{K}^E_{\alpha\beta}(0,i\omega) =& \frac{\pi n e^2 \tau_0}{m}\delta_{\alpha\beta} T \sum_{\varepsilon}\left(1+\frac{\Delta^2-\varepsilon\varepsilon'}{EE'}\right)\\ =& \frac{\pi n e^2 \tau_0}{m}\delta_{\alpha\beta} T \sum_{\varepsilon}\left(1+\frac{\Delta^2+i\varepsilon(i\varepsilon+i\omega)}{\sqrt{\Delta^2-(i\varepsilon)^2}\sqrt{\Delta^2-(i\varepsilon+i\omega)^2}}\right).\end{aligned} \tag{4.63}$$

Because the response is purely diagonal we will drop the α and β notation. Now we can cast the sum into a contour integral using the usual method

$$\mathcal{K}^E(i\omega) = \frac{\pi n e^2 \tau_0}{m}\frac{i}{2\pi}\oint_\Gamma \mathrm{d}z\, f(z)\left(1+\frac{z(z+i\omega)+\Delta^2}{\sqrt{\Delta^2-z^2}\sqrt{\Delta^2-(z+i\omega)^2}}\right). \tag{4.64}$$

The first term has no poles in the the plane outside of the contour and no branch cuts, as shown in the left-hand side of figure 4.3, so this term will evaluate to zero trivially. For the second term the contour can be deformed to enclose the branch cuts that occur due to the square roots, as shown in the right-hand side of figure 4.3, and hence can be written as four contributions: Γ_a through Γ_d.

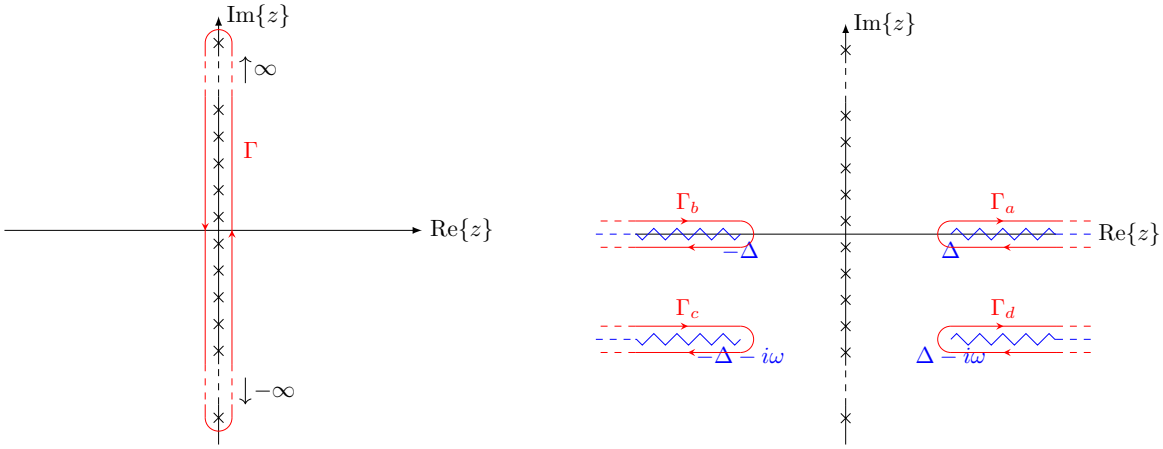

Figure 4.3: The contour that arises when the sum over Matsubara frequencies in the linear response function for a superconductor in an electromagnetic field is converted into a contour integral. The first term in the response function does not contain any poles or branch cuts, shown in the left figure. The second term has two branch cuts due to the square roots and so the contour can be deformed to enclose them, as shown in the right figure.

Our objective here is to eventually analytically continue $i\omega \mapsto \omega + i\delta$ in order to find the linear response in term of real frequencies, however this poses potential problems, as we will moving the branch cut down to the real axis, whilst it is enclosed by a contour. However, we may circumvent any potential dangers with the analytic continuation by removing the contours that enclose the lower two branch cuts, using the transformation $z \mapsto -z - i\omega$. This maps Γ_c and Γ_d exactly to Γ_a and Γ_b respectively, the integrals picking up a minus sign in the process. The Fermi function maps as $f(z) \mapsto f(-z - i\omega) = f(-z)$; using the fact that ω is a Bosonic Matsubara frequency. So all together, using this transformation yields

$$\begin{aligned}
&\frac{i}{2\pi}\oint_{\Gamma} \mathrm{d}z\, f(z) \frac{z(z+i\omega)+\Delta^2}{\sqrt{\Delta^2 - z^2}\sqrt{\Delta^2-(z+i\omega)^2}} \\
=&\frac{i}{2\pi}\int_{\Gamma_a+\Gamma_b} \mathrm{d}z\, (f(z) - f(-z)) \frac{z(z+i\omega)+\Delta^2}{\sqrt{\Delta^2 - z^2}\sqrt{\Delta^2-(z+i\omega)^2}} \\
=&\frac{1}{2\pi i}\int_{\Gamma_a+\Gamma_b} \mathrm{d}z \tanh\Big(\frac{z}{2T}\Big) \frac{z(z+i\omega)+\Delta^2}{\sqrt{\Delta^2 - z^2}\sqrt{\Delta^2-(z+i\omega)^2}}\,. \qquad (4.65)
\end{aligned}$$

Now we are able to analytically continue $i\omega \mapsto \omega + i\delta$ without issue, yielding

$$\mathcal{K}^E(\omega) = \frac{\pi n e^2 \tau_0}{m} \frac{1}{2\pi i}\int_{\Gamma_a+\Gamma_b} \mathrm{d}z \tanh\Big(\frac{z}{2T}\Big) \frac{z(z+\omega)+\Delta^2}{\sqrt{\Delta^2 - z^2}\sqrt{\Delta^2-(z+\omega)^2}}\,, \qquad (4.66)$$

and shifting the contours to those shown in figure 4.4. When $\omega < 2\Delta$ the appropriate contour is that of on the left of the figure and when $\omega > 2\Delta$ one will have a contour of the form on the right.

Taking $z \mapsto x \pm i\delta$ above and below the real axis respectively we can obtain an integral along the real axis, but whilst doing so we must ensure the the sign of the square roots is consistent with the condition enforced by the integrals over ξ performed earlier. The conditions require that $\mathrm{Re}\big\{\sqrt{\Delta^2 - z^2}\big\} > 0$ and $\mathrm{Re}\Big\{\sqrt{\Delta^2-(z+\omega)^2}\Big\} > 0$. Beginning with Γ_a, we can expand out the square root that corresponds to this branch cut into its

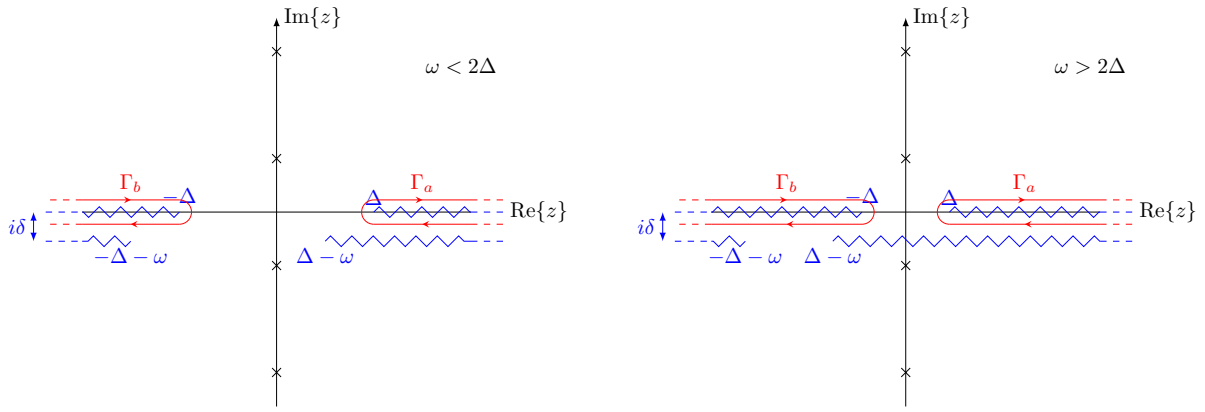

Figure 4.4: The contours in the integral in the linear response function after the lower two contours have been mapped to the upper two and the external frequency, $i\omega$, has been analytically continued to real frequency, $\omega + i\delta$. The left and right figures show the two distinct regimes: when $\omega < 2\Delta$ the lower contour does not crossover with the contour on the opposite side and when $\omega > 2\Delta$ it does. The two regimes lead to different integrals along the real axis due to the different signs of the square roots in the regions of integration relative to the positions of the branch cuts.

real and imaginary parts as follows,

$$\sqrt{\Delta^2 - z^2} \mapsto \sqrt{\Delta^2 - (x \pm i\delta)^2} \simeq \pm i\sqrt{x^2 - \Delta^2}\left[1 \pm \frac{i\delta x}{x^2 - \Delta^2} + \mathcal{O}(\delta^2)\right], \tag{4.67}$$

where we must choose the sign in front of the expression such that the real term is positive.

Since on this branch we have $x > \Delta$,

$$\sqrt{\Delta^2 - z^2} \mapsto -i\sqrt{x^2 - \Delta^2}\,, \quad \text{when} \quad z \mapsto x + i\delta\,, \tag{4.68a}$$

$$\text{and} \quad \sqrt{\Delta^2 - z^2} \mapsto i\sqrt{x^2 - \Delta^2}\,, \quad \text{when} \quad z \mapsto x - i\delta\,. \tag{4.68b}$$

For the Γ_b contour we have the same process except $x < -\Delta$, so

$$\sqrt{\Delta^2 - z^2} \mapsto i\sqrt{x^2 - \Delta^2}\,, \quad \text{when} \quad z \mapsto x + i\delta\,, \tag{4.69a}$$

$$\text{and} \quad \sqrt{\Delta^2 - z^2} \mapsto -i\sqrt{x^2 - \Delta^2}\,, \quad \text{when} \quad z \mapsto x - i\delta\,. \tag{4.69b}$$

All of the contours lie above the branch cut that arises from the $\sqrt{\Delta^2 - (z + \omega)^2}$ term, so by simply making the substitution $x \mapsto x + \omega$, we can use the same process as above

but we only require the $z+\omega \mapsto x+\omega+i\delta$ part. Therefore

$$\sqrt{\Delta^2-(z+\omega)^2} \mapsto -i\sqrt{(x+\omega)^2-\Delta^2} \quad \text{for} \quad x > \Delta-\omega\,, \tag{4.70a}$$

$$\text{and} \quad \sqrt{\Delta^2-(z+\omega)^2} \mapsto i\sqrt{(x+\omega)^2-\Delta^2} \quad \text{for} \quad x < -\Delta-\omega\,. \tag{4.70b}$$

However, there is the third region to consider, $-\Delta-\omega < x < -\Delta$ when $\omega < 2\Delta$ and $-\Delta-\omega < x < \Delta-\omega$ when $\omega > 2\Delta$, where the contour is not directly over the lower branch cut, and so the value of the square root is real without having to pull out a factor of $\pm i$. Thus is this region we will have

$$\begin{aligned} &\sqrt{\Delta^2-(z+\omega)^2} \mapsto \sqrt{\Delta^2-(x+\omega)^2} \\ &\quad \text{for} \quad -\Delta-\omega < x < -\Delta \quad \text{when} \quad x < 2\Delta\,, \\ &\quad \text{or} \quad -\Delta-\omega < x < \omega-\Delta \quad \text{when} \quad x > 2\Delta\,. \end{aligned} \tag{4.71}$$

Using the above results we can write the response function in terms of integrals along the real axis. When $\omega < 2\Delta$ we have

$$\begin{aligned} \mathcal{K}^E(\omega) = \frac{\pi n e^2 \tau_0}{m}\Bigg[&\frac{i}{\pi}\int_{\Delta}^{\infty} \mathrm{d}x \tanh\Big(\frac{x}{2T}\Big) \frac{x(x+\omega)+\Delta^2}{\sqrt{x^2-\Delta^2}\sqrt{(x+\omega)^2-\Delta^2}} \\ &+ \frac{i}{\pi}\int_{-\infty}^{-\Delta-\omega} \mathrm{d}x \tanh\Big(\frac{x}{2T}\Big) \frac{x(x+\omega)+\Delta^2}{\sqrt{x^2-\Delta^2}\sqrt{(x+\omega)^2-\Delta^2}} \\ &- \frac{1}{\pi}\int_{-\Delta-\omega}^{-\Delta} \mathrm{d}x \tanh\Big(\frac{x}{2T}\Big) \frac{x(x+\omega)+\Delta^2}{\sqrt{x^2-\Delta^2}\sqrt{\Delta^2-(x+\omega)^2}} \Bigg]\,, \end{aligned} \tag{4.72}$$

where contributions from above and below the branch cut in each region are identical, giving a factor of two. For $\omega > 2\Delta$ there is an additional integral that appears due to the

region where the lower-right branch cut overlaps with the upper-left. In this case we have

$$\begin{aligned}\mathcal{K}^E(\omega) = \frac{\pi n e^2 \tau_0}{m}\Bigg[&\frac{i}{\pi}\int_{\Delta}^{\infty} \mathrm{d}x \tanh\Big(\frac{x}{2T}\Big)\frac{x(x+\omega)+\Delta^2}{\sqrt{x^2-\Delta^2}\sqrt{(x+\omega)^2-\Delta^2}} \\ &+\frac{i}{\pi}\int_{-\infty}^{-\Delta-\omega} \mathrm{d}x \tanh\Big(\frac{x}{2T}\Big)\frac{x(x+\omega)+\Delta^2}{\sqrt{x^2-\Delta^2}\sqrt{(x+\omega)^2-\Delta^2}} \\ &-\frac{1}{\pi}\int_{-\Delta-\omega}^{\Delta-\omega} \mathrm{d}x \tanh\Big(\frac{x}{2T}\Big)\frac{x(x+\omega)+\Delta^2}{\sqrt{x^2-\Delta^2}\sqrt{\Delta^2-(x+\omega)^2}} \\ &-\frac{i}{\pi}\int_{\Delta-\omega}^{-\Delta} \mathrm{d}x \tanh\Big(\frac{x}{2T}\Big)\frac{x(x+\omega)+\Delta^2}{\sqrt{x^2-\Delta^2}\sqrt{(x+\omega)^2-\Delta^2}}\Bigg]\end{aligned} \tag{4.73}$$

We will begin by examining the case where $\omega < 2\Delta$. We can symmetrise the integrals by making the substitution $x \mapsto x - \frac{\omega}{2}$ in the first term and $x \mapsto -x - \frac{\omega}{2}$ in the latter two terms, which leads to

$$\begin{aligned}\mathcal{K}^E(\omega) = \frac{n e^2 \tau_0}{m}\Bigg[&\int_{\Delta-\frac{\omega}{2}}^{\Delta+\frac{\omega}{2}} \mathrm{d}x \tanh\left(\frac{x+\frac{\omega}{2}}{2T}\right)\frac{(x+\frac{\omega}{2})(x-\frac{\omega}{2})+\Delta^2}{\sqrt{(x+\frac{\omega}{2})^2-\Delta^2}\sqrt{\Delta^2-(x-\frac{\omega}{2})^2}} \\ &-i\int_{\Delta+\frac{\omega}{2}}^{\infty} \mathrm{d}x \left(\tanh\left(\frac{x+\frac{\omega}{2}}{2T}\right)-\tanh\left(\frac{x-\frac{\omega}{2}}{2T}\right)\right)\frac{(x+\frac{\omega}{2})(x-\frac{\omega}{2})+\Delta^2}{\sqrt{(x+\frac{\omega}{2})^2-\Delta^2}\sqrt{(x-\frac{\omega}{2})^2-\Delta^2}}\Bigg]\end{aligned} \tag{4.74}$$

This is as far as we can go analytically for the frequency-dependent linear response in the dirty limit, whilst keeping the temperature and frequency dependencies. If one takes the limit $\omega \to 0$ the first term vanishes and the second term will give an integral over $\mathrm{sech}^2(x)$, reproducing the result in equation 4.62. Alternatively, we can solve for the linear response function exactly when $T = 0$.

In the $T \to 0$ limit, $\tanh\big(\frac{x}{2T}\big) \to \mathrm{sgn}(x)$. This means in the second term we will get a term of the form

$$\mathrm{sgn}(x+\frac{\omega}{2}) - \mathrm{sgn}(x-\frac{\omega}{2})\,. \tag{4.75}$$

In region of integration $x \geq \Delta + \frac{\omega}{2}$ both of the sgn's will be one and so this term will cancel to zero. In the first term the sgn is also one over the entire integration region,

therefore, after some slight rearrangement, we have

$$\mathcal{K}^E(\omega) = \frac{ne^2\tau_0}{m}\int_{\Delta-\frac{\omega}{2}}^{\Delta+\frac{\omega}{2}} \mathrm{d}x\, \frac{x^2 + \left(\Delta - \frac{\omega}{2}\right)\left(\Delta + \frac{\omega}{2}\right)}{\sqrt{x^2 - (\Delta - \frac{\omega}{2})^2}\sqrt{(\Delta + \frac{\omega}{2})^2 - x^2}}\,. \tag{4.76}$$

This integral can be written in the form

$$\mathcal{K}^E(\omega) = \frac{ne^2\tau_0}{m}\left[\int_b^a \mathrm{d}x\, \frac{x^2}{\sqrt{a^2-x^2}\sqrt{x^2-b^2}} + \int_b^a \mathrm{d}x\, \frac{ab}{\sqrt{a^2-x^2}\sqrt{x^2-b^2}}\right], \tag{4.77}$$

where $a = \Delta + \frac{\omega}{2}$ and $b = \Delta - \frac{\omega}{2}$. This can be written using standard results for elliptical integrals (given in results 218.00 and 218.01 in Byrd & Friedman [73]) to yield

$$\begin{aligned}\mathcal{K}^E(\omega) = \frac{ne^2\tau_0}{m}\Bigg[&\left(\Delta + \frac{\omega}{2}\right)E\left(\sqrt{1 - \frac{\left(\Delta - \frac{\omega}{2}\right)^2}{\left(\Delta + \frac{\omega}{2}\right)^2}}\right) \\ &+ \left(\Delta - \frac{\omega}{2}\right)F\left(\sqrt{1 - \frac{\left(\Delta - \frac{\omega}{2}\right)^2}{\left(\Delta + \frac{\omega}{2}\right)^2}}\right)\Bigg],\end{aligned} \tag{4.78}$$

where $E(k)$ the complete elliptic integral of the second kind and $F(k)$ is the complete elliptic integral of the first kind. Note $F(k)$ can be written exactly as a hypergeometric series if one desires, the form of which can also be found in Byrd & Friedman.

When $\omega > 2\Delta$ after symmetrising the integrals and taking the limit $T \to 0$, we find

$$\begin{aligned}\mathcal{K}^E(\omega) = \frac{ne^2\tau_0}{m}\Bigg[&\int_{\frac{\omega}{2}-\Delta}^{\frac{\omega}{2}+\Delta} \mathrm{d}x\, \frac{x^2 - \left(\frac{\omega}{2} - \Delta\right)\left(\frac{\omega}{2} + \Delta\right)}{\sqrt{x^2 - (\frac{\omega}{2} - \Delta)^2}\sqrt{(\frac{\omega}{2} + \Delta)^2 - x^2}} \\ &+ i\int_{\Delta-\frac{\omega}{2}}^{\frac{\omega}{2}-\Delta} \mathrm{d}x\, \frac{x^2 - \left(\frac{\omega}{2} - \Delta\right)\left(\frac{\omega}{2} + \Delta\right)}{\sqrt{(\frac{\omega}{2} - \Delta)^2 - x^2}\sqrt{(\frac{\omega}{2} + \Delta)^2 - x^2}}\Bigg].\end{aligned} \tag{4.79}$$

Noting the latter integral is even, the integrals can be written in the following form

$$\mathcal{K}^E(\omega) = \frac{ne^2\tau_0}{m}\left[\int_b^a \mathrm{d}x\, \frac{x^2 - ab}{\sqrt{a^2-x^2}\sqrt{x^2-b^2}} + 2i\int_0^b \mathrm{d}x\, \frac{x^2 - ab}{\sqrt{a^2-x^2}\sqrt{b^2-x^2}}\right], \tag{4.80}$$

where $a = \frac{\omega}{2} + \Delta$ and $b = \frac{\omega}{2} - \Delta$. The first integral can be solved with the same standard results as above, albeit with different definitions of a and b, and the latter can be solved

with Byrd & Friedman results 219.00 and 219.05, yielding

$$\mathcal{K}^E(\omega) = \frac{ne^2\tau_0}{m}\Bigg[4i\Delta F\left(\frac{\frac{\omega}{2}-\Delta}{\frac{\omega}{2}+\Delta}\right) - 2i\Big(\frac{\omega}{2}+\Delta\Big)E\left(\frac{\frac{\omega}{2}-\Delta}{\frac{\omega}{2}+\Delta}\right) + \Big(\frac{\omega}{2}+\Delta\Big)E\left(\sqrt{1-\frac{\left(\frac{\omega}{2}-\Delta\right)^2}{\left(\frac{\omega}{2}+\Delta\right)^2}}\right) - \Big(\frac{\omega}{2}-\Delta\Big)F\left(\sqrt{1-\frac{\left(\frac{\omega}{2}-\Delta\right)^2}{\left(\frac{\omega}{2}+\Delta\right)^2}}\right)\Bigg]. \tag{4.81}$$

The latter term is identical to that in equation 4.78 and so an equation valid for all ω can be written as

$$\mathcal{K}^E(\omega) = \frac{ne^2\tau_0}{m}\Bigg[i\Bigg[4\Delta F\left(\frac{\frac{\omega}{2}-\Delta}{\frac{\omega}{2}+\Delta}\right) - (\omega+2\Delta)E\left(\frac{\frac{\omega}{2}-\Delta}{\frac{\omega}{2}+\Delta}\right)\Bigg]\Theta(\omega-2\Delta) + \Big(\frac{\omega}{2}+\Delta\Big)E\left(\sqrt{1-\frac{\left(\frac{\omega}{2}-\Delta\right)^2}{\left(\frac{\omega}{2}+\Delta\right)^2}}\right) - \Big(\frac{\omega}{2}-\Delta\Big)F\left(\sqrt{1-\frac{\left(\frac{\omega}{2}-\Delta\right)^2}{\left(\frac{\omega}{2}+\Delta\right)^2}}\right)\Bigg]. \tag{4.82}$$

The real part of the linear response function physically corresponds to the diamagnetic reactivity of the condensate to the alternating applied field, and so is present at all ω. The imaginary part that appears at applied frequencies greater than 2Δ corresponds to excitations of the condensate that are now possible as the frequency is sufficiently high to excite cooper pairs. Because this contribution is imaginary it corresponds to a real part of the conductivity and hence is a measurable 'paramagnetic' response. If we were to calculate this with $T \neq 0$ there would also be a imaginary contribution to the linear response function from the term with the difference of tanh-functions. This term would be another contribution to the paramagnetic response, but now from the quasi-particles that are thermally excited out of the condensate.

4.4 Thermal Conductivity of a Superconductor

The thermal conductivity behaves in a qualitatively different manner to that of of electrical conductivity. This is because the superconducting condensate does not carry entropy, and so does not contribute to thermal conductivity. In other words, there is no 'super'-thermal

current; the only contributions to the thermal conductivity from the electrons will be from those that are not in the condensate. Hence we will calculate the the thermal conductivity, κ, and expect a finite result that tends to zero at $T = 0$.

In the thermal case, in exact analogy to the normal state, the heat current operator will have an additional partial time derivative compared to the electrical current operator; this was shown by Luttinger [33]. Therefore ,we can find the appropriate linear response function for the response to a thermal gradient by constructing a bubble diagram in the same way as for the linear response to an electromagnetic field; the only difference being we will have an additional factor proportional to the average of the Matsubara frequencies from the vertices. This diagrammatic approach was first taken by Ambegaokar and Tewordt [30], following on from earlier papers that used Boltzmann transport equations [58, 74].

Now that we are in a 2×2 matrix formulation we must also be careful about which Pauli matrix the vertex carries. In this case there is an addition minus sign on the down-spin term so we will have a σ_z, as opposed to a σ_0. Hence, in the small q limit the vertex contributions will be given by

$$\frac{\mathbf{k}_F}{m}\left(i\varepsilon + \frac{i\omega}{2}\right)_\alpha \sigma_z \,. \tag{4.83}$$

The bubble diagram is shown in figure 4.5, with the small q limit already taken, and leads to the equation for the heat current - heat current Green's function,

$$\mathcal{G}^T_{\alpha\beta}(i\omega) = \frac{T}{m^2\mathcal{V}} \sum_{\mathbf{k}} \sum_{\varepsilon} \mathbf{k}_{F\alpha}\mathbf{k}_{F\beta}\left(i\varepsilon + \frac{i\omega}{2}\right)^2 \mathrm{Tr}\left[\sigma_z \frac{i\bar{\varepsilon} + \xi\sigma_z - \bar{\Delta}\sigma_x}{\bar{\varepsilon}^2 + \xi^2 + \bar{\Delta}^2}\sigma_z \frac{i\bar{\varepsilon}' + \xi\sigma_z - \bar{\Delta}'\sigma_x}{\bar{\varepsilon}'^2 + \xi^2 + \bar{\Delta}'^2}\right] \tag{4.84}$$

This calculation proceeds, up until the sum over ε, almost identically to the electrical calculation of the previous section. The difference is the extra σ_z terms in the trace, which will simply switch the sign on the Δ term, as the σ_x will anti-commute with the σ_z, whereas the other terms commute. The integral over ξ_k can be completed again with

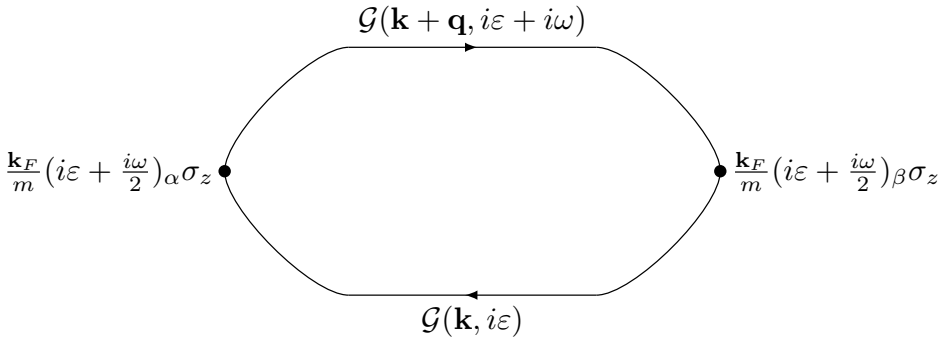

Figure 4.5: Diagrammatic representation of the linear response of of a superconductor to a thermal gradient

the results in equation 4.53 leading to

$$\mathcal{K}^T_{\alpha\beta}(i\omega) = \frac{\pi n \tau_0}{m}\delta_{\alpha\beta} T \sum_\varepsilon \left(i\varepsilon + \frac{i\omega}{2}\right)^2 \frac{EE' - \Delta^2 - \varepsilon\varepsilon'}{EE'(1 + \tau_0 E + \tau_0 E')}\,. \tag{4.85}$$

Examining the dirty limit ($\tau_0 E \ll 1$) we have

$$\mathcal{K}^T_{\alpha\beta}(i\omega) = \frac{\pi n \tau_0}{m}\delta_{\alpha\beta} T \sum_\varepsilon \left(i\varepsilon + \frac{i\omega}{2}\right)^2 \left[1 + \frac{i\varepsilon(i\varepsilon + i\omega) - \Delta^2}{\sqrt{\Delta^2 - (i\varepsilon)^2}\sqrt{\Delta^2 - (i\varepsilon + i\omega)^2}}\right]. \tag{4.86}$$

Next, we convert the Matsubara sum into a contour integral in the z-plane, and the first term will evaluate to zero as there are no poles or branch cuts on the exterior of the contour, leading to

$$\mathcal{K}^T_{\alpha\beta}(i\omega) = \frac{\pi n \tau_0}{m}\delta_{\alpha\beta}\frac{i}{2\pi}\oint_\Gamma \mathrm{d}z\, f(z)\left(z + \frac{i\omega}{2}\right)^2 \frac{z(z + i\omega) - \Delta^2}{\sqrt{\Delta^2 - z^2}\sqrt{\Delta^2 - (z + i\omega)^2}}\,, \tag{4.87}$$

where the contour is the same as in the right-hand side of figure 4.3. We can make the transformation $z \mapsto -z - i\omega$ in the lower two contours to map them to the upper two in the same way as in equation 4.65, because this transformation is still consistent with the additional $(\varepsilon + i\omega/2)$ term. This yields

$$\mathcal{K}^T_{\alpha\beta}(i\omega) = \frac{\pi n \tau_0}{m}\delta_{\alpha\beta}\frac{1}{2\pi i}\int_{\Gamma_a + \Gamma_b} \mathrm{d}z \tanh\left(\frac{z}{2T}\right)\left(z + \frac{i\omega}{2}\right)^2 \frac{z(z + i\omega) - \Delta^2}{\sqrt{\Delta^2 - z^2}\sqrt{\Delta^2 - (z + i\omega)^2}}\,. \tag{4.88}$$

The analytical continuation of $i\omega \mapsto \omega + i\delta$ and $z \mapsto x \pm i\delta$ can be completed fully in analogy with the previous section the only notable difference being after the symmetrisation $x \mapsto x \pm \omega/2$ in the respective terms the $(x+\omega/2)^2$ term will map to x^2. Furthermore, because this is thermal conductivity, we will eventually want to take the limiting case $\omega \to 0$, so we only need consider the contours in the case where $\omega < 2\Delta$. So in conclusion, for the most general expression for the frequency-dependent thermal linear response with $\omega < 2\Delta$, we have

$$\mathcal{K}^T_{\alpha\beta}(\omega) = \frac{n\tau_0}{m}\delta_{\alpha\beta}\Bigg[\int_{\Delta-\frac{\omega}{2}}^{\Delta+\frac{\omega}{2}} \mathrm{d}x\, x^2 \tanh\left(\frac{x+\frac{\omega}{2}}{2T}\right)\frac{(x+\frac{\omega}{2})(x-\frac{\omega}{2})+\Delta^2}{\sqrt{(x+\frac{\omega}{2})^2-\Delta^2}\sqrt{\Delta^2-(x-\frac{\omega}{2})^2}} \\ - i\int_{\Delta+\frac{\omega}{2}}^{\infty} \mathrm{d}x\, x^2\left(\tanh\left(\frac{x+\frac{\omega}{2}}{2T}\right)-\tanh\left(\frac{x-\frac{\omega}{2}}{2T}\right)\right)\frac{(x+\frac{\omega}{2})(x-\frac{\omega}{2})+\Delta^2}{\sqrt{(x+\frac{\omega}{2})^2-\Delta^2}\sqrt{(x-\frac{\omega}{2})^2-\Delta^2}}\Bigg]. \tag{4.89}$$

Next we will proceed with taking the limit $\omega \to 0$. In this case we will be seeking a solution for $T \neq 0$, as we expect the thermal conductivity to be identically zero at $T = 0$. When we take $\omega \to 0$ the first term will vanish, as its integration region tends to zero and the integrand is finite. In the second term the limit of the difference of tanh's will yield a sech^2 as follows,

$$\begin{aligned}\lim_{\omega\to 0}\left[\tanh\left(\frac{x+\frac{\omega}{2}}{2T}\right)-\tanh\left(\frac{x-\frac{\omega}{2}}{2T}\right)\right] &= \omega\lim_{\omega\to 0}\frac{\tanh\left(\frac{x+\frac{\omega}{2}}{2T}\right)-\tanh\left(\frac{x-\frac{\omega}{2}}{2T}\right)}{\omega} \\ &= \omega\frac{\mathrm{d}}{\mathrm{d}x}\tanh\left(\frac{x}{2T}\right) \\ &= \frac{\omega}{2T}\,\mathrm{sech}^2\left(\frac{x}{2T}\right).\end{aligned} \tag{4.90}$$

Furthermore, the numerator and denominator will cancel in this limit, leaving us with

$$\mathcal{K}^T_{\alpha\beta} = \frac{n\tau_0\delta_{\alpha\beta}}{m}\frac{-i\omega}{2T}\int_{\Delta}^{\infty}\mathrm{d}x\, x^2\,\mathrm{sech}^2\left(\frac{x}{2T}\right). \tag{4.91}$$

The final step to obtain the thermal conductivity is to divide the linear response function

by $-i\omega$, therefore

$$T\kappa_s = \frac{n\tau_0}{2mT}\int_{\Delta}^{\infty} \mathrm{d}x\, x^2 \,\mathrm{sech}^2\left(\frac{x}{2T}\right), \tag{4.92}$$

which in agreement with the result presented in Ambegaokar and Griffin [75]. We may also make the substitution $2Ty = x$ to obtain

$$T\kappa_s = \frac{4n\tau_0 T^2}{m}\int_{\frac{\Delta}{2T}}^{\infty} \mathrm{d}y\, y^2 \,\mathrm{sech}^2\left(y\right) \tag{4.93}$$

Although this integral is not analytically tractable and would have to be computed numerically, we can verify that we obtain the normal state thermal conductivity by taking the limit, $\Delta \to 0$. This limit yields

$$T\kappa_n = \frac{4n\tau_0 T^2}{m}\int_{0}^{\infty} \mathrm{d}y\, y^2 \,\mathrm{sech}^2\left(y\right), \tag{4.94}$$

where we can now use the standard result for this integral,

$$\int_{0}^{\infty} \mathrm{d}y\, y^2 \,\mathrm{sech}^2\left(y\right) = \frac{\pi^2}{12}, \tag{4.95}$$

yielding the normal state result as expected.

It can be informative to examine the ratio of the superconducting and normal state results, the prefactors will cancel and we have

$$\frac{\kappa_s}{\kappa_n} = \frac{\int_{\frac{\Delta(T)}{2T}}^{\infty} \mathrm{d}y\, y^2 \,\mathrm{sech}^2\left(y\right)}{\int_{0}^{\infty} \mathrm{d}y\, y^2 \,\mathrm{sech}^2\left(y\right)}. \tag{4.96}$$

So the only difference between the two results is the lower limit of the integral. However, this is deceptively complex because all the temperature dependence is in this limit, remembering that the gap is a function of temperature that has to be determined self consistently (equation 4.22). When this is calculated (either numerically or one can refer back to the work of Bardeen et. al. for an analytic expression [58]) and plotted it shows

the quick suppression of the conductivity as the temperature in decreased below T_c, as can be seen in figure 1.3 in the Introduction.

CHAPTER 5

WEAK LOCALISATION IN A DIRTY SUPERCONDUCTOR

In this chapter we will develop the theory of weak localisation in superconductors. We will begin the first section by calculating the cooperon as a stand-alone term that can then be used in the weak localisation bubble diagram. We make use of the outer-product of Pauli matrices to encode the matrix structure carried on the two vertices of the cooperon. In section 5.2, we calculate the linear response function for the weak localisation to the electrical conductivity, which could be used to calculate the correction to superconducting carrier density [59] or the correction to the linear absorption [61]. However, because we are primarily interested in the thermal conductivity of superconductors, we move on in section 5.3 to calculating the weak localisation correction to the electronic thermal conductivity in dirty superconductors, as usual examining the $\omega \to 0$ limit. We end this section by comparing our results with those of González Rosado et. al. [63]. As well as examining the ratio of the weak localisation correction to the leading order conductivity and draw comparisons to the equivalent ratio in the normal state.

5.1 Calculation of the Cooperon in the Superconducting State

When we calculated the form of the cooperon in the normal state, we did not need to be concerned with the order of Green's functions and interaction vertices. However, in the superconducting state we have seen that we must take the trace over all of the elements of the diagram, the order of which being the order in which those terms appear as we move around the loop. The cooperon connects the upper and lower Nambu Green's functions, so the two vertices of the cooperon will appear at different points in order of the trace. To be able to calculate the cooperon in the superconducting state in isolation (to then use as a term in the weak-localisation bubbles later) we can use a outer-product of the Pauli matrices carried by the upper and lower vertex of the impurity interaction lines to maintain all the information about the cooperon's vertices. In this regime the Dyson equation is constructed in the same way as in section 3.3 with

$$\Gamma_{\mathrm{C}}(\mathbf{q}, i\varepsilon, i\varepsilon + i\omega) = \Gamma_0 + \Gamma_0 \Sigma_{\mathrm{C}}(\mathbf{q}, i\varepsilon, i\varepsilon + i\omega)\Gamma_{\mathrm{C}}(\mathbf{q}, i\varepsilon, i\varepsilon + i\omega)\,. \tag{5.1}$$

Only now we have

$$\Gamma_0 = \frac{1}{2\pi N(0)\tau_0}\sigma_z \otimes \sigma_z \tag{5.2}$$

$$\text{and} \quad \Sigma_{\mathrm{C}}(\mathbf{q}, i\varepsilon, i\varepsilon + i\omega) = \frac{1}{\mathcal{V}}\sum_k \mathcal{G}(\mathbf{q} - \mathbf{k}, i\varepsilon + i\omega) \otimes \mathcal{G}(\mathbf{k}, i\varepsilon)\,. \tag{5.3}$$

Inserting in the Nambu Green's functions and taking leading order in $\mathbf{q}$, we have

$$\Sigma_{\mathrm{C}}(\mathbf{q}, i\varepsilon, i\varepsilon') = N(0)\int \frac{\mathrm{d}\Omega}{4\pi}\int_{-\infty}^{\infty} \mathrm{d}\xi_k \, \frac{(i\bar{\varepsilon}' + (\xi_k - \mu_\theta)\sigma_z - \bar{\Delta}'\sigma_x) \otimes (i\bar{\varepsilon} + \xi_k\sigma_z - \bar{\Delta}\sigma_x)}{(\bar{\varepsilon}'^2 + (\xi_k - \mu_\theta)^2 + \bar{\Delta}'^2)(\bar{\varepsilon}^2 + \xi_k^2 + \bar{\Delta}^2)}\,, \tag{5.4}$$

where $\mu_\theta = \mathbf{k}_F \cdot \mathbf{q}$. Keeping terms that are not odd in ξ_k we can write this as

$$\Sigma_{\mathrm{C}}(\mathbf{q}, i\varepsilon, i\varepsilon') = N(0) \int \frac{\mathrm{d}\Omega}{4\pi} \Bigg[(i\bar{\varepsilon}' - \bar{\Delta}'\sigma_x) \otimes (i\bar{\varepsilon} - \bar{\Delta}\sigma_x) \int_{-\infty}^{\infty} \frac{\mathrm{d}\xi_k}{(\xi_k^2 + \bar{E}^2)((\xi_k - \mu_\theta)^2 + \bar{E}'^2)} + \sigma_z \otimes \sigma_z \int_{-\infty}^{\infty} \frac{\mathrm{d}\xi_k \, \xi_k(\xi_k - \mu_\theta)}{(\xi_k^2 + \bar{E}^2)((\xi_k - \mu_\theta)^2 + \bar{E}'^2)} \Bigg] . \tag{5.5}$$

The integrals over $\mathrm{d}\xi_k$ can both be solved straightforwardly using a contour integrals with the forms:

$$I_1 = \int_{-\infty}^{\infty} \frac{\mathrm{d}\xi}{(\xi^2 + a^2)((\xi + c)^2 + b^2)} = \frac{\pi(a+b)}{ab((a+b)^2 + c^2)} , \tag{5.6a}$$

$$I_2 = \int_{-\infty}^{\infty} \frac{\mathrm{d}\xi \; \xi(\xi + c)}{(\xi^2 + a^2)((\xi + c)^2 + b^2)} = \frac{\pi(a+b)}{(a+b)^2 + c^2} = abI_1 . \tag{5.6b}$$

Using these results we obtain

$$\Sigma_{\mathrm{C}}(\mathbf{q}, i\varepsilon, i\varepsilon') = N(0) \int \frac{\mathrm{d}\Omega}{4\pi} \frac{\pi(\bar{E} + \bar{E}')}{(\bar{E} + \bar{E}')^2 + \mu_\theta^2} \left[\sigma_z \otimes \sigma_z + \frac{(i\bar{\varepsilon}' - \bar{\Delta}'\sigma_x) \otimes (i\bar{\varepsilon} - \bar{\Delta}\sigma_x)}{\bar{E}\bar{E}'} \right] . \tag{5.7}$$

We can use the fact that we are in the diffusive limit to simplify the expression, because we can expand with respect to the the small parameters $\omega\tau_0$ and ql_0. First we use the fact that $\mu_\theta/(\bar{E} + \bar{E}')$ has dimensionality of ql_0 so we can expand to leading order,

$$\frac{\bar{E} + \bar{E}'}{(\bar{E} + \bar{E}')^2 + \mu_\theta^2} \simeq \frac{1}{\bar{E} + \bar{E}'} \left[1 - \left(\frac{\mu_\theta}{(\bar{E} + \bar{E}')^2} \right) + \mathcal{O}\big((ql_0)^4\big) \right] . \tag{5.8}$$

Now we can substitute $\bar{E}$ using equation 4.55 to obtain

$$\frac{\bar{E} + \bar{E}'}{(\bar{E} + \bar{E}')^2 + \mu_\theta^2} \simeq \tau_0 \left[\frac{1}{1 + \tau_0(E + E')} - \frac{(\mu_\theta \tau_0)^2}{(1 + \tau_0(E + E'))^3} \right] . \tag{5.9}$$

We can expand the first term to leading order in $\tau(\bar{E}+\bar{E}')$ and take the zeroth order term in the second, as this term is already leading order in ql_0,

$$\therefore \frac{\bar{E}+\bar{E}'}{(\bar{E}+\bar{E}')^2+\mu_\theta^2} \simeq \tau_0\big[1-\tau_0(E+E')-(\mu_\theta\tau_0)^2\big]\,. \tag{5.10}$$

Now we can complete the angular integral as the only non-trivial term is the one containing μ_θ, which for an isotropic system will simply yield a factor of d^{-1} (where d is the dimensionality of the system). So along with the relation $D=v_F^2\tau_0/d$ we have

$$\Sigma_{\mathrm{C}}(\mathbf{q},i\varepsilon,i\varepsilon') = \pi N(0)\tau_0\gamma\left[\sigma_z\otimes\sigma_z+\frac{(i\bar{\varepsilon}'-\bar{\Delta}'\sigma_x)\otimes(i\bar{\varepsilon}-\bar{\Delta}\sigma_x)}{\bar{E}\bar{E}'}\right] \tag{5.11}$$

$$\text{where}\quad \gamma = \big(1-(Dq^2+E+E')\tau_0\big)\,. \tag{5.12}$$

Finally, we can cancel the factors arising from the barred variables in the last term to obtain the expression for the cooperon self-energy

$$\Sigma_{\mathrm{C}}(\mathbf{q},i\varepsilon,i\varepsilon') = \pi N(0)\tau_0\gamma\left[\sigma_z\otimes\sigma_z+\frac{(i\varepsilon'-\Delta\sigma_x)\otimes(i\varepsilon-\Delta\sigma_x)}{EE'}\right]. \tag{5.13}$$

To obtain the form of the cooperon from the cooperon self-energy we can directly examine the first few terms of the Dyson equation. The first term to examine is

$$\Gamma_0\Sigma_{\mathrm{C}}\Gamma_0 = \frac{\gamma}{4\pi N(0)\tau_0}\sigma_z\otimes\sigma_z\left[\sigma_z\otimes\sigma_z+\frac{(i\varepsilon'-\Delta\sigma_x)\otimes(i\varepsilon-\Delta\sigma_x)}{EE'}\right]\sigma_z\otimes\sigma_z\,. \tag{5.14}$$

Remembering that the two sets of Pauli matrices making up the outer-product obey standard Pauli-commutation relations independently of each other, we can commute the σ_z terms through the self-energy part, the only non-trivial commutation of σ_x and σ_z resulting in a change of sign. So we obtain

$$\Gamma_0\Sigma_{\mathrm{C}}\Gamma_0 = \frac{\gamma}{4\pi N(0)\tau_0}\left[\sigma_z\otimes\sigma_z+\frac{(i\varepsilon'+\Delta\sigma_x)\otimes(i\varepsilon+\Delta\sigma_x)}{EE'}\right]. \tag{5.15}$$

To build up the infinite series from this term we simply need to multiply the previous expression by a factor of $\Gamma_0\Sigma_{\rm C}$,

$$\Gamma_0\Sigma_{\rm C}\Gamma_0\Sigma_{\rm C}\Gamma_0 = \frac{\gamma^2}{8\pi N(0)\tau_0}\sigma_z\otimes\sigma_z\left[\sigma_z\otimes\sigma_z + \frac{(i\varepsilon'-\Delta\sigma_x)\otimes(i\varepsilon-\Delta\sigma_x)}{EE'}\right] \times\left[\sigma_z\otimes\sigma_z + \frac{(i\varepsilon'+\Delta\sigma_x)\otimes(i\varepsilon+\Delta\sigma_x)}{EE'}\right]. \tag{5.16}$$

After expanding this expression out and using appropriate commutation relations, the above expression simplifies to

$$\Gamma_0\Sigma_{\rm C}\Gamma_0\Sigma_{\rm C}\Gamma_0 = \frac{\gamma^2}{4\pi N(0)\tau_0}\left[\sigma_z\otimes\sigma_z + \frac{(i\varepsilon'+\Delta\sigma_x)\otimes(i\varepsilon+\Delta\sigma_x)}{EE'}\right] = \gamma\Gamma_0\Sigma_{\rm C}\Gamma_0\,. \tag{5.17}$$

So we can see that for each term in the infinite series we apply another factor of $\Gamma_0\Sigma_{\rm C}$ which will lead to an additional factor of γ at each order in the series. Therefore the infinite ladder sum can be written as a infinite series in powers of γ like so

$$\begin{aligned}\Gamma_{\rm C} = &= \frac{1}{2\pi N(0)\tau_0}\sigma_z\otimes\sigma_z + \frac{1}{4\pi N(0)\tau_0}\left[\sigma_z\otimes\sigma_z + \frac{(i\varepsilon'+\Delta\sigma_x)\otimes(i\varepsilon+\Delta\sigma_x)}{EE'}\right]\sum_{n=1}^{\infty}\gamma^n \\ &= \frac{1}{4\pi N(0)\tau_0}\left[\sigma_z\otimes\sigma_z\left(1+\sum_{n=0}^{\infty}\gamma^n\right) + \frac{(i\varepsilon'+\Delta\sigma_x)\otimes(i\varepsilon+\Delta\sigma_x)}{EE'}\sum_{n=1}^{\infty}\gamma^n\right] \\ &= \frac{1}{4\pi N(0)\tau_0}\left[\sigma_z\otimes\sigma_z\left(1+\frac{1}{1-\gamma}\right) + \frac{(i\varepsilon'+\Delta\sigma_x)\otimes(i\varepsilon+\Delta\sigma_x)}{EE'}\left(\frac{\gamma}{1-\gamma}\right)\right]\end{aligned} \tag{5.18}$$

Because $Dq^2\tau_0$, $E\tau_0$ and $E'\tau_0$ are all small parameters this means that $\gamma\approx 1$ and hence to leading order

$$1+\frac{1}{1-\gamma}\approx\frac{\gamma}{1-\gamma}\approx\frac{1}{1-\gamma} = \frac{1}{(Dq^2+E+E')\tau_0}\,. \tag{5.19}$$

Therefore the form of the cooperon in the superconducting state is given by

$$\Gamma_{\rm C}(\mathbf{q},i\varepsilon,i\varepsilon') = \frac{1}{4\pi N(0)\tau_0^2}\frac{1}{Dq^2+E+E'}\left[\sigma_z\otimes\sigma_z + \frac{(i\varepsilon'+\Delta\sigma_x)\otimes(i\varepsilon+\Delta\sigma_x)}{EE'}\right] \tag{5.20}$$

5.2 Weak Localisation Correction to Electrical Conductivity in a Superconductor

To calculate the weak localisation correction to conductivity in the superconductor, the calculation can be constructed in analogy with the normal state calculation, by using the cooperon to calculate the infinite series of maximally-crossed diagrams. Except, we will of course be using the Nambu Green's functions and corresponding diagrammatic rules. The diagram we will calculate is shown in figure 5.1 and can be written as

$$\begin{aligned}\mathcal{G}^{\mathrm{WL},E}_{\alpha\beta}(0,i\omega) = \frac{e^2T}{m^2\mathcal{V}^2}\sum_{\mathbf{k},\mathbf{q}}\sum_{\varepsilon}\mathbf{k}_\alpha(\mathbf{q}-\mathbf{k})_\beta\frac{1}{4\pi N(0)\tau_0^2}\frac{1}{Dq^2+E+E'} \\ \times\Bigg[\mathrm{Tr}\left[\mathcal{G}(\mathbf{k},i\varepsilon')\sigma_z\mathcal{G}(\mathbf{q}-\mathbf{k},i\varepsilon')\mathcal{G}(\mathbf{q}-\mathbf{k},i\varepsilon)\sigma_z\mathcal{G}(\mathbf{k},i\varepsilon)\right] \\ +\frac{1}{\bar{E}\bar{E}'}\mathrm{Tr}\left[\mathcal{G}(\mathbf{k},i\varepsilon')(i\bar{\varepsilon}'+\bar{\Delta}'\sigma_x)\mathcal{G}(\mathbf{q}-\mathbf{k},i\varepsilon')\mathcal{G}(\mathbf{q}-\mathbf{k},i\varepsilon)(i\bar{\varepsilon}+\bar{\Delta}\sigma_x)\mathcal{G}(\mathbf{k},i\varepsilon)\right]\Bigg].\end{aligned} \tag{5.21}$$

Note that we have two terms due to the two terms in the cooperon with the σ_z and $(i\varepsilon - \Delta\sigma_x)$ terms placed appropriately in the trace. Also, we have restored the extra factors from the impurities in the second term to make the algebra from the commutation with the Green's functions somewhat neater. Applying the usual formula of inverting the order of the $\mathbf{k}$ and ε sums, taking small $\mathbf{q}$ and converting the $\mathbf{k}$ sum to an integral over

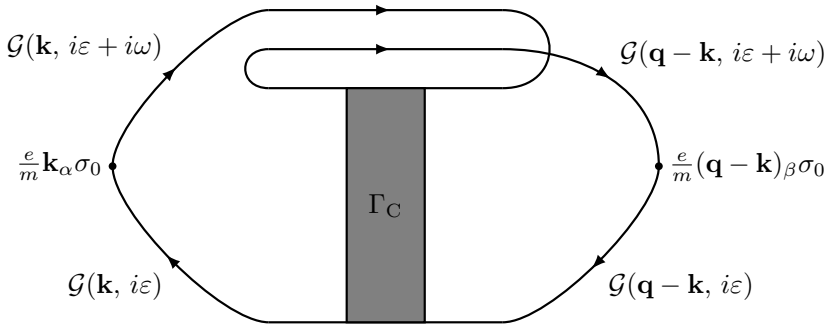

Figure 5.1: Diagrammatic representation of the weak localisation correction to electrical conductivity in a superconductor.

ξ, we can simplify and obtain the linear response function given by

$$\begin{aligned}\mathcal{K}^{\mathrm{WL},E}_{\alpha\beta}(0,i\omega) = &-\frac{e^2N(0)k_F^2}{m^2d}\delta_{\alpha\beta}\frac{1}{4\pi N(0)\tau_0}\frac{1}{\mathcal{V}}\sum_{\mathbf{q}}T\sum_{\varepsilon}\frac{1}{Dq^2+E+E'}\\ &\times\int_{-\infty}^{\infty}\mathrm{d}\xi\left[\mathrm{Tr}\left[\mathcal{G}(\mathbf{k},i\varepsilon')\sigma_z\mathcal{G}(\mathbf{k},i\varepsilon')\mathcal{G}(\mathbf{k},i\varepsilon)\sigma_z\mathcal{G}(\mathbf{k},i\varepsilon)\right]\right.\\ &\left.+\frac{1}{\bar{E}\bar{E}'}\mathrm{Tr}\left[\mathcal{G}(\mathbf{k},i\varepsilon')(i\bar{\varepsilon}'+\bar{\Delta}'\sigma_x)\mathcal{G}(\mathbf{k},i\varepsilon')\mathcal{G}(\mathbf{k},i\varepsilon)(i\bar{\varepsilon}+\bar{\Delta}\sigma_x)\mathcal{G}(\mathbf{k},i\varepsilon)\right]\right].\end{aligned} \tag{5.22}$$

To calculate the trace we can factor out the denominators from all of the Green's functions and hence we are left with two traces given by

$$\begin{aligned}\mathrm{Tr}_1 = \mathrm{Tr}\big[&(i\bar{\varepsilon}'+\xi\sigma_z-\bar{\Delta}'\sigma_x)\sigma_z(i\bar{\varepsilon}'+\xi\sigma_z-\bar{\Delta}'\sigma_x)\\ &\times(i\bar{\varepsilon}+\xi\sigma_z-\bar{\Delta}\sigma_x)\sigma_z(i\bar{\varepsilon}+\xi\sigma_z-\bar{\Delta}\sigma_x)\big]\end{aligned} \tag{5.23a}$$

$$\begin{aligned}\text{and}\quad \mathrm{Tr}_2 = \mathrm{Tr}\big[&(i\bar{\varepsilon}'+\xi\sigma_z-\bar{\Delta}'\sigma_x)(i\bar{\varepsilon}'+\bar{\Delta}'\sigma_x)(i\bar{\varepsilon}'+\xi\sigma_z-\bar{\Delta}'\sigma_x)\\ &\times(i\bar{\varepsilon}+\xi\sigma_z-\bar{\Delta}\sigma_x)(i\bar{\varepsilon}+\bar{\Delta}\sigma_x)(i\bar{\varepsilon}+\xi\sigma_z-\bar{\Delta}\sigma_x)\big].\end{aligned} \tag{5.23b}$$

These traces can be solved with standard commutation relations and making use of the fact that the only non-zero trace in the Pauli matrices comes from the identity, yielding

$$\mathrm{Tr}_1 = 2\big[(\xi^2-\bar{E}'^2)(\xi^2-\bar{E}^2)+4\xi^2(\bar{\Delta}\bar{\Delta}'-\bar{\varepsilon}\bar{\varepsilon}')\big] \tag{5.24a}$$

$$\text{and}\quad \mathrm{Tr}_2 = 2[(\xi^2-\bar{E}^2)(\xi^2-\bar{E}'^2)(\bar{\Delta}\bar{\Delta}'-\bar{\varepsilon}\bar{\varepsilon}')+4\xi^2(\bar{E}\bar{E}')^2]. \tag{5.24b}$$

Substituting these results in the linear response function we have

$$\begin{aligned}\mathcal{K}^{\mathrm{WL},E}_{\alpha\beta}(i\omega) = &-\frac{e^2k_F^2}{2\pi\tau_0^2m^2d}\delta_{\alpha\beta}\frac{1}{\mathcal{V}}\sum_{\mathbf{q}}T\sum_{\varepsilon}\frac{1}{Dq^2+E+E'}\int_{-\infty}^{\infty}\frac{\mathrm{d}\xi}{(\xi^2+\bar{E}^2)^2(\xi^2+\bar{E}'^2)^2}\\ &\times\Bigg[(\xi^2-\bar{E}^2)(\xi^2-\bar{E}'^2)+4\xi^2(\bar{\Delta}\bar{\Delta}'-\bar{\varepsilon}\bar{\varepsilon}')\\ &+\frac{1}{\bar{E}\bar{E}'}\big[(\xi^2-\bar{E}^2)(\xi^2-\bar{E}'^2)(\bar{\Delta}\bar{\Delta}'-\bar{\varepsilon}\bar{\varepsilon}')+4\xi^2(\bar{E}\bar{E}')^2\big]\Bigg].\end{aligned} \tag{5.25}$$

Collecting together terms like so

$$\mathcal{K}^{\mathrm{WL},E}_{\alpha\beta}(i\omega) = -\frac{e^2k_F^2}{2\pi\tau_0^2m^2d}\delta_{\alpha\beta}\frac{1}{\mathcal{V}}\sum_{\mathbf{q}}T\sum_{\varepsilon}\frac{1}{Dq^2+E+E'}\int_{-\infty}^{\infty}\frac{\mathrm{d}\xi}{(\xi^2+\bar{E}^2)^2(\xi^2+\bar{E}'^2)^2} \times\left[(\xi^2-\bar{E}^2)(\xi^2-\bar{E}'^2)\left(1+\frac{\bar{\Delta}\bar{\Delta}'-\bar{\varepsilon}\bar{\varepsilon}'}{\bar{E}\bar{E}'}\right)+4\xi^2(\bar{E}\bar{E}'+\bar{\Delta}\bar{\Delta}'-\bar{\varepsilon}\bar{\varepsilon}')\right], \quad (5.26)$$

we can see that there are integrals over ξ of two forms. The first has the form

$$\int_{-\infty}^{\infty}\mathrm{d}\xi\,\frac{(\xi^2-a^2)(\xi^2-b^2)}{(\xi^2+a^2)^2(\xi^2+b^2)^2}=\frac{2\pi}{(a+b)^3}\,, \quad (5.27)$$

and the second has the form

$$\int_{-\infty}^{\infty}\mathrm{d}\xi\,\frac{4\xi^2}{(\xi^2+a^2)^2(\xi^2+b^2)^2}=\frac{2\pi}{ab(a+b)^3}\,, \quad (5.28)$$

with the requirement that $\mathrm{Re}\{a\},\mathrm{Re}\{b\}>0$. Therefore the ξ integral can be completed to yield

$$\mathcal{K}^{\mathrm{WL},E}_{\alpha\beta}(i\omega) = -\frac{2e^2k_F^2}{\tau_0^2m^2d}\delta_{\alpha\beta}\frac{1}{\mathcal{V}}\sum_{\mathbf{q}}T\sum_{\varepsilon}\frac{1}{Dq^2+E+E'}\frac{1}{(\bar{E}+\bar{E}')^3}\left(1+\frac{\Delta^2-\varepsilon\varepsilon'}{EE'}\right), \quad (5.29)$$

where, because of the extra factor of $1/\bar{E}\bar{E}'$ in the second integral, the two terms become equal and we pick up a factor of two. We also at this stage cancel the impurity factor in the final term. In the dirty limit we can make use of the approximation $1/(\bar{E}+\bar{E}')^3\approx\tau_0^3$ to obtain

$$\mathcal{K}^{\mathrm{WL},E}_{\alpha\beta}(i\omega) = -2e^2D\delta_{\alpha\beta}\frac{1}{\mathcal{V}}\sum_{\mathbf{q}}T\sum_{\varepsilon}\frac{1}{Dq^2+E+E'}\left(1+\frac{\Delta^2-\varepsilon\varepsilon'}{EE'}\right). \quad (5.30)$$

We could proceed further with this calculation to, for example, examine the affect of weak localisation on the number density of superconducting electrons, as was done in the work of Smith and Ambegaokar [59], or the correction to the linear absorption, as in the work of Jujo [61]. However, we know that the weak localisation correction to electrical conductiv-

ity will be negligible in comparison to the contribution from the super-current and hence will be extremely difficult to measure in experiment. So this calculation will simply serve as a useful comparison for the correction to the thermal current, where because there is no super-thermal current one can, in principle, measure the weak localisation correction.

5.3 Weak Localisation Correction to Thermal Conductivity in a Superconductor

To set up the calculation for the weak localisation correction to thermal conductivity in a superconductor we can follow the same procedure as we did for the electrical conductivity case, only needing to change the vertex contributions those appropriate for a thermal-thermal current correlation, for the same reasons as discussed in the previous section. Hence, the diagram we will calculate is given in figure 5.2.

This diagram can be written in terms of its corresponding Green's function,

$$\begin{aligned}\mathcal{G}^{\mathrm{WL},T}_{\alpha\beta}(0,i\omega) = \frac{T}{m^2\mathcal{V}^2}\sum_{\mathbf{k},\mathbf{q}}\sum_{\varepsilon}\mathbf{k}_\alpha(\mathbf{q}-\mathbf{k})_\beta\left(i\varepsilon+\frac{i\omega}{2}\right)^2\frac{1}{4\pi N(0)\tau_0^2}\frac{1}{Dq^2+E+E'}\\ \times\Bigg[\mathrm{Tr}\left[\sigma_z\mathcal{G}(\mathbf{k},i\varepsilon')\sigma_z\mathcal{G}(\mathbf{q}-\mathbf{k},i\varepsilon')\sigma_z\mathcal{G}(\mathbf{q}-\mathbf{k},i\varepsilon)\sigma_z\mathcal{G}(\mathbf{k},i\varepsilon)\right] \qquad (5.31)\\ +\frac{1}{\bar{E}\bar{E}'}\mathrm{Tr}\left[\sigma_z\mathcal{G}(\mathbf{k},i\varepsilon')(i\bar{\varepsilon}'+\bar{\Delta}'\sigma_x)\mathcal{G}(\mathbf{q}-\mathbf{k},i\varepsilon')\sigma_z\mathcal{G}(\mathbf{q}-\mathbf{k},i\varepsilon)(i\bar{\varepsilon}+\bar{\Delta}\sigma_x)\mathcal{G}(\mathbf{k},i\varepsilon)\right]\Bigg].\end{aligned}$$

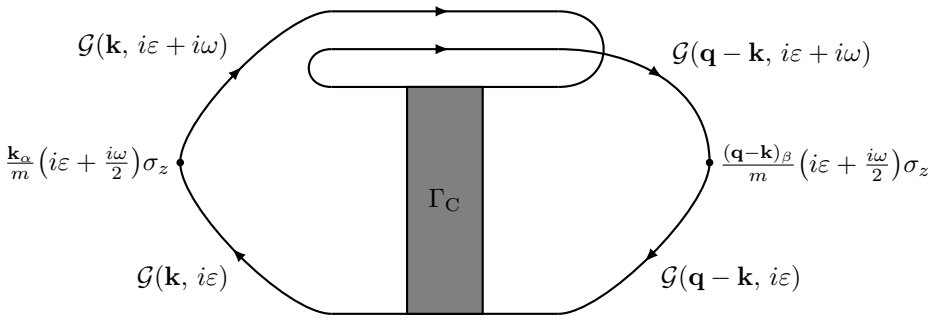

Figure 5.2: Diagrammatic representation of the weak localisation correction to thermal conductivity in a superconductor.

And in the same way as the previous section we can obtain the linear response function from this, given by

$$\begin{aligned}\mathcal{K}^{\mathrm{WL},T}_{\alpha\beta}(0,i\omega) = &-\frac{N(0)k_F^2}{m^2 d}\delta_{\alpha\beta}\frac{1}{4\pi N(0)\tau_0}\frac{1}{\mathcal{V}}\sum_{\mathbf{q}}T\sum_{\varepsilon}\frac{\left(i\varepsilon+\frac{i\omega}{2}\right)^2}{Dq^2+E+E'}\\ &\times\int_{-\infty}^{\infty}\mathrm{d}\xi\left[\mathrm{Tr}\left[\sigma_z\mathcal{G}(\mathbf{k},i\varepsilon')\sigma_z\mathcal{G}(\mathbf{k},i\varepsilon')\sigma_z\mathcal{G}(\mathbf{k},i\varepsilon)\sigma_z\mathcal{G}(\mathbf{k},i\varepsilon)\right]\right.\\ &\left.+\frac{1}{\bar{E}\bar{E}'}\mathrm{Tr}\left[\sigma_z\mathcal{G}(\mathbf{k},i\varepsilon')(i\bar{\varepsilon}'+\bar{\Delta}'\sigma_x)\mathcal{G}(\mathbf{k},i\varepsilon')\sigma_z\mathcal{G}(\mathbf{k},i\varepsilon)(i\bar{\varepsilon}+\bar{\Delta}\sigma_x)\mathcal{G}(\mathbf{k},i\varepsilon)\right]\right].\end{aligned} \tag{5.32}$$

The two traces we must compute are given by

$$\begin{aligned}\mathrm{Tr}_3 = \mathrm{Tr}\big[&\sigma_z(i\bar{\varepsilon}'+\xi\sigma_z-\bar{\Delta}'\sigma_x)\sigma_z(i\bar{\varepsilon}'+\xi\sigma_z-\bar{\Delta}'\sigma_x)\\ &\times\sigma_z(i\bar{\varepsilon}+\xi\sigma_z-\bar{\Delta}\sigma_x)\sigma_z(i\bar{\varepsilon}+\xi\sigma_z-\bar{\Delta}\sigma_x)\big]\end{aligned} \tag{5.33a}$$

$$\begin{aligned}\text{and}\quad \mathrm{Tr}_4 = \mathrm{Tr}\big[&\sigma_z(i\bar{\varepsilon}'+\xi\sigma_z-\bar{\Delta}'\sigma_x)(i\bar{\varepsilon}'+\bar{\Delta}'\sigma_x)(i\bar{\varepsilon}'+\xi\sigma_z-\bar{\Delta}'\sigma_x)\\ &\times\sigma_z(i\bar{\varepsilon}+\xi\sigma_z-\bar{\Delta}\sigma_x)(i\bar{\varepsilon}+\bar{\Delta}\sigma_x)(i\bar{\varepsilon}+\xi\sigma_z-\bar{\Delta}\sigma_x)\big].\end{aligned} \tag{5.33b}$$

The additional σ_z factors in the traces will simply result in some changes in sign on the σ_x terms, when compared to the electrical case. Resulting in the solutions to be traces, given by

$$\mathrm{Tr}_3 = 2\big[(\xi^2-\bar{E}'^2)(\xi^2-\bar{E}^2)-4\xi^2(\bar{\Delta}\bar{\Delta}'+\bar{\varepsilon}\bar{\varepsilon}')\big] \tag{5.34a}$$

$$\text{and}\quad \mathrm{Tr}_4 = 2\big[4\xi^2(\bar{E}\bar{E}')^2-(\xi^2-\bar{E}^2)(\xi^2-\bar{E}'^2)(\bar{\varepsilon}\bar{\varepsilon}'+\bar{\Delta}\bar{\Delta}')\big]. \tag{5.34b}$$

Returning to linear response function, we have

$$\begin{aligned}\mathcal{K}^{\mathrm{WL},T}_{\alpha\beta}(i\omega) = &-\frac{k_F^2}{2\pi\tau_0^2 m^2 d}\delta_{\alpha\beta}\frac{1}{\mathcal{V}}\sum_{\mathbf{q}}T\sum_{\varepsilon}\frac{\left(i\varepsilon+\frac{i\omega}{2}\right)^2}{Dq^2+E+E'}\int_{-\infty}^{\infty}\frac{\mathrm{d}\xi}{(\xi^2+\bar{E}^2)^2(\xi^2+\bar{E}'^2)^2}\\ &\times\left[(\xi^2-\bar{E}'^2)(\xi^2-\bar{E}^2)\left(1-\frac{\bar{\varepsilon}\bar{\varepsilon}'+\bar{\Delta}\bar{\Delta}'}{\bar{E}\bar{E}'}\right)+4\xi^2\big(\bar{E}\bar{E}'-\bar{\varepsilon}\bar{\varepsilon}'-\bar{\Delta}\bar{\Delta}'\big)\right].\end{aligned} \tag{5.35}$$

The integrals over ξ can then be completed using the results given in equations 5.27 and

5.28, yielding

$$\mathcal{K}^{\mathrm{WL},T}_{\alpha\beta}(i\omega) = -\frac{2k_F^2}{\tau_0^2 m^2 d}\delta_{\alpha\beta}\frac{1}{\mathcal{V}}\sum_{\mathbf{q}} T\sum_{\varepsilon}\frac{\left(i\varepsilon+\frac{i\omega}{2}\right)^2}{Dq^2+E+E'}\frac{1}{(\bar{E}+\bar{E}')^3}\left(1-\frac{\Delta^2+\varepsilon\varepsilon'}{EE'}\right) \quad (5.36)$$

Making using of the dirty limit, we can approximate $1/(\bar{E}+\bar{E}')^3 \approx \tau_0^3$ and consolidating the prefactor we arrive at

$$\mathcal{K}^{\mathrm{WL},T}_{\alpha\beta}(i\omega) = -2D\delta_{\alpha\beta}\frac{1}{\mathcal{V}}\sum_{\mathbf{q}} T\sum_{\varepsilon}\frac{\left(i\varepsilon+\frac{i\omega}{2}\right)^2}{Dq^2+E+E'}\left(1-\frac{\Delta^2+\varepsilon\varepsilon'}{EE'}\right). \quad (5.37)$$

The next step is to solve the sum over Matsubara frequencies. We do this by casting the sum into the form of a contour integral and then using analytic continuation to reduce the contour integral to an integral along the real axis. The appropriate contour is the same as shown in the right hand side of figure 4.3, denoted by Γ_2. However, unlike the previous section, both terms in the integral will use this contour with branch cuts because of the additional factor from the cooperon. So we cannot trivially discard the first term as we did in the previous section. The delta function also simply tells us that the response is purely diagonal, or in other words the response is longitudinal with respect to the applied thermal gradient, so from here we will drop the α and β indices as they are redundant. Hence, we can write the linear response function as

$$\mathcal{K}^{\mathrm{WL},T}(i\omega) = -\frac{2D}{\mathcal{V}}\sum_{\mathbf{q}}\frac{i}{2\pi}\oint_{\Gamma}\mathrm{d}z\, f(z)\frac{\left(z+\frac{i\omega}{2}\right)^2}{Dq^2+\sqrt{\Delta^2-z^2}+\sqrt{\Delta^2-(z+i\omega)^2}} \times\left(1-\frac{\Delta^2-z(z+i\omega)}{\sqrt{\Delta^2-z^2}\sqrt{\Delta^2-(z+i\omega)^2}}\right). \quad (5.38)$$

We can use the transformation $z \mapsto -z - i\omega$ in exact analogy to equation 4.65, in order to reduce the integral to one that only encloses the upper two contours (labelled by

Γ_a and Γ_b) with the form

$$\mathcal{K}^{\mathrm{WL},T}(i\omega) = \frac{2D}{\mathcal{V}} \sum_{\mathbf{q}} \frac{i}{2\pi} \int_{\Gamma_{a+b}} \mathrm{d}z \tanh\Big(\frac{z}{2T}\Big) \frac{\big(z+\frac{i\omega}{2}\big)^2}{Dq^2 + \sqrt{\Delta^2 - z^2} + \sqrt{\Delta^2 - (z+i\omega)^2}} \times \left(1 - \frac{\Delta^2 - z(z+i\omega)}{\sqrt{\Delta^2 - z^2}\sqrt{\Delta^2 - (z+i\omega)^2}}\right). \tag{5.39}$$

In the absence of contours enclosing $\pm\Delta - i\omega$ we can safely analytically continue $i\omega \mapsto \omega + i\delta$. Then we can also analytically continue $z \mapsto x \pm i\delta$ for above and below the real axis respectively, remembering that we must choose the signs of the square roots such that the real part is positive, in order to be consistent with the integrals performed in equations 5.27 and 5.28. The correct signs have already been shown in the previous section in equations 4.69 and 4.70. Hence for the Γ_a contour we have

$$\begin{aligned}\int_{\Gamma_a} \cdots = &\int_{\Delta}^{\infty} \mathrm{d}x \tanh\Big(\frac{x}{2T}\Big) \frac{(x+\frac{\omega}{2})^2}{Dq^2 - i\sqrt{x^2-\Delta^2} - i\sqrt{(x+\omega)^2-\Delta^2}} \\ &\times \left(1 - \frac{\Delta^2 - x(x+\omega)}{(-i\sqrt{x^2-\Delta^2})(-i\sqrt{(x+\omega)^2-\Delta^2})}\right) \\ &+ \int_{\infty}^{\Delta} \mathrm{d}x \tanh\Big(\frac{x}{2T}\Big) \frac{(x+\frac{\omega}{2})^2}{Dq^2 + i\sqrt{x^2-\Delta^2} - i\sqrt{(x+\omega)^2-\Delta^2}} \\ &\times \left(1 - \frac{\Delta^2 - x(x+\omega)}{(i\sqrt{x^2-\Delta^2})(-i\sqrt{(x+\omega)^2-\Delta^2})}\right).\end{aligned} \tag{5.40}$$

For brevity, we will relabel $X = \sqrt{x^2-\Delta^2}$ and $X' = \sqrt{(x+\omega)^2-\Delta^2}$ and then simplifying this expression we obtain

$$\begin{aligned}\int_{\Gamma_a} \cdots = \int_{\Delta}^{\infty} \mathrm{d}x \tanh\Big(\frac{x}{2T}\Big)\Big(x+\frac{\omega}{2}\Big)^2 \Bigg[&\frac{1}{Dq^2 - iX - iX'}\left(1 - \frac{x(x+\omega)-\Delta^2}{XX'}\right) \\ &- \frac{1}{Dq^2 + iX - iX'}\left(1 + \frac{x(x+\omega)-\Delta^2}{XX'}\right)\Bigg].\end{aligned} \tag{5.41}$$

Repeating this process for the Γ_b contour and introducing $\bar{X} = \sqrt{\Delta^2 - (x+\omega)^2}$ for the

square root that corresponds to the region outside of the lower branch cut, we find

$$\begin{aligned}\int_{\Gamma_b}\cdots = \int_{-\infty}^{-\Delta-\omega} \mathrm{d}z\,\tanh\Big(\frac{x}{2T}\Big)\Big(x+\frac{\omega}{2}\Big)^2\Bigg[\frac{1}{Dq^2+iX+iX'}\Big(1-\frac{x(x+\omega)-\Delta^2}{XX'}\Big)\\ -\frac{1}{Dq^2-iX+iX'}\Big(1+\frac{x(x+\omega)-\Delta^2}{XX'}\Big)\Bigg]\\ +\int_{-\Delta-\omega}^{-\Delta}\mathrm{d}x\,\tanh\Big(\frac{x}{2T}\Big)\Big(x+\frac{\omega}{2}\Big)^2\Bigg[\frac{1}{Dq^2+iX+\bar{X}}\Big(1-i\frac{x(x+\omega)-\Delta^2}{X\bar{X}}\Big)\\ -\frac{1}{Dq^2-iX+\bar{X}}\Big(1+i\frac{x(x+\omega)-\Delta^2}{X\bar{X}}\Big)\Bigg].\end{aligned} \tag{5.42}$$

Note that because our end goal in thermal quantities is to take $\omega \to 0$, we do not include the additional integral that arises when $\omega > 2\Delta$. Now we symmetrise the integrals; in the Γ_a integral make the transformation $x \mapsto x - \frac{\omega}{2}$, so

$$\begin{aligned}X &\mapsto \sqrt{(x-\frac{\omega}{2})^2-\Delta^2} = X_-\\ X' &\mapsto \sqrt{(x+\frac{\omega}{2})^2-\Delta^2} = X_+\,,\end{aligned} \tag{5.43}$$

and the Γ_b integral make the transformation $x \mapsto -x - \frac{\omega}{2}$, so

$$X \mapsto \sqrt{(x+\frac{\omega}{2})^2-\Delta^2} = X_+ \tag{5.44}$$

$$X' \mapsto \sqrt{(x-\frac{\omega}{2})^2-\Delta^2} = X_- \tag{5.45}$$

$$\bar{X} \mapsto \sqrt{\Delta^2-(x-\frac{\omega}{2})^2} := \widetilde{X}\,. \tag{5.46}$$

Therefore,

$$\begin{aligned}\int_{\Gamma_a}\cdots = \int_{\Delta+\frac{\omega}{2}}^{\infty}\mathrm{d}x\,x^2\tanh\Big(\frac{x-\frac{\omega}{2}}{2T}\Big)\Bigg[\frac{1}{Dq^2-iX_+-iX_-}\Big(1-\frac{(x-\frac{\omega}{2})(x+\frac{\omega}{2})-\Delta^2}{X_+X_-}\Big)\\ -\frac{1}{Dq^2-iX_++iX_-}\Big(1+\frac{(x-\frac{\omega}{2})(x+\frac{\omega}{2})-\Delta^2}{X_+X_-}\Big)\Bigg],\end{aligned} \tag{5.47}$$

and,

$$\int_{\Gamma_b}\cdots = -\int_{\Delta+\frac{\omega}{2}}^{\infty}\mathrm{d}x\,x^2\tanh\left(\frac{x+\frac{\omega}{2}}{2T}\right)\left[\frac{1}{Dq^2+iX_+ +iX_-}\left(1-\frac{(x-\frac{\omega}{2})(x+\frac{\omega}{2})-\Delta^2}{X_+X_-}\right)\right.$$
$$\left.-\frac{1}{Dq^2-iX_+ +iX_-}\left(1+\frac{(x-\frac{\omega}{2})(x+\frac{\omega}{2})-\Delta^2}{X_+X_-}\right)\right]$$
$$-\int_{\Delta-\frac{\omega}{2}}^{\Delta+\frac{\omega}{2}}\mathrm{d}x\,x^2\tanh\left(\frac{x+\frac{\omega}{2}}{2T}\right)\left[\frac{1}{Dq^2+iX_+ +\widetilde{X}}\left(1-i\frac{(x-\frac{\omega}{2})(x+\frac{\omega}{2})-\Delta^2}{X_+\widetilde{X}}\right)\right.$$
$$\left.-\frac{1}{Dq^2-iX_+ +\widetilde{X}}\left(1+i\frac{(x-\frac{\omega}{2})(x+\frac{\omega}{2})-\Delta^2}{X_+\widetilde{X}}\right)\right]. \quad (5.48)$$

After some rearrangement and putting the two terms into the linear response function, we have

$$\mathcal{K}^{WL}(\omega)=\frac{2Di}{\pi\mathcal{V}}\sum_{\mathbf{q}}$$
$$\times\left\{\int_{\Delta+\frac{\omega}{2}}^{\infty}\mathrm{d}x\,x^2\left[\frac{\tanh\left(\frac{x+\frac{\omega}{2}}{2T}\right)}{(Dq^2+iX_-)^2+X_+^2}\left(\frac{x^2-\left(\frac{\omega}{2}\right)^2-\Delta^2}{X_+X_-}(Dq^2+iX_-)+iX_+\right)\right.\right.$$
$$\left.-\frac{\tanh\left(\frac{x-\frac{\omega}{2}}{2T}\right)}{(Dq^2-iX_+)^2+X_-^2}\left(\frac{x^2-(\frac{\omega}{2})^2-\Delta^2}{X_+X_-}(Dq^2-iX_+)-iX_-\right)\right]$$
$$\left.+i\int_{\Delta-\frac{\omega}{2}}^{\Delta+\frac{\omega}{2}}\mathrm{d}x\,x^2\frac{\tanh\left(\frac{x+\frac{\omega}{2}}{2T}\right)}{(Dq^2+\widetilde{X})^2+X_+^2}\left(\frac{x^2-(\frac{\omega}{2})^2-\Delta^2}{X_+\widetilde{X}}(Dq^2+\widetilde{X})+X_+\right)\right\}. \quad (5.49)$$

This is the most general form of the linear response function in the diffusive/dirty limit that one can reach, before taking any further approximations or limits. We can proceed further by examining the $\omega\to 0$ limit, as we are mostly concerned with 'd.c.' thermal currents.

Equation 5.49 is in general complex, but we will only need the real part of the thermal conductivity. Because we divide by $-i\omega$ to get the conductivity from the linear response function this means we only need the $\mathrm{Im}\{\mathcal{K}\}$. The second integral in equation 5.49 is purely real, so we can immediately discard this term. Taking the limit $\omega\to 0$ on the first

integral, we can notice some cancellations will occur. Firstly,

$$\lim_{\omega\to 0}\frac{x^2-\left(\frac{\omega}{2}\right)^2-\Delta^2}{X_+X_-}=\frac{x^2-\Delta^2}{\sqrt{x^2-\Delta^2}\sqrt{x^2-\Delta^2}}=1\,, \tag{5.50}$$

and therefore

$$\mathcal{K}^{WL}(0)=\lim_{\omega\to 0}\frac{2Di}{\pi\mathcal{V}}\sum_{\mathbf{q}}\int_{\Delta+\frac{\omega}{2}}^{\infty}\mathrm{d}x\,x^2\left[\frac{\tanh\left(\frac{x+\frac{\omega}{2}}{2T}\right)}{(Dq^2+iX_-)^2+X_+^2}\big((Dq^2+iX_-)+iX_+\big)\right.$$
$$\left.-\frac{\tanh\left(\frac{x-\frac{\omega}{2}}{2T}\right)}{(Dq^2-iX_+)^2+X_-^2}\big((Dq^2-iX_+)-iX_-\big)\right]. \tag{5.51}$$

This simplification allows a cancellation in the denominators,

$$\frac{(Dq^2+iX_-)+iX_+}{(Dq^2+iX_-)^2+X_+^2}=\frac{1}{Dq^2+iX_--iX_+} \tag{5.52a}$$

$$\text{and}\quad\frac{(Dq^2-iX_+)-iX_-}{(Dq^2-iX_+)^2+X_-^2}=\frac{1}{Dq^2+iX_--iX_+}\,, \tag{5.52b}$$

which leads to

$$\mathcal{K}^{WL}(0)=\lim_{\omega\to 0}\frac{2Di}{\pi\mathcal{V}}\sum_{\mathbf{q}}\int_{\Delta+\frac{\omega}{2}}^{\infty}\mathrm{d}x\,x^2\lim_{\omega\to 0}\left[\frac{\tanh\left(\frac{x+\frac{\omega}{2}}{2T}\right)-\tanh\left(\frac{x-\frac{\omega}{2}}{2T}\right)}{Dq^2+iX_--iX_+}\right]. \tag{5.53}$$

Finally, we can take the limits:

$$\lim_{\omega\to 0}\left[\tanh\left(\frac{x+\frac{\omega}{2}}{2T}\right)-\tanh\left(\frac{x-\frac{\omega}{2}}{2T}\right)\right]=\omega\frac{\mathrm{d}}{\mathrm{d}x}\tanh\left(\frac{x}{2T}\right)=\frac{\omega}{2T}\operatorname{sech}^2\left(\frac{x}{2T}\right), \tag{5.54}$$

and in the denominator

$$\lim_{\omega\to 0}\left[X_+-X_-\right]=\lim_{\omega\to 0}\left[\sqrt{(x+\frac{\omega}{2})^2-\Delta^2}-\sqrt{(x-\frac{\omega}{2})^2-\Delta^2}\right]$$
$$=\omega\frac{\mathrm{d}}{\mathrm{d}x}\sqrt{x^2-\Delta^2}=\omega\frac{x}{\sqrt{x^2-\Delta^2}}\,, \tag{5.55}$$

to obtain

$$\mathcal{K}^{WL}(0) = \frac{2Di}{\pi T\mathcal{V}} \sum_{\mathbf{q}} \int_{\Delta}^{\infty} \mathrm{d}x \, \frac{x^2 \operatorname{sech}^2(\frac{x}{2T})}{Dq^2 - i\omega \frac{x}{\sqrt{x^2-\Delta^2}}} \,. \tag{5.56}$$

From this we can extract the conductivity by dividing by $-i\omega$, then taking the real part, so

$$T\kappa^{WL} = \mathrm{Re}\left\{ -\frac{D}{\pi T\mathcal{V}} \sum_{\mathbf{q}} \int_{\Delta}^{\infty} \mathrm{d}x \, \frac{x^2 \operatorname{sech}^2(\frac{x}{2T})}{Dq^2 - i\omega \frac{x}{\sqrt{x^2-\Delta^2}}} \right\}. \tag{5.57}$$

We have kept leading order in ω because otherwise, when we take the sum over $\mathbf{q}$, the q^2 term in the denominator will lead to a divergence. Of course, if we truly take the limit $\omega \to 0$ this divergence will be present, but by leaving in ω dependence we are able to complete the $\mathbf{q}$ integral see the form of the conductivity for small ω.

As weak localisation effects are most present in 2-dimensional systems, we will perform the $\mathbf{q}$ integral in 2D. We can freely interchange the orders of the sums, so we have

$$T\kappa^{WL} = \mathrm{Re}\left\{ -\frac{D}{\pi T} \int_{\Delta}^{\infty} \mathrm{d}x \, x^2 \operatorname{sech}^2\left(\frac{x}{2T}\right) \frac{1}{\mathcal{V}} \sum_{\mathbf{q}} \frac{1}{Dq^2 - i\omega \frac{x}{\sqrt{x^2-\Delta^2}}} \right\}. \tag{5.58}$$

In the diffusive limit sum should be cut off at $|\mathbf{q}| \sim l_0^{-1}$, or equivalently $Dq^2 \sim \tau_0^{-1}$. So in 2D the sum can be written in integral form as

$$\begin{aligned} \frac{1}{\mathcal{V}} \sum_{\mathbf{q}} \cdots &= \frac{1}{(2\pi)^2} \int_0^{l_0^{-1}} \frac{2\pi q \, \mathrm{d}q}{Dq^2 - i\omega \frac{x}{\sqrt{x^2-\Delta^2}}} \\ &= \frac{1}{4\pi D} \int_0^{\tau_0^{-1}} \frac{\mathrm{d}(Dq^2)}{Dq^2 - i\omega \frac{x}{\sqrt{x^2-\Delta^2}}} \,. \end{aligned} \tag{5.59}$$

Solving this we obtain

$$\begin{aligned} T\kappa^{WL} &= \mathrm{Re}\left\{ -\frac{1}{4\pi^2 T} \int_{\Delta}^{\infty} \mathrm{d}x \, x^2 \operatorname{sech}^2\left(\frac{x}{2T}\right) \ln\left(1 + i\frac{\sqrt{x^2-\Delta^2}}{\omega\tau_0 x}\right) \right\} \\ &= -\frac{1}{8\pi^2 T^2} \int_{\Delta}^{\infty} \mathrm{d}x \, x^2 \operatorname{sech}^2\left(\frac{x}{2T}\right) \ln\left(1 + \frac{x^2-\Delta^2}{(\omega\tau_0 x)^2}\right). \end{aligned} \tag{5.60}$$

Finally, using the dirty limit, $\omega\tau_0 \ll 1$, we have

$$T\kappa^{WL} = -\frac{1}{8\pi^2 T}\int_{\Delta}^{\infty} \mathrm{d}x\, x^2 \operatorname{sech}^2\left(\frac{x}{2T}\right) \ln\left(\frac{x^2-\Delta^2}{(\omega\tau_0 x)^2}\right). \tag{5.61}$$

So we can see from this, if we set $\omega = 0$ we still have a logarithmic divergence in the integrand. However in analogy to the normal state we can introduce the phase breaking rate, τ_ϕ, as a phenomenological parameter to introduce a cut-off to resolve the divergence issue.

If we compare the equation for the cooperon in the superconducting state to the equation in the the normal state (equations 3.56 and 5.20) we can see that, in the superconducting expression, factors in the denominator with the form $\sqrt{\Delta^2+\varepsilon^2}$ take the place of bare Matsubara frequencies in the normal state expression; other than that the form of the factor containing Dq^2 is the same. So to introduce τ_ϕ, we can deduce it should simply enter the denominator in the same way as equation 3.57, meaning

$$\frac{1}{Dq^2+E+E'} \mapsto \frac{1}{Dq^2+E+E'+\tau_\phi^{-1}}\,. \tag{5.62}$$

So returning to the linear response function before the ε sum is taken, we have

$$\mathcal{K}_{\alpha\beta}^{\mathrm{WL},T}(i\omega) = -2D\delta_{\alpha\beta}\frac{1}{\mathcal{V}}\sum_{\mathbf{q}} T\sum_{\varepsilon} \frac{\left(i\varepsilon+\frac{i\omega}{2}\right)^2}{Dq^2+E+E'+\tau_\phi^{-1}}\left(1-\frac{\Delta^2+\varepsilon\varepsilon'}{EE'}\right). \tag{5.63}$$

However, we expect τ_ϕ to only depend on temperature, so it will not take any role in the ε sum; it will simply be a passenger in the calculation. Hence, we can arrive immediately at

$$T\kappa_s^{WL} = \mathrm{Re}\left\{-\frac{D}{\pi T\mathcal{V}}\sum_{\mathbf{q}}\int_{\Delta}^{\infty}\mathrm{d}x\,\frac{x^2\operatorname{sech}^2(\frac{x}{2T})}{Dq^2-i\omega\frac{x}{\sqrt{x^2-\Delta^2}}+\tau_\phi^{-1}}\right\}. \tag{5.64}$$

Now we can set $\omega = 0$ without issue and solve the integral in 2D again, yielding

$$T\kappa_s^{WL} = -\frac{1}{4\pi^2 T}\int_\Delta^\infty \mathrm{d}x\, x^2 \operatorname{sech}^2\left(\frac{x}{2T}\right)\ln\left(1+\frac{\tau_\phi}{\tau_0}\right), \tag{5.65}$$

then use the limit $\tau_\phi \gg \tau_0$, to obtain

$$T\kappa_s^{WL} = -\frac{1}{4\pi^2 T}\int_\Delta^\infty \mathrm{d}x\, x^2 \operatorname{sech}^2\left(\frac{x}{2T}\right)\ln\left(\frac{\tau_\phi}{\tau_0}\right). \tag{5.66}$$

So we can see the form of this is very similar to that of the thermal conductivity we calculated in the previous chapter. If we substitute $y = x/2T$ we can remove the temperature dependence from the sech,

$$T\kappa_s^{WL} = -\frac{2T^2}{\pi^2}\int_{\frac{\Delta(T)}{2T}}^\infty \mathrm{d}y\, y^2 \operatorname{sech}^2(y)\ln\left(\frac{\tau_\phi}{\tau_0}\right), \tag{5.67}$$

so the temperature dependence of the correction is entirely in the lower limit and in the temperature dependence of τ_ϕ. Because the log term does not depend on y, we can in fact factor it out of the integral. If we then examine the ratio of the weak localisation correction to the leading order conductivity, we can see that the integrals will cancel, leaving us with

$$\frac{\kappa_s^{WL}}{\kappa_s} = -\frac{m}{2\pi^2 n\tau_0}\ln\left(\frac{\tau_{\phi,s}}{\tau_0}\right). \tag{5.68}$$

This result is in agreement with the result in González Rosado et. al. for the case of a dirty superconductor [63]. In our calculation we have made no assumption about the validity of this result in different temperate ranges. However, in the work of ref, [63], our result matches for the so called high-temperature region, defined as $T > T_\Delta \approx 0.9T_c$, which defines the region before which the strong exponential suppression of the thermal conductivity sets in. In the low temperature region they argue that the condition $\tau_0 \gg \tau_\phi$ is no longer sufficient to define the diffusive regime, and therefore the lower cutoff of τ_0 in

the integral dq must be replaced with a more complex energy dependent cut-off. However, in the high temperature regime this cutoff returns to simply being given by tau_0 and, as we discussed in the introduction in detail, the high temperature regime is the one of interest when it comes to comparison with experiment results. Thus, we do not fell it is necessary to explore the low temperature region in detail.

The ratio of the weak localisation correction to the leading order conductivity in the normal state has functionally the same form as in the superconducting state,

$$\frac{\kappa_n^{WL}}{\kappa_n} = -\frac{m}{2\pi^2 n\tau_0}\ln\left(\frac{\tau_{\phi,n}}{\tau_0}\right). \tag{5.69}$$

Also, with integrals in the superconducting state ratio cancelling, all the of the temperature dependence comes from τ_ϕ in both ratios. However, note that the phase coherence lifetimes in the normal and superconducting states are in general different, hence why we have labelled them with a s and n subscript. For example, we refer the reader to the work of Reizer [64] where the electron-electron relaxation time was calculated for a dirty superconductor, $\tau_{e-e,s}$. One can see that this calculation is much more involved, and yields a different result, than that of Fukuyama and Abrahams' [44] equivalent calculation of $\tau_{e-e,n}$ in normal disordered metals. One could then use the relaxation times found in these two studies and substitute $\tau_{\phi,n} = \tau_{e-e,n}$ and $\tau_{\phi,s} = \tau_{e-e,s}$ and compare the two resulting weak localisation correction ratios. However, in the following chapter we will turn our attention to the scenario where the phase coherence lifetime is dominated by the scattering lifetime with magnetic impurities, τ_s.

CHAPTER 6

WEAK LOCALISATION IN A SUPERCONDUCTOR INCLUDING MAGNETIC IMPURITIES

In the previous section we included the phase coherence lifetime as a phenomenological parameter, now we wish to introduce a phase breaking mechanism into the formalism directly. We can do so by introducing magnetic impurities. Firstly, in the following section we extend the Nambu-Gorkov formalism to include the interaction with magnetic impurities and show that, unlike with only non-magnetic impurities, the superconducting gap is altered. In section 6.2 we then use this new formalism to examine the frequency dependent linear response of the superconductor with magnetic impurities to an electromagnetic field and, in particular, this section describes in detail how to perform the analytic continuation process in this regime. Though this process is by no means original (for example it can be found in Skalski et. al. [76]), we seek to provide a clear methodology that could then be used by any interested reader. In section 6.3 we then calculate the thermal conductivity using the same analytic continuation techniques and take the $\omega \to 0$

limit; this was first done by Ambegaokar and Griffin [75]. We take this calculation up to the point where the integral would have to be approximated or calculated numerically. Everything up to this point in the chapter is well established in the literature, a review of which can be found in Maki's chapter in Parks' treatise [14].

In section 6.4 we calculate the cooperon with magnetic impurities, which follows the work of Smith [65] up to the acquisition of the general form of the cooperon. The original work of this chapter begins in section 6.5 where we take the leading order approximation of the cooperon in the limit $\tau_s \gg \tau_0$, whilst retaining the frequency dependency of the cooperon. This is because to properly analytically continue we must take the limit $\omega \to 0$ after performing the analytic continuation, in the same way as demonstrated in section 6.2. In section 6.6 we then take the cooperon and use it to construct the weak localisation bubble diagram, and we proceed with this calculation as far as possible analytically. We then end the chapter with some discussion of the result and possible future work.

6.1 Nambu-Gorkov Formalism with Magnetic Impurities

In the previous section we included the phase coherence lifetime as a phenomenological parameter, now we wish to introduce a phase breaking mechanism into the formalism directly. We can do so by introducing magnetic impurities. But before we get ahead of ourselves thinking about the weak localisation correction, we must examine how the magnetic impurities affect the superconducting state.

We have seen that non-magnetic impurities do not have any affect on the transition temperature or superconducting gap (as long as they are in sufficiently low concentrations). However, interaction with magnetic impurities is a time reversal symmetry breaking process for the electrons, and perturbations of this type will affect the gap and transition temperature [14]. Another time reversal symmetry breaking perturbation of note is the application of a magnetic field.

In this section we will be extending the Nambu-Gorkov formalism to include the interaction with magnetic impurities. We will then go on to calculate how the magnetic impurities affect the electrical and thermal conductivity. In the last section we will calculate the form of the cooperon in this regime, with the magnetic impurities providing the phase coherence cut-off.

We begin the set up of the Nambu-Gorkov formulation in the same way as the non-magnetic impurity calculation. We take our Hamiltonian in real space and we include an additional term in our Hamiltonian corresponding to magnetic impurities:

$$\begin{aligned} H_{mag} =& J \int \mathrm{d}\mathbf{r} \sum_j \delta(\mathbf{r}-\mathbf{R}_j) \Big[S_j^x \Big(\psi_\uparrow^\dagger(\mathbf{r})\psi_\downarrow(\mathbf{r}) + \psi_\downarrow^\dagger(\mathbf{r})\psi_\uparrow(\mathbf{r}) \Big) \\ & - i S_j^y \Big(\psi_\uparrow^\dagger(\mathbf{r})\psi_\downarrow(\mathbf{r}) - \psi_\downarrow^\dagger(\mathbf{r})\psi_\uparrow(\mathbf{r}) \Big) + S_j^z \Big(\psi_\uparrow^\dagger(\mathbf{r})\psi_\uparrow(\mathbf{r}) + \psi_\downarrow^\dagger(\mathbf{r})\psi_\downarrow(\mathbf{r}) \Big) \Big] . \end{aligned} \tag{6.1}$$

Where the coupling strength to the magnetic impurities is given by J, the interaction has been taken to be point-like and the component of the j^{th} impurity's spin in each Cartesian direction is given by $S_j^{x,y,z}$.

In a similar way to how we constructed the Nambu-Gorkov-spinors to compactify the BCS term by leveraging the inherent symmetries in the Hamiltonian, we can do the same here by constructing a spin-spinor that reflects the spin flip nature of the magnetic term. In the case of the Nambu-spinor, the symmetry linked a field operator to its conjugate with the opposite spin. In the case of the spin-spinor, it more simply links the operator to its opposite spin partner, hence we will construct them as follows

$$\phi(\mathbf{r}) = \begin{pmatrix} \psi_\uparrow(\mathbf{r}) \\ \psi_\downarrow(\mathbf{r}) \end{pmatrix} \quad ; \quad \phi^\dagger(\mathbf{r}) = \begin{pmatrix} \psi_\uparrow^\dagger(\mathbf{r}) & \psi_\downarrow^\dagger(\mathbf{r}) \end{pmatrix} . \tag{6.2}$$

Then re-writing the magnetic impurity term in the Hamiltonian in terms of the spinors

yields

$$\begin{aligned} H_{mag} =& \int \mathrm{d}\mathbf{r} \sum_j \delta(\mathbf{r}-\mathbf{R}_j)\Big[S_j^x \phi^\dagger(\mathbf{r}) s_x \phi(\mathbf{r}) + S_j^y \phi^\dagger(\mathbf{r}) s_y \phi(\mathbf{r}) + S_j^z \phi^\dagger(\mathbf{r}) s_z \phi(\mathbf{r})\Big] \\ =& J \int \mathrm{d}\mathbf{r} \sum_\beta \delta(\mathbf{r}-\mathbf{R}_j)\mathbf{S}_j \cdot \phi^\dagger(\mathbf{r})\mathbf{s}\phi(\mathbf{r})\,, \end{aligned} \tag{6.3}$$

$$\text{where} \quad \mathbf{s} = \begin{pmatrix} s_x \\ s_y \\ s_z \end{pmatrix} \equiv \begin{pmatrix} \sigma_x \\ \sigma_y \\ \sigma_z \end{pmatrix} \quad ; \quad \mathbf{S}_j = \begin{pmatrix} S_j^x \\ S_j^y \\ S_j^z \end{pmatrix}.$$

Here we have written the Pauli matrices that arise from the use of the the spin-spinor as s_i to distinguish from those that arise from the Nambu-spinor. This helps to keep the notation clear as we move on to the next step, which is to combine both of the spinors together.

To be able to encapsulate the symmetries involved in the formation of Cooper pairs and magnetic interaction, we must combine the two different types of spinors into one rank-4 matrix/spinor representation of the Hamiltonian. So we introduce the magnetic Nambu-Gorkov spinors

$$\Phi(\mathbf{r}) = \begin{pmatrix} \psi_\uparrow(\mathbf{r}) \\ \psi_\downarrow(\mathbf{r}) \\ \psi_\downarrow^\dagger(\mathbf{r}) \\ \psi_\uparrow^\dagger(\mathbf{r}) \end{pmatrix} \quad ; \quad \Phi^\dagger(\mathbf{r}) = \begin{pmatrix} \psi_\uparrow^\dagger(\mathbf{r}) & \psi_\downarrow^\dagger(\mathbf{r}) & \psi_\downarrow(\mathbf{r}) & \psi_\uparrow(\mathbf{r}) \end{pmatrix}; \tag{6.4}$$

so between the first and second elements, and the third and fourth, we have the spin-flip representative of the spin-spinor and between the first and third, and second and fourth, we have the spin flip plus conjugation representative of the Nambu-spinor. Now we can rewrite the terms in the Hamiltonian using this new four component spinor along with

the outer product of the σ and s sets of Pauli matrices:

$$H_0 = \frac{1}{2}\int \mathrm{d}\mathbf{r}\, \Phi^\dagger(\mathbf{r})\left(\frac{\boldsymbol{\nabla}^2}{2m} - \mu\right)[\sigma_z \otimes s_0]\Phi(\mathbf{r}) \tag{6.5a}$$

$$H_{imp} = \frac{U}{2}\sum_i \int \mathrm{d}\mathbf{r}\, \delta(\mathbf{r} - \mathbf{R}_i)\Phi^\dagger(\mathbf{r})[\sigma_z \otimes s_0]\Phi(\mathbf{r}) \tag{6.5b}$$

$$H_{BCS} = -\frac{\Delta}{2}\int \mathrm{d}\mathbf{r}\, \Phi^\dagger(\mathbf{r})[\sigma_x \otimes s_z]\Phi(\mathbf{r}) \tag{6.5c}$$

$$H^x_{mag} = \frac{J}{2}\sum_j \int \mathrm{d}\mathbf{r}\, \delta(\mathbf{r} - \mathbf{R}_j)S^x_j\Phi^\dagger(\mathbf{r})[\sigma_z \otimes s_x]\Phi(\mathbf{r}) \tag{6.5d}$$

$$H^y_{mag} = \frac{J}{2}\sum_\beta \int \mathrm{d}\mathbf{r}\, \delta(\mathbf{r} - \mathbf{R}_j)S^y_j\Phi^\dagger(\mathbf{r})[\sigma_z \otimes s_y]\Phi(\mathbf{r}) \tag{6.5e}$$

$$H^z_{mag} = \frac{J}{2}\sum_\beta \int \mathrm{d}\mathbf{r}\, \delta(\mathbf{r} - \mathbf{R}_j)S^z_j\Phi^\dagger(\mathbf{r})[\sigma_0 \otimes s_z]\Phi(\mathbf{r})\,. \tag{6.5f}$$

The 4×4 matrix structure causes double counting leading to the factor of a half in all of the terms. Now employing the same methods as in previous sections we can obtain the equation of motion for the the magnetic-Nambu-Gorkov Green's function

$$\left[\frac{\mathrm{d}}{\mathrm{d}\tau}\sigma_0 s_0 + \left(\frac{\boldsymbol{\nabla}^2}{2m} - \mu\right)\sigma_z s_0 - \Delta\sigma_x s_x + U\sum_i \delta(\mathbf{r} - \mathbf{R}_i)\sigma_z s_0 \right.$$
$$\left. + J\sum_j \delta(\mathbf{r} - \mathbf{R}_j)\mathbf{S}_j \cdot \boldsymbol{\Omega}\right]\mathcal{G}(\mathbf{r}, \mathbf{r}'; \tau) = -\delta(\mathbf{r} - \mathbf{r}')\delta(\tau)\sigma_0 s_0 \tag{6.6}$$

$$\text{where} \quad \mathcal{G}(\mathbf{r}, \mathbf{r}'; \tau) = -\left\langle T_\tau \Phi(\mathbf{r}, \tau)\Phi^\dagger(\mathbf{r}', 0)\right\rangle \tag{6.7}$$

$$\text{and} \quad \boldsymbol{\Omega} = \begin{pmatrix} \sigma_z s_x \\ \sigma_z s_y \\ \sigma_0 s_z \end{pmatrix}. \tag{6.8}$$

We have employed the convention that the products of the different species of Pauli matrices denotes the outer product, i.e. $\sigma_i s_j \equiv \sigma_i \otimes s_j$.

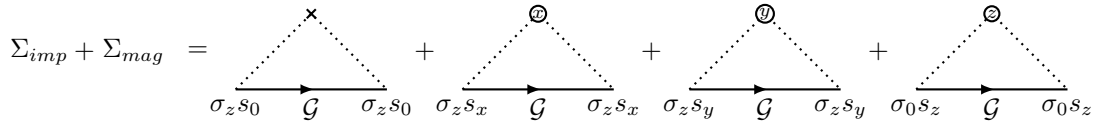

Figure 6.1: The Self-energy part from the Dyson equation for the superconducting Green's function perturbed by non magnetic and magnetic impurities. The left most contribution is from the scattering with non-magnetic impurities and the right-hand are from the three distinct 'species' of magnetic impurities. Each contribution has a different value on the vertex.

The Green's function for a clean superconductor in this new notation would be given by

$$\begin{aligned}\mathcal{G}_0(\mathbf{k}, i\varepsilon) &= \frac{1}{i\varepsilon\sigma_0 s_0 - \xi_k \sigma_z s_0 + \Delta\sigma_x s_z} \\ &= \frac{i\varepsilon\sigma_0 s_0 + \xi_k \sigma_z s_0 - \Delta\sigma_x s_z}{-\varepsilon^2 - \xi_k^2 - \Delta^2}\,. \end{aligned} \tag{6.9}$$

Then we can ensemble average and construct a Dyson equation, as shown in figure 6.1, which proceeds almost identically to the non-magnetic case (including the nested diagram, hence the full $\mathcal{G}$ appears in the self-energy). However, because there are three 'species' of magnetic impurity, when we average over impurity positions we require that the species of magnetic impurity are the same in the average for the term to be non-zero. So if we also assume the magnetic impurities are approximately evenly distributed between species we will pick up a factor of $\frac{1}{3}S(S+1)$ when we take $\langle S^i S^i \rangle$ for each respective spin species. Therefore the self-energy parts will be given by

$$\Sigma_{imp} = n_{imp}|U|^2 \sum_{\mathbf{k}} \sigma_z s_0 \mathcal{G}(\mathbf{k}, i\varepsilon)\sigma_z s_0 \tag{6.10}$$

$$\text{and} \quad \Sigma_{mag} = \frac{1}{3}S(S+1)n_{mag}|J|^2 \sum_{\mathbf{k}} \mathbf{\Omega}\mathcal{G}(\mathbf{k}, i\varepsilon)\cdot\mathbf{\Omega}\,, \tag{6.11}$$

where because the total self-energy for the magnetic impurities is the sum off the contributions from the 3 spin components, we have a dot product of the $\mathbf{\Omega}$ vector with itself; this gives the correct vertex contributions for each respective spin.

We make an ansatz of the same form as in the case with only non-magnetic impurities,

but with a new set of renormalised variables now denoted by a tilde,

$$\Sigma_{imp} + \Sigma_{mag} = i(\varepsilon - \widetilde{\varepsilon})\sigma_0 s_0 + (\Delta - \widetilde{\Delta})\sigma_x s_z \tag{6.12}$$

$$\therefore \mathcal{G}(\mathbf{k}, i\varepsilon) = \frac{1}{i\widetilde{\varepsilon}\sigma_0 s_0 - \xi_k \sigma_z s_0 + \widetilde{\Delta}\sigma_x s_z} = \frac{i\widetilde{\varepsilon}\sigma_0 s_0 + \xi_k \sigma_z s_0 - \widetilde{\Delta}\sigma_x s_z}{-\widetilde{\varepsilon}^2 - \xi_k^2 - \widetilde{\Delta}^2}\,. \tag{6.13}$$

Now we need to examine how the different matrices carried by the vertices of the impurity interactions commute with this Green's function, noting that the outer product essentially allows us to commute the spin and Nambu Pauli matrices independently

$$\text{imp:} \quad \sigma_z s_0 \Big(i\widetilde{\varepsilon}\sigma_0 s_0 + \xi_k \sigma_z s_0 - \widetilde{\Delta}\sigma_x s_z \Big) \sigma_z s_0 = i\widetilde{\varepsilon}\sigma_0 s_0 + \xi_k \sigma_z s_0 + \widetilde{\Delta}\sigma_x s_z \tag{6.14a}$$

$$\text{mag}_\text{x}\text{:} \quad \sigma_z s_x \Big(i\widetilde{\varepsilon}\sigma_0 s_0 + \xi_k \sigma_z s_0 - \widetilde{\Delta}\sigma_x s_z \Big) \sigma_z s_x = i\widetilde{\varepsilon}\sigma_0 s_0 + \xi_k \sigma_z s_0 - \widetilde{\Delta}\sigma_x s_z \tag{6.14b}$$

$$\text{mag}_\text{y}\text{:} \quad \sigma_z s_y \Big(i\widetilde{\varepsilon}\sigma_0 s_0 + \xi_k \sigma_z s_0 - \widetilde{\Delta}\sigma_x s_z \Big) \sigma_z s_y = i\widetilde{\varepsilon}\sigma_0 s_0 + \xi_k \sigma_z s_0 - \widetilde{\Delta}\sigma_x s_z \tag{6.14c}$$

$$\text{mag}_\text{y}\text{:} \quad \sigma_0 s_z \Big(i\widetilde{\varepsilon}\sigma_0 s_0 + \xi_k \sigma_z s_0 - \widetilde{\Delta}\sigma_x s_z \Big) \sigma_0 s_z = i\widetilde{\varepsilon}\sigma_0 s_0 + \xi_k \sigma_z s_0 - \widetilde{\Delta}\sigma_x s_z \tag{6.14d}$$

The non-magnetic term simply flips the sign of the Δ term as it did before. All of the magnetic terms fully commute with the Green's function, which means they will all contribute identically, giving us a factor of 3 which cancels with the 1/3. All together this leaves us with the integrals

$$\Sigma_{imp} = -\, n_{imp} N(0) |U|^2 \int_{-\infty}^{\infty} \mathrm{d}\xi_k \, \frac{i\widetilde{\varepsilon}\sigma_0 s_0 + \xi_k \sigma_z s_0 + \widetilde{\Delta}\sigma_x s_z}{\widetilde{\varepsilon}^2 + \xi_k^2 + \widetilde{\Delta}^2} \tag{6.15}$$

$$\text{and} \quad \Sigma_{mag} = -\, S(S+1) n_{mag} N(0) |J|^2 \int_{-\infty}^{\infty} \mathrm{d}\xi_k \, \frac{i\widetilde{\varepsilon}\sigma_0 s_0 + \xi_k \sigma_z s_0 - \widetilde{\Delta}\sigma_x s_z}{\widetilde{\varepsilon}^2 + \xi_k^2 + \widetilde{\Delta}^2}\,. \tag{6.16}$$

These can be solved in the same way as equation 4.36 yielding

$$\Sigma_{imp} = -\pi n_{imp} N(0) |U|^2 \frac{i\widetilde{\varepsilon}\sigma_0 s_0 + \widetilde{\Delta}\sigma_x s_z}{\sqrt{\widetilde{\varepsilon}^2 + \widetilde{\Delta}^2}} \tag{6.17}$$

$$\text{and} \quad \Sigma_{mag} = -\pi S(S+1) n_{mag} N(0) |J|^2 \frac{i\widetilde{\varepsilon}\sigma_0 s_0 - \widetilde{\Delta}\sigma_x s_z}{\sqrt{\widetilde{\varepsilon}^2 + \widetilde{\Delta}^2}} \tag{6.18}$$

So now we solve for the renormalised variables by solving self consistently with the original ansatz by equating coefficients of the Pauli matrices, along with defining a scattering rate for the magnetic impurities,

$$\tau_s^{-1} = 2\pi S(S+1) n_{mag} N(0) |J|^2 \,, \tag{6.19}$$

we have

$$\varepsilon = \widetilde{\varepsilon}\left(1 - \frac{1}{2}\left(\frac{1}{\tau_0} + \frac{1}{\tau_s}\right)\frac{1}{\sqrt{\widetilde{\varepsilon}^2 + \widetilde{\Delta}^2}}\right) \tag{6.20a}$$

$$\text{and} \quad \Delta = \widetilde{\Delta}\left(1 - \frac{1}{2}\left(\frac{1}{\tau_0} - \frac{1}{\tau_s}\right)\frac{1}{\sqrt{\widetilde{\varepsilon}^2 + \widetilde{\Delta}^2}}\right). \tag{6.20b}$$

Note now that $\frac{\varepsilon}{\Delta} \neq \frac{\widetilde{\varepsilon}}{\widetilde{\Delta}}$, so it is now no longer possible to invert the relations to find $\widetilde{\varepsilon}$ and $\widetilde{\Delta}$ in terms of ε and Δ, therefore the definition of these variables will remain implicit. Also as a result of this the gap and transition temperature will be affected by the addition of magnetic impurities, more specifically they will be suppressed and at a critical concentration the gap will become zero before the superconductivity is completely destroyed, leading to so called gapless superconductivity.

To deduce the form of the suppressed gap we will follow [14] and begin by defining the useful quantity

$$u = \frac{\widetilde{\varepsilon}}{\widetilde{\Delta}} \,. \tag{6.21}$$

We can then re-write the equations in 6.20 like so,

$$\widetilde{\varepsilon} = \varepsilon + \frac{1}{2}\left(\frac{1}{\tau_0} + \frac{1}{\tau_s}\right)\frac{u}{\sqrt{1+u^2}} \tag{6.22a}$$

$$\text{and} \quad \widetilde{\Delta} = \Delta + \frac{1}{2}\left(\frac{1}{\tau_0} - \frac{1}{\tau_s}\right)\frac{1}{\sqrt{1+u^2}} \,. \tag{6.22b}$$

By multiplying the latter equation by u and subtracting it off the former, we can arrive

at

$$\frac{\varepsilon}{\Delta} = u\left(1 - \zeta\frac{1}{\sqrt{1+u^2}}\right), \quad \text{where} \quad \zeta = \frac{1}{\tau_s\Delta}. \tag{6.23}$$

Rewriting this in terms of real frequencies we analytically continue, which will discuss in detail in the following section, but essential we can simply take $iu(i\varepsilon) \mapsto u(\varepsilon)$, which yields

$$\frac{\varepsilon}{\Delta} = u\left(1 - \zeta\frac{1}{\sqrt{1-u^2}}\right), \quad \text{where} \quad \zeta = \frac{1}{\tau_s\Delta}. \tag{6.24}$$

If we, for now, assume that u is purely real we can plot the right-hand side as a function of u, as shown in figure 6.2.

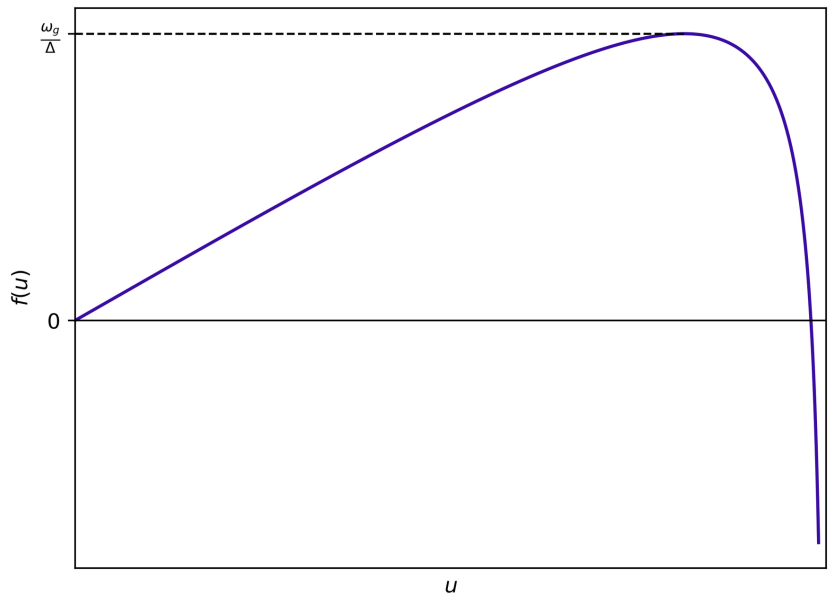

Figure 6.2: Plot of the ratio of the real frequency to the order parameter, ε/Δ, written as a function of u, written in equation 6.24. The maximum of this function can be identified with the suppressed gap, ω_g.

This function has one maximum, which is related to the value of the suppressed gap, ω_g. This is can be shown by looking at the density of states of superconducting electrons,

which can be written as

$$N_s(\varepsilon) = \mathrm{Im}\left\{ \int \frac{\mathrm{d}\mathbf{k}}{(2\pi)^d} \frac{1}{2} \mathrm{Tr}[\mathcal{G}(\mathbf{k}, \varepsilon)] \right\}. \tag{6.25}$$

Substituting in the form of the Green's function, with real frequency, in 3-dimensions we have

$$\begin{aligned} N_s(\varepsilon) &= \frac{1}{2\pi} \mathrm{Im}\left\{ \int \frac{\mathrm{d}^3k}{(2\pi)^3} \frac{1}{2} \mathrm{Tr}\left[\frac{\widetilde{\varepsilon}\sigma_0 s_0 + \xi_k \sigma_z s_0 - \widetilde{\Delta}\sigma_x s_z}{\widetilde{\varepsilon}^2 - \xi_k^2 - \widetilde{\Delta}^2} \right] \right\} \\ &= \frac{1}{2\pi} \mathrm{Im}\left\{ 2N(0) \int_0^\infty \mathrm{d}\xi \, \frac{\widetilde{\varepsilon}}{\widetilde{\varepsilon}^2 - \xi^2 - \widetilde{\Delta^2}} \right\} \\ &= \mathrm{Im}\left\{ N(0) \frac{\widetilde{\varepsilon}}{\sqrt{\widetilde{\Delta}^2 - \widetilde{\varepsilon}^2}} \right\} = N(0) \, \mathrm{Im}\left\{ \frac{u}{\sqrt{1-u^2}} \right\}. \end{aligned} \tag{6.26}$$

Then we can use equation 6.23 along with the fact that ε/Δ is purely real to get

$$N_s(\varepsilon) = N(0)\zeta^{-1} \, \mathrm{Im}\{u\}. \tag{6.27}$$

From this we can conclude that in order for the superconducting density of states to be non-zero, u must have an imaginary part, and in the plot of $\omega/\Delta = f(u)$ we assumed u was purely real. So for $\varepsilon < \omega_g$, $N_s(\varepsilon)$ will be zero and for there to be solutions with $f(u) > \omega_g/\Delta$, u must have an imaginary part and hence N_s is non-zero. Therefore the density of states is gapped for $\varepsilon < \omega_g$.

All that is left to do is to calculate the maximum of this function. We will call the value of u for which $f(u)$ is maximised u_0, then this value simply needs to be substituted into equation 6.23. Following this through, we have

$$\begin{aligned} &\frac{\mathrm{d}f(u)}{\mathrm{d}u} = 0 = 1 - \frac{\zeta}{(1-u_0^2)^{\frac{3}{2}}} \\ &\Rightarrow u_0 = (1 - \zeta^{\frac{2}{3}})^{\frac{1}{2}} \\ &\therefore \omega_g = \Delta(1 - \zeta^{\frac{2}{3}})^{\frac{3}{2}}. \end{aligned} \tag{6.28}$$

6.2 Linear Response of a Superconductor Containing Paramagnetic Impurities to an Electromagnetic Field

The set up of solving for the linear response to an applied field should be very familiar, the only change we must make compared to the calculation in section 4.3 is to use the 'magnetic'-Green's functions defined in the previous section and include a normalisation factor of $\frac{1}{2}$ in the trace due to the double counting of each of the spins. Therefore we will immediately write down the linear response function, in the limit that the external momentum $\mathbf{q} \to 0$:

$$\mathcal{K}^{E,M}_{\alpha\beta}(i\omega) = \frac{e^2 k_F^2 N(0)}{3m^2}\delta_{\alpha\beta} T\sum_{\varepsilon}\int_{-\infty}^{\infty}\frac{\mathrm{d}\xi}{2}\,\mathrm{Tr}\left[\frac{i\widetilde{\varepsilon}'\sigma_0 s_0 + \xi_k\sigma_z s_0 - \widetilde{\Delta}'\sigma_x s_z}{\widetilde{\varepsilon}'^2 + \xi_k^2 + \widetilde{\Delta}'^2}\right.$$
$$\left.\times\frac{i\widetilde{\varepsilon}\sigma_0 s_0 + \xi_k\sigma_z s_0 - \widetilde{\Delta}\sigma_x s_z}{\widetilde{\varepsilon}^2 + \xi_k^2 + \widetilde{\Delta}^2}\right], \tag{6.29}$$

where the M superscript denotes we have included the magnetic impurities. This is a purely diagonal response in this limit, hence we can drop the α and β. Only terms with a matrix dependence of $\sigma_0 s_0$ will contribute to the trace, with a factor of 4, which leads to

$$\mathcal{K}^{E,M}(i\omega) = \frac{ne^2}{m}T\sum_{\varepsilon}\int_{-\infty}^{\infty}\mathrm{d}\xi\,\frac{\xi^2 - \widetilde{\varepsilon}\widetilde{\varepsilon}' + \widetilde{\Delta}\widetilde{\Delta}'}{(\xi^2 + \widetilde{E}^2)(\xi^2 + \widetilde{E}'^2)}\,, \tag{6.30}$$

where $\widetilde{E} = \sqrt{\widetilde{\varepsilon}^2 + \widetilde{\Delta}^2}$. This integral can be solved with the results in equation 4.53 to yield

$$\begin{aligned}\mathcal{K}^{E,M}(i\omega) &= \frac{\pi ne^2}{m}T\sum_{\varepsilon}\frac{\widetilde{E}\widetilde{E}' - \widetilde{\varepsilon}\widetilde{\varepsilon}' + \widetilde{\Delta}\widetilde{\Delta}'}{\widetilde{E}\widetilde{E}'(\widetilde{E} + \widetilde{E}')}\\ &= \frac{\pi ne^2}{m}T\sum_{\varepsilon}\frac{WW' + 1 - uu'}{WW'(\widetilde{\Delta}W + \widetilde{\Delta}'W')}\,,\end{aligned} \tag{6.31}$$

where $W = \sqrt{1+u^2}$. Multiplying through equation 6.22b by a factor of W, we can eliminate $\widetilde{\Delta}$ in favour of Δ to obtain

$$\mathcal{K}^{E,M}(i\omega) = \frac{\pi n e^2}{m} T \sum_{\varepsilon} \frac{WW' + 1 - uu'}{WW'(\Delta W + \Delta W' + \tau_-^{-1})}\,, \tag{6.32}$$

where $\tau_-^{-1} = \tau_0^{-1} - \tau_s^{-1}$. Now to return to units with dimensions of frequency, we multiply the numerator and denominator by Δ^2 and define

$$v = \Delta u \quad \text{and} \quad V = \sqrt{\Delta^2 + v^2}\,, \tag{6.33}$$

so we have

$$\mathcal{K}^{E,M}(i\omega) = \frac{\pi n e^2}{m} T \sum_{\varepsilon} \frac{VV' + \Delta^2 - vv'}{VV'(V + V' + \tau_-^{-1})}\,. \tag{6.34}$$

To proceed we wish to take the sum over ε by writing it as a contour integral, taking $i\varepsilon \mapsto z$. However, it is less clear how this will work now that v and v' are related to ε and $\varepsilon + \omega$ implicitly. However, we can deduce that v must have the same analytic properties as ε with respect to the branch cuts, because if we take the limit $\tau_s^{-1} \to 0$, then $V \to E$ continuously without any breaks in analyticity. So when we take $i\varepsilon \mapsto z$, we will have $iv(i\varepsilon) \mapsto v(z)$ and $iv' \mapsto v(z + i\omega)$, which for brevity we will continue to denote with v and v' respectively. Following from this we will also have $V(z) = \sqrt{\Delta^2 - v^2(z)}$ and $V'(z) = V(z + i\omega) = \sqrt{\Delta^2 - v^2(z + i\omega)}$. So we have

$$\mathcal{K}^{E,M}(i\omega) = \frac{\pi n e^2}{m} \frac{i}{2\pi} \oint_{\Gamma} \mathrm{d}z\, f(z) \frac{VV' + \Delta^2 + vv'}{VV'(V + V' + \tau_-^{-1})}\,, \tag{6.35}$$

where the contour, Γ, is shown in figure 6.3. Note that the primary difference between this contour and the ones that appear without magnetic impurities is that the branch cuts now begin at the the suppressed gap, ω_g.

Next, we wish to remove the contours, Γ_c and Γ_d, that enclose the lower two branches,

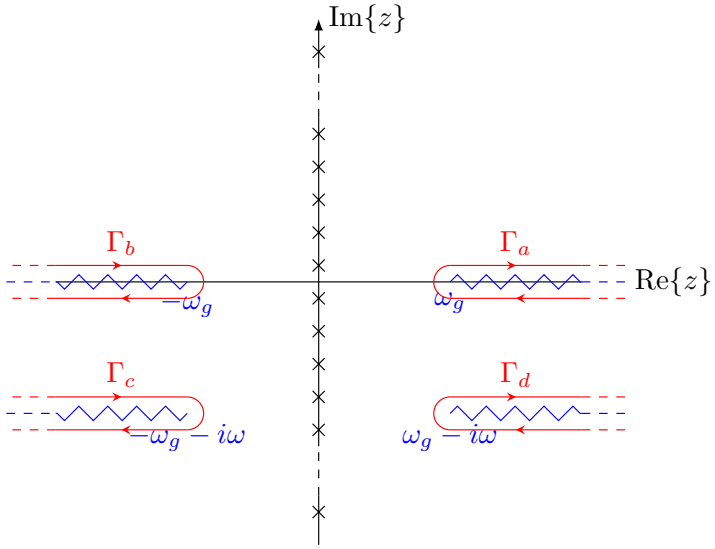

Figure 6.3: Contours arising from Matsubara frequencies in the linear response of a superconductor with magnetic impurities to an electromagnetic field. The primary difference between this case and that without magnetic impurities is that the branch cuts now start at the supressed gap, ω_g, instead of Δ.

so that we can guarantee that when we take $i\omega \mapsto \omega + i\delta$ the contours do not pass over any singularities on the imaginary axis; avoiding any of the complications associated to this. If we examine the relation

$$z = v(z)\left(1 - \frac{1}{\tau_s}\frac{1}{\sqrt{\Delta^2 - v^2(z)}}\right), \tag{6.36}$$

it is straight forward to verify that v has the property $v(-z) = -v(z)$. Therefore, we can make use of the transformation $z \mapsto -z - i\omega$ on Γ_c and Γ_d, because under this transformation $v \mapsto -v'$, $v' \mapsto -v$, $V \mapsto V'$ and $V' \mapsto V$. Thus we have, in analogy to equation 4.65 in section 4.3, a mapping of $\Gamma_c \mapsto \Gamma_a$ and $\Gamma_d \mapsto \Gamma_b$, with $f(z) \mapsto f(-z)$ and picking-up an additional minus sign in the integrals. So we are able to simplify the full contour integral to

$$\mathcal{K}^{E,M}(i\omega) = \frac{\pi n e^2}{m}\frac{1}{2\pi i}\int_{\Gamma_{a+b}} \mathrm{d}z \tanh\left(\frac{z}{2T}\right)\frac{VV' + \Delta^2 + vv'}{VV'(V + V' + \tau_-^{-1})}, \tag{6.37}$$

and then safely analytically continue $i\omega \mapsto \omega$, so that we obtain and equation for $\mathcal{K}^{E,M}(\omega)$

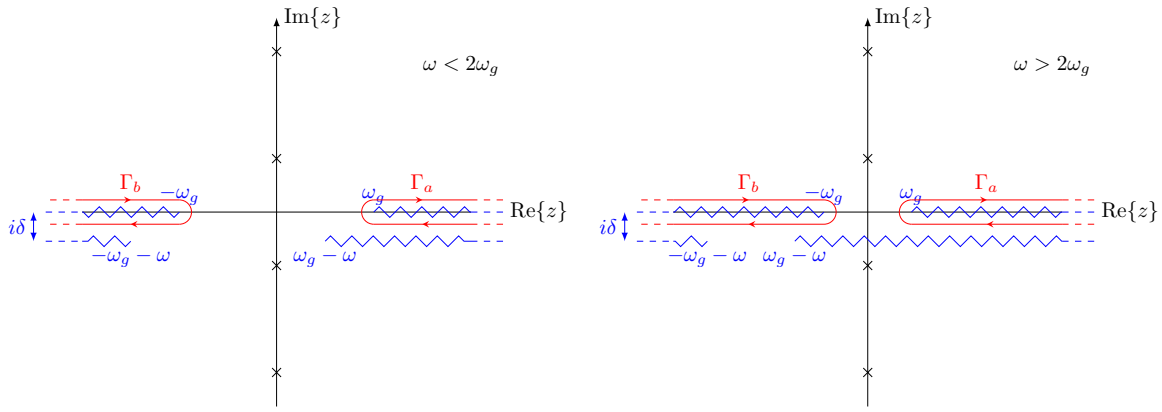

Figure 6.4: Contours arising from Matsubara frequencies in the linear response of a superconductor with magnetic impurities to an electromagnetic field after analytic continuation of $i\omega \mapsto \omega + i\delta$. The left-hand figure shows qualitatively the contours when $\omega < 2\omega_g$ and the right-hand side the case where $\omega > 2\omega_g$.

with contours given in figure 6.4.

To understand the behaviour of v and V as we analytically continue $z \mapsto x \pm i\delta$, we return to the relation in equation 6.36. If we split both z and $v(z)$ into their real and imaginary parts, we have

$$x + iy = (a + ib)\left(1 - \frac{1}{\tau_s}\frac{1}{\sqrt{\Delta^2 - (a+ib)^2}}\right), \quad \text{where} \quad a = \mathrm{Re}\{v\},\, b = \mathrm{Im}\{v\}\,. \tag{6.38}$$

We use the standard result for the square root of a complex number

$$\begin{aligned}\sqrt{\alpha + i\beta} &= \pm\left[\sqrt{\frac{\sqrt{\alpha^2+\beta^2}+\alpha}{2}} + i\,\mathrm{sgn}(\beta)\sqrt{\frac{\sqrt{\alpha^2+\beta^2}-\alpha}{2}}\right], \\ &= \pm\Big[A(\alpha,\beta) + i\,\mathrm{sgn}(\beta)B(\alpha,\beta)\Big]\,, \end{aligned} \tag{6.39}$$

to find

$$\begin{aligned}\sqrt{\Delta^2 - (a+ib)^2} &= \pm\big[A(\Delta^2 - a^2 + b^2, -2ab) + i\,\mathrm{sgn}(-ab)B(\Delta^2 - a^2 + b^2, -2ab)\big] \\ &= \widetilde{A} + i\,\mathrm{sgn}(-ab)\widetilde{B}\,, \end{aligned} \tag{6.40}$$

noting that the functions, $A(\alpha,\beta)$ and $B(\alpha,\beta)$, are real and positive for all α and β. And

remembering that the integral over ξ taken earlier in the calculation requires the real part of $\widetilde{E}$ to be positive, this means we must take the + sign in the $\pm$. Substituting this back into equation 6.38 and rationalising the denominator, we can write this equation as

$$x + iy = \left[a - \frac{1}{\tau_s} \frac{a\widetilde{A} + b\widetilde{B}\mathrm{sgn}(-ab)}{\widetilde{A}^2 + \widetilde{B}^2} \right] + i \left[b - \frac{1}{\tau_s} \frac{b\widetilde{A} - a\widetilde{B}\mathrm{sgn}(-ab)}{\widetilde{A}^2 + \widetilde{B}^2} \right] . \tag{6.41}$$

Now we can see that if we take $y \mapsto -y$, for this equation be be satisfied we must have $b \mapsto -b$, because both $\widetilde{A}$ and $\widetilde{B}$ are even in a and b. Therefore, we can conclude $v(z^*) = v^*(z)$ and hence, as the branch cut is crossed $v \mapsto v^*$. Furthermore, if we refer back to equation 6.40 we can see that taking the conjugate of z will mean $b \mapsto -b$, switching only the sign of the sgn, therefore we have

$$V(z^*) = V^*(z) \, , \tag{6.42}$$

and, similarly to v, we will have $V \mapsto V^*$ as the branch cut is crossed.

Next we will again use the fact that in the limit $\tau_s^{-1} \to 0$ we must recover the analytic properties of the non-magnetic calculation. First, lets examine what will happen when we look at the Γ_a contour. We require that, for $x > \Delta$

$$\begin{aligned} \text{for} \quad z = x + i\delta \quad &: \quad \sqrt{\Delta^2 - v^2(z)} \mapsto -i\sqrt{x^2 - \Delta^2} \quad \text{as} \quad \tau_s^{-1} \to 0 \\ \text{and for} \quad z = x - i\delta \quad &: \quad \sqrt{\Delta^2 - v^2(z)} \mapsto i\sqrt{x^2 - \Delta^2} \quad \text{as} \quad \tau_s^{-1} \to 0 \, . \end{aligned} \tag{6.43}$$

If we expand $v(x + i\delta)$ for small δ we have

$$v(x + i\delta) \simeq v(x) + i\delta \frac{\mathrm{d}v(x)}{\mathrm{d}x} \, , \tag{6.44}$$

where $v(x)$ is in general complex, even though its argument is pure real. Then similarly

to equation 4.67 we can expand out $V(x+i\delta)$ as follows,

$$\sqrt{\Delta^2 - v^2(x+i\delta)} \simeq \pm i\sqrt{v^2(x)-\Delta^2}\left[1 + i\delta\frac{\frac{\mathrm{d}v(x)}{\mathrm{d}x}}{v^2(x)-\Delta^2}\right], \tag{6.45}$$

and because $v(x) \to x$ as $\tau_s^{-1} \to 0$, we can deduce the correct choice of sign must be

$$\sqrt{\Delta^2 - v^2(x+i\delta)} \simeq -i\sqrt{v^2(x)-\Delta^2}. \tag{6.46}$$

Then, as the cut is crossed we have

$$\begin{aligned}\sqrt{\Delta^2 - v^2(x-i\delta)} &= \sqrt{\Delta^2 - v^{*2}(x+i\delta)} \\ &\simeq \pm i\sqrt{v^{*2}(x)-\Delta^2}\left[1 - i\delta\frac{\frac{\mathrm{d}v^*(x)}{\mathrm{d}x}}{v^{*2}(x)-\Delta^2}\right],\end{aligned} \tag{6.47}$$

and hence, to be consistent, we have

$$\sqrt{\Delta^2 - v^2(x-i\delta)} \simeq i\sqrt{v^{*2}(x)-\Delta^2} \tag{6.48}$$

On the Γ_b contour, we can immediately deduce the the appropriate terms above and below the cut using the property $v(-z) = -v(z)$. Because taking $z \to -z$ is equivalent to taking both $x \to -x$ and the complex conjugate, this means that the result above the Γ_a contour should be the same as below the Γ_b contour and visa versa. This is also consistent with the limit $\tau_s^{-1} \to 0$, seeing as in this limit when $x < -\Delta$, we expect

$$\begin{aligned}\text{for} \quad z = x+i\delta \quad &: \quad \sqrt{\Delta^2 - v^2(z)} \mapsto i\sqrt{x^2-\Delta^2} \quad \text{as} \quad \tau_s^{-1} \to 0 \\ \text{and for} \quad z = x-i\delta \quad &: \quad \sqrt{\Delta^2 - v^2(z)} \mapsto -i\sqrt{x^2-\Delta^2} \quad \text{as} \quad \tau_s^{-1} \to 0\,.\end{aligned} \tag{6.49}$$

So all together we have

$$\begin{aligned}
\text{for} \quad x > \omega_g \quad &: \quad \sqrt{\Delta^2 - v^2(x+i\delta)} \simeq -i\sqrt{v^2(x) - \Delta^2} := -iV(x) \\
\text{and} \quad &\sqrt{\Delta^2 - v^2(x-i\delta)} \simeq i\sqrt{v^{*2}(x) - \Delta^2} := iV^*(x)\,, \\
\text{and for} \quad x < -\omega_g \quad &: \quad \sqrt{\Delta^2 - v^2(x+i\delta)} \simeq i\sqrt{v^{*2}(x) - \Delta^2} := iV^*(x) \\
\text{and} \quad &\sqrt{\Delta^2 - v^2(x-i\delta)} \simeq -i\sqrt{v^2(x) - \Delta^2} := -iV(x)\,.
\end{aligned} \tag{6.50}$$

Of course, it is simple to repeat this treatment for $V(z+\omega)$ and the same pattern is found above and below the two lower branch cuts corresponding to this square root, of course with the appropriate regions for the results being $x > \omega_g - \omega$ and $x < -\omega_g - \omega$. The only region that needs addressing is $-\omega_g - \omega < x < -\omega_g$ when $\omega < 2\omega_g$ and $-\omega_g - \omega < x < \omega_g - \omega$ when $\omega > 2\omega_g$, where the integration takes place outside the region of the branch cut. But, we have actually discussed this region at the end of the previous section, as this corresponds to the region where $v(x)$ is purely real and hence the density of states of superconducting carriers is zero. So we will define

$$\begin{aligned}
& v(z+\omega) = \bar{v}(x+\omega) \\
\text{and} \quad & V(z+\omega) = \bar{V}(x+\omega) = \sqrt{\Delta^2 - v^2(x+\omega)} \\
\text{for} \quad & -\omega_g - \omega < x < -\omega_g \quad \text{when} \quad x < 2\omega_g\,, \\
\text{or for} \quad & -\omega_g - \omega < x < \omega_g - \omega \quad \text{when} \quad x > 2\omega_g\,,
\end{aligned} \tag{6.51}$$

where the bars indicate these variables are purely real, to distinguish them from the generally complex $v(z)$. At this stage we must note that the $\omega > 2\omega$ regime is much more relevant when considering magnetic impurities than when without. This is because as ω_g is suppressed by increased concentrations of magnetic impurities, it can decrease to zero leading to gap-less superconductivty. Thus, even when we are considering limits of very small ω we may still be in the regime where $\omega > 2\omega_g$ and so should be careful not to leave out relevant terms in our contour integrals.

Now that we have all the information we need for the analytic continuation of the contours to the real axis, we can begin with writing the integral we obtain from the Γ_a contour

$$\mathcal{K}_a^{E,M}(\omega) = \frac{ne^2}{2im}\Bigg[\int_{\omega_g}^{\infty} \frac{\mathrm{d}x \tanh\left(\frac{x}{2T}\right)}{\tau_-^{-1} - iV(x) - iV(x+\omega)}\left(1 - \frac{v(x)v(x+\omega)+\Delta^2}{V(x)V(x+\omega)}\right) - \int_{\omega_g}^{\infty} \frac{\mathrm{d}x \tanh\left(\frac{x}{2T}\right)}{\tau_-^{-1} + iV^*(x) - iV(x+\omega)}\left(1 + \frac{v^*(x)v(x+\omega)+\Delta^2}{V^*(x)V(x+\omega)}\right)\Bigg]. \quad (6.52)$$

And for the Γ_b contour, in the case where $\omega < 2\omega_g$, we have

$$\begin{aligned}\mathcal{K}_b^{E,M}(\omega) = \frac{ne^2}{2im}\Bigg[&\int_{-\infty}^{-\omega_g-\omega} \frac{\mathrm{d}x \tanh\left(\frac{x}{2T}\right)}{\tau_-^{-1} + iV^*(x) + iV^*(x+\omega)}\left(1 - \frac{v^*(x)v^*(x+\omega)+\Delta^2}{V^*(x)V^*(x+\omega)}\right)\\ &- \int_{-\infty}^{-\omega_g-\omega} \frac{\mathrm{d}x \tanh\left(\frac{x}{2T}\right)}{\tau_-^{-1} - iV(x) + iV^*(x+\omega)}\left(1 + \frac{v(x)v^*(x+\omega)+\Delta^2}{V(x)V^*(x+\omega)}\right)\\ &+ \int_{-\omega_g-\omega}^{-\omega_g} \frac{\mathrm{d}x \tanh\left(\frac{x}{2T}\right)}{\tau_-^{-1} + iV^*(x) + \bar{V}(x+\omega)}\left(1 + \frac{v^*(x)\bar{v}(x+\omega)+\Delta^2}{iV^*(x)\bar{V}(x+\omega)}\right)\\ &- \int_{-\omega_g-\omega}^{-\omega_g} \frac{\mathrm{d}x \tanh\left(\frac{x}{2T}\right)}{\tau_-^{-1} - iV(x) + \bar{V}(x+\omega)}\left(1 - \frac{v(x)\bar{v}(x+\omega)+\Delta^2}{iV(x)\bar{V}(x+\omega)}\right)\Bigg].\end{aligned} \quad (6.53)$$

Now to symmetrise the integrals, in the $\mathcal{K}_a$ term we can make the transformation $x \mapsto x - \omega/2$. Which will transform

$$\begin{aligned} v(x) \mapsto v\Big(x - \frac{\omega}{2}\Big) := v_-\,, \quad v(x+\omega) \mapsto v\Big(x + \frac{\omega}{2}\Big) := v_+ \\ \text{and} \quad V(x) \mapsto V\Big(x - \frac{\omega}{2}\Big) := V_-\,, \quad V(x+\omega) \mapsto V\Big(x + \frac{\omega}{2}\Big) := V_+\,, \end{aligned} \quad (6.54)$$

and in $\mathcal{K}_b$ take $x \mapsto -x - \omega/2$, which yields

$$\begin{aligned} v(x) \mapsto -v\Big(x + \frac{\omega}{2}\Big) := -v_+\,, \quad v(x+\omega) \mapsto -v\Big(x - \frac{\omega}{2}\Big) := -v_-\,, \\ \text{and} \quad V(x) \mapsto V\Big(x + \frac{\omega}{2}\Big) := V_+\,, \quad V(x+\omega) \mapsto V\Big(x - \frac{\omega}{2}\Big) := V_-\,, \\ \text{as well as} \quad \bar{v}(x+\omega) \mapsto -\bar{v}\Big(x - \frac{\omega}{2}\Big) := -\widetilde{v}\,, \quad \bar{V}(x+\omega) \mapsto \bar{V}\Big(x - \frac{\omega}{2}\Big) := \widetilde{V}\,. \end{aligned} \quad (6.55)$$

Using these transformations, we have

$$\begin{aligned}\mathcal{K}^{E,M}(\omega) = \frac{ne^2}{2im}\Bigg[&\int_{\omega_g+\frac{\omega}{2}}^{\infty} \frac{\mathrm{d}x \tanh\left(\frac{x-\frac{\omega}{2}}{2T}\right)}{\tau_-^{-1} - iV_- - iV_+}\left(1 - \frac{v_-v_+ + \Delta^2}{V_-V_+}\right) \\ &- \int_{\omega_g+\frac{\omega}{2}}^{\infty} \frac{\mathrm{d}x \tanh\left(\frac{x-\frac{\omega}{2}}{2T}\right)}{\tau_-^{-1} + iV_-^* - iV_+}\left(1 + \frac{v_-^*v_+ + \Delta^2}{V_-^*V_+}\right) \\ &- \int_{\omega_g+\frac{\omega}{2}}^{\infty} \frac{\mathrm{d}x \tanh\left(\frac{x+\frac{\omega}{2}}{2T}\right)}{\tau_-^{-1} + iV_+^* + iV_-^*}\left(1 - \frac{v_+^*v_-^* + \Delta^2}{V_+^*V_-^*}\right) \\ &+ \int_{\omega_g+\frac{\omega}{2}}^{\infty} \frac{\mathrm{d}x \tanh\left(\frac{x+\frac{\omega}{2}}{2T}\right)}{\tau_-^{-1} - iV_+ + iV_-^*}\left(1 + \frac{v_+v_-^* + \Delta^2}{V_+V_-^*}\right) \\ &- \int_{\omega_g-\frac{\omega}{2}}^{\omega_g+\frac{\omega}{2}} \frac{\mathrm{d}x \tanh\left(\frac{x+\frac{\omega}{2}}{2T}\right)}{\tau_-^{-1} + iV_+^* + \widetilde{V}}\left(1 + \frac{v_+^*\widetilde{v} + \Delta^2}{iV_+^*\widetilde{V}}\right) \\ &+ \int_{\omega_g-\frac{\omega}{2}}^{\omega_g+\frac{\omega}{2}} \frac{\mathrm{d}x \tanh\left(\frac{x+\frac{\omega}{2}}{2T}\right)}{\tau_-^{-1} - iV_+ + \widetilde{V}}\left(1 - \frac{v_+\widetilde{v} + \Delta^2}{iV_+\widetilde{V}}\right)\Bigg] .\end{aligned} \tag{6.56}$$

Next, we can begin to apply the limits that are relevant to our problem. Firstly, we will be in the dirty limit and the diffusive limit, which are the case even without magnetic impurities. The new limit we will be introducing will be that the concentration of magnetic impurities must be much less than than of the non-magnetic impurities, or in term of scattering rates we have $\tau_s^{-1} \ll \tau_0^{-1}$. This is the case because in the regime where $\tau_s^{-1} \sim \tau_0^{-1}$ the magnetic impurities would be at high enough concentrations to destroy the superconductivity entirely. In this limit we can obtain the leading order contribution in the terms with the form

$$\frac{1}{\tau_-^{-1} \pm iV_+ \pm iV_-} \approx \tau_0 \,, \tag{6.57}$$

because the V terms still have dimensionality of $\omega\tau_0$, which is small in this limit. Using this approximation we can see that the '1' terms in each pair of integrals will now cancel

and we are left with

$$\begin{aligned}\mathcal{K}^{E,M}(\omega) = \frac{ne^2\tau_0}{2m}\Bigg[& i\int_{\omega_g+\frac{\omega}{2}}^{\infty} \mathrm{d}x \tanh\left(\frac{x-\frac{\omega}{2}}{2T}\right)\left(\frac{v_-v_+ + \Delta^2}{V_-V_+} + \frac{v_-^*v_+ + \Delta^2}{V_-^*V_+}\right) \\ & - i\int_{\omega_g+\frac{\omega}{2}}^{\infty} \mathrm{d}x \tanh\left(\frac{x+\frac{\omega}{2}}{2T}\right)\left(\frac{v_+^*v_-^* + \Delta^2}{V_+^*V_-^*} + \frac{v_+v_-^* + \Delta^2}{V_+V_-^*}\right) \\ & + \int_{\omega_g-\frac{\omega}{2}}^{\omega_g+\frac{\omega}{2}} \mathrm{d}x \tanh\left(\frac{x+\frac{\omega}{2}}{2T}\right)\left(\frac{v_+^*\widetilde{v} + \Delta^2}{V_+^*\widetilde{V}} + \frac{v_+\widetilde{v} + \Delta^2}{V_+\widetilde{V}}\right)\Bigg].\end{aligned} \tag{6.58}$$

When looking for the real part of the conductivity we must take the imaginary part of the linear response function, remembering they are related by a factor of $-i\omega$. In the first two terms this means we require the real part of the integrand and in the third term the imaginary part. However, if we examine the real part we can see there is some cancellation. Beginning with the first integrand,

$$\begin{aligned}\mathrm{Re}\left\{\frac{v_-v_+ + \Delta^2}{V_-V_+} + \frac{v_-^*v_+ + \Delta^2}{V_-^*V_+}\right\} = & \,\mathrm{Re}\left\{\frac{v_-}{V_-}\right\}\mathrm{Re}\left\{\frac{v_+}{V_+}\right\} - \mathrm{Im}\left\{\frac{v_-}{V_-}\right\}\mathrm{Im}\left\{\frac{v_+}{V_+}\right\} \\ & + \mathrm{Re}\left\{\frac{v_-^*}{V_-^*}\right\}\mathrm{Re}\left\{\frac{v_+}{V_+}\right\} - \mathrm{Im}\left\{\frac{v_-^*}{V_-^*}\right\}\mathrm{Im}\left\{\frac{v_+}{V_+}\right\} \\ & + \mathrm{Re}\left\{\frac{\Delta}{V_-}\right\}\mathrm{Re}\left\{\frac{\Delta}{V_+}\right\} - \mathrm{Im}\left\{\frac{\Delta}{V_-}\right\}\mathrm{Im}\left\{\frac{\Delta}{V_+}\right\} \\ & + \mathrm{Re}\left\{\frac{\Delta}{V_-^*}\right\}\mathrm{Re}\left\{\frac{\Delta}{V_+}\right\} - \mathrm{Im}\left\{\frac{\Delta}{V_-^*}\right\}\mathrm{Im}\left\{\frac{\Delta}{V_+}\right\},\end{aligned} \tag{6.59}$$

the real part will remain the same sign under the complex conjugate, and so sum-up, however taking the conjugate will flip the sign in the imaginary part, causing the terms arising from the imaginary parts to cancel. This will occur in the second integrand too, hence we have

$$\mathrm{Re}\left\{\frac{v_-v_+ + \Delta^2}{V_-V_+} + \frac{v_-^*v_+ + \Delta^2}{V_-^*V_+}\right\} = 2\,\mathrm{Re}\left\{\frac{v_-}{V_-}\right\}\mathrm{Re}\left\{\frac{v_+}{V_+}\right\} + 2\,\mathrm{Re}\left\{\frac{\Delta}{V_-}\right\}\mathrm{Re}\left\{\frac{\Delta}{V_+}\right\}, \tag{6.60}$$

$$\mathrm{Re}\left\{\frac{v_-^*v_+^* + \Delta^2}{V_-^*V_+^*} + \frac{v_-^*v_+ + \Delta^2}{V_-^*V_+}\right\} = 2\,\mathrm{Re}\left\{\frac{v_-}{V_-}\right\}\mathrm{Re}\left\{\frac{v_+}{V_+}\right\} + 2\,\mathrm{Re}\left\{\frac{\Delta}{V_-}\right\}\mathrm{Re}\left\{\frac{\Delta}{V_+}\right\}. \tag{6.61}$$

In the third integral, remembering that $\widetilde{v}$ and $\widetilde{V}$ are purely real, the imaginary part is given by

$$\mathrm{Im}\left\{\frac{v_+^*\widetilde{v}+\Delta^2}{V_+^*\widetilde{V}}+\frac{v_+\widetilde{v}+\Delta^2}{V_+\widetilde{V}}\right\}=\frac{\widetilde{v}}{\widetilde{V}}\,\mathrm{Im}\left\{\frac{v_+^*}{V_+^*}\right\}+\frac{\widetilde{v}}{\widetilde{V}}\,\mathrm{Im}\left\{\frac{v_+}{V_+}\right\}$$
$$+\frac{\Delta}{\widetilde{V}}\,\mathrm{Im}\left\{\frac{\Delta}{V_+^*}\right\}+\frac{\Delta}{\widetilde{V}}\,\mathrm{Im}\left\{\frac{\Delta}{V_+}\right\}. \tag{6.62}$$

But again the taking of the conjugate between terms will cause them to cancel and so

$$\mathrm{Im}\left\{\frac{v_+^*\widetilde{v}+\Delta^2}{V_+^*\widetilde{V}}+\frac{v_+\widetilde{v}+\Delta^2}{V_+\widetilde{V}}\right\}=0\,. \tag{6.63}$$

So collecting this together we find

$$\mathrm{Im}\big\{\mathcal{K}^{E,M}(\omega)\big\}=-\frac{ne^2\tau_0}{m}\int_{\omega_g+\frac{\omega}{2}}^{\infty}\mathrm{d}x\left(\tanh\left(\frac{x+\frac{\omega}{2}}{2T}\right)-\tanh\left(\frac{x-\frac{\omega}{2}}{2T}\right)\right)$$
$$\times\left[\mathrm{Re}\left\{\frac{v_-}{V_-}\right\}\mathrm{Re}\left\{\frac{v_+}{V_+}\right\}+\mathrm{Re}\left\{\frac{\Delta}{V_-}\right\}\mathrm{Re}\left\{\frac{\Delta}{V_+}\right\}\right], \tag{6.64}$$

and hence in terms of conductivity

$$\mathrm{Re}\big\{\sigma^M(\omega)\big\}=\frac{\sigma_{\mathrm{Drude}}}{\omega}\int_{\omega_g+\frac{\omega}{2}}^{\infty}\mathrm{d}x\left(\tanh\left(\frac{x+\frac{\omega}{2}}{2T}\right)-\tanh\left(\frac{x-\frac{\omega}{2}}{2T}\right)\right)$$
$$\times\left[\mathrm{Re}\left\{\frac{v_-}{V_-}\right\}\mathrm{Re}\left\{\frac{v_+}{V_+}\right\}+\mathrm{Re}\left\{\frac{\Delta}{V_-}\right\}\mathrm{Re}\left\{\frac{\Delta}{V_+}\right\}\right]. \tag{6.65}$$

We can return to consider when $\omega > 2\omega_g$. In this regime the contribution from the Γ_b

contour is instead given by

$$\begin{aligned}\mathcal{K}_b^{E,M}(\omega) = \frac{ne^2}{2im}\Bigg[&\int_{-\infty}^{-\omega_g-\omega} \frac{\mathrm{d}x \tanh\left(\frac{x}{2T}\right)}{\tau_-^{-1} + iV^*(x) + iV^*(x+\omega)}\left(1 - \frac{v^*(x)v^*(x+\omega)+\Delta^2}{V^*(x)V^*(x+\omega)}\right) \\ &- \int_{-\infty}^{-\omega_g-\omega} \frac{\mathrm{d}x \tanh\left(\frac{x}{2T}\right)}{\tau_-^{-1} - iV(x) + iV^*(x+\omega)}\left(1 + \frac{v(x)v^*(x+\omega)+\Delta^2}{V(x)V^*(x+\omega)}\right) \\ &+ \int_{-\omega_g-\omega}^{\omega_g-\omega} \frac{\mathrm{d}x \tanh\left(\frac{x}{2T}\right)}{\tau_-^{-1} + iV^*(x) + \bar{V}(x+\omega)}\left(1 + \frac{v^*(x)\bar{v}(x+\omega)+\Delta^2}{iV^*(x)\bar{V}(x+\omega)}\right) \\ &- \int_{-\omega_g-\omega}^{\omega_g-\omega} \frac{\mathrm{d}x \tanh\left(\frac{x}{2T}\right)}{\tau_-^{-1} - iV(x) + \bar{V}(x+\omega)}\left(1 - \frac{v(x)\bar{v}(x+\omega)+\Delta^2}{iV(x)\bar{V}(x+\omega)}\right) \\ &+ \int_{\omega_g-\omega}^{-\omega_g} \frac{\mathrm{d}x \tanh\left(\frac{x}{2T}\right)}{\tau_-^{-1} + iV^*(x) - iV(x+\omega)}\left(1 + \frac{v^*(x)v(x+\omega)+\Delta^2}{V^*(x)V(x+\omega)}\right) \\ &- \int_{\omega_g-\omega}^{-\omega_g} \frac{\mathrm{d}x \tanh\left(\frac{x}{2T}\right)}{\tau_-^{-1} - iV(x) - iV(x+\omega)}\left(1 - \frac{v(x)v(x+\omega)+\Delta^2}{V(x)V(x+\omega)}\right)\Bigg],\end{aligned} \tag{6.66}$$

which after the symmetrisation is taken, is given by

$$\begin{aligned}\mathcal{K}^{E,M}(\omega) = \frac{ne^2}{2im}\Bigg[&\int_{\omega_g+\frac{\omega}{2}}^{\infty} \frac{\mathrm{d}x \tanh\left(\frac{x-\frac{\omega}{2}}{2T}\right)}{\tau_-^{-1} - iV_- - iV_+}\left(1 - \frac{v_-v_+ + \Delta^2}{V_-V_+}\right) \\ &- \int_{\omega_g+\frac{\omega}{2}}^{\infty} \frac{\mathrm{d}x \tanh\left(\frac{x-\frac{\omega}{2}}{2T}\right)}{\tau_-^{-1} + iV_-^* - iV_+}\left(1 + \frac{v_-^*v_+ + \Delta^2}{V_-^*V_+}\right) \\ &- \int_{\omega_g+\frac{\omega}{2}}^{\infty} \frac{\mathrm{d}x \tanh\left(\frac{x+\frac{\omega}{2}}{2T}\right)}{\tau_-^{-1} + iV_+^* + iV_-^*}\left(1 - \frac{v_+^*v_-^* + \Delta^2}{V_+^*V_-^*}\right) \\ &+ \int_{\omega_g+\frac{\omega}{2}}^{\infty} \frac{\mathrm{d}x \tanh\left(\frac{x+\frac{\omega}{2}}{2T}\right)}{\tau_-^{-1} - iV_+ + iV_-^*}\left(1 + \frac{v_+v_-^* + \Delta^2}{V_+V_-^*}\right) \\ &- \int_{\frac{\omega}{2}-\omega_g}^{\frac{\omega}{2}+\omega_g} \frac{\mathrm{d}x \tanh\left(\frac{x+\frac{\omega}{2}}{2T}\right)}{\tau_-^{-1} + iV_+^* + \widetilde{V}}\left(1 + \frac{v_+^*\widetilde{v} + \Delta^2}{iV_+^*\widetilde{V}}\right) \\ &+ \int_{\frac{\omega}{2}-\omega_g}^{\frac{\omega}{2}+\omega_g} \frac{\mathrm{d}x \tanh\left(\frac{x+\frac{\omega}{2}}{2T}\right)}{\tau_-^{-1} - iV_+ + \widetilde{V}}\left(1 - \frac{v_+\widetilde{v} + \Delta^2}{iV_+\widetilde{V}}\right) \\ &- \int_{\omega_g-\frac{\omega}{2}}^{\frac{\omega}{2}-\omega_g} \frac{\mathrm{d}x \tanh\left(\frac{x+\frac{\omega}{2}}{2T}\right)}{\tau_-^{-1} + iV_+^* - iV_-}\left(1 + \frac{v_+^*v_- + \Delta^2}{V_+^*V_-}\right) \\ &+ \int_{\omega_g-\frac{\omega}{2}}^{\frac{\omega}{2}-\omega_g} \frac{\mathrm{d}x \tanh\left(\frac{x+\frac{\omega}{2}}{2T}\right)}{\tau_-^{-1} - iV_+ - iV_-}\left(1 - \frac{v_+v_- + \Delta^2}{V_+V_-}\right)\Bigg].\end{aligned} \tag{6.67}$$

Now making the relevant approximations outlined above, and taking the imaginary part of the response function, the cancellation of terms is identical in the addition integral in this case, and so we can straightforwardly find

$$\begin{aligned}\mathrm{Re}\{\sigma^M(\omega)\} = \frac{\sigma_{\mathrm{Drude}}}{\omega}\Bigg[&\int_{\omega_g+\frac{\omega}{2}}^{\infty} \mathrm{d}x \left(\tanh\left(\frac{x+\frac{\omega}{2}}{2T}\right) - \tanh\left(\frac{x-\frac{\omega}{2}}{2T}\right)\right) \\ &\times \left[\mathrm{Re}\left\{\frac{v_-}{V_-}\right\}\mathrm{Re}\left\{\frac{v_+}{V_+}\right\} + \mathrm{Re}\left\{\frac{\Delta}{V_-}\right\}\mathrm{Re}\left\{\frac{\Delta}{V_+}\right\}\right] \\ -&\int_{\omega_g-\frac{\omega}{2}}^{\frac{\omega}{2}-\omega_g} \mathrm{d}x \tanh\left(\frac{x+\frac{\omega}{2}}{2T}\right) \\ &\times \left[\mathrm{Re}\left\{\frac{v_-}{V_-}\right\}\mathrm{Re}\left\{\frac{v_+}{V_+}\right\} + \mathrm{Re}\left\{\frac{\Delta}{V_-}\right\}\mathrm{Re}\left\{\frac{\Delta}{V_+}\right\}\right]\Bigg].\end{aligned} \tag{6.68}$$

The first term is identical in both regimes and corresponds to the conductivity arising from the quasi particles thermally excited out of the condensate. On the other hand, the latter term only occurs above $2\omega_g$, as it corresponds to excitations of the condensate due to the applied field which must have frequency large enough to excite cooper pairs out of the gapped region. Hence we can write an equation encompassing both regimes as so

$$\begin{aligned}\mathrm{Re}\{\sigma^M(\omega)\} = \frac{\sigma_{\mathrm{Drude}}}{\omega}\Bigg[&\int_{\omega_g+\frac{\omega}{2}}^{\infty} \mathrm{d}x \left(\tanh\left(\frac{x+\frac{\omega}{2}}{2T}\right) - \tanh\left(\frac{x-\frac{\omega}{2}}{2T}\right)\right) \\ &\times \left[\mathrm{Re}\left\{\frac{v_-}{V_-}\right\}\mathrm{Re}\left\{\frac{v_+}{V_+}\right\} + \mathrm{Re}\left\{\frac{\Delta}{V_-}\right\}\mathrm{Re}\left\{\frac{\Delta}{V_+}\right\}\right] \\ -&\int_{\omega_g-\frac{\omega}{2}}^{\frac{\omega}{2}-\omega_g} \mathrm{d}x \tanh\left(\frac{x+\frac{\omega}{2}}{2T}\right)\Theta(\omega-2\omega_g) \\ &\times \left[\mathrm{Re}\left\{\frac{v_-}{V_-}\right\}\mathrm{Re}\left\{\frac{v_+}{V_+}\right\} + \mathrm{Re}\left\{\frac{\Delta}{V_-}\right\}\mathrm{Re}\left\{\frac{\Delta}{V_+}\right\}\right]\Bigg].\end{aligned} \tag{6.69}$$

6.3 Linear response of a Superconductor Containing Paramagnetic Impurities to a Temperature Gradient

To calculate the thermal response we will follow the standard procedure of simply changing the contribution of the vertex compared to the electrical case in the previous section. The only real point of contention is what the appropriate choice of Pauli matrices should be on the vertex in the 4×4 regime. We know from the non-magnetic case that the vertex should carry a σ_z in the Nambu-spinor-space. As far as the appropriate Pauli-matrix for the spin symmetry part of the vertex, the thermal gradient will act on each spin identically, so we should have a s_0 in the spin-space. This is relatively simple to verify if one returns to the heat current operator and writes it in terms of the Φ spinors. Hence, for the linear response function, we have

$$\mathcal{K}^{T,M}_{\alpha\beta}(i\omega) = \frac{k_F^2 N(0)}{3m^2}\delta_{\alpha\beta} T\sum_{\varepsilon}\left(i\varepsilon+\frac{i\omega}{2}\right)^2 \times \int_{-\infty}^{\infty}\frac{\mathrm{d}\xi}{2}\,\mathrm{Tr}\left[\sigma_z s_0 \frac{i\widetilde{\varepsilon}'\sigma_0 s_0 + \xi_k\sigma_z s_0 - \widetilde{\Delta}'\sigma_x s_z}{\widetilde{\varepsilon}'^2+\xi_k^2+\widetilde{\Delta}'^2}\sigma_z s_0 \frac{i\widetilde{\varepsilon}\sigma_0 s_0 + \xi_k\sigma_z s_0 - \widetilde{\Delta}\sigma_x s_z}{\widetilde{\varepsilon}^2+\xi_k^2+\widetilde{\Delta}^2}\right]. \tag{6.70}$$

Commuting the $\sigma_z s_0$ through one of the Green's functions will have the effect of flipping the sign of the Δ term. So, taking trace and using the fact that the response is purely diagonal to drop the delta-function, we can arrive at

$$\mathcal{K}^{T,M}(i\omega) = \frac{n}{m}T\sum_{\varepsilon}\left(i\varepsilon+\frac{i\omega}{2}\right)^2\int_{-\infty}^{\infty}\mathrm{d}\xi\,\frac{\xi^2-\widetilde{\varepsilon}\widetilde{\varepsilon}'-\widetilde{\Delta}\widetilde{\Delta}'}{(\xi^2+\widetilde{E}^2)(\xi^2+\widetilde{E}'^2)}. \tag{6.71}$$

Computing the integral over ξ yields

$$\mathcal{K}^{T,M}(i\omega) = \frac{\pi n}{m}T\sum_{\varepsilon}\left(i\varepsilon+\frac{i\omega}{2}\right)^2\frac{\widetilde{E}\widetilde{E}'-\widetilde{\varepsilon}\widetilde{\varepsilon}'-\widetilde{\Delta}\widetilde{\Delta}'}{\widetilde{E}\widetilde{E}'(\widetilde{E}+\widetilde{E}')}, \tag{6.72}$$

then by multiplying numerator and denominator by factor of $\Delta/\widetilde{\Delta}$ we can write this equation in terms of v and V, like so

$$\mathcal{K}^{T,M}(i\omega) = \frac{\pi n}{m} T \sum_{\varepsilon} \left(i\varepsilon + \frac{i\omega}{2} \right)^2 \frac{VV' - \Delta^2 - vv'}{VV'(V + V' + \tau_-^{-1})} \,. \tag{6.73}$$

We can then convert the sum to a contour integral taking $i\varepsilon \mapsto z$ in the same way described in the previous section, leading to

$$\mathcal{K}^{T,M}(i\omega) = \frac{\pi n}{m} \frac{i}{2\pi} \oint_{\Gamma} \mathrm{d}z \, f(z) \left(z + \frac{i\omega}{2} \right)^2 \frac{VV' - \Delta^2 + vv'}{VV'(V + V' + \tau_-^{-1})} \,, \tag{6.74}$$

where the contour is the same as shown in figure 6.3.

The process for analytic continuation follows the previous section and hence we can immediately write down an expression for the linear response function in terms of integrals along the real axis, as the only difference will be the sign of the Δ^2 terms and the additional $(x + \omega/2)^2$ term in each integral from the vertex. We will also only consider the $\omega < 2\omega_g$ case, with the intention to take $\omega \to 0$ later. Therefore, we have

$$\begin{aligned}
\mathcal{K}^{T,M}(\omega) = \frac{n}{2im} \Bigg[& \int_{\omega_g}^{\infty} \frac{\mathrm{d}x \tanh\left(\frac{x}{2T}\right) \left(x + \frac{\omega}{2}\right)^2}{\tau_-^{-1} - iV(x) - iV(x+\omega)} \left(1 - \frac{v(x)v(x+\omega) - \Delta^2}{V(x)V(x+\omega)} \right) \\
& - \int_{\omega_g}^{\infty} \frac{\mathrm{d}x \tanh\left(\frac{x}{2T}\right) \left(x + \frac{\omega}{2}\right)^2}{\tau_-^{-1} + iV^*(x) - iV(x+\omega)} \left(1 + \frac{v^*(x)v(x+\omega) - \Delta^2}{V^*(x)V(x+\omega)} \right) \\
& + \int_{-\infty}^{-\omega_g - \omega} \frac{\mathrm{d}x \tanh\left(\frac{x}{2T}\right) \left(x + \frac{\omega}{2}\right)^2}{\tau_-^{-1} + iV^*(x) + iV^*(x+\omega)} \left(1 - \frac{v^*(x)v^*(x+\omega) - \Delta^2}{V^*(x)V^*(x+\omega)} \right) \\
& - \int_{-\infty}^{-\omega_g - \omega} \frac{\mathrm{d}x \tanh\left(\frac{x}{2T}\right) \left(x + \frac{\omega}{2}\right)^2}{\tau_-^{-1} - iV(x) + iV^*(x+\omega)} \left(1 + \frac{v(x)v^*(x+\omega) - \Delta^2}{V(x)V^*(x+\omega)} \right) \\
& + \int_{-\omega_g - \omega}^{-\omega_g} \frac{\mathrm{d}x \tanh\left(\frac{x}{2T}\right) \left(x + \frac{\omega}{2}\right)^2}{\tau_-^{-1} + iV^*(x) + \bar{V}(x+\omega)} \left(1 + \frac{v^*(x)\bar{v}(x+\omega) - \Delta^2}{iV^*(x)\bar{V}(x+\omega)} \right) \\
& - \int_{-\omega_g - \omega}^{-\omega_g} \frac{\mathrm{d}x \tanh\left(\frac{x}{2T}\right) \left(x + \frac{\omega}{2}\right)^2}{\tau_-^{-1} - iV(x) + \bar{V}(x+\omega)} \left(1 - \frac{v(x)\bar{v}(x+\omega) - \Delta^2}{iV(x)\bar{V}(x+\omega)} \right) \Bigg] \,.
\end{aligned} \tag{6.75}$$

Then by making the transformations $x \mapsto x - \omega/2$ in the first two integrals and $x \mapsto$

$-x-\omega/2$ in the latter four, the integrals can be symmetrised to yield

$$\begin{aligned}\mathcal{K}^{T,M}(\omega)=\frac{n}{2im}\Bigg[&\int_{\omega_g+\frac{\omega}{2}}^{\infty}\frac{\mathrm{d}x\,x^2\tanh\left(\frac{x-\frac{\omega}{2}}{2T}\right)}{\tau_-^{-1}-iV_--iV_+}\left(1-\frac{v_-v_+-\Delta^2}{V_-V_+}\right)\\&-\int_{\omega_g+\frac{\omega}{2}}^{\infty}\frac{\mathrm{d}x\,x^2\tanh\left(\frac{x-\frac{\omega}{2}}{2T}\right)}{\tau_-^{-1}+iV_-^*-iV_+}\left(1+\frac{v_-^*v_+-\Delta^2}{V_-^*V_+}\right)\\&-\int_{\omega_g+\frac{\omega}{2}}^{\infty}\frac{\mathrm{d}x\,x^2\tanh\left(\frac{x+\frac{\omega}{2}}{2T}\right)}{\tau_-^{-1}+iV_+^*+iV_-^*}\left(1-\frac{v_+^*v_-^*-\Delta^2}{V_+^*V_-^*}\right)\\&+\int_{\omega_g+\frac{\omega}{2}}^{\infty}\frac{\mathrm{d}x\,x^2\tanh\left(\frac{x+\frac{\omega}{2}}{2T}\right)}{\tau_-^{-1}-iV_++iV_-^*}\left(1+\frac{v_-v_+^*-\Delta^2}{V_+V_-^*}\right)\\&-\int_{\omega_g-\frac{\omega}{2}}^{\omega_g+\frac{\omega}{2}}\frac{\mathrm{d}x\,x^2\tanh\left(\frac{x+\frac{\omega}{2}}{2T}\right)}{\tau_-^{-1}+iV_+^*+\widetilde{V}}\left(1+\frac{v_+^*\widetilde{v}-\Delta^2}{iV_+^*\widetilde{V}}\right)\\&+\int_{\omega_g-\frac{\omega}{2}}^{\omega_g+\frac{\omega}{2}}\frac{\mathrm{d}x\,x^2\tanh\left(\frac{x+\frac{\omega}{2}}{2T}\right)}{\tau_-^{-1}-iV_++\widetilde{V}}\left(1-\frac{v_+\widetilde{v}-\Delta^2}{iV_+\widetilde{V}}\right)\Bigg].\end{aligned}\tag{6.76}$$

Taking the limits outlined in the previous section, we can approximate using equation 6.57 to obtain

$$\begin{aligned}\mathcal{K}^{T,M}(\omega)=\frac{n\tau_0}{2m}\Bigg[&i\int_{\omega_g+\frac{\omega}{2}}^{\infty}\mathrm{d}x\,x^2\tanh\left(\frac{x-\frac{\omega}{2}}{2T}\right)\left(\frac{v_-v_+-\Delta^2}{V_-V_+}+\frac{v_-^*v_+-\Delta^2}{V_-^*V_+}\right)\\&-i\int_{\omega_g+\frac{\omega}{2}}^{\infty}\mathrm{d}x\,x^2\tanh\left(\frac{x+\frac{\omega}{2}}{2T}\right)\left(\frac{v_+^*v_-^*-\Delta^2}{V_+^*V_-^*}+\frac{v_+v_-^*-\Delta^2}{V_+V_-^*}\right)\\&+\int_{\omega_g-\frac{\omega}{2}}^{\omega_g+\frac{\omega}{2}}\mathrm{d}x\,x^2\tanh\left(\frac{x+\frac{\omega}{2}}{2T}\right)\left(\frac{v_+^*\widetilde{v}-\Delta^2}{V_+^*\widetilde{V}}+\frac{v_+\widetilde{v}-\Delta^2}{V_+\widetilde{V}}\right)\Bigg].\end{aligned}\tag{6.77}$$

When finding the imaginary part of the thermal linear response function, we can follow the same process as shown in equations 6.59 to 6.64, only with $\Delta^2\mapsto-\Delta^2$. Thus we have

$$\begin{aligned}\mathrm{Im}\big\{\mathcal{K}^{T,M}(\omega)\big\}=-\frac{n\tau_0}{m}\int_{\omega_g+\frac{\omega}{2}}^{\infty}&\mathrm{d}x\,x^2\left(\tanh\left(\frac{x+\frac{\omega}{2}}{2T}\right)-\tanh\left(\frac{x-\frac{\omega}{2}}{2T}\right)\right)\\&\times\left[\mathrm{Re}\left\{\frac{v_-}{V_-}\right\}\mathrm{Re}\left\{\frac{v_+}{V_+}\right\}-\mathrm{Re}\left\{\frac{\Delta}{V_-}\right\}\mathrm{Re}\left\{\frac{\Delta}{V_+}\right\}\right].\end{aligned}\tag{6.78}$$

Once again, we will hone-in on the $\omega=0$ limit when looking at thermal conductivity.

In this limit the difference of tanh's will give a sech^2, as shown in equation 4.90, and v_+ and v_- will both collapse down to $v(x)$, all-together yielding

$$\mathrm{Im}\{\mathcal{K}^{T,M}(0)\} = -\frac{n\omega\tau_0}{2mT}\int_{\omega_g}^{\infty} \mathrm{d}x\, x^2\, \mathrm{sech}^2\left(\frac{x}{2T}\right)\left[\mathrm{Re}\left\{\frac{v(x)}{V(x)}\right\}^2 - \mathrm{Re}\left\{\frac{\Delta}{V(x)}\right\}^2\right], \quad (6.79)$$

$$\Rightarrow \mathrm{Re}\{\kappa^M\} = \frac{n\tau_0}{2mT^2}\int_{\omega_g}^{\infty} \mathrm{d}x\, x^2\, \mathrm{sech}^2\left(\frac{x}{2T}\right)\left[\mathrm{Re}\left\{\frac{v(x)}{V(x)}\right\}^2 - \mathrm{Re}\left\{\frac{\Delta}{V(x)}\right\}^2\right]. \quad (6.80)$$

6.4 Calculation of the Cooperon in a Superconductor with Magnetic Impurities

In the following section we will be computing the cooperon in the the Superconducting state of a superconductor doped with a small concentrations of magnetic impurities. This follows the work of Smith [65]. However, the principal deviation is that the work of Smith was only concerned with the calculation of the weak localisation correction the the superconducting carrier density, where the frequency in the cooperon can be set to zero, whereas in order to calculate the weak localisation correction to conductivity (thermal or electrical), one must go through the analytic continuation process as outlined in the previous sections. This means that we must must retain the frequency dependence in the cooperon at least until after the analytic continuation has been completed, only after which we would set the frequency to zero for the thermal conductivity calculations we are interested in. Similarly to the work of Smith we are interested in the case of weak doping of magnetic impurities such that $\tau_s^{-1} \ll \tau_0^{-1}$, so the magnetic impurities can be the primary phase coherence breaking mechanism, but not so large that it completely destroys the superconductivity.

To construct the cooperon in the superconducting state including magnetic impurities, we use the same logic as in section 5.1, where we use an outer-product construction. Only in this case we will, of course, be working with the 4×4 products of Pauli matrices on the vertices. Furthermore, there are two types of impurity scattering that can now occur:

those involving the non-magnetic impurities and those involving the magnetic impurities. However, it is straightforward to see that with a construction like that which is shown in figure 6.5 (where the non-magnetic impurities are denoted by crosses and the three species of magnetic impurity are denoted by the circle), we can obtain the Dyson equation that includes all possible sequences of scattering events. So the Dyson equation can be defined in the usual way with the bare impurity part given by

$$\begin{aligned}\Gamma_0 = &\frac{1}{2\pi N(0)\tau_0}[\sigma_z s_0 \otimes \sigma_z s_0] \\ &+ \frac{1}{6\pi N(0)\tau_s}[\sigma_z s_x \otimes \sigma_z s_x + \sigma_z s_y \otimes \sigma_z s_y + \sigma_0 s_z \otimes \sigma_0 s_z]\,,\end{aligned} \tag{6.81}$$

and the self-energy given by

$$\Sigma_C(\mathbf{q}, i\varepsilon, i\varepsilon') = \frac{1}{\mathcal{V}}\sum_{\mathbf{k}} \mathcal{G}(\mathbf{q}-\mathbf{k}, i\varepsilon') \otimes \mathcal{G}(\mathbf{k}, i\varepsilon)\,. \tag{6.82}$$

As we will be stacking up quite a few Pauli matrices in succession in the coming calculation, we will drop the outer product symbol and take the convention that each set of four Pauli matrices together will all be outer producted with each other. Thus, we can write the self-energy as

$$\begin{aligned}\Sigma_C(\mathbf{q}, i\varepsilon, i\varepsilon') = N(0)\int \frac{\mathrm{d}\Omega}{4\pi}\int_{-\infty}^{\infty}\mathrm{d}\xi \Bigg[&\frac{i\widetilde{\varepsilon}'\sigma_0 s_0 + (\xi+\mu_\theta)\sigma_z s_0 - \widetilde{\Delta}'\sigma_x s_z}{\widetilde{\varepsilon}'^2 + (\xi+\mu_\theta)^2 + \widetilde{\Delta}'^2} \\ &\times \frac{i\widetilde{\varepsilon}\sigma_0 s_0 + \xi\sigma_z s_0 - \widetilde{\Delta}\sigma_x s_z}{\widetilde{\varepsilon}^2 + \xi^2 + \widetilde{\Delta}^2}\Bigg]\,.\end{aligned} \tag{6.83}$$

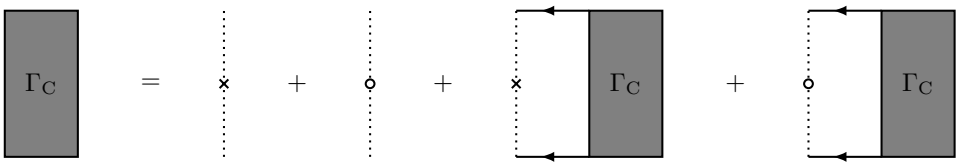

Figure 6.5: The Dyson equation for the cooperon with both non-magnetic and magnetic impurities. The cross represents the non-magnetic impurities and the circle represents the magnetic impurities that will constitute of three terms for each magnetic species.

Breaking these terms up such that we have integrals of the form given in equations 5.27 and 5.28, we have

$$\begin{aligned}\Sigma_C(\mathbf{q}, i\varepsilon, i\varepsilon') = N(0)\int \frac{\mathrm{d}\Omega}{4\pi}\Bigg[&(i\widetilde{\varepsilon}'\sigma_0 s_0 - \widetilde{\Delta}'\sigma_x s_z)(i\widetilde{\varepsilon}\sigma_0 s_0 - \widetilde{\Delta}\sigma_x s_z)\\ &\times\int_{-\infty}^{\infty}\frac{\mathrm{d}\xi}{(\widetilde{\varepsilon}'^2 + (\xi+\mu_\theta)^2 + \widetilde{\Delta}'^2)(\widetilde{\varepsilon}^2 + \xi^2 + \widetilde{\Delta}^2)}\\ &+\sigma_z s_0\sigma_z s_0\int_{-\infty}^{\infty}\frac{\mathrm{d}\xi\ \xi(\xi+\mu_\theta)}{(\widetilde{\varepsilon}'^2 + (\xi+\mu_\theta)^2 + \widetilde{\Delta}'^2)(\widetilde{\varepsilon}^2 + \xi^2 + \widetilde{\Delta}^2)}\Bigg],\end{aligned} \tag{6.84}$$

which can then be solved using the standard results to yield

$$\Sigma_C(\mathbf{q}, i\varepsilon, i\varepsilon') = \widetilde{\gamma}\left[\sigma_z s_0\sigma_z s_0 + \frac{(i\widetilde{\varepsilon}'\sigma_0 s_0 - \widetilde{\Delta}'\sigma_x s_z)(i\widetilde{\varepsilon}\sigma_0 s_0 - \widetilde{\Delta}\sigma_x s_z)}{\widetilde{E}\widetilde{E}'}\right] \tag{6.85}$$

$$\text{where}\quad \widetilde{\gamma} = N(0)\int\frac{\mathrm{d}\Omega}{4\pi}\frac{\pi(\widetilde{E}+\widetilde{E}')}{(\widetilde{E}+\widetilde{E}')^2 + \mu_\theta^2}\,. \tag{6.86}$$

The main difference between this and the calculation without magnetic impurities is that with $\frac{\varepsilon}{\Delta} \neq \frac{\widetilde{\varepsilon}}{\widetilde{\Delta}}$ there is no cancellation of the impurity-factors in the numerator and denominator. Therefore, for now we will not make any approximations in γ, other than assuming an isotropic system, and we can complete the angular integral as follows,

$$\begin{aligned}\widetilde{\gamma} &= \pi N(0)\int\frac{\mathrm{d}\Omega}{4\pi}\frac{1}{(\widetilde{E}+\widetilde{E}')\left(1-\left(\frac{\mu_\theta}{(\widetilde{E}+\widetilde{E}'}\right)^2\right)}\\ &\approx \pi N(0)\int\frac{\mathrm{d}\Omega}{4\pi}\left[\frac{1}{\widetilde{E}+\widetilde{E}'} - \frac{\mu_\theta^2}{(\widetilde{E}+\widetilde{E}')^3}\right]\\ &= \frac{\pi N(0)}{\widetilde{E}+\widetilde{E}'}\left[1 - \frac{q^2 v_F^2}{d(\widetilde{E}+\widetilde{E}')^2}\right],\end{aligned} \tag{6.87}$$

where the order one piece in the second line was discarded because it averages to zero under the angular integral.

Next, we will find it convenient to absorb this factor of $\widetilde{\gamma}$ into the definition of Γ_0

removing it from the self-energy part, so the Dyson equation is redefined as

$$\Gamma_C = (1 - \Gamma_0 \Sigma_C)^{-1} \frac{\Gamma_0}{\widetilde{\gamma}} \,, \tag{6.88}$$

$$\text{with} \quad \Sigma_C = \sigma_z s_0 \sigma_z s_0 + \frac{(i\widetilde{\varepsilon}'\sigma_0 s_0 - \widetilde{\Delta}'\sigma_x s_z)(i\widetilde{\varepsilon}\sigma_0 s_0 - \widetilde{\Delta}\sigma_x s_z)}{\widetilde{E}\widetilde{E}'} \,, \tag{6.89}$$

$$\text{and} \quad \Gamma_0 = \mu X + \lambda Y \,, \tag{6.90}$$

$$\text{where} \quad X = \sigma_z s_0 \sigma_z s_0 \quad , \quad Y = \sigma_z s_x \sigma_z s_x + \sigma_z s_y \sigma_z s_y + \sigma_0 s_z \sigma_0 s_z$$

$$\text{and} \quad \mu = \frac{\widetilde{\gamma}}{2\pi N(0)\tau_0} \quad , \quad \lambda = \frac{\widetilde{\gamma}}{6\pi N(0)\tau_s} \,.$$

So now the problem is reduced to the matrix inversion of the $(1 - \Gamma_0 \Sigma_C)$ term, that we will label as

$$M = (1 - (\mu X + \lambda Y)\Sigma_C)^{-1} \,. \tag{6.91}$$

But one can notice that Y commutes with both X and Σ_C, and therefore is trivial in the matrix inversion. So to simplify the problem we can set Y to the identity and to restore the appropriate factors of Y in the final expression we can take $\lambda^n \mapsto \lambda^n \Lambda^n P_\lambda$, where Λ is an eigenvalue of Y and P_Λ is the projector onto the eigenvalue. Hence, we can instead solve for the simpler matrix

$$M' = (1 - (\mu X + \lambda)\Sigma_C)^{-1} \,. \tag{6.92}$$

Before proceeding with solving for M' this we will find the eigenvalues and projectors for Y. One can go through the tedium of writing out the 16×16 matrix for Y and solving for the eigenvalues manually (luckily it is block diagonal, so it reduces to solving two 8×8 matrices), however we can skip this by making use of the Cayley-Hamilton theorem. If we examine what happens when we square Y we immediate arrive at the characteristic

equation, as there are only two eigenvalues,

$$\begin{aligned} Y^2 &= (\sigma_z s_x \sigma_z s_x + \sigma_z s_y \sigma_z s_y + \sigma_0 s_z \sigma_0 s_z)^2 \\ &= 3\sigma_0 s_0 \sigma_0 s_0 - 2\sigma_z s_x \sigma_z s_x - 2\sigma_z s_y \sigma_z s_y - 2\sigma_0 s_z \sigma_0 s_z \\ &= 3 - 2Y \,. \end{aligned} \tag{6.93}$$

Therefore we can immediately deduce

$$\Lambda = 1 \,,\, -3 \,. \tag{6.94}$$

We can construct the projectors under the requirements:

$$P_1^2 = P_1 \quad , \quad P_{-3}^2 = P_{-3} \quad \text{and} \quad P_1 P_{-3} = 0 \,.$$

One can easily verify that these requirements are satisfied by

$$P_1 = \frac{1}{4}(3 + Y) \quad \text{and} \quad P_{-3} = \frac{1}{4}(1 - Y) \,. \tag{6.95}$$

Now that we have all we need with respect to the eigenvalues of Y, we can return to solving M'.

For convenience, we can expand out the expression for Σ_C and label the coefficients of each distinct matrix, like so

$$\Sigma_C = -(a\sigma_0 s_0 \sigma_0 s_0 + b\sigma_z s_0 \sigma_z s_0 + c\sigma_x s_z \sigma_x s_z + d\sigma_0 s_0 \sigma_x s_z + e\sigma_x s_z \sigma_0 s_0) \,, \tag{6.96}$$

$$\text{where} \quad a = \frac{\widetilde{\varepsilon}\widetilde{\varepsilon}'}{\widetilde{E}\widetilde{E}'} \,, \quad b = -1 \,, \quad c = -\frac{\widetilde{\Delta}\widetilde{\Delta}'}{\widetilde{E}\widetilde{E}'} \,, \quad d = \frac{i\widetilde{\varepsilon}'\widetilde{\Delta}}{\widetilde{E}\widetilde{E}'} \quad \text{and} \quad e = \frac{i\widetilde{\varepsilon}\widetilde{\Delta}'}{\widetilde{E}\widetilde{E}'} \,. \tag{6.97}$$

Note that these coefficients have the property

$$(d \pm e)^2 = (a \pm c)^2 - b^2 \,, \tag{6.98}$$

as we will need this later.

There are only eight unique matrices that appear in the matrix multiplication of M', which we will label as follows

$$S_1 = \sigma_0 s_0 \sigma_0 s_0 \qquad S_2 = \sigma_z s_0 \sigma_z s_0 \qquad S_3 = \sigma_x s_z \sigma_x s_z \qquad S_4 = \sigma_0 s_0 \sigma_x s_z$$
$$S_5 = \sigma_x s_z \sigma_0 s_0 \qquad S_6 = \sigma_y s_z \sigma_y s_z \qquad S_7 = i\sigma_z s_0 \sigma_y s_z \qquad S_8 = i\sigma_y s_z \sigma_z s_0 \,. \tag{6.99}$$

M'^{-1} can then be written in terms of these matrices, as

$$\begin{aligned} M'^{-1} &= S_1 + (\lambda S_1 + \mu S_2)(aS_1 + bS_2 + cS_3 + dS_4 + eS_5) \qquad (6.100)\\ &= (1 + \lambda a + \mu b)S_1 + (\lambda b + \mu a)S_2 + \lambda c S_3 + \lambda d S_4 + \lambda e S_5 - \mu c S_6 + \mu d S_7 + \mu e S_8 \end{aligned}$$

Because the S-matrices (along with their negative counterparts) form a closed group under multiplication, as shown by the multiplication table 6.6, it is possible to write M' as a linear combination of the S-matrices with unknown coefficients, that are to be determined,

$$M' = A_1 S_1 + A_2 S_2 + A_3 S_3 + A_4 S_4 + A_5 S_5 + A_6 S_6 + A_7 S_7 + A_8 S_8 \,. \tag{6.101}$$

S_1	S_2	S_3	S_4	S_5	S_6	S_7	S_8
S_2	S_1	$-S_6$	S_7	S_8	$-S_3$	S_4	S_5
S_3	$-S_6$	S_1	S_5	S_4	$-S_2$	S_8	S_7
S_4	$-S_7$	S_5	S_1	S_3	S_8	$-S_2$	S_6
S_5	$-S_8$	S_4	S_3	S_1	S_7	S_6	$-S_2$
S_6	$-S_3$	$-S_2$	$-S_8$	$-S_7$	S_1	$-S_5$	$-S_4$
S_7	$-S_4$	S_8	S_2	$-S_6$	S_5	$-S_1$	$-S_3$
S_8	$-S_5$	S_7	$-S_6$	S_2	S_4	$-S_3$	$-S_1$

Figure 6.6: Multiplication table for the S-matrices defined in equation 6.99, where the matrix displayed in the left column is multiplied on the left into the matrix displayed in the top row on the right.

Now because $M'M'^{-1} = S_1$ we can multiply together equations 6.100 and 6.101 to obtain a set of eight equations for the eight unknowns A_i, which we can represent as a

matrix, like so

$$\begin{bmatrix} \chi & \nu & \lambda c & \lambda d & \lambda e & -\mu c & -\mu d & -\mu e \\ \nu & \chi & \mu c & -\mu d & -\mu e & -\lambda c & \lambda d & \lambda e \\ \lambda c & \mu c & \chi & \lambda e & \lambda d & -\nu & -\mu e & -\mu d \\ \lambda d & \mu d & \lambda e & \chi & \lambda c & -\mu e & -\nu & -\mu c \\ \lambda e & \mu e & \lambda d & \lambda c & \chi & -\mu d & -\mu c & -\nu \\ -\mu c & -\lambda c & -\nu & \mu e & \mu d & \chi & -\lambda e & -\lambda d \\ \mu d & \lambda d & \mu e & -\nu & -\mu c & \lambda e & \chi & \lambda c \\ \mu e & \lambda e & \mu d & -\mu c & -\nu & -\lambda d & \lambda c & \chi \end{bmatrix} \begin{bmatrix} A_1 \\ A_2 \\ A_3 \\ A_4 \\ A_5 \\ A_6 \\ A_7 \\ A_8 \end{bmatrix} = \begin{bmatrix} 1 \\ 0 \\ 0 \\ 0 \\ 0 \\ 0 \\ 0 \\ 0 \end{bmatrix}, \tag{6.102}$$

where we have made the substitutions $\chi = 1 + \lambda a + \mu b$ and $\nu = \lambda b + \mu a$ for clarity. Note that the order in which M' and M'^{-1} are multiplied does matter, as one can see from the multiplication table for the S-matrices, changing the order of multiplication can lead to changes in sign. Therefore, the form of the matrix equation we obtain will differ if the order is exchanged. The construction of this matrix equation can be understood as follows: after M' is multiplied into the left-hand side of M'^{-1} one can collect terms into coefficients of each S_i; the j^{th} row in the matrix is then related coefficient of S_i with the element in the j^{th} row is the multiplicative factor of A_j; then the coefficient of S_i is equated with the right-hand side, which only has the identity, S_1, so all elements on the right-hand side of the matrix equation are zero, except the first which carries the factor of 1 from the identity.

It is not simple to spot how to proceed from here, but it happens that we can solve this matrix equation by noticing that we can add and subtract rows in specific pairs. The pairs are rows 1 and 2, 3 and 6, 4 and 7 and finally 5 and 8. One can notice this pattern because it is matching up, in each respective column, elements with a factor of c, d, e and the χ and ν terms. So if we define

$$B_1 = A_1 + A_2\,, \quad B_2 = A_3 - A_6\,, \quad B_3 = A_4 + A_7 \quad \text{and} \quad B_4 = A_5 + A_8\,, \tag{6.103}$$

we can obtain a new matrix equation

$$\begin{bmatrix} \chi+\nu & (\lambda+\mu)c & (\lambda-\mu)d & (\lambda-\mu)e \\ (\lambda+\mu)c & \chi+\nu & (\lambda-\mu)e & (\lambda-\mu)d \\ (\lambda+\mu)d & (\lambda+\mu)e & \chi-\nu & (\lambda-\mu)c \\ (\lambda+\mu)e & (\lambda+\mu)d & (\lambda-\mu)c & \chi-\nu \end{bmatrix} \begin{bmatrix} B_1 \\ B_2 \\ B_3 \\ B_4 \end{bmatrix} = \begin{bmatrix} 1 \\ 0 \\ 0 \\ 0 \end{bmatrix}, \tag{6.104}$$

where $\chi+\nu = 1+(\lambda+\mu)(a+b)$ and $\chi-\nu = 1+(\lambda-\mu)(a-b)$. Similarly, we can define another set

$$C_1 = A_1 - A_2\,, \quad C_2 = A_3 + A_6\,, \quad C_3 = A_4 - A_7 \quad \text{and} \quad C_4 = A_5 - A_8\,, \tag{6.105}$$

to obtain the matrix equation

$$\begin{bmatrix} \chi-\nu & (\lambda-\mu)c & (\lambda+\mu)d & (\lambda+\mu)e \\ (\lambda-\mu)c & \chi-\nu & (\lambda+\mu)e & (\lambda+\mu)d \\ (\lambda-\mu)d & (\lambda-\mu)e & \chi+\nu & (\lambda+\mu)c \\ (\lambda-\mu)e & (\lambda-\mu)d & (\lambda+\mu)c & \chi+\nu \end{bmatrix} \begin{bmatrix} C_1 \\ C_2 \\ C_3 \\ C_4 \end{bmatrix} = \begin{bmatrix} 1 \\ 0 \\ 0 \\ 0 \end{bmatrix}. \tag{6.106}$$

We repeat this process again, pairing up rows 1 and 2, and 3 and 4, to obtain a set of four 2×2 matrix equations:

$$\begin{bmatrix} 1+(\lambda+\mu)(a+b+c) & (\lambda-\mu)(d+e) \\ (\lambda+\mu)(d+e) & 1+(\lambda-\mu)(a-b+c) \end{bmatrix} \begin{bmatrix} B_1+B_2 \\ B_3+B_4 \end{bmatrix} = \begin{bmatrix} 1 \\ 0 \end{bmatrix}, \tag{6.107}$$

$$\begin{bmatrix} 1+(\lambda-\mu)(a-b+c) & (\lambda+\mu)(d+e) \\ (\lambda-\mu)(d+e) & 1+(\lambda+\mu)(a+b+c) \end{bmatrix} \begin{bmatrix} C_1+C_2 \\ C_3+C_4 \end{bmatrix} = \begin{bmatrix} 1 \\ 0 \end{bmatrix}, \tag{6.108}$$

$$\begin{bmatrix} 1+(\lambda+\mu)(a+b-c) & (\lambda-\mu)(d-e) \\ (\lambda+\mu)(d-e) & 1+(\lambda-\mu)(a-b-c) \end{bmatrix} \begin{bmatrix} B_1-B_2 \\ B_3-B_4 \end{bmatrix} = \begin{bmatrix} 1 \\ 0 \end{bmatrix}, \tag{6.109}$$

$$\begin{bmatrix} 1+(\lambda-\mu)(a-b-c) & (\lambda+\mu)(d-e) \\ (\lambda-\mu)(d-e) & 1+(\lambda+\mu)(a+b-c) \end{bmatrix} \begin{bmatrix} C_1-C_2 \\ C_3-C_4 \end{bmatrix} = \begin{bmatrix} 1 \\ 0 \end{bmatrix}. \tag{6.110}$$

We can then simply invert these using the standard matrix inversion routine for a 2×2 matrix and take only the left-hand column because the inverse will multiply into the right-hand side, where the 0 will kill the contribution from the right-hand column. Thus, we have:

$$\begin{bmatrix} B_1+B_2 \\ B_3+B_4 \end{bmatrix} = \frac{1}{D_1} \begin{bmatrix} 1+(\lambda-\mu)(a-b+c) \\ -(\lambda+\mu)(d+e) \end{bmatrix}, \tag{6.111}$$

$$\begin{bmatrix} C_1+C_2 \\ C_3+C_4 \end{bmatrix} = \frac{1}{D_1} \begin{bmatrix} 1+(\lambda+\mu)(a+b+c) \\ -(\lambda-\mu)(d+e) \end{bmatrix}, \tag{6.112}$$

$$\begin{bmatrix} B_1-B_2 \\ B_3-B_4 \end{bmatrix} = \frac{1}{D_2} \begin{bmatrix} 1+(\lambda-\mu)(a-b-c) \\ -(\lambda+\mu)(d-e) \end{bmatrix}, \tag{6.113}$$

$$\begin{bmatrix} C_1-C_2 \\ C_3-C_4 \end{bmatrix} = \frac{1}{D_2} \begin{bmatrix} 1+(\lambda+\mu)(a+b-c) \\ -(\lambda-\mu)(d-e) \end{bmatrix}, \tag{6.114}$$

where the determinants, D_1 and D_2, from the inversion are given by

$$D_1 = (1+(\lambda+\mu)(a+b+c))(1+(\lambda-\mu)(a-b+c)) - (\lambda+\mu)(\lambda-\mu)(d+e)^2$$
$$\text{and} \quad D_2 = (1+(\lambda+\mu)(a+b-c))(1+(\lambda-\mu)(a-b-c)) - (\lambda+\mu)(\lambda-\mu)(d-e)^2\,.$$

These can be simplified by expanding out and making use of the identity in equation 6.98, along with $b=-1$, to obtain

$$D_1 = 1+2\lambda(a+c)-2\mu\,, \tag{6.115a}$$
$$\text{and} \quad D_2 = 1+2\lambda(a-c)-2\mu\,. \tag{6.115b}$$

To work our way back to expressions for the set of A_i, we must once again add and subtract equations 6.111 - 6.114 in pairs. Firstly, finding expressions for B_i:

$$B_1 = \frac{1+(\lambda-\mu)(a+c+1)}{2D_1} + \frac{1+(\lambda-\mu)(a-c+1)}{2D_2}\,, \tag{6.116a}$$
$$B_2 = \frac{1+(\lambda-\mu)(a+c+1)}{2D_1} - \frac{1+(\lambda-\mu)(a-c+1)}{2D_2}\,, \tag{6.116b}$$
$$B_3 = -\frac{(\lambda+\mu)(d+e)}{2D_1} - \frac{(\lambda+\mu)(d-e)}{2D_2} \tag{6.116c}$$
$$\text{and} \quad B_4 = -\frac{(\lambda+\mu)(d+e)}{2D_1} + \frac{(\lambda+\mu)(d-e)}{2D_2}\,. \tag{6.116d}$$

Then for C_i, we have

$$C_1 = \frac{1+(\lambda+\mu)(a+c-1)}{2D_1} + \frac{1+(\lambda+\mu)(a-c-1)}{2D_2}\,, \tag{6.117a}$$
$$C_2 = \frac{1+(\lambda+\mu)(a+c-1)}{2D_1} - \frac{1+(\lambda+\mu)(a-c-1)}{2D_2}\,, \tag{6.117b}$$
$$C_3 = -\frac{(\lambda-\mu)(d+e)}{2D_1} - \frac{(\lambda-\mu)(d-e)}{2D_2}\,, \tag{6.117c}$$
$$\text{and} \quad C_4 = -\frac{(\lambda-\mu)(d+e)}{2D_1} + \frac{(\lambda-\mu)(d-e)}{2D_2}\,. \tag{6.117d}$$

Finally, repeating this process again to find the set of A_i:

$$A_1 = \frac{1+\lambda(a+c)-\mu}{2D_1} + \frac{1+\lambda(a-c)-\mu}{2D_2}, \tag{6.118a}$$

$$A_3 = \frac{1+\lambda(a+c)-\mu}{2D_1} - \frac{1+\lambda(a-c)-\mu}{2D_2}, \tag{6.118b}$$

$$A_2 = \frac{\lambda-\mu(a+c)}{2D_1} + \frac{\lambda-\mu(a-c)}{2D_2}, \tag{6.118c}$$

$$-A_6 = \frac{\lambda-\mu(a+c)}{2D_1} - \frac{\lambda-\mu(a-c)}{2D_2}, \tag{6.118d}$$

$$A_4 = -\frac{\lambda(d+e)}{2D_1} - \frac{\lambda(d-e)}{2D_2}, \tag{6.118e}$$

$$A_5 = -\frac{\lambda(d+e)}{2D_1} + \frac{\lambda(d-e)}{2D_2}, \tag{6.118f}$$

$$A_7 = -\frac{\mu(d+e)}{2D_1} - \frac{\mu(d-e)}{2D_2}, \tag{6.118g}$$

$$\text{and} \quad A_8 = -\frac{\mu(d+e)}{2D_1} + \frac{\mu(d-e)}{2D_2} \tag{6.118h}$$

We have ordered the expression for each A_i suggestively to highlight the patterns that emerge:

- the expressions are related in pairs: $A_1 \leftrightarrow A_3$, $A_2 \leftrightarrow -A_6$, $A_4 \leftrightarrow A_5$ and $A_7 \leftrightarrow A_8$,
- each pair of A_i's is related by switching the sign on the D_2 term
- for each individual A_i the first and second terms are related by $a+c \leftrightarrow a-c$, $d+e \leftrightarrow d-e$ and $D_1 \leftrightarrow D_2$.

Therefore, we can write the expression for M' as such

$$\begin{aligned} M' = \frac{1}{2D_1}\Big[&(1+\lambda(a+c)-\mu)(S_1+S_3) + (\lambda-\mu(a+c))(S_2-S_6) \\ &- \lambda(d+e)(S_4+S_5) - \mu(d+e)(S_7+S_8)\Big] \\ +\frac{1}{2D_2}\Big[&(1+\lambda(a-c)-\mu)(S_1-S_3) + (\lambda-\mu(a-c))(S_2+S_6) \\ &- \lambda(d-e)(S_4-S_5) - \mu(d+e)(S_7-S_8)\Big]. \end{aligned} \tag{6.119}$$

By using the multiplication table for S_i we can notice that we can pull out a factor of

$(S_1 + S_3)$ and $(S_1 - S_3)$ in the first and second term respectively, to obtain

$$\begin{aligned} M' = \frac{1}{2D_1}\Big[&(1+\lambda(a+c)-\mu)S_1 + (\lambda-\mu(a+c))S_2 \\ &- \lambda(d+e)S_4 - \mu(d+e)S_7\Big](S_1+S_3) \\ +\frac{1}{2D_2}\Big[&(1+\lambda(a-c)-\mu)S_1 + (\lambda-\mu(a-c))S_2 \\ &- \lambda(d-e)S_4 - \mu(d+e)S_7\Big](S_1-S_3)\,. \end{aligned} \tag{6.120}$$

To obtain M from M' we must restore the terms corresponding to the $\Lambda = -3$ eigenvalue of Y and apply appropriate projectors on the eigen-spaces. Recall that M' corresponds to the part of M with $\Lambda = 1$. So all that needs to be done to this term is to multiply by the projector onto $\Lambda = 1$, $P_1 = \frac{1}{4}(3S_1 + Y)$. To find the other term corresponding to $\Lambda = -3$ we make the substitution $\lambda \mapsto -3\lambda$ and multiply by the projector, $P_{-3} = \frac{1}{4}(S_1 - Y)$. Putting this all together leads to the equation for M,

$$\begin{aligned} M = \frac{1}{8D_1}\Big[&(1+\lambda(a+c)-\mu)S_1 + (\lambda-\mu(a+c))S_2 \\ &- \lambda(d+e)S_4 - \mu(d+e)S_7\Big](S_1+S_3)(3S_1+Y) \\ +\frac{1}{8D_2}\Big[&(1+\lambda(a-c)-\mu)S_1 + (\lambda-\mu(a-c))S_2 \\ &- \lambda(d-e)S_4 - \mu(d+e)S_7\Big](S_1-S_3)(3S_1+Y) \\ +\frac{1}{8D_3}\Big[&(1-3\lambda(a+c)-\mu)S_1 - (3\lambda+\mu(a+c))S_2 \\ &+ 3\lambda(d+e)S_4 - \mu(d+e)S_7\Big](S_1+S_3)(S_1-Y) \\ +\frac{1}{8D_4}\Big[&(1-3\lambda(a-c)-\mu)S_1 - (3\lambda+\mu(a-c))S_2 \\ &+ 3\lambda(d-e)S_4 - \mu(d+e)S_7\Big](S_1-S_3)(S_1-Y)\,, \end{aligned} \tag{6.121}$$

where D_3 and D_4 are D_1 and D_2 respectively, with the substitution $\lambda \mapsto -3\lambda$, i.e.

$$D_3 = 1 - 6\lambda(a+c) - 2\mu\,, \tag{6.122}$$

$$\text{and} \quad D_4 = 1 - 6\lambda(a-c) - 2\mu\,. \tag{6.123}$$

To find the form of the cooperon from M, we return to the relation

$$\widetilde{\gamma}\Gamma_C = M\Gamma_0 = M(\mu S_2 + \lambda Y)\,. \tag{6.124}$$

Note that Γ_0 commutes with the $(S_1 \pm S_3)$ terms and with the projectors, but as well as this, the projectors have the effect of 'projecting' the Y term in Γ_0 to its respective eigenvalue, i.e.

$$(3S_1 + Y)(\mu S_2 + \lambda Y) = (\mu S_2 + \lambda)(3S_1 + Y)$$

$$\text{and} \quad (S_1 - Y)(\mu S_2 + \lambda Y) = (\mu S_2 - 3\lambda)(S_1 - Y)\,.$$

Examining the first term first, we have

$$\begin{aligned}\widetilde{\gamma}\Gamma_C^{(1)} &= \frac{1}{8D_1}\Big[(1 + \lambda(a+c) - \mu)S_1 + (\lambda - \mu(a+c))S_2 \\ &\qquad - \lambda(d+e)S_4 - \mu(d+e)S_7\Big](\mu S_2 + \lambda)(S_1 + S_3)(3S_1 + Y) \\ &= \frac{1}{8D_1}\Big[\big(\lambda + (\lambda^2 - \mu^2)(a+c)\big)S_1 + \big(\lambda^2 + \mu(1-\mu)\big)S_2 \\ &\qquad - (\lambda^2 - \mu^2)(d+e)S_4\Big](S_1 + S_3)(3S_1 + Y)\,.\end{aligned} \tag{6.125}$$

Examining the third term, we notice that this term is identical to first, up to the projector and, therefore, the transformation $\lambda \mapsto -3\lambda$. Therefore we can immediately arrive at

$$\begin{aligned}\widetilde{\gamma}\Gamma_C^{(3)} = \frac{1}{8D_3}\Big[&\big(-3\lambda + (9\lambda^2 - \mu^2)(a+c)\big)S_1 + \big(9\lambda^2 + \mu(1-\mu)\big)S_2 \\ &- (9\lambda^2 - \mu^2)(d+e)S_4\Big](S_1 + S_3)(S_1 - Y)\,.\end{aligned} \tag{6.126}$$

Then to obtain the second and fourth terms, we can simply make the substitutions, $(a+c)$, $(d+e)$, $(S_1+S_3) \mapsto (a-c)$, $(d-e)$, (S_1-S_3) in the first and third respectively, yielding

$$\widetilde{\gamma}\Gamma_C^{(2)} = \frac{1}{8D_2}\Big[\big(\lambda + (\lambda^2-\mu^2)(a-c)\big)S_1 + \big(\lambda^2+\mu(1-\mu)\big)S_2 - (\lambda^2-\mu^2)(d-e)S_4\Big](S_1-S_3)(3S_1+Y) \tag{6.127}$$

and

$$\widetilde{\gamma}\Gamma_C^{(4)} = \frac{1}{8D_4}\Big[\big(-3\lambda + (9\lambda^2-\mu^2)(a-c)\big)S_1 + \big(9\lambda^2+\mu(1-\mu)\big)S_2 - (9\lambda^2-\mu^2)(d-e)S_4\Big](S_1-S_3)(S_1-Y)\,. \tag{6.128}$$

So all in all, for the most general form of the cooperon, before we begin to take relevant limits, we have

$$\begin{aligned}\Gamma_C = \frac{1}{8\widetilde{\gamma}}\Bigg[&\frac{1}{D_1}\Big[\big(\lambda + (\lambda^2-\mu^2)(a+c)\big)S_1 + \big(\lambda^2+\mu(1-\mu)\big)S_2 - (\lambda^2-\mu^2)(d+e)S_4\Big](S_1+S_3)(3S_1+Y)\\ &+\frac{1}{D_2}\Big[\big(\lambda + (\lambda^2-\mu^2)(a-c)\big)S_1 + \big(\lambda^2+\mu(1-\mu)\big)S_2 - (\lambda^2-\mu^2)(d-e)S_4\Big](S_1-S_3)(3S_1+Y)\\ &+\frac{1}{D_3}\Big[\big(-3\lambda + (9\lambda^2-\mu^2)(a+c)\big)S_1 + \big(9\lambda^2+\mu(1-\mu)\big)S_2 - (9\lambda^2-\mu^2)(d+e)S_4\Big](S_1+S_3)(S_1-Y)\\ &+\frac{1}{D_4}\Big[\big(-3\lambda + (9\lambda^2-\mu^2)(a-c)\big)S_1 + \big(9\lambda^2+\mu(1-\mu)\big)S_2 - (9\lambda^2-\mu^2)(d-e)S_4\Big](S_1-S_3)(S_1-Y)\Bigg]\end{aligned} \tag{6.129}$$

6.5 Leading Order Approximation of the Cooperon for Weak Doping of Magnetic Impurities

Next, we will examine the limiting case that is relevant to the problem. It is at this stage that we diverge from he previous work of Smith [65]. The methodology for finding the leading order contribution follows closely, however, the major difference is that we will *not* be taking the zero frequency case at this stage, as we are interested in more that just the superconducting carrier density.

We can take both the dirty and diffusive limits, that are applicable for superconductors with sufficiently high numbers of non-magnetic impurities and for weak localisation respectively. But on top of this can assume $\tau_s^{-1} \ll \tau_0^{-1}$, to ensure we are still firmly in the superconducting state. Therefore, in this limit we have $\widetilde{E} = \bar{E}$ in $\widetilde{\gamma}$ and we can use the same approximations as in the calculation in section 5.1,

$$\begin{aligned}\widetilde{\gamma} &\approx \frac{\pi N(0)}{\bar{E}+\bar{E}'}\left(1 - \frac{q^2 v_F^2}{d(\bar{E}+\bar{E}')^2}\right) \\ &\approx \pi N(0)\tau_0\big(1 - (Dq^2 + \bar{E} + \bar{E}')\tau_0\big)\,. \end{aligned} \tag{6.130}$$

However, we can find the leading order behaviour by taking the further simplification that

$$\widetilde{\gamma} \approx \pi N(0)\tau_0 \tag{6.131}$$

in all terms, except for the denominators, D_i. Where this approximation is taken, we have

$$\begin{aligned} \lambda &= \frac{\widetilde{\gamma}}{6\pi N(0)\tau_s} \approx \frac{\tau_0}{3\tau_s} \to 0 \text{because} \quad \tau_0 \ll \tau_s \\ \text{and} \quad \mu &= \frac{\widetilde{\gamma}}{2\pi N(0)\tau_0} \approx \frac{1}{2}\,. \end{aligned} \tag{6.132}$$

Leading to a much simplified expression for Γ_C, given by

$$\begin{aligned}\Gamma_C \approx \frac{1}{32\pi N(0)\tau_0}\Bigg[&\frac{1}{D_1}\Big[-(a+c)S_1+S_2+(d+e)S_4\Big](S_1+S_3)(3S_1+Y)\\&+\frac{1}{D_2}\Big[-(a-c)S_1+S_2+(d-e)S_4\Big](S_1-S_3)(3S_1+Y)\\&+\frac{1}{D_3}\Big[-(a+c)S_1+S_2+(d+e)S_4\Big](S_1+S_3)(S_1-Y)\\&+\frac{1}{D_4}\Big[-(a-c)S_1+S_2+(d-e)S_4\Big](S_1+S_3)(S_1-Y)\Bigg].\end{aligned} \tag{6.133}$$

By multiplying in the factors of $(S_1 \pm S_3)$, we can collect together terms like so

$$\begin{aligned}\Gamma_C = \frac{1}{32\pi N(0)\tau_0}\Bigg[&\Big(\frac{1}{D_1}+\frac{1}{D_2}\Big)\Big[-aS_1+S_2-cS_3+dS_4+eS_5\Big](3S_1+Y)\\&+\Big(\frac{1}{D_1}-\frac{1}{D_2}\Big)\Big[-aS_1+S_2-cS_3+dS_4+eS_5\Big]S_3(3S_1+Y)\\&+\Big(\frac{1}{D_3}+\frac{1}{D_4}\Big)\Big[-aS_1+S_2-cS_3+dS_4+eS_5\Big](S_1-Y)\\&+\Big(\frac{1}{D_3}-\frac{1}{D_4}\Big)\Big[-aS_1+S_2-cS_3+dS_4+eS_5\Big]S_3(S_1-Y)\Bigg].\end{aligned} \tag{6.134}$$

Substituting for $(a)-(e)$ we obtain a term, that will label as Σ_M, that is reminiscent of previous cooperon calculations,

$$\begin{aligned}\Sigma_M &= \Big[-aS_1+S_2-cS_3+dS_4+eS_5\Big]\\&= \Big[\sigma_z s_0\sigma_z s_0+\frac{(i\widetilde{\varepsilon}'\sigma_0 s_0+\widetilde{\Delta}'\sigma_x s_z)(i\widetilde{\varepsilon}\sigma_0 s_0+\widetilde{\Delta}\sigma_x s_z)}{\widetilde{E}\widetilde{E}'}\Big]\\&= \Big[\sigma_z s_0\sigma_z s_0+\frac{(iv'\sigma_0 s_0+\Delta\sigma_x s_z)(iv\sigma_0 s_0+\Delta\sigma_x s_z)}{VV'}\Big],\end{aligned} \tag{6.135}$$

which we have rewritten in terms of v in the last line. We will find it most convenient to not multiply in the factors of S_3, $(3+Y)$ and $(1-Y)$ when it comes to completing the traces, when the weak-localisation bubble is constructed.

The next step is to find the leading order term arising from the denominators. Using

$$a \pm c = \frac{\widetilde{\varepsilon}\widetilde{\varepsilon}' \mp \widetilde{\Delta}\widetilde{\Delta}'}{\widetilde{E}\widetilde{E}'} \tag{6.136}$$

and substituting this into the denominators, we have

$$\begin{aligned} D_{1,2} &= 1 + \left[\frac{1}{3\tau_s}\left(\frac{\widetilde{\varepsilon}\widetilde{\varepsilon}' \mp \widetilde{\Delta}\widetilde{\Delta}'}{\widetilde{E}\widetilde{E}'}\right) - \frac{1}{\tau_0}\right]\frac{1}{\widetilde{E}+\widetilde{E}'}\left(1 - \frac{q^2 v_F^2}{d(\widetilde{E}+\widetilde{E}')^2}\right) \\ \text{and} \quad D_{3,4} &= 1 - \left[\frac{1}{\tau_s}\left(\frac{\widetilde{\varepsilon}\widetilde{\varepsilon}' \mp \widetilde{\Delta}\widetilde{\Delta}'}{\widetilde{E}\widetilde{E}'}\right) + \frac{1}{\tau_0}\right]\frac{1}{\widetilde{E}+\widetilde{E}'}\left(1 - \frac{q^2 v_F^2}{d(\widetilde{E}+\widetilde{E}')^2}\right). \end{aligned} \tag{6.137}$$

We can write this in terms of v and V, following the process shown in equations 6.31 to 6.34, like so

$$\begin{aligned} D_{1,2} &= 1 + \left[\frac{1}{3\tau_s}\left(\frac{vv' \mp \Delta^2}{VV'}\right) - \frac{1}{\tau_0}\right]\frac{1}{V+V'+\tau_-^{-1}}\left(1 - \frac{q^2 v_F^2}{d(V+V'+\tau_-^{-1})^2}\right) \\ \text{and} \quad D_{3,4} &= 1 - \left[\frac{1}{\tau_s}\left(\frac{vv' \mp \Delta^2}{VV'}\right) + \frac{1}{\tau_0}\right]\frac{1}{V+V'+\tau_-^{-1}}\left(1 - \frac{q^2 v_F^2}{d(V+V'+\tau_-^{-1})^2}\right). \end{aligned} \tag{6.138}$$

Examining the latter part of each denominator, that we will label $\mathcal{D}$, we can extract a factor of τ_0^{-1} from each $(V + V' + \tau_-^{-1})$ term,

$$\begin{aligned} \mathcal{D} &= \frac{1}{V+V'+\tau_-^{-1}}\left(1 - \frac{q^2 v_F^2}{d(V+V'+\tau_-^{-1})^2}\right) \\ &= \frac{\tau_0}{\tau_0 V + \tau_0 V' + 1 - \frac{\tau_0}{\tau_s}}\left(1 - \frac{Dq^2\tau_0}{(\tau_0 V + \tau_0 V' + 1 - \frac{\tau_0}{\tau_s})^2}\right). \end{aligned} \tag{6.139}$$

We can then expand the term out in front in the small parameters, $1 \gg \frac{\tau_0}{\tau_s}$, $\tau_0 V$, $\tau_0 V'$, because we can treat $\tau_0 V$ as like order $\varepsilon\tau_0$. So, in the first term we expand to first order in these parameters, but the second term is already small in the parameter $Dq^2\tau_0$, as this term is like ql_0, so we only need to the zeroth order part. Hence, we have

$$\mathcal{D} \simeq \tau_0\left(1 + \frac{\tau_0}{\tau_s} - \tau_0 V - \tau_0 V'\right)(1 - Dq^2\tau_0). \tag{6.140}$$

Seeing as we are only keeping the leading order part, we can discard the cross-term between the order ql_0 and $\varepsilon\tau_0$ parts. Therefore, we are left with

$$\mathcal{D} \simeq \tau_0\left(1 + \frac{\tau_0}{\tau_s} - \tau_0 V - \tau_0 V' - Dq^2\tau_0\right). \tag{6.141}$$

Putting this back into $D_{1,2}$ and then once again, discarding cross-terms that are sub-leading-order, we find

$$\begin{aligned} D_{1,2} &= 1 + \left[\frac{1}{3\tau_s}\left(\frac{vv' \mp \Delta^2}{VV'}\right) - \frac{1}{\tau_0}\right]\tau_0\left(1 + \frac{\tau_0}{\tau_s} - \tau_0 V - \tau_0 V' - Dq^2\tau_0\right) \\ &\simeq \frac{\tau_0}{3\tau_s}\left(\frac{vv' \mp \Delta^2}{VV'}\right) - \frac{\tau_0}{\tau_s} + \tau_0 V + \tau_0 V' + Dq^2\tau_0 \end{aligned} \tag{6.142}$$

and, similarly, for $D_{3,4}$ we have

$$D_{3,4} \simeq -\frac{\tau_0}{\tau_s}\left(\frac{vv' \mp \Delta^2}{VV'}\right) - \frac{\tau_0}{\tau_s} + \tau_0 V + \tau_0 V' + Dq^2\tau_0\,. \tag{6.143}$$

Now if we extract the common factor of τ_0, we arrive at our final expression for the cooperon in the weakly-doped regime,

$$\begin{aligned} \Gamma_C(\mathbf{q}, i\varepsilon, i\varepsilon') \approx \frac{1}{32\pi N(0)\tau_0^2}\Bigg[&\left(\frac{1}{D_1} + \frac{1}{D_2}\right)\Sigma_M(3S_1 + Y) + \left(\frac{1}{D_1} - \frac{1}{D_2}\right)\Sigma_M S_3(3S_1 + Y) \\ &+ \left(\frac{1}{D_3} + \frac{1}{D_4}\right)\Sigma_M(S_1 - Y) + \left(\frac{1}{D_3} - \frac{1}{D_4}\right)\Sigma_M S_3(S_1 - Y)\Bigg] \end{aligned} \tag{6.144}$$

$$\begin{aligned} \text{now with} \quad D_{1,2} &= Dq^2 + V + V' - \frac{1}{\tau_s} + \frac{1}{3\tau_s}\left(\frac{vv' \mp \Delta^2}{VV'}\right), \\ D_{3,4} &= Dq^2 + V + V' - \frac{1}{\tau_s} - \frac{1}{\tau_s}\left(\frac{vv' \mp \Delta^2}{VV'}\right). \end{aligned}$$

We can examine the limit $\tau_s^{-1} \to 0$ to check that this form of the cooperon matches that

of equation 5.20. In this limit we have $v, v', V, V' \to \varepsilon, \varepsilon', E, E'$ and hence

$$\begin{aligned} &D_{1,2,3,4} \to Dq^2 + E + E' \\ \text{and} \quad &\Sigma_M \to \Big[\sigma_z s_0 \sigma_z s_0 + \frac{(i\varepsilon'\sigma_0 s_0 + \Delta\sigma_x s_z)(i\varepsilon\sigma_0 s_0 + \Delta\sigma_x s_z)}{EE'}\Big]. \end{aligned} \tag{6.145}$$

Thus we can see the second and fourth terms will simply cancel to zero (suggesting these terms are indicative of an effect that is only present with the inclusion of magnetic impurities), leaving us with

$$\begin{aligned} \Gamma_C \to &\frac{1}{16\pi N(0)\tau_0^2}\frac{1}{Dq^2 + E + E'} \\ &\times \Big[\sigma_z s_0 \sigma_z s_0 + \frac{(i\varepsilon'\sigma_0 s_0 + \Delta\sigma_x s_z)(i\varepsilon\sigma_0 s_0 + \Delta\sigma_x s_z)}{EE'}\Big](3S_1 + Y + S_1 - Y) \\ = &\frac{1}{4\pi N(0)\tau_0^2}\frac{1}{Dq^2 + E + E'}\Big[\sigma_z s_0 \sigma_z s_0 + \frac{(i\varepsilon'\sigma_0 s_0 + \Delta\sigma_x s_z)(i\varepsilon\sigma_0 s_0 + \Delta\sigma_x s_z)}{EE'}\Big], \end{aligned} \tag{6.146}$$

because all that is left is the identity term, S_1, that will not have any affect on the traces, we can simply take this as a factor 4. So the only difference between this and the cooperon in equation 5.20 is that we have the 4×4 matrices, but when we take a normalised trace this will yield the exact results we desire. Hence, this provides a good check that this form of the cooperon with magnetic impurities is accurate.

6.6 Partial Calculation of Weak Localisation Correction in a Superconductor with Magnetic Impurities

In the following section, we will make partial progress through the weak localisation correction calculation to the thermal conductivity using the cooperon from the previous section. We will compute the traces and the integral over ξ to take us to the point at which analytic continuation would have to be performed. By taking the calculation to

this stage, we will be able provide some discussion of the functional form of the resulting equation.

We can construct the weak-localisation diagram in analogy to chapter 5, where the first pair of $\sigma_i s_i$ in the cooperon are inserted into the trace around the loop at the top of the cooperon ladder and the latter pair is inserted at the bottom. The new consideration with regards to the output of the traces is the addition of the Y, S_1 S_3 terms.

S_1 is just the identity thereofre this has no interesting behaviour in the traces. Y is made up of three terms containing $\sigma_z s_x$, $\sigma_z s_y$ and $\sigma_0 s_z$ respectively and we find that all of these terms commute with every other term that appears in the trace. This means that we can trivially commute together the two additional terms that appear due to Y in each trace, reducing them to the same form as that which only contains the identity. In other words, once we take the trace we can replace Y with a factor of 3, meaning $(3S_1 + Y) \to 6$ and $(S_1 - Y) \to -2$.

Now we will examine the weak-localisation Green's function term by term, labelling each term with a numbered subscript, starting with

$$\begin{aligned}\mathcal{G}^{WL,M}_{\alpha\beta,1} = \frac{6}{32\pi N(0)\tau_0^2}\frac{T\delta_{\alpha\beta}}{m^2\mathcal{V}^2}\sum_{\mathbf{q}}\sum_{\mathbf{k}}\sum_{\varepsilon}\mathbf{k}_\alpha(\mathbf{q}-\mathbf{k})_\beta\left(i\varepsilon+\frac{i\omega}{2}\right)^2\left(\frac{1}{D_1}+\frac{1}{D_2}\right)\\ \times\Big[\operatorname{Tr}\left\{\sigma_z s_0\mathcal{G}(\mathbf{k},i\varepsilon')\sigma_z s_0\mathcal{G}(\mathbf{q}-\mathbf{k},i\varepsilon')\sigma_z s_0\mathcal{G}(\mathbf{q}-\mathbf{k},i\varepsilon)\sigma_z s_0\mathcal{G}(\mathbf{k},i\varepsilon)\right\}\\ +\frac{1}{\widetilde{E}\widetilde{E}'}\operatorname{Tr}\big\{\sigma_z s_0\mathcal{G}(\mathbf{k},i\varepsilon')(i\widetilde{\varepsilon}'\sigma_0 s_0+\widetilde{\Delta}'\sigma_x s_z)\mathcal{G}(\mathbf{q}-\mathbf{k},i\varepsilon')\\ \times\sigma_z s_0\mathcal{G}(\mathbf{q}-\mathbf{k},i\varepsilon)(i\widetilde{\varepsilon}\sigma_0 s_0+\widetilde{\Delta}\sigma_x s_z)\mathcal{G}(\mathbf{k},i\varepsilon)\big\}\Big],\end{aligned} \tag{6.147}$$

where it is most convenient to put the parts appearing in the trace from the Σ_M part in ε form for the time being. Next we can take all the appropriate steps to obtain the linear-response function from the Green's function which one should be familiar with from the previous sections. We will drop out any Pauli-identity-matrices at this stage as well for brevity, but we must remember that the identity is still a 4×4 matrix and so we

introduce the factor of 1/2 to normalise the trace. Doing all of this leads us to

$$\begin{aligned}\mathcal{K}_1^{WL,M} = -\frac{3D}{32\pi\tau_0^3}\frac{T}{\mathcal{V}}\sum_{\mathbf{q}}\sum_{\varepsilon}\left(i\varepsilon+\frac{i\omega}{2}\right)^2\left(\frac{1}{D_1}+\frac{1}{D_2}\right)\int_{-\infty}^{\infty}\frac{\mathrm{d}\xi}{(\xi^2+\widetilde{E}^2)^2(\xi^2+\widetilde{E}'^2)^2}\\ \times\Big[\operatorname{Tr}\left\{\sigma_z(i\widetilde{\varepsilon}'+\xi\sigma_z-\widetilde{\Delta}'\sigma_x s_z)\sigma_z(i\widetilde{\varepsilon}'+\xi\sigma_z-\widetilde{\Delta}'\sigma_x s_z)\right.\\ \left.\times\,\sigma_z(i\widetilde{\varepsilon}+\xi\sigma_z-\widetilde{\Delta}\sigma_x s_z)\sigma_z(i\widetilde{\varepsilon}+\xi\sigma_z-\widetilde{\Delta}\sigma_x s_z)\right\} \qquad (6.148)\\ +\frac{1}{\widetilde{E}\widetilde{E}'}\operatorname{Tr}\big\{\sigma_z(i\widetilde{\varepsilon}'+\xi\sigma_z-\widetilde{\Delta}'\sigma_x s_z)(i\widetilde{\varepsilon}'+\widetilde{\Delta}'\sigma_x s_z)(i\widetilde{\varepsilon}'+\xi\sigma_z-\widetilde{\Delta}'\sigma_x s_z)\\ \times\,\sigma_z(i\widetilde{\varepsilon}+\xi\sigma_z-\widetilde{\Delta}\sigma_x s_z)(i\widetilde{\varepsilon}+\widetilde{\Delta}\sigma_x s_z)(i\widetilde{\varepsilon}+\xi\sigma_z-\widetilde{\Delta}\sigma_x s_z)\big\}\Big]\end{aligned}$$

The computation of these traces in fact proceeds in an identical manner to that outlined in equations 5.33 - 5.36, despite the new 4×4 matrices. Therefore we can immediately write

$$\begin{aligned}\mathcal{K}_1^{WL,M} &= -\frac{3}{2}\frac{D}{\tau_0^3}\frac{T}{\mathcal{V}}\sum_{\mathbf{q}}\sum_{\varepsilon}\left(i\varepsilon+\frac{i\omega}{2}\right)^2\left(\frac{1}{D_1}+\frac{1}{D_2}\right)\frac{1}{(\widetilde{E}+\widetilde{E}')^3}\left(1-\frac{\widetilde{\varepsilon}\widetilde{\varepsilon}'+\widetilde{\Delta}\widetilde{\Delta}'}{\widetilde{E}\widetilde{E}'}\right) \qquad (6.149)\\ &= -\frac{3}{2}\frac{D}{\tau_0^3}\frac{T}{\mathcal{V}}\sum_{\mathbf{q}}\sum_{\varepsilon}\left(i\varepsilon+\frac{i\omega}{2}\right)^2\left(\frac{1}{D_1}+\frac{1}{D_2}\right)\frac{1}{(V+V'+\tau_-^{-1})^3}\left(1-\frac{vv'+\Delta^2}{VV'}\right).\end{aligned}$$

To leading order we can take $V+V'+\tau_-^{-1}\approx\tau_0^{-1}$, cancelling in the prefactor to yield

$$\mathcal{K}_1^{WL,M} = -\frac{3D}{2}\frac{T}{\mathcal{V}}\sum_{\mathbf{q}}\sum_{\varepsilon}\left(i\varepsilon+\frac{i\omega}{2}\right)^2\left(\frac{1}{D_1}+\frac{1}{D_2}\right)\left(1-\frac{vv'+\Delta^2}{VV'}\right) \qquad (6.150)$$

The third term has the exact same structure as the first, only with a factor -2 instead of 6 and the substitution $D_{1,2}\mapsto D_{3,4}$. Therefore we have

$$\mathcal{K}_3^{WL,M} = \frac{D}{2}\frac{T}{\mathcal{V}}\sum_{\mathbf{q}}\sum_{\varepsilon}\left(i\varepsilon+\frac{i\omega}{2}\right)^2\left(\frac{1}{D_3}+\frac{1}{D_4}\right)\left(1-\frac{vv'+\Delta^2}{VV'}\right). \qquad (6.151)$$

For the second and fourth terms we must examine how S_3 affects the traces. The two

traces we have to calculate now have the forms

$$\begin{aligned}\mathrm{Tr}_1 = \mathrm{Tr}\big\{&\sigma_z(i\widetilde{\varepsilon}' + \xi\sigma_z - \widetilde{\Delta}'\sigma_x s_z)\sigma_z(\sigma_x s_z)(i\widetilde{\varepsilon}' + \xi\sigma_z - \widetilde{\Delta}'\sigma_x s_z)\\ &\times \sigma_z(i\widetilde{\varepsilon} + \xi\sigma_z - \widetilde{\Delta}\sigma_x s_z)\sigma_z(\sigma_x s_z)(i\widetilde{\varepsilon} + \xi\sigma_z - \widetilde{\Delta}\sigma_x s_z)\big\}, \qquad (6.152)\\ \mathrm{Tr}_2 = \mathrm{Tr}\big\{&\sigma_z(i\widetilde{\varepsilon}' + \xi\sigma_z - \widetilde{\Delta}'\sigma_x s_z)(i\widetilde{\varepsilon}' + \widetilde{\Delta}'\sigma_x s_z)(\sigma_x s_z)(i\widetilde{\varepsilon}' + \xi\sigma_z - \widetilde{\Delta}'\sigma_x s_z)\\ &\times \sigma_z(i\widetilde{\varepsilon} + \xi\sigma_z - \widetilde{\Delta}\sigma_x s_z)(i\widetilde{\varepsilon} + \widetilde{\Delta}\sigma_x s_z)(\sigma_x s_z)(i\widetilde{\varepsilon} + \xi\sigma_z - \widetilde{\Delta}\sigma_x s_z)\big\} \qquad (6.153)\end{aligned}$$

These traces can be calculated similarly to previous cases, noting that the additional $\sigma_x s_z$ terms commute with everything but the σ_z terms, with which they anti-commute. This yields

$$\mathrm{Tr}_1 = 4(\xi^2 + \widetilde{E}^2)(\xi^2 + \widetilde{E}'^2) \qquad (6.154a)$$

$$\mathrm{Tr}_2 = 4(\xi^2 + \widetilde{E}^2)(\xi^2 + \widetilde{E}'^2)(\widetilde{\varepsilon}\widetilde{\varepsilon}' + \widetilde{\Delta}\widetilde{\Delta}') \qquad (6.154b)$$

Using these results in the linear response function, we have

$$\begin{aligned}\mathcal{K}_2^{WL,M} = -\frac{3D}{8\pi\tau_0^3}\frac{T}{\mathcal{V}}\sum_{\mathbf{q}}\sum_{\varepsilon}&\left(i\varepsilon + \frac{i\omega}{2}\right)^2\left(\frac{1}{D_1} - \frac{1}{D_2}\right)\\ &\times \int_{-\infty}^{\infty}\frac{\mathrm{d}\xi}{(\xi^2 + \widetilde{E}^2)(\xi^2 + \widetilde{E}'^2)}\left(1 + \frac{\widetilde{\varepsilon}\widetilde{\varepsilon}' + \widetilde{\Delta}\widetilde{\Delta}'}{\widetilde{E}\widetilde{E}'}\right). \qquad (6.155)\end{aligned}$$

This integral can be solved using the result in equation 4.53 yielding

$$\begin{aligned}\mathcal{K}_2^{WL,M} &= -\frac{3D}{8\tau_0^3}\frac{T}{\mathcal{V}}\sum_{\mathbf{q}}\sum_{\varepsilon}\left(i\varepsilon + \frac{i\omega}{2}\right)^2\left(\frac{1}{D_1} - \frac{1}{D_2}\right)\frac{1}{\widetilde{E}\widetilde{E}'(\widetilde{E} + \widetilde{E}')}\left(1 + \frac{\widetilde{\varepsilon}\widetilde{\varepsilon}' + \widetilde{\Delta}\widetilde{\Delta}'}{\widetilde{E}\widetilde{E}'}\right)\\ &= -\frac{3D}{2\tau_0^3}\frac{T}{\mathcal{V}}\sum_{\mathbf{q}}\sum_{\varepsilon}\left(i\varepsilon + \frac{i\omega}{2}\right)^2\left(\frac{1}{D_1} - \frac{1}{D_2}\right) \qquad (6.156)\\ &\qquad \times \frac{1}{(2V + \tau_-^{-1})(2V' + \tau_-^{-1})(V + V' + \tau_-^{-1})}\left(1 + \frac{vv' + \Delta^2}{VV'}\right),\end{aligned}$$

which when we take the leading order part reduces to

$$\mathcal{K}_2^{WL,M} \simeq -\frac{3D}{2}\frac{T}{\mathcal{V}}\sum_{\mathbf{q}}\sum_{\varepsilon}\left(i\varepsilon+\frac{i\omega}{2}\right)^2\left(\frac{1}{D_1}-\frac{1}{D_2}\right)\left(1+\frac{vv'+\Delta^2}{VV'}\right). \tag{6.157}$$

Similarly for the final term, we have

$$\mathcal{K}_4^{WL,M} \simeq \frac{D}{2}\frac{T}{\mathcal{V}}\sum_{\mathbf{q}}\sum_{\varepsilon}\left(i\varepsilon+\frac{i\omega}{2}\right)^2\left(\frac{1}{D_3}-\frac{1}{D_4}\right)\left(1+\frac{vv'+\Delta^2}{VV'}\right). \tag{6.158}$$

Finally, collecting all of the terms together there is some cancellation and we find

$$\mathcal{K}^{WL,M} = -\frac{DT}{\mathcal{V}}\sum_{\mathbf{q}}\sum_{\varepsilon}\left(i\varepsilon+\frac{i\omega}{2}\right)^2\left[3\left(\frac{1}{D_1}-\frac{1}{D_2}\frac{vv'+\Delta^2}{VV'}\right)-\left(\frac{1}{D_3}-\frac{1}{D_4}\frac{vv'+\Delta^2}{VV'}\right)\right]. \tag{6.159}$$

6.7 Discussion and Future work

We first perform a sanity check to see whether this result is consistent with established results. We can take the limit $\tau_s^{-1} \to 0$ and once again we have $v, v', V, V' \to \varepsilon, \varepsilon', E, E'$ and $D_{1,2,3,4} \to Dq^2 + E + E'$. Therefore we will simply be able to factor out the denominators, as they are now all the same, and thus the two terms will cancel, yielding a factor of 2 and the familiar coherence factor, $1-(\varepsilon\varepsilon'+\Delta^2)/EE'$. This reproduces equation 5.37, therefore this result is consistent with the case that has no magnetic impurities.

It is illuminating to draw comparisons between the different weak localisation calculations we have covered in this thesis, and indeed part of the motivation for including them is so that the structural similarities in the equations are clear. We can compare the different calculations from two different angles: electrical vs thermal, and normal state vs the superconducting state vs superconducting state with magnetic impurities. We will collate the results here for easy reference and we will present them at the stage just before the sum over Matsubara frequencies is completed, as it is at this stage the functional

comparisons are clearest:

$$
\begin{aligned}
K_n^{WL,E} &= -\frac{4e^2DT}{\mathcal{V}}\sum_{\mathbf{q}}\sum_{\varepsilon}\frac{1}{Dq^2+|\omega|+\tau_\phi^{-1}}\Theta(-\varepsilon(\varepsilon+\omega))\,,\\
K_s^{WL,E} &= -\frac{2e^2DT}{\mathcal{V}}\sum_{\mathbf{q}}\sum_{\varepsilon}\frac{1}{Dq^2+E+E'+\tau_\phi^{-1}}\left(1-\frac{\varepsilon\varepsilon'-\Delta^2}{EE'}\right),\\
K_n^{WL,T} &= -\frac{4DT}{\mathcal{V}}\sum_{\mathbf{q}}\sum_{\varepsilon}\left(i\varepsilon+\frac{i\omega}{2}\right)^2\frac{1}{Dq^2+|\omega|+\tau_\phi^{-1}}\Theta(-\varepsilon(\varepsilon+\omega))\,,\\
K_s^{WL,T} &= -\frac{2DT}{\mathcal{V}}\sum_{\mathbf{q}}\sum_{\varepsilon}\left(i\varepsilon+\frac{i\omega}{2}\right)^2\frac{1}{Dq^2+E+E'+\tau_\phi^{-1}}\left(1-\frac{\varepsilon\varepsilon'+\Delta^2}{EE'}\right),\\
K_{s,mag}^{WL,T} &= -\frac{DT}{\mathcal{V}}\sum_{\mathbf{q}}\sum_{\varepsilon}\left(i\varepsilon+\frac{i\omega}{2}\right)^2\left[3\left(\frac{1}{D_1}-\frac{1}{D_2}\frac{vv'+\Delta^2}{VV'}\right)-\left(\frac{1}{D_3}-\frac{1}{D_4}\frac{vv'+\Delta^2}{VV'}\right)\right],
\end{aligned}
\tag{6.160}
$$

Firstly, we can discuss the difference between the electrical and thermal equations. We can see that there are three key differences, all of which are a result of the difference in the contribution from the vertices in the bubble diagrams. The simplest of which is the additional factor of e^2 in the prefactor of the electrical equations. The factor of $(i\varepsilon+i\omega/2)^2$ is a result of the partial time derivative that is present in the heat current operator, but not in the electrical current operator. This additional factor is mathematically the origin of the Wiedemann-Franz law in the normal state. In the superconducting equations we also see that the Δ^2 term switches sign; this is a result of the additional σ_z matrices on the vertices causing a sign flip in the traces. These three changes can be thought of as a set of informal 'rules' for converting between electrical and thermal calculations.

The relation between the normal state and superconducting calculations for electrical conductivity can be related in a much more formal sense via the method of exact eigenstates [59]. This method functions because the weak localisation effect is caused only by the interaction with a one body potential in the form of static impurities, therefore normal state and superconducting state can be related via the matrix elements of the current operator. We will not work through the derivation here, but practically speaking this manifests again in a set of 'rules' that relate the normal and superconducting calculations as long as there are no two-body potentials. To obtain the superconducting equation

from the normal, the $|\omega|$ is replaced with $E + E'$ and the Heaviside function is replaced with the coherence factor, $1 - (\varepsilon\varepsilon' - \Delta^2)/EE'$. In the limit $\Delta \to 0$ by using the fact that $E \to |\varepsilon|$ one can also regain the normal state result from the superconducting one. The exact eigenstates method does not transfer precisely in the formal mathematical sense to the thermal calculations, as a result of the partial time derivative in the heat current operator. However, by using a combination of the two sets of rules outlined above, one can clearly see the connections between the first four results. A deeper investigation into the limitations of this set of 'rules' and whether or not the exact eigenstates method can be applied in some way to thermal conductivity could be an interesting area for future work.

Unlike the relations between the equations we have discussed so far, the relation between the superconducting thermal weak localisation corrections with and without magnetic impurities appears to be very non-trivial. This is because the spin-flip scattering caused by paramagnetic impurities is a pair-breaking mechanism. This is clear when we compare to a system where spin-orbit scattering is the only interaction, other than the interaction with the non-magnetic impurities. Hikami et. al. [77] showed that in the normal state with spin-orbit scattering, but no spin-flip scattering, one would obtain a logarithmic correction of the same form as with only non-magnetic impurities, but with an additional factor of $-1/2$, creating a weak anti-localisation effect. González Rosado et. al. [63] found a similar result in the thermal conductivity superconducting state: finding the ratio of the weak localisation effect to the leading order conductivity was only altered by a factor of $-1/2$ when spin-orbit scattering was introduced. The key point here is that the functional form of the correction was not altered, even in superconductors, when the scattering mechanism is not pair-breaking. Whereas, the inclusion of magnetic impurities clearly transforms the structure of the weak localisation correction, as we can see from equation 6.159.

We can see that in $K^{WL,T}_{s,mag}$ the factor of $(i\varepsilon + i\omega/2)^2$ from the vertices remains the same, whilst the rest of the terms have a structure that resembles the coherence factor,

but with a number of differences. Firstly, v and V take the place of ε and E, which implicitly contain τ_s, because the relations between ε and $\widetilde{\varepsilon}$, and Δ and $\widetilde{\Delta}$, can no longer be disentangled. Secondly, there are now two distinct terms that can be traced back to the two eigenvalues of Y in the derivation of the cooperon: the former with the factor of 3 comes from the $\Lambda = 1$ eigenvalue (spin singlet) and the latter with the factor of -1 comes from the $\Lambda = -3$ eigenvalue (spin triplet). We have already discussed above how these terms will reduce the the non-magnetic superconducting result in the limit $\tau_s^{-1} \to 0$. It is interesting that there appears to be a simultaneous enhancement of the correction by a factor of 3/2 and introduction of an anti-localisation term that, at least to leading order, seems to cancel with this enhancement. We are careful to say to leading order, because all of the denominators are similar but distinct. We note that if one could factor out all of the denominators we would be left with a term that looks like

$$1 - \frac{vv' + \Delta^2}{VV'}\,, \tag{6.161}$$

which has the same form as the coherence factor one would expect for thermal conductivity, only with v's for the reason mentioned above.

Finally, we will examine the forms of the denominators. All of these have the same basic structure with only one term varying between them, hence we can write them in the form

$$\begin{aligned} D_i &= Dq^2 + V + V' - \frac{1}{\tau_s} + X_i\,, \qquad (6.162)\\ \text{with}\quad X_1 &= \frac{1}{3\tau_s}\frac{vv' - \Delta^2}{VV'}\,, \quad X_2 = \frac{1}{3\tau_s}\frac{vv' + \Delta^2}{VV'}\,,\\ X_3 &= -\frac{1}{\tau_s}\frac{vv' - \Delta^2}{VV'} \quad \text{and} \quad X_4 = -\frac{1}{\tau_s}\frac{vv' + \Delta^2}{VV'}\,. \end{aligned}$$

The first two denominators with the factor of 1/3 correspond to the $\Lambda = 1$ eigenvalue and the latter two correspond to the $\Lambda = -3$ eigenvalue. We also note that the pairs of denominators that appear in each coherence factor-like term only differ by the sign

of Δ^2. So when Δ is small close to T_c (which we recall we are most interested in the region $T \gtrapprox 0.9T_c$), these denominators may become approximately equal, allowing for some simplification. However, approximations should really take place after the analytical continuation has been performed, which leads us to the discussion of future work.

The next logical step to make this work more complete is to perform the full analytic continuation on $K^{WL,T}_{s,mag}$. We have made an effort to include a complete description of how to perform this process in sections 6.2 and 6.3, so that this thesis contains all of the information necessary to perform this next step in the calculation. Without having to go through the analytic continuation we are able to make some qualitative predictions based on what we know about the analytic continuation process and the structure the of the equation. The major complication of the analytic continuation for $K^{WL,T}_{s,mag}$ is that the denominators can no longer be approximated away compared to the calculations of $K^{E,M}_s$ and $K^{T,M}_s$, where we were able to take $(\tau_-^{-1} \pm iV \pm iV') \approx \tau_0^{-1}$, due to being in the dirty limit for disordered superconductors. Whereas, in D_i it is not clear whether any term is appreciably small or large compared to the others. In the conductivity calculations this lead to cancellation of the 1's in the coherence factors from above and below the branch cuts. In the weak localisation case there would not be an exact cancellation, however for the $1/D_1$ and $1/D_3$ terms we would end up with a difference in two terms that only vary by the analyticity of v and V. For proof of concept, the D_1 term would end up with an integral from the Γ_a contour given by

$$\int_{\omega_g}^{\infty} \mathrm{d}x \left(x + \frac{\omega}{2}\right)^2 \tanh\!\left(\frac{x}{2T}\right) \left[\frac{1}{Dq^2 - iV(x) - iV'(x) - \frac{1}{\tau_s} + \frac{1}{3\tau_s}\left(\frac{v(x)v'(x)+\Delta^2}{V(x)V'(x)}\right)} \right. \tag{6.163}$$
$$\left. - \frac{1}{Dq^2 + iV^*(x) - iV'(x) - \frac{1}{\tau_s} - \frac{1}{3\tau_s}\left(\frac{v^*(x)v'(x)+\Delta^2}{V^*(x)V'(x)}\right)} \right].$$

This term clearly does not exactly cancel, but it may be formally small in comparison to the D_2 and D_4 terms, because we know that the additional factors of i from the $(vv' + \Delta^2)/VV'$ term cause the contributions from either side of the contour to sum

instead of subtract. Again we can examine the contribution from Γ_a for the D_2 term to see this,

$$-\int_{\omega_g}^{\infty} \mathrm{d}x \left(x+\frac{\omega}{2}\right)^2 \tanh\left(\frac{x}{2T}\right) \left[\frac{\left(\frac{v(x)v'(x)-\Delta^2}{V(x)V'(x)}\right)}{Dq^2 - iV(x) - iV'(x) - \frac{1}{\tau_s} + \frac{1}{3\tau_s}\left(\frac{v(x)v'(x)-\Delta^2}{V(x)V'(x)}\right)} \right. \tag{6.164}$$
$$\left. + \frac{\left(\frac{v^*(x)v'(x)-\Delta^2}{V^*(x)V'(x)}\right)}{Dq^2 + iV^*(x) - iV'(x) - \frac{1}{\tau_s} - \frac{1}{3\tau_s}\left(\frac{v^*(x)v'(x)-\Delta^2}{V^*(x)V'(x)}\right)} \right].$$

We also note that eventually we would want to take the limit $\omega \to 0$ as this is a thermal measurement and this raises some interesting considerations how the $-\tau_s^{-1}$ and X_i terms will combine. At a simple level it appears as though in this limit $X_2 \to \frac{1}{3\tau_s}$ and $X_4 \to -\frac{1}{\tau_s}$, but because v is complex, its analyticity will change over the branch cut and the situation is likely not as simple as this. However, this may be indicative of the leading order behaviour of these terms. This would lead to terms like $\frac{2}{3\tau_s}$ and/or $\frac{4}{3\tau_s}$ in D_2 and $\frac{2}{\tau_s}$ and/or a cancellation to zero in D_4 depending on which combinations of signs occur in the analytic continuation. Though we cannot say anything concrete without the full analytic continuation, this is reassuring as terms of this type often appear in weak localisation calculations including magnetic and/or spin-orbit scattering [42, 45, 65], and certainly it would be pertinent in future work to confirm in the limit $\Delta \to 0$ along with $\omega \to 0$ one would return to the normal state results.

In conclusion, there are certainly a variety of interesting avenues to explore as far as limiting approximations after the full analytic continuation is completed. The resulting integrals both prior to and after any approximations would almost certainly have to be tackled numerically. This could then be compared to any future experimental curves of the thermal conductivity as a function of the temperature. However, as we have discussed in the introduction, experimental results in this area are virtually non-existent, so we believe this would be an interesting area to explore in the future. The extension of the theory to include spin-orbit as well as spin-flip scattering would open up the possibility of weak anti-localisation effects. This may be more interesting from an experimental viewpoint, as

the addition of impurities leading to an increase in conductivity is perhaps a more novel effect.

CHAPTER 7

CONCLUSION

In this thesis we began by establishing the Green's function methodology that is at the heart of diagrammatic quantum field theory and used this to derive the impurity Green's function that serves as the main building block of transport calculations. In chapter 3 we used this methodology to derive the Drude electrical conductivity from the linear response to an electromagnetic field and the thermal conductivity from the equivalent linear response to a thermal gradient. We showed that these results obeyed the Wiedemann-Franz law as expected. We then demonstrated how the self-intersecting paths that lead to the weak localisation effect can be interpreted diagrammatically, and went on to calculate this correction in one, two and three dimensions, demonstrating that the weak localisation correction in the normal state also obeys the Wiedemann-Franz law. We also showed that by considering the pair propagator that appears in the superconducting-fluctuation correction to conductivity, we can derive diagrammatically the BCS result for the transition temperature for clean and dirty superconductors.

In chapter 4 we derived the Nambu-Gorkov formalism from the BCS Hamiltonian that allows the diagrammatic formalism to be applicable in the superconducting state and used it to recover the BCS self-consistency equation for the gap. We showed how impurities can be included into this formalism perturbatively, in analogy with the normal state, allowing us to perform calculations for dirty superconductors. With this machinery in

place, we calculated the linear response of the dirty superconductor to an electromagnetic field, using this to derive the superconducting carrier density and the frequency-dependent linear response at zero temperature, which describes infrared absorption and transmission. We then calculated the response of the superconductor to a thermal gradient and by examining the zero-frequency case, we found an expression for the electronic component of the thermal conductivity of a superconductor.

Chapter 5 was the beginning of the original work of this thesis. We developed the theory of the cooperon in the superconducting state making use of the outer-product to encode the matrix structure on both vertices of the cooperon into one mathematical object. We then used this to calculate the weak localisation correction to thermal conductivity in a dirty superconductor, with the phase coherence lifetime introduced as a phenomenological parameter. Our result was in agreement with the result in González Rosado et. al. [63] for dirty superconductors, in the high temperature regime where the cutoff of the momentum integral is provided by the impurity scattering rate, τ_0^{-1}. We also discussed in the Introduction how the exponential suppression of the carriers with decreasing temperature makes the high temperature regime the most interesting for experimental observation of weak localisation in superconductors.

In chapter 6, we first extend the Nambu-Gorkov formalism to include the spin-flip scattering caused by magnetic impurities and showed how this leads to a suppression of the gap. We calculated the real part of the electrical and thermal conductivity, paying close attention to how to perform the analytic continuation of the integrals, as this process carries over to the weak localisation calculation. We provided a full derivation of the form of the cooperon with magnetic impurities providing the phase coherence lifetime cut-off in the dirty limit. We built upon the previous work of Smith [65], by taking the leading order approximation of the cooperon in the limit $\tau_s^{-1} \ll \tau_0^{-1}$ whilst maintaining the frequency dependence. This is because, although we would eventually take the limit $\omega \to 0$, we can see from the calculations earlier in chapter 6 that we must do this after the analytic continuation. So having access to the frequency-dependent cooperon is essential

for calculating the weak localisation correction to thermal conductivity in this regime. We then completed the first part of the calculation of the weak localisation correction using the magnetic impurity cooperon, up to the point at which we would have to perform the analytic continuation.

In future work we hope to complete the full analytic continuation and take the $\omega \to 0$ limit relevant for thermal conductivity. At first inspection it appears as though the increased complexity of the linear response function means that the neat cancellations which occur in the conductivity calculations in the first half of chapter 6 will not be possible in the weak localisation case. However, we propose that an investigation into the small Δ limit may be fruitful from an analytical viewpoint. Considering that we are primarily focused on temperature just below T_c, there may be an appreciable temperature range where this approximation will be valid. Otherwise, a numerical calculation of the resulting real integrals from the analytic continuation will be possible, even without any further approximation. This could in principle be compared to experimental measurements, with particular interest in the fitting in the region just below T_c. However, to the author's best knowledge at this time there are no experiments investigating the weak localisation correction to thermal conductivity in superconductors, much less ones specifically interested in doping with paramagnetic impurities. Thus, we hope that this area will be explored in the future in order to provide results with which to compare future numerical calculations.

APPENDIX A

DERIVATION OF THE KUBO FORMULA FOR LINEAR RESPONSE

We will derive the linear response of an operator to a small perturbation of the Hamiltonian. The method that will be employed is to express the expectation value of the operator in the basis of energy eigenvalues of the Hamiltonian in the Schrodinger representation. Then, switch to the interaction representation and expand to first order in the interaction evolution operator. We have

$$H(t) = H_0 + H'(t)\Theta(t), \tag{A.1}$$

so the Hamiltonian is perturbed at $t = 0$. The expectation value of an arbitrary operator, $\hat{A}$, before the perturbation can be expressed as

$$\langle A \rangle = \frac{1}{Z_0} \operatorname{Tr}\{\rho_0 A\} \tag{A.2}$$

$$\text{where} \quad \rho_0 = e^{-\beta H_0} = \sum_m |m\rangle\langle m| \, e^{-\beta E_m}$$

$$\text{and} \quad Z_0 = \operatorname{Tr}\{\rho_0\}$$

$$\Rightarrow \langle A \rangle = \frac{1}{Z_0} \sum_{nm} \langle n|m\rangle \ \langle m|e^{-\beta E_m} A|n\rangle$$

$$= \frac{1}{Z_0} \sum_{nm} \delta_{nm} \langle m|e^{-\beta E_m} A|n\rangle$$

$$= \frac{1}{Z_0} \sum_n \langle n|A|n\rangle \, e^{-\beta E_n} \tag{A.3}$$

Now consider the expectation value of A at some time $t > 0$ after the perturbation has been applied. In the Schrodinger picture the time dependence of this expectation value is encapsulated in the time dependence of the eigenstates, i.e.

$$\langle A(t) \rangle = \frac{1}{Z} \operatorname{Tr}\{\rho(t) A\} \tag{A.4}$$

$$\text{where} \quad \rho(t) = \sum_m |m(t)\rangle\langle m(t)| \, e^{-\beta E_m}$$

Following the same process as before, the only difference being also obtaining a $\delta(t - t')$, we find

$$\langle A(t) \rangle = \frac{1}{Z} \sum_n \langle n(t)|A|n(t)\rangle \, e^{-\beta E_n} \tag{A.5}$$

Now switch to the interaction picture to absorb the trivial time evolution due to H_0 into the eigenstates and operators and leave only the evolution due the perturbation we are interested in. We denote the interaction picture states and operators with hats:

$$|\hat{n}(t)\rangle = e^{iH_0 t} \, |n(t)\rangle \quad \text{and} \quad \hat{A}(t) = e^{iH_0 t} A e^{-iH_0 t} \tag{A.6}$$

The time evolution due to the perturbation can be written in terms of these states as

$$|\hat{n}(t)\rangle = \hat{U}(t)\,|\hat{n}(0)\rangle \;\; ; \quad \hat{U}(t) = T_t e^{-\int_0^t \hat{H}'(t')dt'} \tag{A.7}$$

where T_t is the time ordering operator. Now using the fact that the interaction picture and Schrodinger picture states must be the same up to $t = 0$ when the perturbation is applied (this can also be easily seen by setting $t = 0$ in equation 6), we obtain

$$|n(t)\rangle = e^{-iH_0 t}\,|\hat{n}(t)\rangle = e^{-iH_0 t}\hat{U}(t)\,|\hat{n}(0)\rangle = e^{-iH_0 t}\hat{U}(t)\,|n\rangle \tag{A.8}$$

Now substituting this into equation 5

$$\begin{aligned}\langle A(t)\rangle &= \frac{1}{Z}\sum_n \langle n|\hat{U}^\dagger(t)e^{iH_0 t}Ae^{-iH_0 t}\hat{U}(t)|n\rangle\, e^{-\beta E_n} \\ &= \frac{1}{Z}\sum_n \langle n|\hat{U}^\dagger(t)\hat{A}(t)\hat{U}(t)|n\rangle\, e^{-\beta E_n}\end{aligned} \tag{A.9}$$

Expanding $\hat{U}(t)$ to first order in $\hat{H}'(t)$

$$\begin{aligned}\langle A(t)\rangle &= \frac{1}{Z}\sum_n \langle n|\left(1 + i\int_0^t \hat{H}'(t')dt'\right)\hat{A}(t)\left(1 - i\int_0^t \hat{H}'(t')dt'\right)|n\rangle\, e^{-\beta E_n} \\ &= \frac{1}{Z}\sum_n \langle n|\hat{A}(t)|n\rangle - i\int_0^t dt'\,\langle n|(\hat{A}(t)\hat{H}'(t') - \hat{H}'(t')\hat{A}(t))|n\rangle\, e^{-\beta E_n} \\ &= \frac{1}{Z}\sum_n \left(\langle n|\hat{A}(t)|n\rangle - i\int_0^t dt'\,\langle n|[\hat{A}(t),\hat{H}'(t')]|n\rangle\right) e^{-\beta E_n} \\ &= \langle\hat{A}(t)\rangle_0 - i\int_0^t dt'\left\langle[\hat{A}(t),\hat{H}'(t')]\right\rangle_0\end{aligned} \tag{A.10}$$

$$\begin{aligned}\therefore \delta\langle A(t)\rangle &= \langle A(t)\rangle - \langle\hat{A}(t)\rangle_0 \\ &= -i\int_0^t dt'\left\langle[\hat{A}(t),\hat{H}'(t')]\right\rangle_0\end{aligned} \tag{A.11}$$

where the zero subscript on the expectation value denotes the average with respect to the unperturbed Hamiltonian. Explicit spatial dependence of the operators can be included introducing an integral over space and if A is a vector operator we can treat each compo-

nent, labelled by α, separately. We will also employ the convention to combine the two variables $(\mathbf{r}, t)$ into a single index $(\mathbf{1})$.

$$\begin{aligned}\delta\langle A_\alpha(\mathbf{r},t)\rangle &= -i\int_V d\mathbf{r}'\int_0^t dt'\left\langle[\hat{A}_\alpha(\mathbf{r},t),\hat{H}'(\mathbf{r}',t')]\right\rangle_0\\ \delta\langle A_\alpha(\mathbf{1})\rangle &= -i\int d\mathbf{1}'\left\langle[\hat{A}_\alpha(\mathbf{1}),\hat{H}'(\mathbf{1}')]\right\rangle_0\end{aligned} \tag{A.12}$$

This the Kubo formula for linear response.

Now consider a perturbation of the form

$$H'(\mathbf{1}) = \phi_\beta(\mathbf{1})B_\beta(\mathbf{r}) \tag{A.13}$$

where B is an operator and ϕ is a classical field. Using the Kubo formula we can write

$$\begin{aligned}\delta\langle A_\alpha(\mathbf{1})\rangle &= -i\int d\mathbf{1}'\phi_\beta(\mathbf{1}')\left\langle[\hat{A}_\alpha(\mathbf{1}),\hat{B}_\beta(\mathbf{1}')]\right\rangle_0 &\text{(A.14)}\\ &= \int d\mathbf{1}'\phi_\beta(\mathbf{1}')G^R_{A_\alpha B_\beta}(\mathbf{1},\mathbf{1}')\\ G^R_{A_\alpha B_\beta}(\mathbf{1},\mathbf{1}') &= -i\left\langle[\hat{A}_\alpha(\mathbf{1}),\hat{B}_\beta(\mathbf{1}')]\right\rangle_0\Theta(t-t') &\text{(A.15)}\end{aligned}$$

$G^R_{A_\alpha B_\beta}$ is the retarded Green's function (GF) relating the operators A and B and is in general a matrix when the operators are vectors. If there is temporal translational invariance, then G can only depend of differences in time, $t - t'$. Then if the time integration is extended back from $0 \to -\infty$ (which is reasonable if one is not interested in transient behaviour) $\delta\langle A\rangle$ has the form of a convolution and the Fourier transform (FT) in time can be taken immediately to give

$$\delta\langle A_\alpha(\mathbf{r},\omega)\rangle = \int_V d\mathbf{r}'\phi_\beta(\mathbf{r}',\omega)G^R_{A_\alpha B_\beta}(\mathbf{r},\mathbf{r}',\omega) \tag{A.16}$$

Similarly for spatial translational invariance:

$$\delta \langle A_\alpha(\mathbf{q},\omega)\rangle = \phi_\beta(\mathbf{q},\omega) G^R_{A_\alpha B_\beta}(\mathbf{q},\omega) \tag{A.17}$$

Note that one may have to be more careful when taking these FTs if the GF contains terms like ∂_t or $\boldsymbol{\nabla}$ as one would pick up extra factors of frequency or momentum from the exponent in the FT. Also, there may be remaining internal degrees of freedom contained within the GF that still need to to summed/integrated over.

APPENDIX B

DERIVATION OF THE OPERATOR REPRESENTATION OF CURRENT DENSITY

Take a simple classical Hamiltonian for a particle in a EM-field

$$H_0(\mathbf{p}, \mathbf{A}) = \frac{1}{2m}(\mathbf{p} - q\mathbf{A})^2 \tag{B.1}$$

Where $\mathbf{A} = \mathbf{A}(\mathbf{r}, \mathbf{t})$ is the vector potential, which is in general a function of space and time, and is related to the $\mathbf{E}$ and $\mathbf{B}$ fields (in the Weyl/Hamiltonian/temporal gauge where the scalar potential is zero) by

$$\mathbf{E} = -\partial_t \mathbf{A} \quad \text{and} \quad \mathbf{B} = \boldsymbol{\nabla} \times \mathbf{A} \tag{B.2}$$

The current density operator can be related to the change in this Hamiltonian due to a small perturbation of $\mathbf{A}$.

$$H(\mathbf{p}, \mathbf{A} + \delta\mathbf{A}) = \frac{1}{2m}(\mathbf{p} - q(\mathbf{A} + \delta\mathbf{A}))^2 \tag{B.3}$$

$$= \frac{1}{2m}((\mathbf{p} - q\mathbf{A})^2 - 2q(\mathbf{p} - q\mathbf{A}) \cdot \delta\mathbf{A} + \mathcal{O}(\delta\mathbf{A}^2))$$

$$\Rightarrow \delta H = -\frac{q}{m}(\mathbf{p} - q\mathbf{A}) \cdot \delta\mathbf{A} \tag{B.4}$$

$$= -q\mathbf{v} \cdot \delta\mathbf{A}$$

$$= -\mathbf{J} \cdot \delta\mathbf{A}$$

$$= -\int d\mathbf{r}\ \mathbf{j} \cdot \delta\mathbf{A} \tag{B.5}$$

Now we will follow an analogous process of applying a small perturbation on $\mathbf{A}$ on a quantum mechanical Hamiltonian and manipulate it into the form given in equation 4 to find the form of the quantum current density operator.

$$H(\mathbf{A}) = \frac{1}{2m}\sum_\sigma \int d^3r\ \psi_\sigma^\dagger(\mathbf{r})(-i\boldsymbol{\nabla} - q\mathbf{A})^2\psi_\sigma(\mathbf{r}) \tag{B.6}$$

$$= H(0) + \frac{1}{2m}\sum_\sigma \int d^3r\ \psi_\sigma^\dagger(\mathbf{r})\Big[iq\big(\boldsymbol{\nabla} \cdot \mathbf{A} + \mathbf{A} \cdot \boldsymbol{\nabla}\big) + q^2\mathbf{A}^2\Big]\psi_\sigma(\mathbf{r}) \tag{B.7}$$

Integrate the first term in the integral by parts:

$$\int d^3r\ \psi_\sigma^\dagger(\mathbf{r})\boldsymbol{\nabla} \cdot \mathbf{A}\psi_\sigma(\mathbf{r}) = \Big[\psi_\sigma^\dagger(\mathbf{r})\mathbf{A}\psi_\sigma(\mathbf{r})\Big]_{\partial V} - \int d^3r\ \mathbf{A} \cdot \big(\boldsymbol{\nabla}\psi_\sigma^\dagger(\mathbf{r})\big)\psi_\sigma(\mathbf{r}) \tag{B.8}$$

The boundary term must tend to zero, hence we have

$$H(\mathbf{A}) - H(0) = \frac{1}{2m}\sum_\sigma \int d^3r\ \left[iq\mathbf{A} \cdot \Big(\psi_\sigma^\dagger(\mathbf{r})\boldsymbol{\nabla}\psi_\sigma(\mathbf{r}) - \boldsymbol{\nabla}\psi_\sigma^\dagger(\mathbf{r})\psi_\sigma(\mathbf{r})\Big) + q^2\mathbf{A}^2\psi_\sigma^\dagger(\mathbf{r})\psi_\sigma(\mathbf{r})\right] \tag{B.9}$$

Now the change in H due to a small perturbation in $\mathbf{A}$ is

$$\begin{aligned}\delta H &= H(\mathbf{A}+\delta\mathbf{A}) - H(\mathbf{A}) \\ &= \frac{1}{2m}\sum_{\sigma}\int d^3r\,\left[iq\,\delta\mathbf{A}\cdot\Big(\psi^\dagger_\sigma(\mathbf{r})\boldsymbol{\nabla}\psi_\sigma(\mathbf{r}) - \boldsymbol{\nabla}\psi^\dagger_\sigma(\mathbf{r})\psi_\sigma(\mathbf{r})\Big) + 2q^2\delta\mathbf{A}\cdot\mathbf{A}\psi^\dagger_\sigma(\mathbf{r})\psi_\sigma(\mathbf{r})\right]\end{aligned} \tag{B.10}$$

Comparing this to equation 4 we can read off the current density operator per spin:

$$\mathbf{j}_\sigma(\mathbf{r}) = -\frac{iq}{2m}\Big(\psi^\dagger_\sigma(\mathbf{r})\boldsymbol{\nabla}\psi_\sigma(\mathbf{r}) - \boldsymbol{\nabla}\psi^\dagger_\sigma(\mathbf{r})\psi_\sigma(\mathbf{r})\Big) - \frac{q^2}{m}\mathbf{A}(\mathbf{r})\psi^\dagger_\sigma(\mathbf{r})\psi_\sigma(\mathbf{r}) \tag{B.11}$$

This can be separated out into two parts: the paramagnetic part, $\mathbf{j}^{\boldsymbol{\nabla}}_\sigma$, and the diamagnetic part, $\mathbf{j}^{\mathbf{A}}_\sigma$, given by

$$\mathbf{j}^{\boldsymbol{\nabla}}_\sigma(\mathbf{r}) = -\frac{iq}{2m}\Big(\psi^\dagger_\sigma(\mathbf{r})\boldsymbol{\nabla}\psi_\sigma(\mathbf{r}) - \boldsymbol{\nabla}\psi^\dagger_\sigma(\mathbf{r})\psi_\sigma(\mathbf{r})\Big) \tag{B.12}$$

$$\mathbf{j}^{\mathbf{A}}_\sigma(\mathbf{r}) = -\frac{q^2}{m}\mathbf{A}(\mathbf{r})\psi^\dagger_\sigma(\mathbf{r})\psi_\sigma(\mathbf{r}) \tag{B.13}$$

APPENDIX C

CALCULATION OF THE DRUDE CONDUCTIVITY WHERE THE DIVERGENCE ISSUE IS EXPLICITLY ADDRESSED

We begin with

$$\begin{aligned}
\mathbf{J}_\alpha(\mathbf{q},\omega) &= -K_{\alpha\beta}(\mathbf{q},\omega)\mathbf{A}_\beta(\mathbf{q},\omega) \\
K_{\alpha\beta}(\mathbf{q},\omega) &= G^R_{\mathbf{j}\alpha\beta}(\mathbf{q},\omega) + \frac{ne^2}{m}\delta_{\alpha\beta} \\
G^E_{\mathbf{j}\alpha\beta}(\mathbf{q},i\omega) &= \frac{2e^2T}{4m^2V}\sum_{\mathbf{k}}\sum_{\epsilon}(2\mathbf{k}+\mathbf{q})_\alpha(2\mathbf{k}+\mathbf{q})_\beta G(\mathbf{k},i\epsilon)G(\mathbf{k}+\mathbf{q},i\epsilon+i\omega)
\end{aligned} \tag{C.1}$$

Note that the order of summations over momenta and frequency have been explicitly ordered and due to potential problems with divergences one cannot switch the order trivially. Using form of the single particle impurity Green's functions, we immediately

write them in terms of their spectral functions,

$$G_{\mathbf{j}\alpha\beta}(\mathbf{q}, i\omega) = \frac{2e^2T}{4m^2V}\sum_{\mathbf{k}}\sum_{\epsilon}(2\mathbf{k}+\mathbf{q})_\alpha(2\mathbf{k}+\mathbf{q})_\beta\int_{-\infty}^{\infty}\mathrm{d}x\ \mathrm{d}y\ \frac{\mathcal{A}(\mathbf{k},x)\mathcal{A}(\mathbf{k}+\mathbf{q},y)}{(i\epsilon-x)(i\epsilon+i\omega-y)} \tag{C.2}$$

$$\mathcal{A}(\mathbf{k},x) = \frac{1}{2\pi\tau_0}\frac{1}{(\xi_k - x + \frac{i}{2\tau_0})(\xi_k - x - \frac{i}{2\tau_0})} \tag{C.3}$$

Now we will assume that $|\mathbf{q}| \ll |\mathbf{k}|$ and $\mathbf{k} \sim \mathbf{k}_F$. The first assumption physically means that we want to only look at the long wavelength behaviour of the response, to which a macroscopic conductivity value would correspond. The second is to say that the perturbation caused by the field is sufficiently small such that the only electron that take part in the conduction are those close to the Fermi surface, and further that they are not excited far above the Fermi surface.

$$G_{\mathbf{j}\alpha\beta}(\mathbf{q}, i\omega) = \frac{2e^2N(0)T}{m^2}\int\frac{\mathrm{d}\Omega}{4\pi}\mathbf{k}_{F\alpha}\mathbf{k}_{F\beta}\int_{-\infty}^{\infty}\mathrm{d}\xi_k\sum_{\epsilon}\int_{-\infty}^{\infty}\mathrm{d}x\ \mathrm{d}y\ \frac{\mathcal{A}(\mathbf{k},x)\mathcal{A}(\mathbf{k}+\mathbf{q},y)}{(i\epsilon-x)(i\epsilon+i\omega-y)} \tag{C.4}$$

where $N(0)$ is the density of states at the Fermi surface, the integral over $\mathrm{d}\Omega$ is a solid angle integral over the Fermi surface and the integral over $\mathrm{d}\xi_k$ is over the kinetic energy of the electrons. The order of summation over Matsubara frequencies and integrals over $\mathrm{d}x$ and $\mathrm{d}y$ can be reordered without any problems so we can perform the sum first. To do this we can perform the usual 'trick' by writing the sum as a contour integral where the residues of the Fermi function 'count' over the Matsubara frequencies up the imaginary axis and then taking the sum of the residues on the rest of the complex plane instead.

$$T\sum_{\epsilon}\frac{\mathcal{A}(\mathbf{k},x)\mathcal{A}(\mathbf{k}+\mathbf{q},y)}{(i\epsilon-x)(i\epsilon+i\omega-y)} = -\frac{1}{2\pi i}\oint\mathrm{d}z\ f(z)\frac{\mathcal{A}(\mathbf{k},x)\mathcal{A}(\mathbf{k}+\mathbf{q},y)}{(z-x)(z+i\omega-y)} \tag{C.5}$$

$$\text{let}\quad F(z) := f(z)\frac{\mathcal{A}(\mathbf{k},x)\mathcal{A}(\mathbf{k}+\mathbf{q},y)}{(z-x)(z+i\omega-y)} \tag{C.6}$$

$$\Rightarrow\ -\frac{1}{2\pi i}\oint \mathrm{d}z\ F(z) = \mathrm{Res}(F(z),x) + \mathrm{Res}(F(z),y-i\omega)$$
$$= f(x)\frac{\mathcal{A}(\mathbf{k},x)\mathcal{A}(\mathbf{k}+\mathbf{q},y)}{x-y+i\omega} + f(y)\frac{\mathcal{A}(\mathbf{k},x)\mathcal{A}(\mathbf{k}+\mathbf{q},y)}{y-i\omega-x}$$
$$= \big(f(x)-f(y)\big)\frac{\mathcal{A}(\mathbf{k},x)\mathcal{A}(\mathbf{k}+\mathbf{q},y)}{x-y+i\omega} \tag{C.7}$$

As we have the temperature GFs in terms of their spectral functions it is safe to analytically continue from Matsubara frequencies to real frequencies to obtain retarded GFs, so we formally replace $i\omega$ with ω that is analytic in the upper half plane. Now complete the integral over one of $\mathrm{d}x$ and $\mathrm{d}y$ in each term to eliminate one of the dummy variables

$$\int_{-\infty}^{\infty}\mathrm{d}y\ f(x)\frac{\mathcal{A}(\mathbf{k},x)\mathcal{A}(\mathbf{k}+\mathbf{q},y)}{x-y+\omega} = f(x)\mathcal{A}(\mathbf{k},x)\int_{-\infty}^{\infty}\mathrm{d}y\ \frac{\mathcal{A}(\mathbf{k}+\mathbf{q},y)}{(\omega+x)-y} \tag{C.8}$$
$$= f(x)\mathcal{A}(\mathbf{k},x)G^R(\mathbf{k}+\mathbf{q},\omega+x)$$
$$= f(x)\mathcal{A}(\mathbf{k},x)\frac{1}{\omega+x-\xi_{k+q}+\frac{i}{2\tau_0}}$$
$$\int_{-\infty}^{\infty}\mathrm{d}x\ f(y)\frac{\mathcal{A}(\mathbf{k},x)\mathcal{A}(\mathbf{k}+\mathbf{q},y)}{x-y+\omega} = -f(y)\mathcal{A}(\mathbf{k}+\mathbf{q},y)\int_{-\infty}^{\infty}\mathrm{d}x\ \frac{\mathcal{A}(\mathbf{k},x)}{(y-\omega)-x} \tag{C.9}$$
$$= -f(y)\mathcal{A}(\mathbf{k}+\mathbf{q},y)G^R(\mathbf{k},y-\omega)$$
$$= f(y)\mathcal{A}(\mathbf{k}+\mathbf{q},y)\frac{1}{\omega-y+\xi_k+\frac{i}{2\tau_0}}$$

Using this, relabelling y to x in the second term, we have

$$G^R_{\mathbf{j}\alpha\beta}(\mathbf{q},\omega) = \frac{2e^2N(0)}{m^2}\int\frac{\mathrm{d}\Omega}{4\pi}\mathbf{k}_{F\alpha}\mathbf{k}_{F\beta}\int_{-\infty}^{\infty}\mathrm{d}\xi_k$$
$$\times\int_{-\infty}^{\infty}\mathrm{d}x\, f(x)\left(\frac{\mathcal{A}(\mathbf{k},x)}{\omega+x-\xi_{k+q}+\frac{i}{2\tau_0}} - \frac{\mathcal{A}(\mathbf{k}+\mathbf{q},x)}{\omega-x+\xi_k+\frac{i}{2\tau_0}}\right) \tag{C.10}$$

As $|\mathbf{q}| \ll |\mathbf{k}|$ use $\xi_{k+q} \approx \xi_k + \mathbf{k}_F\cdot\mathbf{q} := \xi + \mu_\theta$.

$$G^R_{\mathbf{j}\alpha\beta}(\mathbf{q},\omega) = \frac{2e^2N(0)}{m^2}\int\frac{\mathrm{d}\Omega}{4\pi}\mathbf{k}_{F\alpha}\mathbf{k}_{F\beta}\int_{-\infty}^{\infty}\mathrm{d}\xi$$
$$\times\int_{-\infty}^{\infty}\mathrm{d}x\ f(x)\left(\frac{\mathcal{A}(\mathbf{k},x)}{\omega+x-\xi-\mu_\theta+\frac{i}{2\tau_0}} - \frac{\mathcal{A}(\mathbf{k}+\mathbf{q},x)}{\omega-x+\xi+\frac{i}{2\tau_0}}\right) \tag{C.11}$$

We now want to be able to change to order of integration over $\mathrm{d}x$ and and $\mathrm{d}\xi$ but it is not immediately clear that there is sufficient convergence to allow this, so we must demonstrate explicitly if it is possible. The integrals have the form

$$\mathcal{I} = \int_{-\infty}^{\infty} \mathrm{d}\xi \int_{-\infty}^{\infty} \mathrm{d}x \; f(x)F(x-\xi) \tag{C.12}$$

where $F(x-\xi)$ is an arbitrary function of $x-\xi$. Integrate by parts first w.r.t ξ, then x (all boundary terms are assumed to vanish):

$$\begin{aligned}
\mathcal{I} &= -\int_{-\infty}^{\infty} \mathrm{d}\xi \; \xi \frac{\mathrm{d}}{\mathrm{d}\xi} \int_{-\infty}^{\infty} \mathrm{d}x \; f(x)F(x-\xi) \\
&= -\int_{-\infty}^{\infty} \mathrm{d}\xi \; \xi \int_{-\infty}^{\infty} \mathrm{d}x \; f(x) \frac{\mathrm{d}}{\mathrm{d}\xi} F(x-\xi) \\
&= \int_{-\infty}^{\infty} \mathrm{d}\xi \; \xi \int_{-\infty}^{\infty} \mathrm{d}x \; f(x) \frac{\mathrm{d}}{\mathrm{d}x} F(x-\xi) \\
&= -\int_{-\infty}^{\infty} \mathrm{d}\xi \; \xi \int_{-\infty}^{\infty} \mathrm{d}x \; \frac{\mathrm{d}f(x)}{\mathrm{d}x} F(x-\xi)
\end{aligned} \tag{C.13}$$

The $\frac{\mathrm{d}f(x)}{\mathrm{d}x}$ term ensures sufficient convergence to switch the order of the integrals. Hence we have

$$\begin{aligned}
G^R_{\mathbf{j}\alpha\beta}(\mathbf{q},\omega) = -\frac{2e^2N(0)}{m^2} \int \frac{\mathrm{d}\Omega}{4\pi} \mathbf{k}_{F\alpha}\mathbf{k}_{F\beta} \\
\times \int_{-\infty}^{\infty} \mathrm{d}x \; \frac{\mathrm{d}f(x)}{\mathrm{d}x} \int_{-\infty}^{\infty} \mathrm{d}\xi \left(\frac{\mathcal{A}(\mathbf{k},x)}{\omega + x - \xi - \mu_\theta + \frac{i}{2\tau_0}} - \frac{\mathcal{A}(\mathbf{k}+\mathbf{q},x)}{\omega - x + \xi + \frac{i}{2\tau_0}} \right)
\end{aligned} \tag{C.14}$$

Using the form of $\mathcal{A}$ given in equation 5 we can now perform the integral over $\mathrm{d}\xi$ as a contour integral. We will consider one term at a time

$$\begin{aligned}
\mathcal{I}_1 &= \int_{-\infty}^{\infty} \frac{\mathrm{d}\xi}{2\pi\tau_0} \frac{\xi}{\left(x - \xi - \mu_\theta + \omega + \frac{i}{2\tau_0}\right)\left(\xi - x + \frac{i}{2\tau_0}\right)\left(\xi - x - \frac{i}{2\tau_0}\right)} \\
&= -\int_{-\infty}^{\infty} \frac{\mathrm{d}\xi}{2\pi\tau_0} \frac{\xi}{\left(\xi - (x + \omega - \mu_\theta + \frac{i}{2\tau_0})\right)\left(\xi - (x - \frac{i}{2\tau_0})\right)\left(\xi - (x + \frac{i}{2\tau_0})\right)}
\end{aligned} \tag{C.15}$$

As x, μ_θ and ω are all pure real the half plane that the poles are in is entirely dictated by the sign of the $\frac{i}{2\tau_0}$ term. Hence we can chose a contour that closes in the lower half plane to only pick up one residue.

$$\mathcal{I}_1 = -\oint_{\Gamma_1} \frac{dz}{2\pi\tau_0} \frac{z}{\left(z-(x+\omega-\mu_\theta+\frac{i}{2\tau_0})\right)\left(z-(x-\frac{i}{2\tau_0})\right)\left(z-(x+\frac{i}{2\tau_0})\right)} \tag{C.16}$$

$$= \frac{2\pi i}{2\pi\tau_0}\left[\frac{z}{\left(z-(x+\omega-\mu_\theta+\frac{i}{2\tau_0})\right)\left(z-(x+\frac{i}{2\tau_0})\right)}\right]_{z=x-\frac{i}{2\tau_0}}$$

$$= \frac{i}{\tau_0}\frac{x-\frac{i}{2\tau_0}}{\left(-\omega+\mu_\theta-\frac{i}{\tau_0}\right)\left(-\frac{i}{\tau_0}\right)} = \frac{x-\frac{i}{2\tau_0}}{\omega-\mu_\theta+\frac{i}{\tau_0}} \tag{C.17}$$

Now examining the $\mathcal{I}_2$ term we notice that we can close the contour in the upper half plane, leading to

$$\mathcal{I}_2 = -\int_{-\infty}^{\infty} \frac{\mathrm{d}\xi}{2\pi\tau_0} \frac{\xi}{\left(\xi-(x-\omega-\frac{i}{2\tau_0})\right)\left(\xi-(x-\mu_\theta-\frac{i}{2\tau_0})\right)\left(\xi-(x-\mu_\theta+\frac{i}{2\tau_0})\right)}$$

$$= -\oint_{\Gamma_2} \frac{dz}{2\pi\tau_0} \frac{z}{\left(z-(x-\omega-\frac{i}{2\tau_0})\right)\left(z-(x-\mu_\theta-\frac{i}{2\tau_0})\right)\left(z-(x-\mu_\theta+\frac{i}{2\tau_0})\right)} \tag{C.18}$$

$$= -\frac{2\pi i}{2\pi\tau_0}\left[\frac{z}{\left(z-(x-\omega-\frac{i}{2\tau_0})\right)\left(z-(x-\mu_\theta-\frac{i}{2\tau_0})\right)}\right]_{z=x-\mu_\theta+\frac{i}{2\tau_0}}$$

$$= -\frac{i}{\tau_0}\frac{x-\mu_\theta+\frac{i}{2\tau_0}}{\left(\omega-\mu_\theta+\frac{i}{\tau_0}\right)\left(\frac{i}{\tau_0}\right)} = -\frac{x-\mu_\theta+\frac{i}{2\tau_0}}{\omega-\mu_\theta+\frac{i}{\tau_0}} \tag{C.19}$$

So putting the two terms together, we have

$$\mathcal{I}_1+\mathcal{I}_2 = \frac{x-\frac{i}{2\tau_0}}{\omega-\mu_\theta+\frac{i}{\tau_0}} - \frac{x-\mu_\theta+\frac{i}{2\tau_0}}{\omega-\mu_\theta+\frac{i}{\tau_0}} = \frac{\mu_\theta-\frac{i}{\tau_0}}{\omega-\mu_\theta+\frac{i}{\tau_0}}\,. \tag{C.20}$$

Now complete the next integral over $\mathrm{d}x$,

$$\int_{-\infty}^{\infty}\mathrm{d}x\ \frac{\mathrm{d}f(x)}{\mathrm{d}x}\frac{\mu_\theta-\frac{i}{\tau_0}}{\omega-\mu_\theta+\frac{i}{\tau_0}} = \frac{\mu_\theta-\frac{i}{\tau_0}}{\omega-\mu_\theta+\frac{i}{\tau_0}}\int_{-\infty}^{\infty} df(x) \tag{C.21}$$

$$= \frac{\mu_\theta-\frac{i}{\tau_0}}{\omega-\mu_\theta+\frac{i}{\tau_0}}\left[\frac{1}{1+e^{\beta x}}\right]_{-\infty}^{\infty}$$

$$= \frac{-\mu_\theta+\frac{i}{\tau_0}}{\omega-\mu_\theta+\frac{i}{\tau_0}} = 1-\frac{\omega}{\omega-\mu_\theta+\frac{i}{\tau_0}} \tag{C.22}$$

Thus far we have

$$G^R_{\mathbf{j}\alpha\beta} = \frac{2e^2N(0)}{m^2}\int\frac{\mathrm{d}\Omega}{4\pi}\mathbf{k}_{F\alpha}\mathbf{k}_{F\beta}\left(\frac{\omega}{\omega-\mu_\theta+\frac{i}{\tau_0}}-1\right) \tag{C.23}$$

Consider the term

$$-\frac{2e^2N(0)}{m^2}\int\frac{\mathrm{d}\Omega}{4\pi}\mathbf{k}_{F\alpha}\mathbf{k}_{F\beta} = -\frac{2e^2N(0)}{m^2}\frac{k_F^2}{3}\delta_{\alpha\beta} = -\frac{ne^2}{m}\delta_{\alpha\beta} \tag{C.24}$$

using $n = \frac{4}{3}N(0)\xi_F$. This term exactly cancels the contribution from the diamagnetic term, therefore the linear response function is given by

$$\begin{aligned} K_{\alpha\beta}(\mathbf{q},\omega) &= \frac{2e^2N(0)}{m^2}\int\frac{\mathrm{d}\Omega}{4\pi}\mathbf{k}_{F\alpha}\mathbf{k}_{F\beta}\frac{\omega}{\omega-\mu_\theta+\frac{i}{\tau_0}} \\ &= \frac{3ne^2}{mk_F^2}\int\frac{\mathrm{d}\Omega}{4\pi}\mathbf{k}_{F\alpha}\mathbf{k}_{F\beta}\,\frac{\omega}{\omega-\mu_\theta+\frac{i}{\tau_0}} \end{aligned} \tag{C.25}$$

Relating this back to the equation for current

$$\mathbf{J}(\mathbf{q},\omega) = \frac{3ne^2}{mk_F^2}\int\frac{\mathrm{d}\Omega}{4\pi}\frac{\omega\,\mathbf{k}_F\,\mathbf{k}_F\cdot\mathbf{A}(\mathbf{q},\omega)}{\omega-\mathbf{v}_F\cdot\mathbf{q}+\frac{i}{\tau_0}} \tag{C.26}$$

$$\mathbf{E}(\mathbf{q},\omega) = -i\omega\mathbf{A}(\mathbf{q},\omega)$$

$$\mathbf{J}(\mathbf{q},\omega) = \frac{3ne^2i}{mk_F^2}\int\frac{\mathrm{d}\Omega}{4\pi}\frac{\mathbf{k}_F\,\mathbf{k}_F\cdot\mathbf{E}(\mathbf{q},\omega)}{\omega-\mathbf{v}_F\cdot\mathbf{q}+\frac{i}{\tau_0}} \tag{C.27}$$

The D.C. conductivity is obtained when the electric field is static and uniform, there we only require the Fourier components with $\mathbf{q}=0$ and $\omega=0$. As the electric field is static we can easily evaluate the angular integral as before yielding

$$\begin{aligned} \mathbf{J}(0,0) &= \frac{3ne^2i}{mk_F^2}\frac{k_F^2}{3}\frac{\mathbf{E}(0,0)}{\frac{i}{\tau_0}} \\ &= \frac{ne^2\tau_0}{m}\mathbf{E}(0,0) \end{aligned} \tag{C.28}$$

$$\therefore\ \sigma_{\mathrm{DC}} = \frac{ne^2\tau_0}{m} \quad \text{as required.} \tag{C.29}$$

APPENDIX D

STANDARD FORMULA FOR THE INTEGRAL OF IMPURITY GREEN'S FUNCTIONS IN THE DIFFUSIVE LIMIT

In the diffusive limit, $\omega\tau_0 \ll 1$ (where τ_0 is the elastic scattering lifetime), we can generalise the result of summation over $\mathbf{k}$ of n Green's functions with positive Matsubara frequencies and m Green's functions with negative Matsubara frequencies.

$$\mathcal{I}_{nm} = \sum_{\mathbf{k}} G^{+}(\mathbf{k}, i\omega_1)^n G^{-}(\mathbf{k}, i\omega_2)^m \quad ; \quad \omega_1 > 0 \ , \ \omega_2 < 0 \tag{D.1}$$

$$= \sum_{\mathbf{k}} \frac{1}{\left(i\omega_1 - \xi + \frac{i}{2\tau}\right)^n} \frac{1}{\left(i\omega_2 - \xi - \frac{i}{2\tau}\right)^m}$$

$$= N(0) \int \frac{d\Omega}{4\pi} \int_{-\infty}^{\infty} d\xi \, \frac{1}{\left(i\omega_1 - \xi + \frac{i}{2\tau}\right)^n} \frac{1}{\left(i\omega_2 - \xi - \frac{i}{2\tau}\right)^m} \tag{D.2}$$

As there is no angular dependence the angular integral simply evaluates to 4π cancelling the denominator. Closing the contour in upper half plane for ξ integral we obtain

$$\begin{aligned}
\mathcal{I}_{nm} &= 2\pi i N(0)(-1)^{n+m}\frac{1}{(n-1)!}\lim_{\xi\to i\omega+\frac{i}{2\tau}}\frac{\mathrm{d}^{n-1}}{\mathrm{d}\xi^{n-1}}\frac{1}{\left(\xi-i\omega_2+\frac{i}{2\tau}\right)^m} \qquad \text{(D.3)}\\
&= 2\pi i N(0)(-1)^{n+m}\frac{1}{(n-1)!}(-m)(-(m+1))...(-(m+n-2))\frac{1}{\left(i\omega_1-i\omega_2+\frac{i}{\tau}\right)^{m+n-1}}\\
&= 2\pi i N(0)(-1)^{n+m}(-1)^{n-1}\frac{(m+n-2)!}{(n-1)!(m-1)!}\frac{1}{(\frac{i}{\tau})^{m+n-1}}\ ; \quad \text{using} \quad \omega \ll \frac{1}{\tau}\\
&= 2\pi i N(0)\,\frac{(m+n-2)!}{(n-1)!((m+n-2)-(n-1))!}\,(-1)^{2n}(-1)^{m-1}(-i\tau)^{m+n-1}\\
&= 2\pi N(0)\begin{pmatrix} m+n-2 \\ n-1 \end{pmatrix} i(-i\tau)^n(i\tau)^{m-1}\\
&= 2\pi N(0)\tau\begin{pmatrix} m+n-2 \\ n-1 \end{pmatrix}(-i\tau)^{n-1}(i\tau)^{m-1}\,. \qquad \text{(D.4)}
\end{aligned}$$

APPENDIX E

STANDARD METHOD TO CONVERT A SUM OVER MATSUBARA FREQUENCIES TO A CONTOUR INTEGRAL

We make heavy use of linear response functions constructed using temperature Green's functions. In these calculations we will often have sums over the Matsubara frequencies. Here we will establish the method we use to evaluate these sums, when they cannot be simply completed directly. We follow the method outlined in appendix B of Rickayzen [56].

A sum over Matsubara frequencies has the general form

$$S = T \sum_{\varepsilon} F(i\varepsilon)\,, \tag{E.1}$$

we have Fermionic Matsubara frequencies,

$$\varepsilon = 2\pi T(n + \frac{1}{2})\,. \tag{E.2}$$

Now consider the function defined in the complex plane, $F(z)$, multiplied by the Fermi-function,

$$g(z) = f(z)F(z) = \frac{F(z)}{e^{\beta z} + 1}\,. \tag{E.3}$$

This new function will have the same analytic properties as the original function but will have an addition set of simple poles when

$$e^{\beta z} + 1 = 0\,. \tag{E.4}$$

These points occur when $z = i\varepsilon$. Provided $F(z)$ does not have any poles that coincide exactly with $f(z)$ then $g(z)$ has simple poles at the Matsubara frequencies on the imaginary axis with residues of $-TF(i\varepsilon)$. There fore if we construct a contour, Γ, that encloses all the poles due to $f(z)$, but none that are due to the original function $F(z)$, we have

$$S = \frac{i}{2\pi} \oint \mathrm{d}z\, f(z)F(z)\,. \tag{E.5}$$

This contour is shown in figure E.1. The contour can then be deformed instead to enclose

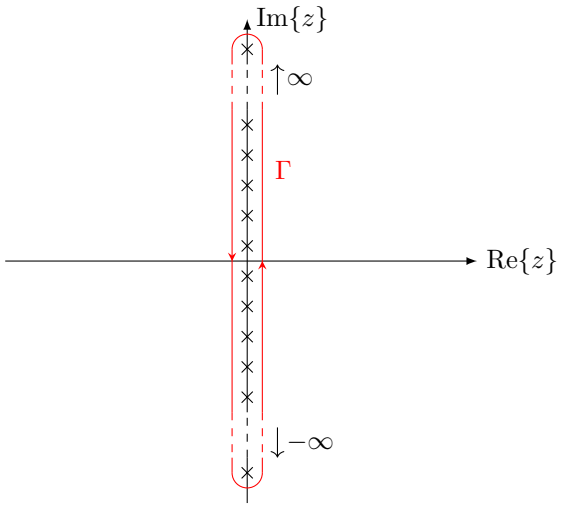

Figure E.1: The contour enclosing the poles of the Fermi-function that allows the sum over Matsubara frequencies to converted to a contour integral in the complex plane.

the left and right hand planes, provided that

$$\lim_{|z|\to 0} |zg(z)| = 0\,, \tag{E.6}$$

so the integrals enclosing the plane tend to zero as their radius tends to infinity.

If $F(z)$ has poles, this contour will now enclose them and the sum can be evaluated by calculating the residues. If $F(z)$ has any branch cuts then the contour will have to be deformed around the cuts and the evaluation of the sum will involve integrals along the cuts. The second case arises in the linear response function of superconductors in chapter 4 and beyond.

BIBLIOGRAPHY

[1] N. Ashcroft and N. Mermin. *Solid state physics*. Holt-Saunders, 1976.

[2] S. Simon. *The Oxford Solid state basics*. Oxford University press, 2013.

[3] C. Kittel. *Introduction to solid state physics*. John Wiley & Sons, 1986.

[4] H. Kamerlingh-Onnes. On the change of the electrical resistance of pure metals at very low temperature, etc v the disappearance of the resistance of mercury. *Proceedings of the koninklijke akademie van wetenschappen te amsterdam*, 14, 1911.

[5] A. Rose-Innes and E. Rhoderick. *Introduction of Superconductivity*. Pergamon Press, 1969.

[6] W. Meissner and R. Ochsenfeld. Ein neuer effekt bei eintritt der supraleitfähigkeit. *Naturwissenschaften*, 21, 1933.

[7] F. London and H. London. The electromagnetic equations of the supraconductor. *Proceedings of the Royal society A: Mathematical, physical and engineering sciences*, 149, 1935.

[8] Ginzburg V. and L. Landau. On the theory of superconductivity. *Zh. Eksp. Fiz.*, 20, 1950.

[9] G. Rickayzen. *Theory of Superconductivity*. Interscience Publishers, 1965.

[10] A. Abrikosov. On the magnetic properties of superconductors. *Sov. Phys. JETP*, 32, 1957.

[11] M. Tinkham. *Introduction to Superconductivity*. Dover Publications, 2nd edition, 1996.

[12] L. Cooper. Bound electron pairs in a degenerate fermi gas. *Phys. Rev.*, 104, 1956.

[13] J. Bardeen, L. Cooper, and J. Schrieffer. Theory of superconductivity. *Phys. Rev.*, 108, 1957.

[14] K. Maki. Gapless superconductivity. In R. Parks, editor, *Superconductivity*, volume 2. Marcel Dekker Inc., 1969.

[15] A. Abrikosov and L. Gor'kov. Contribution to the theory of superconducting alloys with paramagnetic impurities. *Zh. Eksp. Teor. Fiz.*, 39, 1960.

[16] F. Reif and M. Woolf. Energy gap in superconductors containing paramagnetic impurities. *Phys. Rev. Lett.*, 9, 1962.

[17] H. Frölich. Theory of the superconducting state. i. the ground state at the absolute zero of temperature. *Phys. Rev.*, 79, 1950.

[18] E. Maxwell. Isotope effect in the superconductivity of mercury. *Phys. Rev.*, 78, 1950.

[19] C. Reynolds, B. Serin, W. Wright, and L. Nesbitt. Superconductivity of isotopes of mercury. *Phys. Rev.*, 78, 1950.

[20] T. Matsubara. A new approach to quantum-statistical mechanics. *Progress of Theoretical Physics*, 14(4), 1955.

[21] R. Kubo. A general expression for the conductivity tensor. *Canadian Journal of Physics*, 34, 1956.

[22] R. Kubo. Statistical-mechanical theory of irreversible processes. i. general theory and simple applications to magnetic and conduction problems. *Journal of the Physical Society of Japan*, 12(6), 1957.

[23] S. Edwards. A new method for the evaluation of electrical conductivity in metals. *Philisophical Magazine*, 3, 1958.

[24] J. Langer. Theory of impurity resistance in metals. *Phys. Rev.*, 120, 1960.

[25] J. Langer. Theory of impurity resistance in metals. ii. *Phys. Rev.*, 124, 1961.

[26] J. Langer. Evaluation of kubo's formula for the impurity resistance of an interacting electron gas. *Phys. Rev.*, 127, 1962.

[27] L. Gor'kov. Energy spectrum of superconductors. [quantum field theory]. *Sov. Phys. - JETP (Engl. Transl.); (United States)*, 7(3), 1958.

[28] Y. Nambu. Quasi-particles and gauge invariance in the theory of superconductivity. *Phys. Rev.*, 117, 1960.

[29] J. Langer. Thermal conductivity of a system of interacting electrons. *Phys. Rev.*, 128, 1962.

[30] V. Ambegaokar and L. Tewordt. Theory of the electronic thermal conductivity of superconductors with strong electron-phonon coupling. *Phys. Rev.*, 134, 1964.

[31] G. Mahan. *Many particle physics*. Plenum, 2000.

[32] J. Luttinger. Theory of thermal transport coefficients. *Phys. Rev.*, 135, 1964.

[33] J. Luttinger. Thermal transport coefficients of a superconductor. *Phys. Rev.*, 136, 1964.

[34] B. Al'tshuler and A. Aronov. Contribution to the theory of disordered metals in strongly doped semiconductors. *Sov Phys. - JETP*, 77, 1979.

[35] L. Aslamarkov and A. Larkin. Effect of fluctuations on the properties of a superconductor above the critical temperature. *Sov. Phys. Solid State*, 10, 1968.

[36] K. Maki. Critical fluctuation of the order parameter in a super conductor i. *Progress of Theoretical Physics*, 40, 1968.

[37] R. Thompson. Microwave, flux flow, and fluctuation resistance of dirty type-ii superconductors. *Phys. Rev. B*, 1, 1970.

[38] J. Langer and T. Neal. Breakdown of the concentration expansion for the impurity resistivity of metals. *phys. Rev. Lett.*, 16, 1966.

[39] E. Abrahams, P. Anderson, D. C. Licciardello, and T. Ramakrishnan. Scaling theory of localization: Absence of quantum diffusion in two dimensions. *Phys. Rev. Lett.*, 42, 1979.

[40] P. Lee and T. Ramakrishnan. Disordered electronic systems. *Rev. Mod. Phys.*, 57, 1985.

[41] L. Gor'kov, A. Larkin, and D. Kheml'nitskii. Particle conductivity in a two-dimensional random potential. *Sov. Phys. - JETP Lett.*, 30, 1979.

[42] Gerd Bergmann. Weak localization in thin films: a time-of-flight experiment with conduction electrons. *Physics Reports*, 107, 1984.

[43] G. Dolan and D. Osheroff. Nonmetallic conduction in thin metal films at low temperatures. *Phys. Rev. Lett.*, 43, 1979.

[44] H. Fukuyama and E. Abrahams. Inelastic scattering time in two-dimensional disordered metals. *Phys. Rev. B*, 27, 1963.

[45] B. Altshuler and A. Aronov. Electron - electron interaction in disordered conductors. In A. Efros and M. Pollak, editors, *Electron-electron interaction in disordered systems*. Elsevier Science Publishers, 1985.

[46] V. Bayot, L. Piraux, J. Michenaud, and J. Issi. Evidence for weak localization in the thermal conductivity of a quasi-two-dimensional electron system. *Phys. Rev. Lett.*, 65, 1990.

[47] D. Stornaiuolo, S. Gariglio, A. Fête, M. Gabay, D. Li, D. Massarotti, and J.-M. Triscone. Weak localization and spin-orbit interaction in side-gate field effect devices at the laalo$_3$/srtio$_3$ interface. *Phys. Rev. B*, 90, 2014.

[48] A. Kuzanyan and S. Harutyunyan. Weak localisation and weak anti-localisation in ultra thin sb$_2$te$_3$ nanoplates. *Journal of Contemporary Physics*, 56, 2021.

[49] T. I. Baturina, S. V. Postolova, A. Yu. Mironov, A. Glatz, M. R. Baklanov, and V. M. Vinokur. Superconducting phase transitions in ultrathin tin films. *Europhysics Letters*, 97(1), 2012.

[50] J. Wang, W. Powers, Z. Zhang, M Smith, B. McIntosh, S. Bac, and L. Riney. Observations of coexisting weak localistion and superconducting fluctuations in strained $sn_{1-x}in_xte$ thin films. *Nano Lett.*, 22, 2022.

[51] K. Schwab, E. Henriksen, J. Worlock, and M. Roukes. Measurement of the quantum of thermal conductance. *Nature*, 404, 2000.

[52] G. Di Battista, P. Seifert, K. Watanabe, T. Taniguchi, K. Fong, A. Principi, and D. Efetov. Revealing the thermal properties of superconducting magic-angle twisted bilayer graphene. *Nano Letters*, 22(16), 2022.

[53] M. Sutherland, J. Dunn, W. Toews, E. O'Farrell, J. Analytis, I. Fisher, and R. Hill. Low-energy quasiparticles probed by heat transport in the iron-based superconductor lafepo. *Phys. Rev. B*, 85, 2012.

[54] D. Ginsberg and L. Hebel. Non-equilibrium properties: Comparison of experimental results and predictions of the bcs theory. In R. Parks, editor, *Superconductivity*, volume 1. Marcel Dekker Inc., 1969.

[55] G. Gladstone, M. Jensen, and J. Schrieffer. Superconductivity in the transition metals. In R. Parks, editor, *Superconductivity*, volume 2. Marcel Dekker Inc., 1969.

[56] G. Rickayzen. *Green's functions and condensed matter*. Courier Corporation, 2013.

[57] C. Satterthwaite. Thermal conductivity of normal and superconducting aluminum. *Phys. Rev.*, 125, 1962.

[58] J. Bardeen, G. Rickayzen, and L. Tewordt. Theory of the thermal conductivity of superconductors. *Phys. Rev.*, 113, 1959.

[59] R.. Smith and V. Ambegaokar. Weak-localization correction to the number density of superconducting electrons. *Phys. Rev. B*, 45, 1992.

[60] Y. Yong-Hong, Yu G., W. Yong-Gang, and L. Mei. Weak-localization effect on the density of states in disordered d-wave superconductors*. *Communications in Theoretical Physics*, 42(2), 2004.

[61] T. Jujo. Weak localization correction to linear absorption in conventional superconductors. *Journal of the Physical Society of Japan*, 90(1), 2021.

[62] F. Hajiloo, F. Hassler, and J. Splettstoesser. Mesoscopic effects in the heat conductance of superconducting-normal-superconducting and normal-superconducting junctions. *Phys. Rev. B*, 99, 2019.

[63] L. González Rosado, F. Hassler, and G. Catelani. Weak localization corrections to the thermal conductivity in s-wave superconductors. *Phys. Rev. B*, 101, 2020.

[64] M. Reizer. Electron-electron interactions in two-dimensional impure superconductors. *Phys. Rev. B*, 61, 2000.

[65] R. Smith. *The interplay of localization and interaction in dirty superconducting films and mesoscopic metal rings*. PhD thesis, Cornell University, 1993.

[66] H. Bruus and K. Flensberg. *Many-body quantum theory in condensed matter physics: an introduction*. Oxford university press, 2004.

[67] A. Abrikosov, L. Gorkov, and I. Dzyaloshinski. *Methods of quantum field theory in statistical physics*. Courier Corporation, 2012.

[68] V. Ambegaokar. The green's function method. In R. Parks, editor, *Superconductivity*, volume 1. Marcel Dekker Inc., 1969.

[69] L. Kanadoff and P. Martin. Hydrodynamic equations and correlation functions. *Annals of Physics*, 24, 1963.

[70] G. Chester and A. Thellung. The law of wiedemann and franz. *Proceedings of the Physical Society*, 77(5), 1961.

[71] M. Kearney and P. Butcher. Thermal transport in disordered systems. *Journal of Physics C: Solid State Physics*, 21(9), 1988.

[72] A. Abrikosov and L. Gor'kov. On the theory of superconducting alloys. i. the electrodynamics of alloys at absolute zero. *Sov. Phys. JETP*, 35(6), 1958.

[73] P. Byrd and M. Friedman. *Handbook of elliptic integrals for engineers and scientists*. Springer-Verlag Berlin Heidelberg, 1971.

[74] L. Tewordt. Theory of the instrinsic electronic thermal conductivity of superconductors. *Phys. Rev.*, 129, 1963.

[75] V. Ambegaokar and A. Griffin. Theory of the thermal conductivity of superconducting alloys with paramagnetic impurities. *Phys. Rev.*, 137, 1965.

[76] S. Skalski, O. Betbeder-Matibet, and P. R. Weiss. Properties of superconducting alloys containing paramagnetic impurities. *Phys. Rev.*, 136, 1964.

[77] S. Hikami, A. I. Larkin, and Y. Nagaoka. Spin-orbit interaction and magnetoresistance in the two dimensional random system. *Progress of Theoretical Physics*, 63(2), 1980.